Transcriptional targets of Pax3 during development

By

Benjamin Fenby

Thesis submitted for the degree of doctor of philosophy at the University of Edinburgh

May 2005

"….it seems we are converging on mutual indifference."

R. Connolly, 2003

Disclaimer

I (Benjamin Fenby) performed all of the experiments presented in this thesis unless otherwise clearly stated in the text. No part of this work has been, or is being, submitted for any other degree or qualification

Acknowledgements

Numerous people have been indispensable to the completion this work.

John Mason has tirelessly supervised me over the past 4 years. This is in spite of me foisting myself into his lab uninvited and proceeding to throw regular tantrums whilst spending quite a frightening quantity of cash. He receives top thanks and probably some kind of serious karmic upgrade for the next life I should imagine.

Karen Chapman, Lesley Forrester and Mike Clinton all kindly agreed to sit on my Thesis Committee; their advice and guidance was invaluable.

Technical support (a term which never properly reflects how impossible work like this would be without it) from Katy Gillies and Duncan McNeil must also be warmly applauded.

My contemporaries in the Price / Mason / Kind / Spears / West labs for kindness, help and above all tolerance over the years.

These data would not have been obtained without the breeding and sacrificing of mice. Whilst this was always kept to the barest minimum (partly due to my being rubbish at dissection), I acknowledge and state this was performed as humanely as possible.

Finally, J. Fenby, S. Fenby, R. Fenby, P. Zaki, D. Tyas, J. Newbold, J. Pinson, J. Buscombe, D. Hancock, I. Simpson, L. Newbold, C. McCardle, S. Heasman, D. Icely, V. Fotaki, K. Hochweiller, A. Aboobaker, R. Pickering, H. Munn, C. Naughton, H. Woolnough, C. Yap, T. Hill, J. Nelson, S. Scudamore, N. Coller, P. Kind, C. Berry, A. Woolnough, S. Artois, M. Lights, G. Sian and R. Connolly all deserve a piece of this.

T. Ellender gets a much bigger bit.

Table of Contents

Abbreviations

Term	Definition
5'UTR	5' Untranslated Region
ATP	Adenosine triphosphate
BSA	Bovine Serum Albumin
cDNA	Complementary DNA
ChIP	Chromatin Immunoprecipitation
CNS	Central Nervous System
ddH2O	Doube distilled, column purified water
DNA	Deoxyribonucleic Acid
dNTP	Deoxyribonucleotides
LacZ	B-Galactosidase
mRNA	Messenger RNA
NCAM	Neural Cell Adhesion Molecule
NEB	New England Biolabs
ORF	Open Reading Frame
PAC	P1 Artificial Chromosome
PCIA	Phenol Chloroform Iso-amly Alcohol
PCR	Polymerase Chain Reaction
PEXT	Primer extension
QRTPCR	Quantified RTPCR
RA	Retinoic Acid
RACE	Rapid Amplification of cDNA Ends
RLU	Reative Light Units
RNA	Ribonucleic Acid
RPA	Ribonuclease Protection Assay
rpm	Rotations per minute
RT	Room Temperature (18-20 °C)
RTPCR	Reverse Transcriptase PCR
SAP	Shrimp Alkaline Phosphatase
SDS-PAGE	SDS Polyacrylamide Gel Electrophoresis
Sp^{2H}	Splotch -null mutant allele of *Pax3*
TEPCR	Template Enriched PCR
TTLB	Tail Tip Lysis Buffer

Abstract

Transcription factors play multiple and important roles during embryonic development. The *Pax* gene family have been shown to be essential in these processes, and mutations which abrogate their function disrupt the development of a range of embryonic tissues. One member of this family, *Pax3*, is characterised by a semidominant mutant phenotype and is involved in the proper formation of the brain, central and peripheral nervous system, hypaxial musculature, and cardiac outflow vessels. *Pax3* is a transcription factor and its biological role involves the binding of specific sequences in genomic DNA to regulate the expression of a set of target genes. Defects observed in animals harbouring a mutation in *Pax3* are assumed to arise from the misregulation of the transcriptional targets of this gene.

In dissecting the precise biological function of *Pax3*, it is important to differentiate between primary and secondary phenotypes in the mutant animal; specifically, between defects caused by the direct misregulation of *Pax3* targets and those generated by the compounded knock-on effects of a dysfunctional master-regulator such as *Pax3*. A simple comparison of expression profiles between wild type and mutant animals, using microarray or differential display based methodologies, would not achieve this aim. To date, no attempt to perform a comprehensive screen for direct *Pax3* targets in development has been performed.

This thesis presents a development of the tools necessary to perform the task of identifying direct targets of *Pax3 in vivo*. Firstly, two candidate genes for direct *Pax3* regulation are considered, *Wnt1* and *Pax7*. These candidates are implicated from previous work on *Pax3* although no direct transcriptional link has ever been

established. Firstly, differences in the expression of these genes between the *Pax3* mutant and wild type embryos is quantitatively analysed. In the case of *Pax7*, little work had been performed to identify the regulatory elements controlling its expression in the mouse. Described here is a series of experiments mapping the 5' end of the transcript, the delineation of a putative promoter region and the identification and cloning of a highly conserved enhancer element within the first intron. The *Wnt1* regulatory elements have been well described elsewhere. A series of experiments are then performed to confirm the interaction between these regulatory regions and *Pax3* and the identification and testing of specific *Pax3* binding sites is reported.

To confirm these interactions *in vivo*, chromatin immunoprecipitation, using a novel mono-specific anti-*Pax3* antibody designed for the purposes of this thesis, is used. This technique, having been verified on these two direct *Pax3* targets in this way, could then be used to screen for novel direct targets of *Pax3* regulation *in vivo* and in the wild type; expanding our understanding of the pathways and developmental function of this gene in future.

Chapter One: Introduction

The transcription factor *Pax3* is involved in a range of developmental and pathological processes, ranging from the patterning and specification of the central nervous system to the progression of cancer (Chi and Epstein, 2002). In animal models where the function of the *Pax3* gene has been ablated or modified, a number of interesting phenotypes have been observed. These include neural tube closure defects, which are similar to the condition *spina bifida* in humans, severe brain defects, such as anencephaly and exencephaly, problems in a range of tissues which are normally populated by a migratory population of stem cells originating from the embryonic spinal cord known as the neural crest (in humans these defects are categorised under the umbrella term neurocristopathies) and defects in the proper septation and morphology of the heart. In humans the condition Waardenburg's Syndrome has been attributed to mutations in *Pax3* (Epstein, 1996). Patients suffering from this congenital disorder have a heterozygous mutation in the *Pax3* gene (only one *Pax3* homozygous mutant human has been reported at term (Zlogotara, 1995)) and exhibit characteristic pigmentation defects (including a white forelock reminiscent of the white belly spot found on *Pax3* heterozygous mice), deafness, craniofacial abnormalities, and even defects in limb musculature.

Understanding such developmental processes, and using the *Pax3* gene as a tool to probe these further, should ultimately enable the better understanding and more appropriate treatment of a range of diseases in future.

The *Pax3* protein acts as a transcription factor, binding to DNA and regulating the expression of other genes (Epstein et al., 1991). Whilst much work has been done to describe the role *Pax3* plays in different developmental processes, relatively few direct targets of *Pax3* have been established and no comprehensive screen for *Pax3* target genes has been performed. This is important since, without an understanding of the direct targets of *Pax3*, any appreciation of the specific pathways this gene modulates is difficult. Furthermore, the interpretation of data obtained from manipulations of the *Pax3* gene, whether knockouts, overexpressions, or even the use of *Pax3* as a developmental marker, will be enhanced by a comprehensive understanding of the gene's transcriptional function.

This thesis therefore aims to identify novel targets of direct regulation by *Pax3* and defines the specific elements through which *Pax3* is acting. These targets are then confirmed *in vivo* through the optimisation of a technique which can then be used as a tool for performing a more comprehensive screen for *Pax3* target genes in future.

Pax3 *Biochemistry*

The paired DNA binding domain is found in several *Drosophila* genes, such as *Paired*, *gooseberry-proximal/distal* (Mansouri, 1996). These are involved in the segmentation patterning and development of the embryo. The paired domain is found throughout evolution, and represents a highly conserved 128 amino acid motif that forms a helix-turn-helix structure to contact DNA. In vertebrates, the first paired domain containing proteins identified were the *Pax* family.

The Pax *Gene Family*

Pax genes encode a family of DNA binding proteins. These proteins are expressed in a temporally and spatially dynamic manner in the mammalian embryo. The disruption or misregulation of these factors has been shown to have serious consequences for the process of development and ultimate function of many tissues. *Pax* genes are 9 in number in the mouse and are all thought to bind DNA and act as transcription factors, regulating the expression of downstream target genes. These proteins are thought to bind to specific sequences in the promoters and enhancers (*cis*-regulatory sequences) of their targets and regulate their expression via the recruitment of either inhibitory or activatory transcriptional complexes (for general reviews, see (Chi and Epstein, 2002; Epstein, 1996; Mansouri, 1996)). The known roles of the *Pax* genes in mouse development are summarised in Figure 1.1.

Pax Gene	**Paired, homeodomain, or octapeptide**	**Name and Phenotype of mutant**	**Reference**
Pax1 (I)	Paired + octapeptide	*Undulated (Un).* Axial skeletal defects.	(Wallin, 1994)
Pax2 (III)	Paired + octapeptide + truncated homeodomain	k/o defects in urogenital tract, optic nerve, cochlea defects	(Torres, 1995)

Pax3 (II)	Paired + octapeptide + homeodomain	*Splotch (Sp)* Open neural tube, lethal by E15 due to cardiac outflow tract phenotype	(Epstein et al., 1991)
Pax4 (IV)	Paired + homeodomain	k/o defects in pancreatic α-cells	(Habener and Stoffers, 1998)
Pax5 (III)	Paired + octapeptide + truncated homeodomain	k/o defects in midbrain and ablation of B cell development	(Urbanek, 1994)
Pax6 (IV)	Paired + homeodomain	*Small eye (Sey)* Forebrain defects, micropthalmia lethal at birth	(Hill, 1991)
Pax7 (II)	Paired + octapeptide + homeodomain	k/o defects in cephalic neural crest derivatives	(Mansouri et al., 1996)
Pax8 (III)	Paired + octapeptide + truncated homeodomain	k/o absent follicular cells of Thyroid gland	(Mansouri, 1998)
Pax9	Paired +	k/o absent thymus,	(Peters,

(I)	octapeptide	teeth, extra digits and ectopic skeletal growth	1998)

Figure 1.1 : The roles of Pax *genes in development, reviewed in (Chi and Epstein, 2002; Eccles, 2002; Mansouri, 1996). Numbers in roman numerals denote the subfamily to which the factor belongs; i.e.* Pax1 *and* Pax9 *are within sub-family I (classification from (JacksonLabs))*

The *Pax* genes are divided into subfamilies on the basis of their domain composition, as shown in Figure 1.1. Members of the same subfamily have highly conserved DNA binding domains, with sequence divergence occurring towards the 3' end of the gene (C-terminus of the protein). This implies similar DNA sequence recognition by members of the same sub-family and may account for functional redundancy between family members *in vivo*. It is important to note that *Pax* proteins may also have other functions, aside from their roles as transcription factors, which are not highlighted in these studies.

The Pax3 *gene and its isoforms*

Pax3 was first identified in 1991 in the mouse and was shown to have a dynamic expression pattern during embryogenesis. Clones were isolated from a cDNA library using the *Pax1* paired box as a probe. The *Pax3* gene was shown to be expressed from the onset of neurulation (E8.5) in the developing CNS (Goulding et al., 1991). This

has since been confirmed in several other studies (Bang et al., 1999; Natoli et al., 1997) and *Pax3* is further expressed in the adult hair follicle (Lang, 2005). The *Pax3* gene maps to mouse chromosome 1 (Epstein et al., 1991) and encodes a protein product of 479 amino acids (53 KDa). The *Pax3* locus spans 95kb (ensembl) in the mouse and homologous loci have been identified in humans, *Xenopus*, *Fugu* and rat. A schematic of the *Pax3* protein, highlighting the major domains, is illustrated in Figure 1.2.

The *Pax3* locus encodes up to 10 exons (Barber et al., 1999) with transcripts varying in length from 900 bp (Tsukamoto et al., 1994) to 3.6 kb (Goulding et al., 1991). Six exon splice variants (named *PAX3a* to *Pax3f*, respectively) were originally reported between human and mice (Barber et al., 1999). A recent study has identified a new isoform generated through the use of a novel splice site formed at the junction of exons 7 and 8 (*Pax3(Δ8)*) in the mouse. This isoform removes part of the transactivation site of *Pax3* (encoded by exon 8) and has been shown to result in a transcriptionally dominant negative protein *in vitro* (Pritchard, 2003).

The biological importance of many of these isoforms has yet to be determined experimentally. Indeed *PAX3a* and *PAX3b*, whilst thought to potentially also encode dominant negative forms of *Pax3* (Tsukamoto et al., 1994), have yet to be confirmed as biologically functional at the protein level or even existant in the mouse. Similarly, *Pax3e* and *Pax3f* have not been characterised in any

Figure 1.2:
Scale drawing of mouse *Pax3* protein illustrating major domains and features. NT = Amino-terminus, CT = Carboxy-terminus

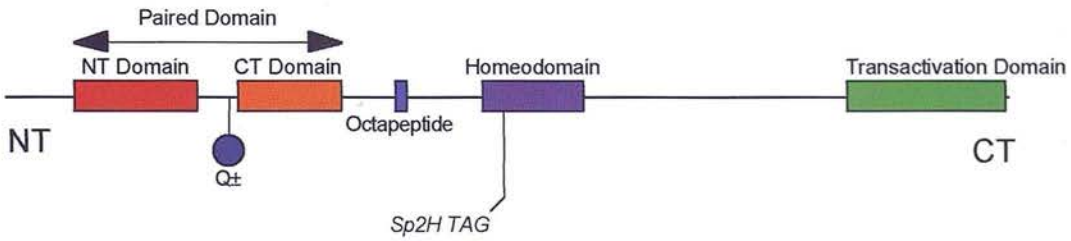

more detail than the sequencing of RTPCR clones (Barber et al., 1999). *Pax3c* was the original full length transcript reported for the mouse by (Goulding et al., 1991). *Pax3d* is identical to *Pax3c*, but has an extra C-terminal coding exon (exon 9). Because no functional difference between *Pax3c* and *Pax3d* could be detected, (Barber et al., 1999), the major *Pax3c* isoform has been used throughout this thesis.

Another major source of transcript variation for this gene is the inclusion or exclusion of a glutamine (Q) codon generated by an alternative splicing event at the exon 2 - exon 3 junction, see Figure 1.3E (Vogan et al., 1996). All 8 of the *Pax3* transcripts denoted above also therefore have a Q± status, bringing the total number of splice variants to 16 recorded so far.

The inclusion of a glutamine residue at position 76 in the *Pax3* protein was first identified by (Vogan et al., 1996). This glutamine residue is positioned between the two DNA binding sub-domains of the paired domain, see (Czerny, 1993). This places the splice variation in the C-terminal sub-domain of the *Pax3* paired domain in a similar position to exon 5a in the *Pax6-5a* isoform (shown to be important in changing the sequence specificity of *Pax6* see (Kozmik, 1997) and below). The inclusion of the *Pax3* Q residue was shown *in vitro* to mediate changes in binding affinity of the paired domain to artificial consensus sites (the Q- isoform binding with around 5 times greater affinity to specific sequences as the Q+). *In vivo* the Q+ isoform is by far the most abundant of the isoforms (Vogan et al., 1996) and no dynamic change in the relative abundance of the isoforms was observed during development. Later

Figure 1.3:
Genomic *Pax3* locus, from www.ensembl.org.
A) *Pax3* in context of mouse chromosome 1
B) expanded contig view
C) exon / intron schematic
D) protein domain structure of transcript
E) illustration of Q± alternative splicing between exon 2 and exon 3 in *Pax3*. Blue = exon sequence, green = splice donor / acceptor sites, red = glutamate codon, arrows = alternative splice acceptor sites

A

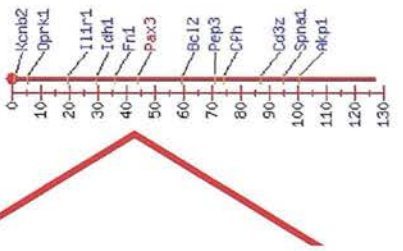

B

C

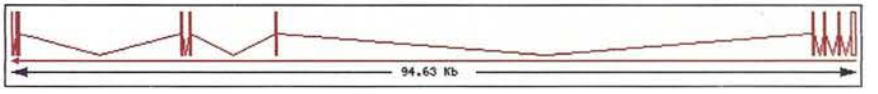

D

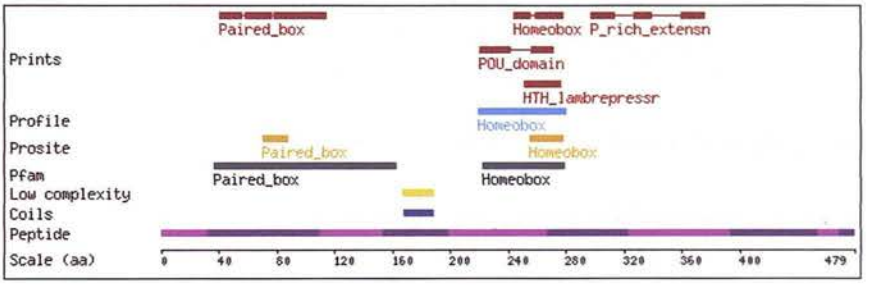

E

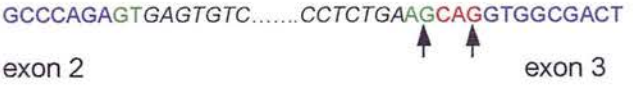

studies have revealed that, when selected for using *in vitro* Selex* based methodologies, *Pax3*Q+ and *Pax3*Q- may also have affinities for slightly different sequences (Vogan and Gros, 1997).

It is plausible that the two isoforms are generated by stochastic splicing events in the cell due to the existence of similarly high affinity splice acceptor sites. Since both isoforms do recognise identical sequences, it is possible that the difference generates such a minor change in functionality (and target sequence specificity (Vogan and Gros, 1997; Vogan et al., 1996)) that evolution has not selected for one or the other isoform and hence both are observed. This view may be supported by the fact that, to date, no differences in transcriptional targets have been observed for these isoforms *in vivo*. In this thesis the most abundant, Q+, isoform has been used for all experiments.

The Pax3 *Protein*

The *Pax3* protein has been studied extensively and its functional domains mapped in detail. The N-terminus of the protein holds the paired and homeodomain, separated by an octapeptide motif, and the transactivating domain is found towards the C-terminal end of the protein (Figure 1.2). The functional significance of the conserved octapeptide motif is unclear, in spite of its presence in most *Pax* family proteins (with the exception of Pax4/6).

* Selex is an *in vitro* method for selecting oligonucleotides which bind to a protein with high affinity using several rounds of PCR amplification

One group (Ziman and Kay, 1998) has proposed that this region is of regulatory importance at the DNA level, and that the octapeptide motif is in fact a site directing methyltransferase activity to regulate the transcription of *Pax3* (i.e. DNA sequence is conserved over codon use between species). In Pax5, however, the octapeptide has been shown to interact with the *Groucho* family of co-repressors (Chi and Epstein, 2002) and *Ets* co-regulators (Wheat, 1999). Similarly the ability of Pax3 to interact with the hDaxx repressor protein has been shown to be partially compromised on deletion of an N-terminally extended octapeptide domain (Hollenbach et al., 1999). The functional significance of this *in vivo* was not investigated by this group, however.

The binding by the N terminal domains of the protein to specific sequences in genomic DNA during development is thought to represent the core biochemical function of the *Pax3* protein*. Structural studies on the related human Pax6 and *Drosophila* paired proteins indicate a common mechanism for DNA interaction by this domain family (Xu, 1995; Xu, 1999). Much work has been done *in vitro* to dissect the precise components of these domains and how they interact with one another. It is generally accepted that, in Pax3, the paired domain imparts much of the sequence specificity of the protein and indeed plays an important role in modulating the DNA binding affinity of the homeodomain and its ability to dimerise on palindromic DNA sequences (Fortin et al., 1998; Underhill, 1997). This finding is reinforced by the *Splotch delayed* (Sp^{d}) mutant, a missense *Pax3* mutant harbouring a

* Interestingly, the regulation of p53 by Pax3 may be post-transcriptional since differences in p53 protein and not mRNA can be observed between a Sp^{2H} -/- and wild type background, see **Pani, L., Horal, M. and Loeken, M. R.** (2002). Rescue of neural tube defects in Pax-3-deficient embryos by p53 loss of function: implications for Pax-3- dependent development and tumorigenesis. *Genes Dev* **16**, 676-80.

glycine to alanine substitution within position 9 of the paired domain. This mutation abrogates DNA binding by both domains and confers a null phenotype *in vivo*. Therefore, correct DNA – paired domain interactions are essential for the proper selection of Pax3 targets during development.

The role of the homeodomain of Pax3 in binding DNA is also complex. (Underhill, 1997) demonstrate that the paired domain of Pax3 affects the sequence specificity of the homeodomain and the spacing of the ATTA palindromic recognition sequence for this part of the protein. Spacing between the homeodomain and paired domain recognition sequences has been shown to affect the DNA binding affinity of the *Pax3* protein (Phelan and Loeken, 1998). The DNA binding of the paired and homeodomain are also reciprocally related, and abrogation of DNA binding in one can lead to loss of DNA binding in both (Apuzzo, 2004; Apuzzo and Gros, 2002). The paired and homeodomain of Pax3 are therefore considered functionally interdependent.

The C-terminal portion of the *Pax3* protein is responsible for the transactivatory functions (Chalepakis et al., 1994) and is not thought to be directly involved in DNA binding. The postulated role for this part of the protein in mediating transactivation of target genes has been borne out by functional dissections of the *Pax3* protein *in vitro* (Chalepakis et al., 1994). Pax3 has clearly been shown to be able to up-regulate as well as down-regulate target genes, presumably depending on the transcriptional context within a particular cell type and target locus. Examples of *Pax3* having both transactivatory and transrepressive functions *in vitro* (Chalepakis et al., 1994; Lang, 2005) and *in vivo* (Kwang et al., 2002; Lang and Epstein, 2003) can be found in the

literature. The C terminal domain of *Pax3* has also been shown to modulate the binding activity of the N terminal domains of the protein (Cao and Wang, 2000). This is supported by the *in vivo* observation that the *Pax3* protein, and the *Pax3-FKHR* fusion oncogene product (generated by a chromosomal translocation mutation common in alveolar rabdomyosarcoma (Lam et al., 1999) replacing the *Pax3* C-terminus with the transactivation domain of one of the forkhead family of transcription factors) have the potential to transactivate different target genes in spite of their identical DNA binding protein domains (Barber et al., 2002; Begum, 2005; Du, 2005). The phenomenon of long-range structural alterations affecting the functionality of transcription factors has also been observed in a completely heterogenous context; the glucocorticoid nuclear receptors undergo similar long-range conformational changes on DNA binding (Pearce, 1998; van Tilborg, 2000).

Pax3 *Target Sequences*

The root functionality of a transcription factor comes from its ability to bind to *cis*-regulatory sequences of target genes and hence mediate either up- or down-regulation of their expression. To understand the role Pax3 plays during vertebrate development, it is therefore necessary to identify the target sequences to which it binds. Several attempts have been made using *in vitro* techniques to identify the consensus sequences recognised by Pax3. This was first performed by Chalepakis et al (Chalepakis and Gruss, 1995) using a PCR selection based Selex analysis of the Pax3 paired domain to generate a 13bp consensus sequence. One of the most interesting results of this early work was the observation that, with the exception of the four 5' nucleotides, the *Pax3* consensus sequence obtained was extremely similar to other

binding consensus sites derived for Pax2 and Pax6. Furthermore, the sequences of previously described high affinity paired domain binding oligo sequences CD19-2A and PRS9 (from the *Drosophila* e5 promoter) were conserved to the 3' end of the consensus sequence. These data were interpreted as meaning that the 3' end of this recognition sequence represented a high affinity Paired domain binding site (hence the homology to both other Pax sites and high affinity oligo sequences), and the 5' nucleotides may impart the actual sequence specificity to the *Pax3* protein. Recent software designed to identify transcription factor binding sites (MatInspector) cites these first four base pairs as the core binding motif for *Pax3*. Some published *Pax3* consensus sites are summarised in Figure 1.4.

This consensus sequence is thought to represent binding of the N-terminal sub-domain of the *Pax3* protein only. In the *Pax6* protein, an alternative splicing event in the DNA encoding the paired domain acts a molecular "toggle" to shift binding preference from the N to C-terminal sub-domain of the *Pax6* paired domain, through the inclusion of the 5a exon (Kozmik, 1997). This dramatically alters the sequence specificity of the *Pax6* protein. The presence of an alternatively spliced glutamine residue between the N and C terminal sub-domains of the paired domain in Pax3 obviously represents an attractive model for a similar post-transcriptional level of regulation. Several papers have addressed this *in vitro* (Vogan and Gros, 1997; Vogan et al., 1996) and have obtained target sequences with a higher affinity for one or other isoforms. No absolute changes in binding specificity or *in vivo* target selection has yet been identified for these isoforms, however.

Figure 1.4 :
Comparison of Pax3 paired domain consensus sites previously reported in the literature. Predicted core consensus sites are highlighted in red.

Experimental Source	**Consensus Sequence**	**Reference**
in vitro, Selex methodology	TCGTCACRCHYHA	Chalepakis and Gruss, 1995
in vitro, Selex methodology	GTCACGCTT	Vogan et al, 1996
in vitro, Selex methodology	TCGTCACSCTT-A	Vogan and Gross, 1997
in vivo, c-RET enhancer	TGTCACACTGCC	Lang and Epstein, 2003

The above studies enable the identification of putative Pax3 DNA binding sites *in vivo* via sequence analysis. As pointed out by many authors, however (Wasserman and Sandelin, 2004), the presence of a Pax3 consensus does not automatically imply a Pax3 responsive site *in vivo*. Functional studies are always essential to confirm the significance of any potential Pax3 binding site. Indeed, (Phelan and Loeken, 1998), observed that many of the Pax3 responsive genes confirmed so far actually contain low affinity Pax3 consensus sites, and not the high affinity sites identified by *in vitro* methodologies. This suggests that a simple sequence based approach to identifying new Pax3 targets may not be appropriate and that a more direct method for identifying *Pax3* target genes *in vivo* may be required.

Pax3 also interacts with other proteins *in vivo*. These interactions can occur via both the paired domain (Hollenbach et al., 2002; Lang and Epstein, 2003; Wheat, 1999) and homeodomain (Hollenbach et al., 1999; Stamataki et al., 2001) and can elicit both negative and positive transcriptional responses from the target genes in question. Thus it is important to appreciate that, whichever sequences the Pax3 protein binds to during development, the binding of co-factors and ultimately the recruitment of the RNA polymerase machinery is core to the function of this transcription factor.

Pax3 *In Neural Tube and Neural Crest Development*

The induction of neural tube from ectoderm occurs early in the development of the mouse and involves a complex array of signals. The formation of the neural tube and neural crest cells probably represents one of the earliest events in the evolution of vertebrates and therefore a high degree of conservation in the mechanisms and signals

used between species is thought to exist (Meulemans and Bronner-Fraser, 2004). After gastrulation, the ectoderm is organised into neuroectodermal and ectodermal regions through the action of the Spemann's Organiser (in amphibians) or equivalent (the node in mice and chick). These structures secrete neural inducers, such as *chordin* and *noggin*, which enable the establishment of neural cell fates from non-neural ectoderm through the inhibition of the high levels of BMP signalling (LaBonne and Bronner-Fraser, 1998; LaBonne and Bronner-Fraser, 1999). Once the neuroectoderm has been specified in this manner, the tissue invaginates to form the neural fold and ultimately closes completely to generate the neural tube (Figure 1.5). It is the interface between neural and non-neural ectoderm which stimulates the generation of the neural crest population (Selleck and Bronner-Fraser, 1995). In mice, *noggin* mutants are still able to express many of the dorsal neural tube markers by E10.5, and some migratory neural crest cells are still observed (McMahon, 1998), implying that other signals must be involved in this process, such as Wnt and FGF (Monsoro-Burq, 2003).

Intermediate levels of BMP signals from the ectoderm are however essential in the early stages of this process, and help to induce the expression of *Msx1* at the neural plate boundary (LaBonne and Bronner-Fraser, 1999; Liem, 1997; Monsoro-Burq, 2004). *Msx1* and a *Wnt8* signal from the underlying non-axial mesoderm (Bang, 1997; Bang et al., 1999) then induce *Pax3* expression in the lateral edges of the neural plate. This is then restricted dorsally by *Shh* signals from the notochord and floor plate (Goulding, 1993) as neural tube closure proceeds, generating a *Pax3* expression pattern restricted to the dorsal half of the developing neural tube. Another important gene, *Zic1*, is expressed in the dorsal neural tube after induction by *BMP4* and *BMP7*

Figure 1.5:
Schematic of neural tube closure and neural crest induction highlighting the expression domains of the major genes outlined in the text. (Source image taken from Bronner-Fraser, 2002)

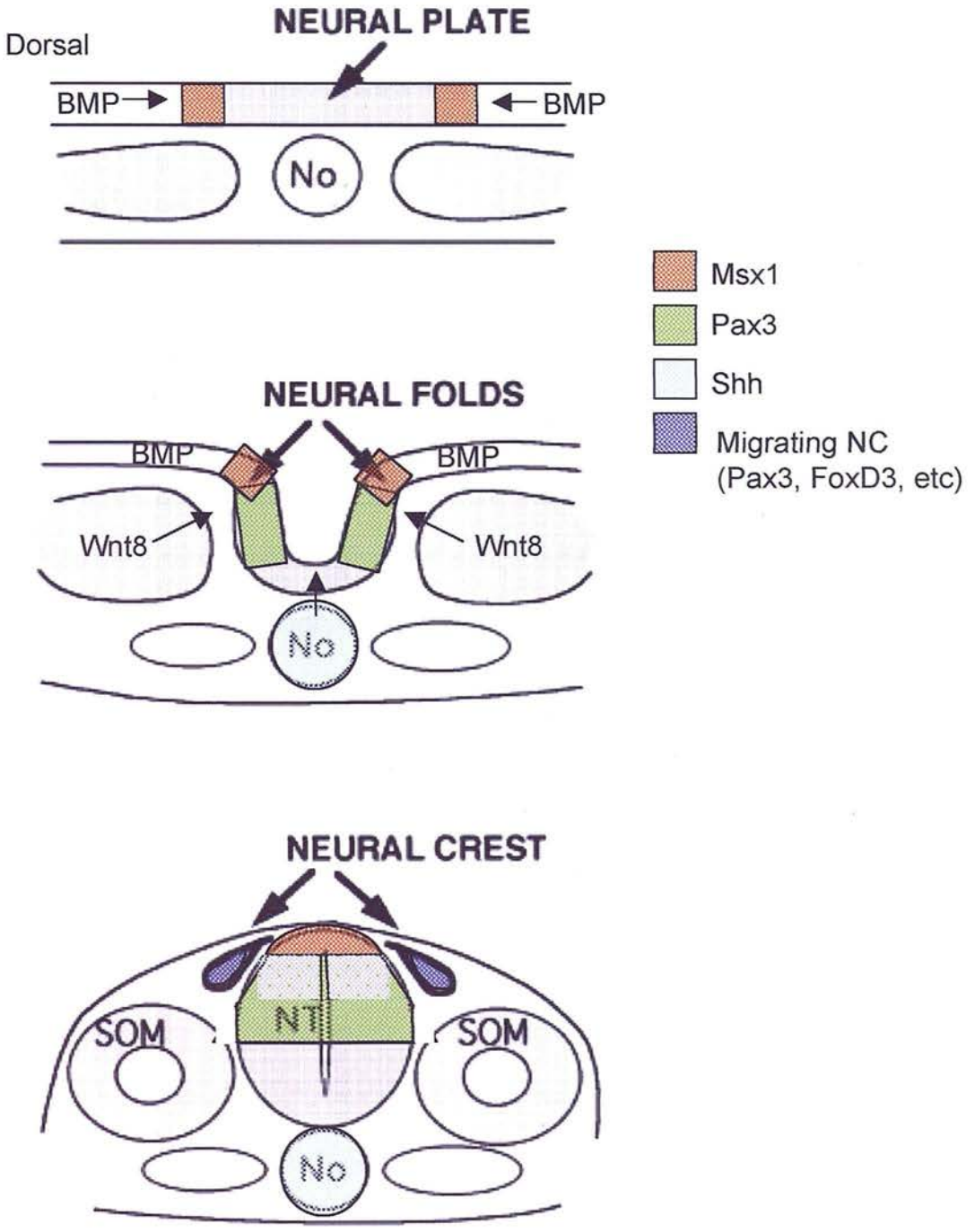

from adjacent ectoderm and is restricted to dorsal neural tube by *Shh* in a manner analogous to *Pax3* (Aruga, 2002). The activities of these genes converge to stimulate the expression of neural crest markers such as *Slug*, *Snail* and *Foxd3* which are important in establishing the neural crest lineage (Dottori et al., 2001; Kos, 2001; LaBonne and Bronner-Fraser, 1999; Mennerich and Braun, 2001). One interesting study has proposed that a major function of *Pax3* is the inhibition of p53 mediated apoptosis (Pani et al., 2002). This is based on the rescue of neural tube defects on a Sp^{2H} -/- *p53* -/- double mutant background due to reduced cell death. It is important to consider the role of *Pax3* as a cell survival signal therefore, in addition to the regulation of developmental target genes.

The precise role of *Pax3* in the process of switching on the genes specifying the neural crest lineage is still unclear. Whilst *Pax3* is genetically upstream of *Foxd3* (Dottori et al., 2001), direct interaction between *Pax3* and the regulatory elements of *Foxd3* has not been shown. Furthermore, the induction of *Slug* by the combined activities of *Zic1* and *Pax3* (Monsoro-Burq, 2004) have been shown to be mediated by Wnt signalling. These observations are in keeping with those made on *Pax3* chimeras (Mansouri et al., 2001) that, whilst *Pax3* null cells cannot be rescued by wild type counterparts in somites, a non-cell autonomous role exists for the gene in the development of the neural crest. If *Pax3* requires a non-cell autonomous signal to enable the instruction of downstream target genes involved in neural crest development, suitable candidate factors should be considered.

Wnts are attractive signals to facilitate this role of *Pax3*. In *Xenopus*, the induction of neural crest cell fates in the dorsal neural tube has been shown to be dependent upon

Wnt1 and *Wnt3a*, synergising with neuralising factors such as *noggin* (Saint-Jeannet et al., 1997). This activity could not be replaced with *Wnt5a* or *Wnt8*, implying that the Wnt signal responsible for inducing *Pax3* expression and that involved in neural crest specification are different (Bang et al., 1999; Saint-Jeannet et al., 1997). Similarly in Zebrafish, Wnt signalling has been shown to be essential during neural crest induction from underlying mesoderm (Lewis, 2003) (in *Xenopus* neural crest (Bang et al., 1999) this mesodermal signal has been shown to be *Wnt8*) but this signal is distinct from a second Wnt activity, however, which specifies a neural crest lineage. Both the "two signal" model of neural crest induction (where the induction of neuroectoderm by *chordin* and *noggin* requires a second signal to express neural crest specific markers (LaBonne and Bronner-Fraser, 1998)) and the "double gradient" model (where default anterior neural tissue is patterned combined lateralising and posteriorising gradients (Villanueva, 2002)) in *Xenopus* depend upon canonical Wnt signalling. In chick, inhibition of Wnt signalling similarly perturbs the expression of neural crest marker genes (Garcia-Castro, 2002).

Other Wnt genes that are expressed in this tissue at this stage are *Wnt1* and *Wnt3a*. Compound knockouts of these genes (Ikeya et al., 1997) show major defects in their neural crest populations and neural crest derived structures but not in the overall dorsoventral patterning of the neural tube, suggesting these factors act after the establishment of patterning within the neural tube itself. Further experiments investigating the expression and function of Wnt receptors in Xenopus neural crest, the frizzled protein family, have revealed that the *Wnt1* specific receptor *Frz3* is necessary for the induction of neural crest in the developing *Xenopus* embryo in association with the Kermit co-receptor (Deardorff, 2001; Tan, 2001).

The expression of *Wnt1* and *Wnt3a* in the *Pax3* mutant has been investigated, and whilst the expression of *Wnt3a* did not change, *in situ* data for *Wnt1* did imply a significant downregulation in the neural tube of Sp^{2H} homozygotes (Conway et al., 2000). *Wnt1* therefore represents an attractive candidate gene for direct regulation by *Pax3* in this system.

Wnt1 *and* Wnt1 *Regulation*

Much work has been done on *Wnt1* and the regulation of this gene, and will be briefly dealt with here (for a comprehensive review of Wnt biology in this and other systems see (Logan, 2004; Miller, 2001)). *Wnt1* was the first of the *Wnt* genes to be discovered, and was originally identified as the site of a mouse mammary tumour viral insertion into the 5' and 3' regulatory regions of the gene (Van Ooyen, 1984). Later sequence alignments revealed that the gene was the mammalian homologue of the *Drosophila Wingless (Wg)* gene, and the ability of *Wnt1* to transform mammary cells when inappropriately expressed led to its categorisation as a proto-oncogene and suggested a biological role in proliferation (Dickinson et al., 1994; Nusse et al., 1990). Knockout strategies (McMahon and Bradley, 1990; Thomas, 1990) revealed an essential role for *Wnt1* in the development of midbrain and cerebellar structures. Neither of these studies illustrated defects in neural tube development in spite of the strong dynamic expression of this gene. Similarly, *Wnt3a* knockout mice (Takada, 1994) displayed defects in somitogenesis but not in the neural tube or neural crest derivatives. A redundancy in Wnt signalling in the neural tube was therefore

postulated and *Wnt1* / *Wnt3a* double mutant embryos exhibit a severe neural crest phenotype (Ikeya et al., 1997).

If *Wnt1* represents a direct target of *Pax3* regulation in the developing embryo, an elucidation of the *cis*-regulatory elements driving the expression of this gene is required. Due to the insertion of the provirus into the region 5' proximal to the gene causing inappropriate *Wnt1* regulation (Nusse et al., 1990; Van Ooyen, 1984), initial analysis of the *Xenopus Wnt1* 5' proximal promoter was performed to delineate a functional promoter with luciferase reporter genes (Gao et al., 1994). Attempts in mouse to generate LacZ transgenics which recapitulate the expression pattern of *Wnt1* using 5' proximal regions of the *Wnt1* genomic locus failed to show a repeatable or faithful pattern of expression (J. Mason, unpublished data and (Echelard et al., 1994)). In the mouse, a 5.5kb 3' distal element has been shown to direct the expression of *Wnt1* in the developing CNS (Echelard et al., 1994) which was later remarkably reduced to a highly conserved 110bp element sufficient for driving expression of a reporter in the midbrain and even rescuing the knockout phenotype in this region of the *Wnt1* mutant embryo (Rowitch et al., 1998). This 110 bp element does not drive expression in the developing neural tube, however. The 3' distal enhancer is generally considered the region of major regulatory importance controlling the expression of *Wnt1*.

It should be noted that some studies (Lagutin et al., 2003; St-Arnaud and Moir, 1993) have demonstrated the importance of the *Wnt1* promoter in regulating expression of the gene in forebrain and RA differentiated P19 cells, respectively. This region of the

Wnt1 locus should not, therefore, be excluded *a priori* from an investigation into the regulation of *Wnt1* expression.

Pax3 *and Cardiac Development*

One of the most interesting phenotypes observed in the *Pax3* mutant mouse is the presence of a defect in cardiac development, see (Epstein, 1996) and (Creazzo, 1998) for a general overview. The cardiac defect in the *Splotch* mouse was first observed in 1954 (Auerbach, 1954) and is characterised by failure in the outflow vessels of the heart to properly septate and position over the chambers of the heart. This typically leads to anatomical conditions of the Persisting Truncus Arteriosus (PTA) family or, in less severe examples, Double Outlet Right Ventricle (DORV) (Creazzo, 1998). These defects are identical to those observed in avian models of neural crest ablation, and specifically in those where the ablation is limited to regions of cranial neural crest between mid-otic placode and somite 3 (Van den Hoff, 2000). Similarly, fate mapping neural crest cells in the mouse embryo reveals an important role for neural crest derivatives in the development of the outflow tracts of the heart (Jiang, 2000) .The *Splotch* alleles have been shown to be mutations of the *Pax3* locus (Epstein et al., 1991) and the nature of the mid-gestational lethality in Sp^{2H} homozygous mice was convincingly shown to correlate exactly with the incidence of congenic heart malformation (Conway et al., 1997b) and not with the neural tube related phenotypes demonstrated by these mutants. The immunolocalisation of the *slug* protein (a marker of neural crest, downstream of *Pax3* (Monsoro-Burq, 2004)) in the outflow tracts of the avian heart further supports the hypothesis that neural crest are important in the

proper development of these tissues since *slug* represents a downstream marker of *Pax3* function in avians (Carmona, 2000).

Much work has been done to characterise the nature of this defect. Transgenic rescue of the cardiac malformations in *Pax3* mutants using *Pax3* driven by a promoter specific to the neural tube and not the somites (another major region of *Pax3* expression) (Li et al., 1999) has shown that the cardiac defects observed in these animals is due to the expression of *Pax3* in ectodermally derived tissues (i.e., the neural tube and neural crest). More recent work has precisely labelled the source of cardiac neural crest in the mouse to originate from the neural tube opposite somite two, and for migration to occur from the seven somite stage (~ E9.5). The route of migration of these cells is through pharyngeal arches 3, 4 and 6 and into the developing heart (Chan et al., 2004). In the Sp^{2H} mutant, the number of these cells migrating to the heart and ultimately present in the developing outflow tract (and other neural crest populated structures such as the dorsal root ganglia) is defective (Conway et al., 1997b). Contrasting studies have been performed to assess whether the lack of cardiac neural crest cells reaching the outflow tract of the heart is due to defects in the migratory competence of these cells (Conway et al., 1997a; Epstein et al., 2000) or their proliferative ability (Conway et al., 2000). Reciprocal grafts of cardiac neural crest cells between wild type and Sp^{2H} -/- tissues (Chan et al., 2004) have clearly demonstrated that a mutation in *Pax3* affects both the migrating cells themselves and their ability to navigate in their environment. This finding is in keeping with earlier work (Mansouri et al., 2001) which found that, whilst *Pax3* function seemed to be cell autonomous in the neural tube and somites, its role in neural crest was not. Candidate molecules mediating this defect in cell – cell

communication in *Pax3* mutants include integrins (Bajanca and Thorsteinsdottir, 2002), NCAM (Glogarova and Buckiova, 2004), and versican (Henderson et al., 1997). Given the number of genes the overexpression of *Pax3* in a cell line can alter (almost 300 (Mayanil et al., 2001)), and the range of phenotypes exhibited by Sp^{2H} -/- mice, a complexity of cell autonomy phenotype of this nature is not necessarily surprising.

Could one of the non-cell autonomous features of this defect in Sp^{2H} mice be due to a defect in *Wnt1* signalling due to the absence of *Pax3*? The establishment of *Wnt1* as a direct target of *Pax3 in vivo* would clearly be a significant step towards the resolution of this issue. Interestingly, *in vitro*, the expression of *Pax3* in Saoss cells has been shown to activate the c-Jun-N-terminal kinase mediated non-canonical Wnt signalling cascade (Wiggan and Hamel, 2002), implying that the activation of Wnt signalling in response to *Pax3* need not be mediated by the canonical β-catenin pathway alone.

A further line of evidence suggesting a role for Wnt signalling in the development of the outflow tract of the heart has also recently been reported (Clevers, 2002). In these studies in the mouse, a mutant component of the Wnt signalling pathway, *Dishevelled 2 (Dvl2)*, was shown to have an identical phenotype to the Sp^{2H} homozygote cardiac outflow tract (Hamblet, 2002) with an similar penetrance of ~ 50 – 60% to that previously reported for outflow tract defects in Sp^{2H} mice (Conway et al., 1997b). These mice also exhibited neural tube and somite defects, again reminiscent of the *Pax3* mutation. Further analysis of this pathway revealed that the transcription factor *Pitx2* (Kioussi, 2002) is a target of the *Wnt/Dvl2* pathway in cardiac malformations, and that this transcription factor mediates its response through the regulation of the

G1 growth control genes (Hee Baek, 2003). Two interesting results are reported in the findings of this group. Firstly, *Pax3* expression appears to be unperturbed in *Pitx2* knockouts, suggesting the cardiac phenotype is not due to an indirect effect of *Pax3* misregulation in these experiments and that *Pax3* expression is genetically upstream of these defects. Secondly, *Wnt1* and *Pitx2* expression co-localise in migrating neural crest cells in the 3rd and 4th pharyngeal arches (through which the cardiac neural crest migrate (Chan et al., 2004)) (Kioussi, 2002). This expression domain mirrors the route of the cardiac neural crest in the wild type (Chan et al., 2004).

The regulation of *Wnt1* by *Pax3* in this process could therefore link the cardiac phenotypes of the *Pax3* and *Dvl2 / Pitx2* mutants to a common pathway, and indicate a specific Wnt molecule involved in the developmental processes examined in these papers.

Finally, whilst the *Wnt1* knockout mice themselves do not show any reported signs of cardiac malformations and are largely carried to term, which would argue against the presence of a severe cardiac defect (McMahon and Bradley, 1990; Thomas, 1990), the possible redundancy between *Wnt1* and *Wnt3a* in the development of neural crest may explain this lack of cardiac phenotype in the *Wnt1* knockout animals. Where both *Wnt1* and *Wnt3a* are knocked out (Ikeya et al., 1997), no examination of cardiac outflow tract was reported and these embryos did not survive to term. It is also pertinent to point out that in this study the expression domain of *Pax3* in the hindbrain of *Wnt1* homozygote mutants appears normal, again arguing its position as genetically upstream. In the compound *Wnt1/Wnt3a* mutant it was reduced, however. Whether this reduction in the double mutant reflects the presence of *Pax3* in a downstream

genetic context to *Wnt1* or *Wnt3a*, or whether this is due to the observed reduction in cell proliferation in these mutants was not determined. One group have also reported cardiac defects in mouse embryos injected with *Wnt1* antisense RNA constructs (Augustine et al., 1993).

Subsequently, the following hypothesis was investigated in this thesis:

Hypothesis One

Pax3 up regulates Wnt1 transcription directly, probably through the 3' distal enhancer region, in vivo *during the development of the neural crest.*

Since the beginning of this project, one major paper concerning the development of the cardiac outflow tract in the mouse has been published (Kwang et al., 2002). In this paper a central role for the gene *Msx2* in the development of an outflow tract defect in mice is evidenced. The authors demonstrate that *Pax3* acts as a negative regulator of *Msx2* expression in the wild type. In the Sp^{2H} homozygote an increased level and ectopic expression domain of *Msx2* is reported; the breeding of the Sp^{2H} allele onto an *Msx2* -/- background to generate a compound mutant rescues the heart defect of the Sp^{2H} mutant animal. Interestingly, other neural crest derived structures (dorsal root ganglia, thyroid and thymus) defective in Sp^{2H} homozygotes were not rescued. Similarly, non-neural crest defects observed in *Pax3* mutants (neural tube closure, exencephaly) remained in the compound embryos. The authors conclude that *Msx2* is the principal downstream effector of *Pax3* in the development of the murine outflow tract.

To establish whether *Wnt1* plays a role in the development of the outflow tract it was reasoned that, if *Pax3* can be shown to regulate *Wnt1*, the ectopic expression of *Msx2* in the Sp^{2H} mutant would be hypothesised to have a negative effect on the expression of *Wnt1*. In support of this hypothesis, analysis of *Wnt1* expression (as determined by expression of a *Wnt1*-LacZ reporter gene) on a Sp^{2H} homozygous background illustrates a loss of expression in a population of cells migrating from the neural tube, presumably the neural crest (although it should be noted that no sections are presented in this work at an appropriate level to represent cardiac neural crest) (Serbedzija and McMahon, 1997). Similarly in Sp^{2H} -/- embryos, *in situ* hybridization for *Msx2* transcript illustrates an expansion of *Msx2* expression in the region of the embryo from which the cardiac neural crest would normally originate (Kwang et al., 2002). If a negative interaction between *Msx2* and *Wnt1* could be established, this would provide specific evidence for a role for *Wnt1* in cardiac neural crest development. *Msx2* and *Msx1/Msx2* compound mutants do not display any cardiac defects (Kwang et al., 2002; Satokata, 2000). No experiments examining the expression of *Wnt1* in these mutants was reported.

The following hypothesis was therefore also investigated.

Hypothesis Two

Wnt1 transcription is directly downregulated by Msx2, most probably by the distal 3' enhancer element, in vivo *with implications for the normal development of the cardiac neural crest.*

Hypothesis One and Hypothesis Two are addressed in Chapters 3 and 6 of this thesis.

Pax3 *and Somite and Limb Muscle Development*

Another major area of *Pax3* expression in the developing embryo is in the tissues that contribute to and populate the developing limb musculature. The area of tissue adjacent to the newly formed neural tube, the presomitic paraxial mesoderm (PSM) is induced to bud off into somites during vertebrate development, and this is one of the most easily observed developmental processes. The PSM buds off sequentially to form individual somites in a rostrocaudal wave of development, (see (Buckingham, 2001; Buckingham et al., 2003; Christ and Brand-Saberi, 2002) for a general overview of these processes), with more rostral somites developing first. Somites are staged numerically as they form. For example, a stage IV somite would have three somites caudal before un-segmented mesoderm, a stage XX would have nineteen and so forth. This enables both the staging of somites between different ages and allows comparative analysis of somite development between species.

Sp^{2H} homozygous mutants have severe defects in their hypaxial musculature (Franz, 1993) and the *Pax3* gene has been shown to be expressed in both PSM, developing somites and in the developing limb mesenchyme (Buckingham et al., 2003; Franz, 1993). Clearly many important targets for *Pax3* regulation may exist in these mesodermal tissues.

An overview of somitogenesis is illustrated in Figure 1.6. The PSM buds off to generate the epithelial somite which expands and then, in response to signals from the notochord (Goulding et al., 1994), differentiates into the sclerotome ventrally (characterised by the expression of Pax1 and Pax9 and fated to become skeletal and cartilaginous tissues) and dermomyotome dorsally. The dermomyotome is patterned in response to factors released from the neural tube and ectoderm (Amthor, 1999). As the name would suggest, the dermomyotome constitutes the future cells of the dermis and musculature, and can be separated into the epaxial (medial) and hypaxial (lateral) components. As these structures progress further throughout their development, the myotome differentiates from the dermomyotome to lie between this tissue and the sclerotome, and ultimately generates epaxial musculature (Denetclaw, 1997). At the level of the limb buds, the ventrolateral edge of the dermomyotome generates migrating muscle precursors (which express *Pax3*) which then progress into the limb bud before differentiating into muscle fibres (Tremblay, 1998). It has been suggested that the paraxial mesoderm is an entirely naive tissue, and the dorsoventral and mediolateral patterning events which ultimately generate the sclerotome, myotome and dermomyotome are thought to be generated by multiple, often redundant signals arising from the neural tube, notochord, overlying ectoderm (Dietrich, 1997) and adjacent lateral plate mesoderm (Pourquie, 1995).

Factors regulating Pax3 *in the mesoderm*

Pax3 expression is initially found throughout the PSM (Goulding et al., 1994). Once the epithelial somite is formed, this expression is restricted dorsally by signals emanating from the notochord (Goulding et al., 1994), probably *Shh* in a manner

Figure 1.6

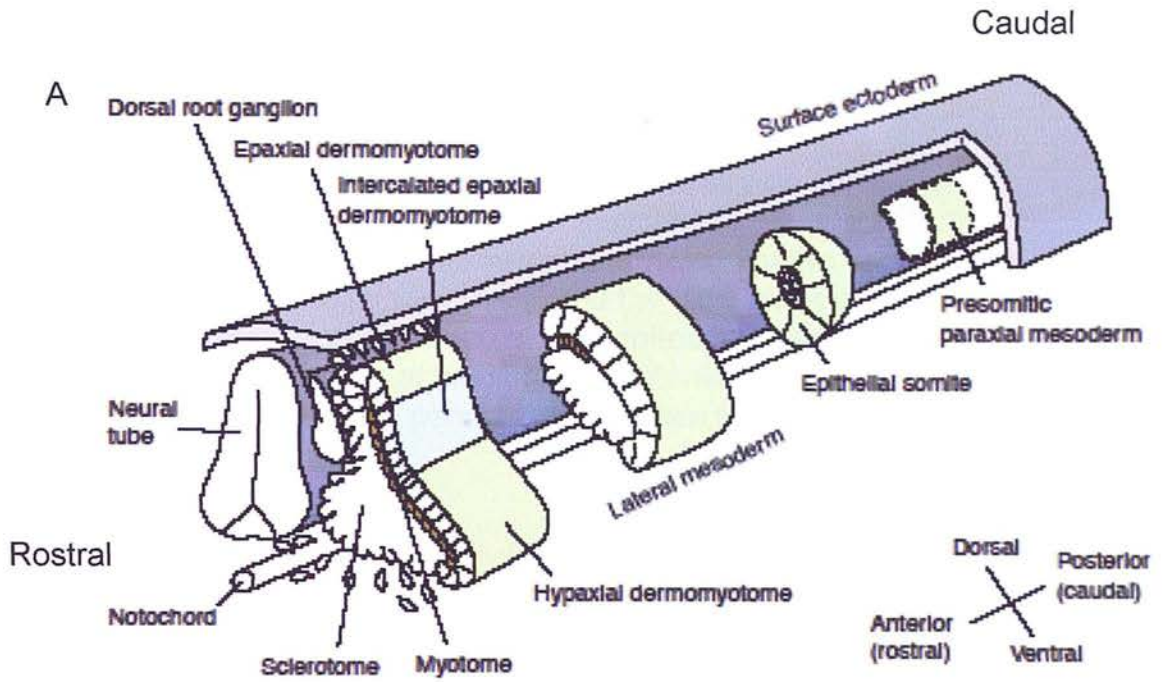

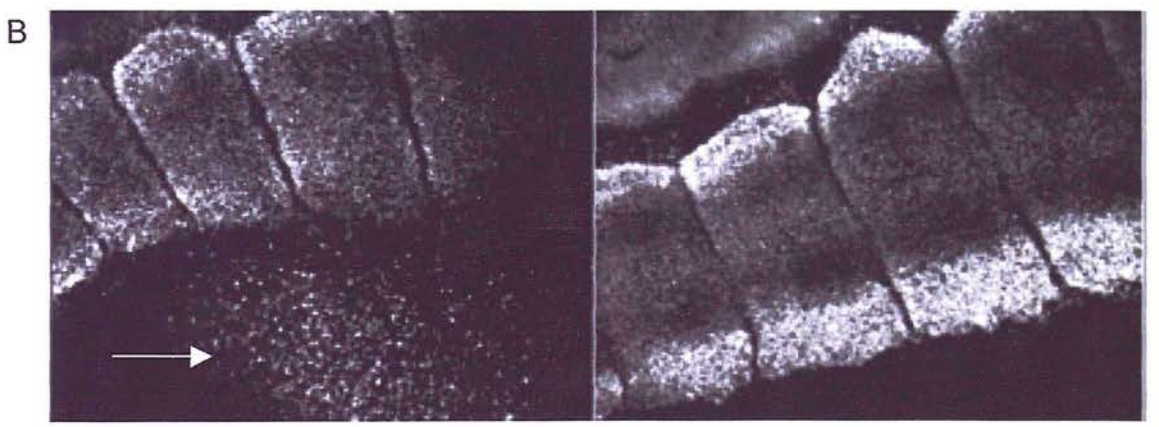

Forelimb level

Interlimb level

Figure 1.6:
A) Schematic representation of somitogenesis. Somites are formed and develop in a rostrocaudal gradient on both sides of the neural tube (Image taken from Buckingham, 2001)
B) Pax3 whole mount immunohistochemistry on chick embryo. Illustrating migration of muscle precursor cells into the forelimb from the ventrolateral edge of the dermomyotome (white arrow), and the high levels of Pax3 expression observed at the ventrolateral and dorsomedial edges of the somite at interlimb levels. Dorsal is up on both panels (Image taken from Venters et al, 2004)

analogous to that in the neural tube (Fan, 1997). The initial induction of *Pax3* is likely to be mediated by BMP signals, specifically *BMP4* from surface ectoderm and this has been shown to be important in the maintenance of *Pax3* in proliferating populations of muscle precursor cells (Amthor, 1999). Sustained *Pax3* expression requires constant exposure to dorsalising signals throughout somitogenesis. Later expression and maintenance of *Pax3* in the somites is also likely to be Wnt dependent, since the expression patterns reported for *BMP4* in the chick embryo would not enable prolonged expression of *Pax3* (Dietrich, 1997). Wnt signals have been shown *in vitro* to induce *Pax3* expression in culture (Fan, 1997), and the Wnt's 1, 3, 3a, 4 and 6 are expressed in the appropriate patterns to induce *Pax3* expression in the somite from dorsal neural tube (*Wnt1*, *Wnt3*, *Wnt3a*, Wnt4) and surface ectoderm (*Wnt4*, *Wnt6*) (Parr, 1993). Ectopic *Wnt1* expression has been shown to up-regulate *Pax3* and other dorsal somite markers (Capdevilla, 1998; Maroto et al., 1997). Furthermore, the downstream components of canonical Wnt signalling (Frz1, Lef and β-catenin) are also present in the presomitic mesoderm and are up-regulated in the dorsal somite where *Pax3* is expressed (Schimdt, 2000).

Contrasting evidence has shown that neither expression of ectopically active β-catenin nor LiCl treatment (which activates the β-catenin pathway) can actually induce the expression of myogenic genes within the somite, however (Chen, 2004). Similarly, the expression of *Lef1* and β-catenin in the somites is restricted to the myotomal compartment as development proceeds, and this expression is dependent upon a *Shh* signal from the notochord (Schimdt, 2000). Given that *Pax3* is not expressed in the myotome, only in the dermomyotome, and that *Shh* signals are repressive to *Pax3* expression in these tissues (Goulding et al., 1994), the maintenance

of this expression by Wnt signals from surrounding tissues seems unlikely to be operating via the canonical signalling pathway alone. A non-canonical Wnt responsive pathway, utilising adenylate cyclase, PKA, and CREB has been shown to both co-localise to *Pax3* expressing dermomyotome and induce *Pax3* expression *in vitro* (Chen, 2004). The specific Wnt signal involved *in vivo* in this system has yet to be identified, although both *Wnt1* and *Wnt7a* were implicated in this study. The lack of somite or dermomyotomal defects reported in the *Wnt1/Wnt3a* compound mutant mice, in spite of their survival to E18.5, suggests that these Wnt's may not be significant *in vivo* inducers of *Pax3* in the mesoderm (Ikeya et al., 1997). (Oddly, *Wnt3a* mutants, however, do demonstrate a defect in somitogenesis, however (Takada, 1994)). The closer proximity of *Wnt7a* in the dorsal ectoderm to the *Pax3* positive dermomyotome would present this factor as a much more attractive *Pax3* inductive signal (Parr, 1993). It is likely that multiple, possibly redundant, signals converge on this process of somatic differentiation, however.

As development proceeds, the expression pattern of *Pax3* changes, as illustrated in figure 1.6B. The later expression of *Pax3* in the dermomyotome exhibits a strong expression in the dorsomedial and ventrolateral domains, with weaker expression in the intermediate regions (Venters et al., 2004). The cells expressing *Pax3* at the ventrolateral lip of the dermomyotome migrate into the developing limb bud (Figure 1.6B, white arrow), and are essential for the later expression of myogenic differentiation markers (i.e. *MyoD*) (Venters et al., 2004; Williams, 1994). Furthermore, the expression of *Pax3* in the developing limb bud has been shown to originate from this migratory population, and is not due to *de novo Pax3* expression in limb mesenchyme by Quail – Chick Chimeras (Williams, 1994).

Pax3 *function in mesoderm*

The roles of *Pax3* in the developing somite and limb bud have been studied by several groups. Measurement of cell proliferation through the incorporation of BrdU into *Pax3* positive cells, as observed by (Amthor, 1998) led to the implication of *Pax3* as a regulator of cell cycle control and the proliferation of the dermomyotome population. Implicit with this is the converse regulation of *MyoD*, a basic helix-loop-helix transcription factor known to signal terminal differentiation of the myogenic lineage in the myotomal compartment (Amthor, 1998). Observations of somite development in the Sp^{2H} and Sp^{d} compound mutant (a Sp^{2H} / Sp^{d} genotype was used to enable the embryos to develop further than the cardiac defect in Sp^{2H} homozygotes would normally allow) are in agreement with this role (Tremblay, 1998). Mutant dermomyotome fails to elongate and organize properly at both the medial and lateral edges implying a defective proliferation or organisation of the cells in this region. This is consistent with the strong bands of *Pax3* expression recorded at these positions in the wild type (Venters et al., 2004). Similarly, the sclerotomal compartments (denoted by *paraxis* expression) and the myotomal compartments (denoted by *MyoD* and *Myf5* expression) are truncated in the Sp^{2H} homozygous mutant (Henderson et al., 1999), indicating a general function in overall somite proliferation for *Pax3*.

Another aspect of the *Splotch* phenotype is attributed to the inability of *Pax3* mutant cells from the dermomyotome to undertake the long-range migration required to populate the limbs at bud level. This can clearly be observed in contrasting *Pax3*-LacZ reporter gene activity at this position between wild type and Sp^{2H} homozygotes

(Buckingham et al., 2003). A study of muscle precursor migration in the Sp^{2H} homozygote reveals that the lack of muscle differentiation genes expressed in the developing limb bud is due to a migratory defect, as assessed by DiI labelling, and not incompetence for dermomyotome precursors to adopt myogenic cell fates since Sp^{2H} -/- somites transplanted into wild type limb buds are competent to express *myogenin* (Daston, 1996).

This migratory defect of dermomyotome derived hypaxial precursors in a *Pax3* null background has been attributed to the loss of expression of the *c-met* transcript in these cells. The *c-met* gene encodes a tyrosine kinase receptor which is necessary for the migration of these precursors in the mouse (Bladt, 1995). No expression of this gene can be detected in the Sp^{2H} homozygote embryo (Daston, 1996) (or detected at massively reduced levels, see (Mennerich, 1998)), and *Pax3* has been shown to both bind and transactivate the human *c-met* promoter in culture via a defined consensus site (Epstein et al., 1996). In support of this interaction, the *c-met* ligand, scatter factor or hepatocyte growth factor (HGF), is expressed in the limb bud under control of signals from both the apical ectodermal ridge and zone of polarising activity and controls the motility and positioning of myogenic precursor cells (and *Pax3* expressing cells in particular) in this tissue (Scaal, 1999). One group have additionally demonstrated expression patterns of specific integrin dimers corresponding to the expression domain of *Pax3* in migrating muscle precursors (Bajanca and Thorsteinsdottir, 2002). This may provide these cells with the extracellular proteins necessary to complete their migration into the developing limb bud. The further observation by this group that the pattern of integrin expression changes on the surface of these cells after the induction of *Myf5*, another marker of terminal

myogenic differentiation, may also indicate a mechanism for changes in cell – cell contacts to reflect the morphological changes adopted by developing muscle fibres (see (Buckingham, 2001) for a review of this later process).

Pax3 is also involved in other regulatory cascades in the developing musculature. The *Six* family of homeodomain proteins are involved in myogenesis, and mutations in the *Six1* gene generates a muscle hypoplasia phenotype which particularly affects the hypaxial muscles (Laclef et al., 2003). Dominant negative *Pax3* expression results in the inhibition of *Six1* and its regulatory co-factor *Eya2* (Ridgeway and Skerjanc, 2001), implying that *Pax3* lies functionally upstream of these factors. In contrast to these findings a recent study generating a *Six1/Six4* compound mutant mouse with an aggravated muscular phenotype has reported *Pax3* and *c-Met* expression to be downstream of *Six* gene regulation (Grifone, 2005). Direct regulatory interactions between *Pax3* and *Six* homeoproteins are not established in these studies and this contradictory evidence has yet to be resolved.

Lbx1 is another important target of *Pax3* regulation and mice harbouring mutations in this gene also demonstrate defects in their musculature, particularly in the more distal hypaxial components (Brohmann, 2000; Gross, 2000). These mice demonstrate normal *Pax3* and *c-met* expression in the dermomyotome (Brohmann, 2000). Sp^{2H} homozygous mice demonstrate no expression of *Lbx1* transcripts and a *Pax3* signal is at least partially required for the expression of this gene in the ventrolateral tips of the dermomyotome (Mennerich, 1998). These studies implicate *Pax3* as a regulator of *Lbx1* in the developing somite.

The expression of *Pax3* in migrating muscle cells is essential for the later expression of myogenic determination genes, and the cells which delaminate from the dermomyotome, under the control of factors such as *Pax3* and *Lbx1*, are thought to be committed to a myogenic fate despite not expressing myogenic markers such as *MyoD* or *Mrf5* (Bober et al., 1994). *Pax3* is essential for the expression of *MyoD*, since Sp^{2H} mutants cannot express this gene in hypaxial muscles, and double *Myf5* / *Pax3* mutants exhibit a total absence of body musculature (Tajbakhsh et al., 1997). Furthermore, ectopic expression of *Pax3* alone in undifferentiated mesoderm is sufficient to cause the expression of *MyF5*, *MyoD* and *myogenin* markers (Maroto et al., 1997). This contrasts with the observations in the somite and migrating muscle precursors that the expression domains of *Pax3* and *MyoD* do not overlap. The observation that in the wild type, *Pax3* expression may determine myogenically fated but undifferentiated cells is of interest. The expression of *Msx1* in the ventrolateral tip of the dermomyotome and *Pax3* positive migrating muscle precursor cells may explain this phenomenon (Bendall et al., 1999). *Msx1* expression in these cells was shown to maintain this population in an undifferentiated state by antagonising the transcriptional activation of *MyoD* by *Pax3*. Even more remarkably, the ectopic expression of *Msx1* in terminally differentiated myotubes can completely repress the expression of *MyoD*, *Mrf4* and *myogenin* and enable clonal populations to be re-differentiated into non-myogenic cell types (Odelberg, 2000). One caveat to the above is the observed ability of somites obtained from a *Pax3* null (Sp^{2H}) background transplanted into a wild type chick limb bud to acquire a myogenic fate, as determined by *myogenin* expression (Daston, 1996). One possible explanation for this is that a second signalling pathway is able to switch on *myogenin* expression in this context,

such as one controlled by *Mrf4*, which may act at least partially independently from the *Pax3/Myf5* specification of muscle cell types (Kassar-Duchossoy, 2004).

Pax3 and Pax7

In the developing mouse, another *Pax* gene, *Pax7*, is expressed in a highly dynamic and specific manner in the neural tube and developing musculature (Jostes et al., 1990). *Pax7* is of particular interest in muscle development due to its importance in the regulation of adult muscle regeneration, which is thought to be partially due to a reprisal of embryonic developmental pathways (Zhao and Hoffman, 2004). In regenerating muscle, a group of muscle derived stem cells can be isolated, and are induced to activate *Myf5* and *MyoD* expression in response to appropriate signals (i.e. damage) through the activation of *Pax7* expression generating so-called satellite cells (Seale et al., 2004). The role of *Pax7* in these adult populations has interesting parallels with *Pax3* in the developing musculature. *Pax7* knock-out animals display a total absence of satellite cells, but do contain a stem cell population within muscle tissues (Seale et al., 2000). In these mutants this population is competent to differentiate into a significantly greater range of cell types than those isolated from wild type mice, indicating that *Pax7*, like *Pax3* in the migrating muscle precursors of the embryonic limb, acts to commit these cells to a myogenic lineage. Interestingly, one group have also noted that differing allelic forms of the *Pax7* homeodomain correspond to differing efficiencies of muscle regeneration, implicating this portion of the protein in the regulation of the myogenic pathway (Kay et al., 1995)

An interesting aspect of this phenomenon with respect to embryonic development is that, in spite of *Pax7* being involved in the regulation of myogenic targets in regenerating adult muscle, *Pax7* is incompetent to replace the myogenic function of *Pax3 in utero* in transgenic mice (Relaix et al., 2004). Since *Pax3* and *Pax7* form a *Pax* gene subfamily, and have almost identical protein sequences across their DNA binding domains, see Figure 1.7, this difference in ability may reflect the transactivatory potential of their C-termini, rather than a difference in transcriptional targets. In keeping with this hypothesis the activation of the *c-met* receptor, essential in migrating muscle precursor cells and a target of *Pax3* induction in the wild type (Bladt, 1995; Epstein et al., 1996), is described as "inefficient" rather than absent in these mice (Relaix et al., 2004). *Pax7* knockout mice also do not demonstrate significant defects in musculature at birth, although a growth retarded post natal phenotype is demonstrated, leading to almost all (97%) of these homozygotes dying within 3 weeks after birth (Mansouri et al., 1996), possibly due to defective muscle regeneration and growth.

Pax3 has been implicated in the regulation of *Pax7* through the observation of expression patterns in Sp^{2H} homozygotes (Borycki et al., 1999). This study shows a clear expansion in the expression pattern of *Pax7* in the neural tube of *Pax3* mutants. Normally, *Pax7* is expressed in dorsal neural tube, but omitted from the roof plate (Jostes et al., 1990). In Sp^{2H} mice, the expression level is higher than in the wild type and includes the roof plate. Similarly, in the somites, the expression of *Pax7* seems to extend from dorsal regions to the ventrolateral lip of the dermomyotome. This would imply a negative regulation of *Pax7* by *Pax3*. In contrast to this, (Relaix et al., 2004) show that *Pax7* does not appear to be significantly over expressed in either the neural

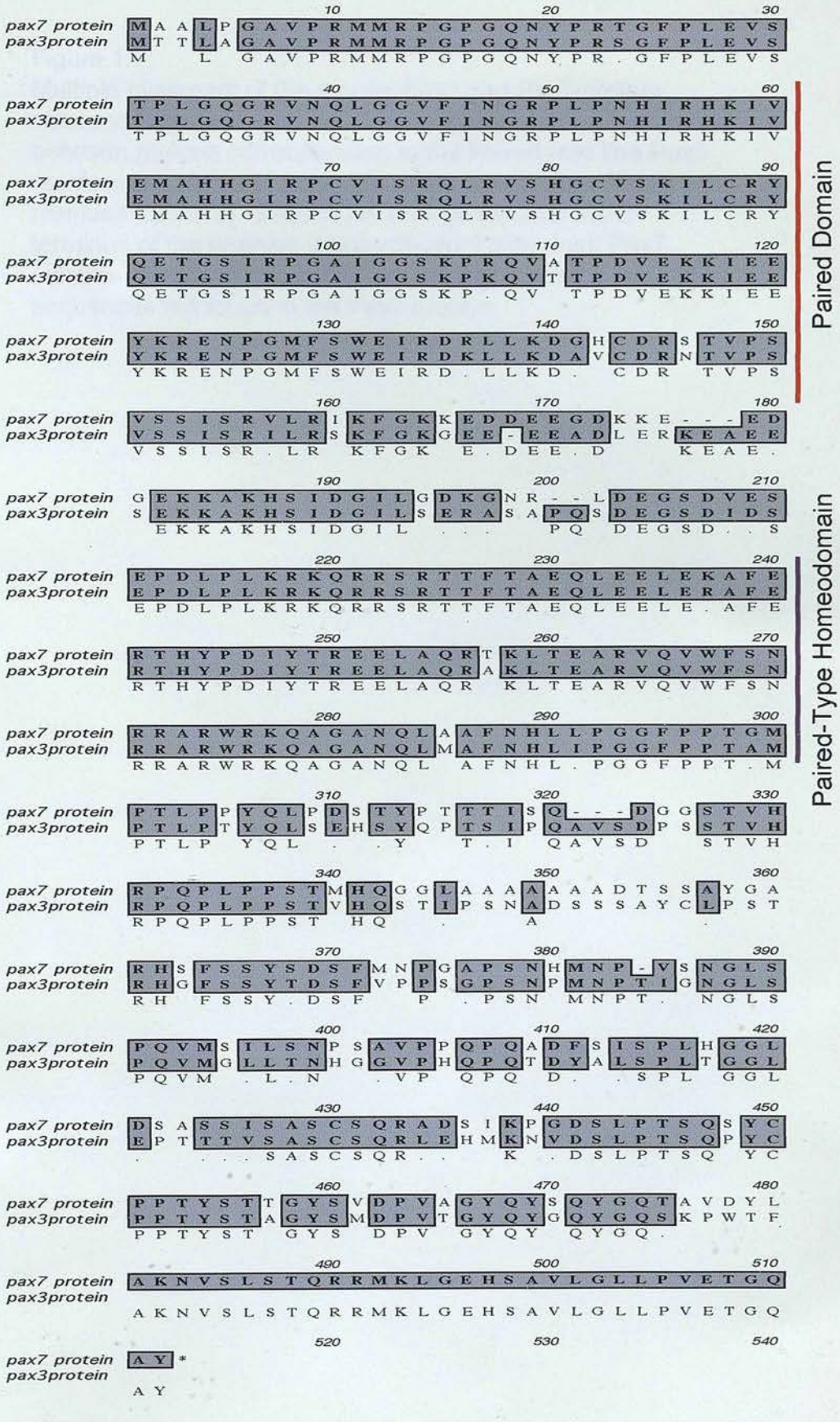
pax7 protein
pax3protein
Paired Domain
Paired-Type Homeodomain

Figure 1.7:
Multiple alignment of the mouse Pax3 and Pax7 protein sequences (N to C-terminal). Note high level of conservation between regions corresponding to the Paired (red line,Pax3 residues 34:162) and homeodomains (purple line, Pax3 residues 228:278). Sequences diverge towards the C-terminus of the proteins (transactivatory domains); Pax7 exhibits an extended C-terminal domain containing residue sequences not found in the Pax3 protein.

tube or somites in the *Pax3* mutant mouse. These investigators attribute this difference to either genetic background or a possible truncated form of *Pax3* expressed from the Sp^{2H} allele interfering with *Pax7* expression. This latter explanation seems unlikely since it would imply a wild type interaction between the genes, and no truncated *Pax3* protein product has yet been reported as expressed from the Sp^{2H} allele. Finally, induction of P19 EC cells to a myogenic cell fate using DMSO, known to induce *Pax3* expression in this line, also induces *Pax7* (Ziman et al., 2001). Whether this effect is dependent on prior *Pax3* expression has not been established. Two very recent studies have indicated that a population of *Pax3 / Pax7* positive cells provide an important of pool of skeletal muscle progenitor cells in both the embryo and the adult, and represent the common origin for satellite cells in mature muscle (Gros, 2005; Relaix, 2005). Such a cell population presents an attractive target for potential therapeutic intervention in muscular diseases and, given the requirement of *Pax3* and *Pax7* co-expression for the proliferation and expansion of this population (Relaix, 2005), any regulatory interaction between these genes may be of interest in this context.

Since no direct regulatory relationship between *Pax3* and *Pax7* has yet been explored in the literature, this thesis will also examine the possibility that *Pax7* represents a direct target of *Pax3* transcriptional regulation.

Hypothesis Three

Pax7 is directly downregulated by Pax3, in vitro *and* in vivo, *via defined regulatory elements and with implications for the development of both neural and mesodermal tissues.*

Hypothesis Three is addressed in Chapters 4 and 6 of this thesis.

In contrast with *Wnt1*, where well-defined *cis*-regulatory elements have been described in the mouse, at the start of this study no investigation into equivalent elements controlling transcription at the *Pax7* locus has been described*. To date four studies have been performed analysing either the transcriptional start site of the human *Pax7* gene (therefore providing an obvious location for a putative minimal promoter) (Schafer et al., 1994; Vorobyov et al., 1997) or the region of genomic sequence 5' proximal to this start site for *cis*-regulatory activity (Murmann et al., 2000; Syagailo et al., 2002). These investigators identified transcripts of varying length at the 5' end, ranging from 664bp (Syagailo et al., 2002) to 60bp (Murmann et al., 2000). This thesis will initially establish a 5' UTR for the mouse *Pax7* transcript, and use this to examine the proximal region of genomic sequence for basal promoter activity. A bioinformatic approach has also been used to try and identify putative functional elements for the mouse *Pax7* gene. The regulatory sequences identified were then assayed for *Pax3* responsiveness and binding both *in vitro* and *in vivo*.

---

* Since the start of this investigation, one paper describing these elements in the mouse has been reported. These data will be considered later in detail, and related to the findings reported here. See **Lang, D., Brown, C. B., Milewski, R., Jiang, Y. Q., Lu, M. M. and Epstein, J. A.** (2003). Distinct enhancers regulate neural expression of Pax7. *Genomics* **82**, 553-60.

Conclusion

The above introduction presents an overview of two major developmental pathways within which *Pax3* is known to play an important biological role, namely the development of neural crest and somites. The identification of two putative targets for direct *Pax3* regulation, and the resulting hypotheses directing much of the experimental work in the following chapters, are also included. This is not intended as an exhaustive review of all *Pax3* functions or previously reported target genes. Another major omission is an increasingly large body of work describing the function of *Pax3* (and *Pax7*) in the development of alveolar rhabdomyosarcomas due to a common chromosomal translocation event fusing the DNA binding domains of these factors to the transactivatory domain of the *FKHR* gene (see (Barr, 2001) for review). Since this reflects a pathological state only, and some groups describe a difference in the sets of target genes regulated by *Pax3* and *Pax3-FKHR* (Barber et al., 2002; Begum, 2005), this fusion protein has not been considered further in this thesis, except where directly relevant.

In addition to the hypotheses described above, the aims of this investigation were to develop a potential methodology for determining new, direct, targets of *Pax3* regulation *in vivo*. The target genes described above were verified and then used as positive controls to verify the application of this methodology *in vivo*. The determination of direct *Pax3* targets *de novo* enables an enhanced understanding of this transcription factor's biological role. It also helps to clarify some of the existing unresolved issues surrounding *Pax3* function that have been generated by the conflicting evidence presented in the past.

Chapter 2: Materials and Methods

Introduction

This chapter will describe the rationale and methodologies behind the techniques used in the following results chapters. The following is intended as a reference to enable both an appreciation of the precise methods used and a starting point for any investigator wishing to reproduce or extend the findings outlined in this thesis. General molecular biology protocols were taken from (Sambrook and Russell, 2005) and adapted where necessary. Where more specialised protocols have been utilised (i.e. QRTPCR) a discussion of the experimental rationale and data treatment has also been included. All protocols referred to in this thesis are described below, unless stated otherwise in the text. Manufacturers instructions have been referred to where appropriate and should be consulted for detailed instructions where necessary. COSHH forms and risk assessments for these methods can be obtained by contacting the University of Edinburgh. Sigma was the supplier of basic reagents and chemicals, unless otherwise stated. Supplier catalogues should be consulted to obtain information for ordering.

Organisms

Bacteria

Escherichia coli (*E. coli*) were used for all steps involving bacteria. Sterile conditions were used throughout, excess cultures were disposed of in 5% Virkon, and glassware washed in 5% Virkon after use. All liquid cultures were grown in 2XTY, shaken at

220 rpm for 16 hours at 37 °C, and inoculated directly from LBA plates (with the exception of Maxi-preps where a 5ml starter culture was inoculated and incubated for 8 hours before being added to the 250ml 2XTY).

2XTY	1.6% Tryptone 1% Yeast Extract 86.2mM NaCl

The following volumes were used for different size cultures throughout the project, depending on the quantity of plasmid DNA required:

Culture Size	**Volume 2XTY**
Mini-prep	1.5ml
Midi-prep	50ml
Maxi-prep	250ml (5ml starter culture)

E. Coli were plated out on LB Agar (LBA) plates. LB was made using LB tablets (Sigma) and Agar added to 1%. This was then autoclaved to sterilise and 10cm plates poured (using appropriate antibiotic) before cooling.

Antibiotics

The antibiotics used in this thesis were Ampicilin and Kanamycin as appropriate. Ampicillin was used at a final concentration of 1000 μg / ml. Kanamycin was used at a final concentration of 500 μg / ml.

Mammalian Cell Culture

Cell lines

Two cell lines were used in this thesis, and were ordered from ECACC. These were C2C12 (91031101) and NIH-3T3 (93061524). They were both maintained as described below.

Maintenance

All mammalian cell lines were maintained in sterile conditions, according to Class II procedures. Waste cultures and glassware were washed in 5% Virkon after use. Cells were grown at 37 °C and 5% CO_2, in a humidified incubator. All cell lines were grown to ~70% confluence (monitored by microscopy and estimated) before being routinely passaged:

1) Wash cells in 1X PBS (Phosphate Buffered Saline, Invitrogen)
2) Add 5ml 1X Trypsin-EDTA (Invitrogen)
3) Incubate at 37 °C for 5 minutes
4) Remove cells from incubator and ensure they have detached from flask
5) Add 5ml full growth medium
6) Take 1ml cell suspension and add to 30ml fresh growth medium in a new T75 Tissue Culture flask (Grenier)
7) Replace in incubator

Growth Medium (Invitrogen)	440ml DMEM-N12 1X glycine 1X Penicillin / Streptomycin 10% Foetal Calf Serum (FCS)

Mouse Colony

CBA x C57BL/6F1 mice were maintained as according to Home Office regulations, on site, in a dedicated facility. Several breeding pairs were held over the course of the project, constituting one male heterozygote and one female wild type. The *Splotch* mutation is characterised by a white belly spot in the heterozygote. Only offspring carrying a white belly spot were kept, after we had confirmed by PCR genotyping strict concurrence of belly spot phenotype with a splotch heterozygous genotype.

Mouse Embryos

Mouse embryos were obtained by mating male and female mice, and observing vaginal plugs. Observation of a plug was taken as Embryonic Day 0.5 (E0.5), and litters were dated accordingly. Litters were collected on the day specified in the experimental protocol by anesthetising the mother, performing cervical dislocation and dissecting the embryos. Further embryo dissection was performed as described, using a dissecting microscope.

Genotyping of Mice

Genomic DNA was extracted from tails (adult) or amniotic sac (embryos) for PCR genotyping as described below.

Nucleic Acids

DNA Extraction

Plasmid

Plasmid DNA was extracted from bacteria using Qiagen mini, midi, or maxi-prep kits at the volumes described. DNA was then restricted to confirm the nature of the plasmid and quantify yield before any further experiments were undertaken.

PAC (P1 Artificial Chromosome)

Bacteria carrying PAC constructs were grown in 2XTY using 50% kanamycin, and incubated at 37 °C for 16 hours. PAC DNA was extracted as follows:

1) Spin cultures down at 6,000 rpm, 15 minutes, 4 °C
2) Re-suspend in 7.5ml solution PAC1
3) Add 7.5ml solution PAC2
4) Invert gently 4-6 times
5) Incubate at RT for 5 minutes
6) Add 7.5ml solution PAC3, agitating gently
7) Invert 4-6 times
8) Incubate on ice for 5 minutes
9) Spin at 10,000 rpm for 10 minutes at 4 °C
10) Place tubes on ice, transfer the supernatant to a fresh tube by filtering through gauze
11) Add 20ml isopropanol
12) Incubate on ice for 5 minutes
13) Spin at 10,000 rpm, 15 minutes at 4 °C
14) Wash twice in 70% ethanol, spinning for 5 minutes to recover
15) Air dry pellet
16) Re-suspend in 500µl ddH_2O

Solutions:

PAC1	15mM Tris-HCl (pH 8.0) 10mM EDTA 100µg/ml RNaseA
PAC2	0.2M NaOH 1% (w/v) SDS
PAC3	3M K.OAc (pH 5.5)

Genomic DNA

Genomic DNA was extracted from mouse tail tips (adults) or amniotic sac (embryos) for genotyping as follows:

1. Add proteinase K (100mg/ml) to TTLB
2. Add 500µl of this to each sample
3. Incubate at 55 °C for 16 hours
4. Vortex and spin for 15 minutes at 13,000 rpm
5. Pour off supernatant into tubes containing 500µl isopropanol
6. Mix gently and spin at 13,000 rpm for 5 minutes
7. Discard supernatant
8. Dry at 37 °C for 30 minutes
9. Add 250µl ddH2O, shake for 30 minutes at 55 °C
10. Add 250µl PCIA, vortex and incubate at RT for 5 minutes
11. Spin 13,000 rpm for 5 minutes
12. Remove upper layer into new tubes
13. Precipitate DNA as described
14. Re-suspend pellet in 100µl ddH_2O

TTLB	1% SDS (w/v) 10mM Tris-Base, pH7.4 1mM EDTA

PCR genotyping was then performed using primers P3GENOL/R, 1.5mM $MgCl_2$, on program 60^30 (see PCR section for a description of this nomenclature). Products of 127bp (wild type allele) and 95bp (Sp^{2H} allele) were resolved using a 2.5% agarose gel and ethidium bromide staining. Heterozygotes were identified by a doublet.

RNA Extraction

RNA was extracted from both cell cultures (70-80% confluence) or embryos (E9.5 – E12.5, various) using several different techniques. These are outlined below.

Trizol

Trizol (GibcoBRL) was used to extract total RNA from both cells and embryos according to manufacturer's instructions. This is a Phenol-Chloroform based protocol.

RNeasy Mini

RNeasy Mini kits (Qiagen) were used to extract total RNA from cell cultures according to manufacturer's instructions. This is a column based protocol for small quantities of starting tissue.

RNeasy Midi

RNeasy Midi kits (Qiagen) were used to extract total RNA from embryos, according to their weight and manufacturer's instructions. This is a column based protocol for larger quantities of starting tissue (i.e. whole embryo RNA)

mRNA

A Micro-FastTrack 2.0 Kit (Invitrogen) was used to isolate mRNA specifically from both cell cultures and embryos, according to manufacturer's instructions. This is a column based protocol, using oligo (dT) cellulose to specifically isolate mRNA from tissues.

NP-40 isolation of cytoplasmic RNA

To isolate cytoplasmic RNA, excluding hnRNA, NP-40 Lysis Buffer protocol was used on cell cultures as follows (based on one 70-80% confluent T75 flask of cells):

1) Trypsinise cells (as above)
2) Spin at 1,000 rpm for 5 minutes at RT
3) Wash in 1X PBS
4) Spin at 1,000 rpm for 5 minutes at RT
5) Re-suspend pellet in 400µl NP-40 Lysis Buffer
6) Transfer to an Eppendorf and spin at 13,000 rpm for 2 minutes at 4°C
7) Transfer supernatant to a new Eppendorf, discarding the pellet of cell nuclei
8) Add 400µl phenol, 50µl 10% (w/v) SDS
9) Vortex
10) Incubate at RT for 5 minutes
11) Spin at 13,000 rpm for 5 minutes
12) Transfer aqueous phase to a new tube
13) Precipitate RNA
14) Re-suspend in 50µl ddH_2O

NP40 Lysis Buffer	150mM NaCl 10mM Tris-HCl (pH7.4) 0.5% NP40 (w/v) 1mM $MgCl_2$

DNA / RNA precipitation

DNA and RNA were precipitated using ammonium acetate. The following general protocol was used for a given volume *n* of nucleic acid:

1. Add 0.4 x *n* 5M NH_4.OAc, pH5.5
2. Add 2.5 x *n* 100% ethanol
3. Vortex
4. Spin at 13,000 rpm for 30 minutes at 4 °C
5. Discard Supernatant
6. Wash in 75% ethanol
7. Spin at 13,000 rpm for 10 minutes at 4 °C
8. Air dry pellet
9. Re-suspend in appropriate volume of ddH_2O

DNA Quantification

Plasmid DNA was quantified using agarose gel electrophoresis and comparing to a known quantity of ladder DNA. Ethidium bromide and an UV transilluminator, in conjunction with imaging software, were used. DNA would be linearised by restriction digest and the band intensity, quantified by the software, compared to that of a band on a DNA ladder of known concentration. Every six months the accuracy of the equipment would be tested using serial dilutions of ladder and linearised plasmid of a concentration specified by a supplier to ensure operating range and accuracy.

RNA Quantification

RNA was quantified using an UV spectrometer by measuring the absorbance at λ = 260 nm.

DNA Sequencing

DNA was sequenced using the MWG Sequencing Facility (http://www.mwg-biotech.com). Briefly, plasmids were precipitated as described (1μg per sequencing reaction) and posted off for sequencing. Primers used in the sequencing reactions were either supplied by MWG-Biotech or defined as required to extend sequencing runs, and synthesised by MWG-Biotech for sequencing on-site.

Agarose Electrophoresis

DNA and RNA were routinely separated using agarose electrophoresis. Low melting point agarose was dissolved by boiling in 1X TBE. Ethidium Bromide (at 10μg/ml) was added to 1μl/ml TBE-Agarose. Gels were left to set (~30 minutes) at RT before being covered in 1X TBE, samples loaded, and electrophoresed at 45mA/cm for varying amounts of time.

Polyacrylamide Electrophoresis (Denaturing)

DNA and RNA were routinely separated using denaturing polyacrylamide electrophoresis. 6% polyacrylamide gels containing 8M Urea were made to as follows:

Acrylamide Gel Mix	1X TBE 15% Acrylamide / Bis-acrylamide (40% mix) 8M Urea

20cm glass plates designed to fit in a BioRad Protean II electrophoresis system were cleaned, and the outer plate inner surface coated in RepelcoteVS (BDH). The plates were then assembled using 1mm spacers and a comb of appropriate size. A 10% (w/v) ammonium persulphate solution was then made, and 1ml added to the acrylamide gel mix to remove oxygen from solution (this is inhibitory to the polymerisation reaction). 100 µl of TEMED (N,N,N',N'-Tetramethyl-1,2-diaminomethane) was then added to initiate the radical based polymerisation. The gel mix was then poured between the plates, with care to avoid bubbles, and allowed to set. Gels were run in 1X TBE at 450 V for 2.5 hours, fixed in a solution of 5% acetic acid and 15% methanol for 15 minutes, and dried under vacuum overnight prior to exposure to X-ray film.

Cloning

Throughout the thesis several cloning strategies have been employed to manipulate DNA for various experimental purposes. The following is a general description of the techniques involved in every case. Specific cloning strategies can be found in the

results chapters pertaining to specific constructs. A full list of all DNA constructs made in this thesis and their cloning strategies can be found in Appendix 1.

Restriction Digests

Restriction enzymes were typically obtained from New England Biolabs (NEB), Promega or Fermentas, dependent on availability. Digests were conducted at 37 °C (unless the enzyme was active at a different temperature) for one to two hours. A general protocol for a single digest was as follows:

Digest of 20 µl	2 µl 10X Reaction Buffer 2 µl 10X BSA 1 µl Enzyme (10 units) n µl DNA (required µg quntitiy) (20 - (5 + n)) µl ddH_2O

Reaction buffer at 10X was supplied by the manufacturer, 100X BSA was supplied by the manufacturer and made to 10X fresh for each digest with ddH_2O. Whilst digest volumes and quantities of DNA were altered as required, all digests were scaled according to the above and the final concentration of total enzyme never exceeded 10% of the reaction volume.

Phosphatasing to remove end phosphate groups

Shrimp Alkaline Phosphatase (SAP, Roche) was used to phosphatase nucleic acids as according to the manufacturer's instructions. Phosphatasing was used either to

prevent open vectors from self-ligating if that were a possibility, or to remove end phosphates from a DNA ladder to enable kinase radiolabelling in Primer Extension or RPA protocols.

Kinasing

T4 Polynucleotide Kinase (NEB) was used to add phosphate groups to nucleic acids according to manufacturer's instructions. For radiolabelling, $^{32}P\gamma$-ATP (Amersham) was added to the reaction mixture (quantities described for each protocol, below).

Ligations

Ligations were performed using T4 Ligase (Promega). T4 Ligase buffer was separated into 10 µl aliquots and a fresh aliquot used for each ligation reaction. Ligations were generally set up as follows:

Ligation Reaction 20µl	2 µl 10X T4 Reaction Buffer 1 µl T4 Ligase (10 units) x µl Insert (required µg) y µl Vector (required µg) (20 – (3 + x + y)) µl ddH_2O

Quantities and ratios of vector and insert were determined empirically and were often a range within a given set of ligation experiments. Ligations were conducted at 16 °C for 16 hours before being transformed into competent *E. coli* as described and plated out on LBA with the appropriate antibiotic selection.

TOPO-cloning

A major method of creating plasmid clones of PCR products used in this thesis utilised a topoisomerase method rather than conventional ligase based cloning. These protocols used a range of vectors from Invitrogen where a topoisomerase enzyme is cross linked to an open vector designed to facilitate the rapid and efficient recombination of different PCR products before further cloning steps. Often these vectors were intermediates to enable more efficient downstream cloning steps or to enable rapid sequencing screening before further manipulation. The vectors used were as follows:

PCR Product Type	**TOPO vector used**
Taq amplified, 3' A overhang	pCR-II-TOPO-TA
Pfu amplified, no overhang	pCR-II-TOPO-Blunt
Large product (> 2 kb)	pCR-II-XL-TOPO

For detailed protocols, see manufacturer's instructions.

Heat-Shock Transformation

Plasmids and ligations were transformed into super competent (10^9 colonies μg^{-1} plasmid DNA). Top-10 *E. coli* (Invitrogen) using the heat shock protocol (at 42 °C) specified in the manufacturer's instructions. Bacteria were then plated out on LBA with the appropriate antibiotic and incubated overnight at 37 °C.

PCR (Polymerase Chain Reaction)

PCR was used widely throughout this thesis. The following describes the general conditions used for every reaction, methods of optimisation typically used where this was required, followed by the notation used to define experimental conditions in each specific reaction. Primers were designed using MacVector 7.2 software. The names of primers used in each reaction are given in the results chapters; a table of all primers used and their sequences can be found in Appendix 2.

PCR Reaction Conditions

All PCR reactions used the following basic set of conditions, reagents were generally supplied by Promega and primers synthesised to order by MWG-Biotech.

PCR Reaction Mix	2.5 µl 10X Reaction Buffer x µl 25mM $MgCl_2$ 1.25 µl 5' Primer (10µM) 1,25 µl 3' Primer (10µM) 1 µl dNTP mix (Promega) y µl DNA Template (required µg) 0.5 µl Taq Polymerase (5 units) (25 – (x + y)) µl ddH_2O
PCR Program	Step 1 : 1 Minute at 95 °C Step 2 : 1 Minute at 95 °C Step 3 : 30 Seconds at T_m Step 4 : 1 Minute at 72 °C Step 5 : Go To Step 2 n Times Step 6 : 10 Minutes at 72 °C Step 7 : 4 °C Forever

The variations to this protocol specific to each reaction were T_m (annealing temperature for Primer and template) and the number of cycles (n). These are annotated throughout as T_m ^ n (i.e. 55^35 would denote a T_m of 55 °C and 35 cycles of amplification). All reactions were optimised to have identical reaction conditions otherwise.

PCR Optimisation

PCR reactions were optimised using the above basic reaction program and by varying the concentration of $MgCl_2$ between 0.5mM and 2.5mM and T_m spread over the mean average predicted by the software used to design the primers. The T_m, cycle number, and [$MgCl_2$] used in each reaction are specified where relevant, although it is the experience of this investigator that PCR reaction conditions are generally indiosyncratic to the specific equipment, reagents and source material used. Independent optimisation of conditions should be anticipated in every case.

TEPCR

Template Enriched PCR (TEPCR) was used to clone from DNA where conventional, restriction digest mediated cloning was difficult. This protocol uses high concentrations of template and primers, combined with low PCR cycle number, to maximise product concentration in the final reaction mix. It was reasoned a lower cycle number would minimise the number of mutations generated by the polymerase

during the amplification cycle and therefore the number of colonies screened before an appropriate clone was found. Typically 10 – 15 cycles were used in each case.

RTPCR

Reverse Transcriptase PCR (RTPCR) was performed in a number of experiments. This technique uses the RT enzyme to generate a cDNA copy of mRNA which can then be amplified using gene specific primers. In each experiment, RNA was isolated using one of the methods described, quantified, and subjected to an RT step using SuperScript III Reverse Transcriptase (Invitrogen), as per the manufacturer's instructions. PCR steps were then conducted on the cDNA template as previously described, product confirmed by agarose electrophoresis, and where necessary, cloning and sequencing. No RT controls were included where appropriate, and when possible primers were designed to span introns to control for contamination from genomic DNA.

QRTPCR

To enable the repeatable and rapid quantification of levels of transcript between wild type and mutant embryos, Quantified Reverse Transcriptase PCR (QRTPCR) was used (for a review see (Bustin, 2000)). In this method the incorporation of a fluorescent dye into PCR product is measured over the course of a PCR reaction. Since the dye fluoresces only when it intercalates into dsDNA (in a mechanism analogous to ethidium bromide), the level of fluorescence observed in a sample is

linearly proportional to the quantity of DNA of a given range of product sizes (>250bp). Since these samples were cDNA's synthesised from DNase treated total RNA preparations, and since all no RT controls performed during the PCR steps of this protocol were negative, the only dsDNA available for the incorporation of fluorescent dye must be PCR product derived from the amplification of cDNA. The following derivation has been adapted and simplified from (Livak and Schmittgen, 2001).

In the linear phases of a PCR reaction, the quantity of product after n cycles, X_n , is related to the quantity of starting material X_o by the relationship:

$$X_n = X_o \times (1 + E_X)^n$$

Where E_X represents the efficiency of amplification of product X in the reaction (i.e. if the efficiency was 100% $E_X = 1$, $(1 + E_X)^n = 2^n$ or a doubling every cycle).

If the level of fluorescence after n cycles, F_n, is directly proportional to X_n (i.e. $F_n \alpha X_n$) then it follows:

$$F_n / c.(1 + E_X)^n = X_o$$

Therefore, for any samples where E_X is equivalent, a measurement of F_n at cycle number n is equivalent to a measure of the quantity of starting material in that sample. Conversely, a difference of F_n after the same number of cycles in two different

samples (where E_x is equivalent) is a measure of the difference in amount of starting material between those samples.

To ensure that E_x is invariant between reactions, a plot of the difference of the number of cycles required to reach a given level of fluorescence against the difference in concentration of starting product must be linear. If

$$F_1 / c.(1 + E_1)^n = X_1 \text{ and } F_2 / c.(1 + E_2)^n = X_2$$

Then

$$X_1 - X_2 = F_1 / c.(1 + E_1)^n - F_2 / c.(1 + E_2)^n$$

If

$$E_1 = E_2$$

Then

$$k.\Delta X = \Delta F$$

Where k = amplification constant $c.(1 + E_2)^n$.

Experimentally this can be tested by a dilution series of cDNA (X) against fluorescence (F) after *n* cycles. If this plot is linear then the efficiency of PCR

amplification is identical across that range of cDNA concentrations, and then the measurement of fluorescence can be interpreted as an indicator of quantity of starting material.

The purpose of the QRTPCR experiments conducted in this thesis was to determine the difference in quantity of mRNA of each product between wild type and mutant embryo samples. This was performed in the following manner.

Firstly, two Sp^{2H} +/- were mated to generate embryos which were genotyped using PCR as described, and Sp^{2H} +/+ and Sp^{2H} -/- E9.5 sibling pairs used in the experiments. Total RNA was extracted and quantified as described, and equal quantities of RNA were used in three separate RT experiments for each embryo (with one –RT for each embryo). These replicates control for variation in cDNA synthesis from each sample.

For each of the genes analysed (i.e. for each PCR), a series of dilutions for the wild type samples were performed, from 1.0 µl of cDNA to 0.01 µl of cDNA. This generates a plot of concentration of cDNA vs. Fluorescence observed after *n* cycles (cycle threshold). In every case this was linear, showing that amplification efficiencies were identical over this concentration range.

This also generates an standard curve of arbitrary units where the wild type samples are set at 1 (undiluted). Each of the three +RT reactions from the wild type and mutant embryos are then interpolated off of this graph, at this cycle threshold, to show the relative amounts of starting material present in the cDNA.

Each sibling pair generates 18 readings. Three sets of 6 readings for each of these genes analysed, namely GAPDH, *Wnt1* and *Pax7*. For each gene, there are 3 wild type and 3 mutant readings. Variation between these replicates is a measure of the variability of the production of cDNA from the RNA samples, samples where the variation was high were excluded from the final data pool.

Four sibling pairs were analysed in this way and contributed to the final data pool. Mean averages of the level of expression of each transcript in the Sp^{2H} mutants were expressed as % of wild type expression.

i.e. wild type = ~1.0 or each gene (since we are quantifying relative expression from the standard curve generated by serial dilution of wild type cDNA), and mutant = < 1.0 if the transcript is less represented than the wild type or > 1.0 if more abundant in the mutant.

This method does not simply normalise by the value obtained for GAPDH but tests to ensure GAPDH transcript levels remain unchanged. If this is the case, any changes in transcript levels observed have been assumed to be real.

Total RNA was extracted from littermate wild type and Sp^{2H} -/- embryos as described, and quantified. Identical μg quantities of RNA were then subjected to an RT step (above) and the cDNAs then used with QuantiTect SYBR Green reagent (Qiagen) in PCR reactions on an Opticon single wavelength PCR machine and data analysed using the Opticon Monitor software. Dilution series were performed for all genes

analysed to ensure linearity of response across a concentration gradient, and to enable relative quantisation of each transcript. All reactions were run on the program 55^40, and [$MgCl_2$] 1.5mM. Amplicons were all < 250bp to ensure linearity of SYBR Green incorporation (i.e. c is identical between all reactions, Qiagen), and melting point curves were examined to ensure the specificity of each reaction. Levels of Sp^{2H} -/- transcript expression were expressed as % of wild type, and GAPDH was used a normalising control.

Site Directed Mutagenesis

Mutation of the core Pax3 binding consensus was performed using the QuikChange Site Directed Mutagenesis Kit (Stratagene) according to manufacturer's instructions. Briefly, this protocol uses primers carrying the desired mutations to anneal to the unmutated sequence on the plasmid of interest. A *Pfu* polymerase then extends the primers around the plasmids on both strands, generating nicked, non methylated complementary strands. The parental DNA (methylated) is then digested away with the DpnI enzyme leaving only the new, mutated strands. These are then annealed and transformed into *E. coli* as described above.

Primers used were W1_sub_FWD/REV in conjunction with the pW1P(1.2)Luc plasmid and P7_sub_FWD/REV in conjunction with the p1.5I1RLuc plasmid. Colonies were grown up and plasmid DNA extracted for sequencing, as described, to confirm the substitution of the Pax3 core consensus site.

Primer extension

Primer extension was used to size the 5' Untranslated Region (UTR) of the *Pax7* mRNA, a diagrammatic representation of this method can be seen in Chapter 4 (Figure 4.3A). Briefly this method employs a radiolabelled primer which anneals to a known sequence within the transcript of interest (i.e. *Pax7* coding exons) and is then used by the RT enzyme to prime a cDNA extension to the 5' end of the mRNA. Since the primer is first kinase labelled with ^{32}P at the 5' end, this can be visualised on a denaturing poyacrlyamide gel against an ssDNA ladder (also radiolabeled). This enables the 5'UTR of the transcript to be sized.

Total and messenger RNA was extracted from C2C12 (*Pax7* positive) cells and embryos as described above. This was quantified and 8μg RNA used in each extension step. Primers were ordered from MWG-Biotech (detailed in Chapter 4 and Appendix 2) and 100 pmol kinase labelled with ^{32}P γ-ATP at 3000 Ci/mMole using the T4 polynucleotide kinase protocol. Labelled primer was then separated from unincorporated ^{32}P γ-ATP by application of the reaction mix to a G-25 size exclusion column (Amersham). Purified, labelled primer were then frozen and equal quantities used in each extension experiment.

8 μg of RNA was then placed in the following reaction mix:

Extension Mix (uses SuperScript RT (Invitrogen) reagents)	8 μl $MgCl_2$ (25mM) 4 μl 10X Reaction Buffer 4 μl dNTP mix (Promega) 1 μl RNase OUT (Ambion) n μl RNA (8 μg)

	(35 – (17+ n)) µl ddH_2O

This was then heated to 70 °C for 10 minutes to denature RNA secondary structure and then snap cooled on ice for 5 minutes. 4 µl Labelled Primer was then added and the mixture incubated at RT for 5 minutes to allow primer – RNA complexes to form. 1 µl SuperScript III RT (Invitrogen, final reaction volume 40 µl) was then added and the mixture incubated at 55 °C for 45 minutes. Reactions were then stopped by heating to 100 °C for 5 minutes. Samples were then boiled in Formamide Loading Buffer II (Ambion) and analysed by running on a 1mm thick 6% polyacrylamide 8M Urea denaturing gel (see above). A DNA ladder of pBR322 (MspI, NEB) was phosphatased using SAP (Roche) and then kinase labelled using ^{32}P γ-ATP as described. This was used to size the primer extension fragments.

The gels were ran for 2.5 hours at 450 V and then fixed in a solution of 5% acetic acid and 15% methanol in ddH_2O for 20 minutes. The gels were then dried overnight under vacuum, and exposed to X-ray film (Kodak) for 12, 24, 48 and 72 hours at –80 °C in an imaging cassette.

5'RACE

To further examine the *Pax7* transcript, 5' RACE (Rapid Amplification of cDNA Ends) was used to amplify, clone and sequence the 5'UTR. This methodology uses a set of gene specific primers and a set of primers complementary to sequences annealed to the 5' end of the transcript to perform nested PCR and amplify the 5'UTR of the gene. Oligonucleotides of known sequence are generally annealed to the very

5' end of the mRNA or cDNA. The precise method by which this occurs differs from protocol to protocol, and is described below. Once these linker sequences have been annealed, PCR or RTPCR (depending on whether the linkers anneal to the mRNA or cDNA population) can then be used to specifically amplify the gene of interest.

The SMART RACE cDNA amplification kit was used in the first instance (Clontech). In this protocol total RNA is extracted from the source of interest (in this instance C2C12 or wild type E11.5 embryos) and an RT step performed with an enzyme blend designed to leave an oligo-C overhang at the very 3' end of the cDNA. This is then used to anneal a primer containing an oligo-G 5' end with a 3' known sequence. The RT enzyme then switches templates and extends along this new primer, generating a cDNA with a known 5' sequence. This population of cDNA's can then be used in a conventional nested PCR reaction using gene specific primers to isolate and sequence the 5'UTR required.

Due to the seemingly foreshortened nature of many of the 5'RACE clones isolated with the above method when compared to the primer extension data (see Chapter 4), a second method of performing 5'RACE was then utilised to try and exclusively select for full length transcripts. A FirstChoice RACE-Ready cDNA kit (Ambion) was used. This method selects for full length 5'UTR's by exploiting the 5' terminal 7-methylguanine cap present only on full length mRNA's. Firstly, a phosphatase activity is used to remove phosphates from any RNA species without a 5' cap (i.e. those partially degraded). Next the 5' cap guianine is removed from full length mRNA molecules. This generates a population of RNA's in which only those which were full length will have a 5' phosphate moiety capable of accepting the ligation of

an RNA primer of known sequence to the 5' end of the transcript. Thus a population of mRNA's with a 5' end of known sequence are generated. This is then used in an RTPCR reaction with primers designed against this sequence and within the gene of interest to amplify and clone the 5'UTR.

Cytoplasmic RNA was isolated from C2C12 cells of wild type embryos, and quantified, as described. Gene specific primers were designed using MacVector, and the 5'RACE followed according to the manufacturer's instructions. PCR products were TOPO cloned and sequenced using MWG-Biotech. Sequences were aligned to the genomic using a CustalW local alignment.

Ribonuclease Protection Assay (RPA)

RPA analysis was employed to further analyse the *Pax7* 5'UTR. RPA utilises a radio labelled antisense RNA probe against the sequence of interest (see figure 4.5A) to anneal to the mRNA. This forms an RNA-RNA duplex where the sequences are complementary. RNase is then used to digest away un-annealed RNA and probe sequences, leaving a probe – target complex intact. These are then purified and run out on a denaturing polyacrylamide gel. Since the probe sequence is known (and overlaps with the coding sequence of *Pax7* at one end), this can be used to size the 5'UTR accurately. Since the probe was designed to cover the UTR's predicted by both primer extension and 5'RACE it was hoped that this method might help resolve differences between the 5'UTR's predicted by PEXT and 5'RACE for *Pax7*.

A probe was cloned into a vector containing an SP6 promoter in the appropriate orientation (see Chapter 4). This was linearised at a final concentration of 0.5μg/μl and *in vitro* transcription performed with the MAXIscript *in vitro* transcription kit (Ambion) according to manufacturer's instructions and using ^{32}P α-UTP at 800Ci/mmol as the radiolabel. Probes were then subjected to DNaseI digestion and a G-25 size exclusion column used to purify as described previously. Probes were then run out on a 6% acrylamide gel and exposed to X-ray film for 1 hour to position within the gel. Full length probes were then extracted overnight into buffer.

RNA was then extracted from C2C12 cells (cytoplasmic RNA) or E11.5 wild type embryos (total RNA) and quantified. 5μg of RNA was used in each RPA reaction and this was made up to 50μg RNA using yeast tRNA (a negative control reaction using *Pax7* negative NIH-3T3 was also performed). Hybridisation was conducted using the HybSpeed RPA kit (Ambion) according to manufacturer's instructions. Samples were then treated with RNase and protected fragments separated on a denaturing polyacrylamide gel, as described. Fragments were sized using pBR322(MspI) kinase – labelled ladder as before, fixed, dried and either exposed to X-ray film for two weeks or to a phosphorimager.

PAC Library Screen

A mouse PAC genomic library was utilised to clone the mouse *Pax7* genomic locus. PAC clones can carry up to 150kb of insert and, given the size of the *Pax7* genomic region (figure 4.1A), these were deemed an appropriate source from which to clone

this region of DNA. The PAC library, gridded on to nylon filters, was obtained from the HGMP. A probe was synthesised from plasmid pP7HYB (520bp EcoRI fragment, human sequence, see Chapter 4) using ^{32}P α-CTP and the HighPrime kit (Roche). Unincorporated radioactivity was removed by applying the reaction mix to a G-25 size exclusion column (Amersham). Filters were probed using the following protocol:

1) Soak filters in 2X SSC for 1 hour at RT
2) Remove from 2X SSC
3) Stack filters one on top of another, DNA facing upwards, with a nylon membrane placed between the sheets
4) Roll filters up and place into a Hybridisation Tube
5) Add 20ml Church Hybridisation Mix
6) Incubate at 65 °C for 2 hours (pre-hybridisation step)
7) Pre-warm 15ml Church Hybridisation Mix to 65 °C
8) Pour Church pre-hybridisation solution off filters and discard
9) Add labelled probe to 15ml pre-warmed Church Hybridisation Mix
10) Place in tube with filters, rotate for 16 hours at 65 °C, ensuring even coverage of filters with probe solution
11) Remove probe solution and discard
12) Wash filters three times in Church Wash solution, pre-warmed to 65 °C
13) Monitor filters for background
14) Starting with 2X SSC, wash filters with increasing stringency of SSC until filter background is acceptable and specific hot spots can be detected
15) Wrap films in cling film
16) Expose to X-ray film in imaging cassette at –80 °C for 24 hours to one week, depending on signal strength
17) Identify positive clones and order from HGMP collection

The solutions used were as follows:

20X SSC	3M NaCl 300mM Na-citrate
1M $NaPO_4$ pH 7.2	1M $Na_2HPO_4.7H_2O$ 0.4% H_3PO_4
Church Hybridisation Mix	250 mM $NaPO_4$ pH 7.2 7% SDS (w/v) 1mM EDTA 1% BSA (w/v)
Church Wash	1% SDS

	1mM EDTA 40 mM $NaPO_4$ pH 7.2

Southern Blot

To map and confirm the PAC clones identified by the PAC library screen, southern blotting was performed using a 770bp PCR probe amplified from mouse genomic DNA, see Chapter 4. Probes were labelled as described for the PAC library screen. PAC clones were grown up and PAC DNA extracted as described. The DNA obtained from each clone was then digested with 7 different enzymes for 16 hours at 37 °C. The digests were then run out on a large (200ml) 1.2% agarose gel for 16 hours at 30 V. The gels were then stained and photographed to ensure digestion and separation. Southern blotting was then conducted as follows:

1) Wash gel in ddH_2O for 30 minutes, shaking gently on a rotating platform
2) Wash gel in ddH_2O with 12.5ml concentrated HCl for 30 minutes
3) Wash gel in 2 x excess of Denaturing Solution for 30 minutes each
4) Wash gel in 2 x excess of Neutralising Solution for 30 minutes each
5) Place gel on blotting set-up containing 20X SSC
6) Cover with cling film and cut a hole around the gel, removing this
7) Cover gel surface with 2X SSC
8) Cut nitrocellulose filter to the size of the gel and place on top, taking care to remove any air bubbles
9) Wet filter with 2X SSC
10) Place two pieces of Whatmann paper, soaked in 2X SSC, cut to the appropriate size on top of the filter
11) Stack absorbent paper towels on top of the Whatmann papers
12) Apply heavy weight to the top of the blotting set up
13) Leave for 16 hours
14) Replace Whatmann paper and towels, re-apply weight
15) Leave for a further 8 hours
16) Remove filter, wrap in cling film
17) UV cross link
18) Air dry, then bake at 120 °C for 15 minutes
19) Place filter in hybridisation tube with nylon membranes
20) Add 20ml Church Hybridisation Mix, pre-warmed to 65 °C, containing 20 µl denatured salmon sperm DNA

21) Pre-hyb for 30 minutes
22) Remove pre-hyb solution
23) To 10ml pre-warmed Church Wash add 10 µl denatured Salmon Sperm DNA and radiolabeled probe
24) Rotate in a hybridisation oven for 16 hours at 65 °C
25) Remove probe wash
26) Wash filter 4 x 30 minutes in 20 ml Church Wash
27) Wrap moist filter in cling film
28) Expose to X-ray film in an imaging cassette for 24, 48 and 72 hours, as required

The solutions used were as follows:

20X SSC	As above
1M $NaPO_4$ pH 7.2	As above
Church Hybridisation Mix	As above
Church Wash	As above
Denaturing Solution	0.5M NaOH 1.5M NaCl
Neutralising Solution pH 7.5	0.5M Tris Base 1.5M NaCl pH with HCl or NaOH

Transfections

Luciferase Assay Transfections (protocol for adherent NIH-3T3 and C2C12 cells)

Cultures of NIH-3T3 and C2C12 cells were maintained in class II conditions as described. One day prior to transfection, cells were trypsinised and re-suspended in antibiotic free DMEM N-12. Cells were counted using a haemocytometer and 2 x 10^6 cells were added to each well of a sterile 24 well plate containing 500µl antibiotic free DMEM N-12. These cultures were left incubated for 16 hours to reach 80-90% confluence prior to transfection. 2 hours prior to transfection the growth medium was

aspirated, the cells washed with PBS twice and covered in 500µl Opti-MEM transfection medium (Invitrogen) per well. Cultures were then replaced in the incubator for two hours prior to transfection.

Plasmid DNA was grown and purified as described before being linearised and quantified. Equal µg quantities of DNA were added to the cells in each transfection. Also, equal µg quantities of CMV and SV40 strong and weak promoters were added to the cells where appropriate. This was to prevent variations in luciferase output and Renilla / luciferase ratios due to promoter – promoter interactions and competition for transcription factors between experiments. For example:

	µg luciferase plasmid DNA	**µg Renilla plasmid DNA**	**µg pCMV-PAX3 plasmid DNA**	**µg pCMV-Script plasmid DNA**
Well A	0.5	0.1	0.0	0.4
Well B	0.5	0.1	0.05	0.35
Well C	0.5	0.1	0.1	0.3

Here, all three wells have a total of 1µg plasmid DNA added, varying the amount of *Pax3* expression plasmid, enabling the effect of several concentrations of *Pax3* expression to be investigated on the luciferase reporter plasmid, the total amount of CMV promoter is constant. (NB. Since the sizes of pCMV-Script and pCMV-Pax3 vary this is not strictly speaking true. pCMV-Pax3 is 25% larger and so, weight for weight, will carry 25% fewer 'molecules' of CMV promoter into the transfection. Since an excess of the smaller plasmid is used in each experiment, the actual difference in number of CMV promoters is minimal, i.e. 0.4 in Well A compared with

(0.3 + (0.75 x 0.1)) = 0.375 = 6% difference in Well C). Since the observed luciferase induction was always much greater than these small differences in CMV promoter composition, and DNA-Lipofectamine ratios thought to have a much greater effect on transfection ratios, (Invitrogen, product insert), this was considered acceptable). For 24 well plates the optimal total amount of DNA was found to be 1.5μg per well for both cell lines.

μg luciferase plasmid DNA	**μg Renilla plasmid DNA**	**μg pCMV-PAX3 plasmid DNA**	**μg pCMV-Script plasmid DNA**
0.5	0.1	x	0.4 + y

Where x + y = 0.5μg DNA

Lipofectamine-2000 reagent was then used to transfect the plasmid DNA into each well as follows:

1) Add all DNA to 50μl Opti-MEM
2) Mix and incubate at RT
3) Add Lipofectamine-2000 to a second 50μl Opti-MEM. Add nμl Lipofectamine-2000 where n = (μg DNA x 2). For example, 1μg total DNA = 2ul Lipoectamine-2000
4) Mix and incubate at RT for 5 minutes
5) Mix DNA - Opti-MEM and Lipofectamine-2000 – Opti-MEM together
6) Incubate at RT for 30 minutes
7) Add to well containing 500μl Opti-MEM
8) Mix gently and incubate at 37 ^{o}C, 5% CO_2 for 24 hours

After 24 hours, cells were washed in PBS and harvested using the Passive Lysis Buffer component of the Dual Luciferase Reporter Assay System (Promega). Luciferase and Renilla Luciferase expression was then assayed according to manufacturers instructions and using a TD-20/20 Luminometer (Turner Biosystems).

Relative Light Units (RLU) were measured for each luciferase, and recorded for every sample. RLU was measured cumulatively over 10 seconds and performed twice for each sample to ensure accuracy of measurement. Individual transfections were conducted in triplicate in each run to ensure each set of conditions gave a reliable result within a run of transfections. These runs were repeated between 3 and 12 times, depending on the specific experiment, and this is then recorded as the n value for each experiment.

Appendix 4 contains a detailed description of the Luciferase rationale and data treatment used in this thesis.

Transfections for Western Blotting

To confirm the expression of Pax3 and Msx2 full length protein product from the plasmids pCMV-Pax3 and pCMV-Msx2 Western blotting was also used. These plasmids were transfected into both NIH-3T3 and C2C12 and the proteins harvested for Western blotting. Transfections containing varying quantities of expression vector and pCMV-Script, or pCMV-Script alone (negative control), were conducted as described above but in 6 well plates. All quantities of cells and reagents were multiplied by 5 to account for the larger size of the wells and transfections conducted using Lipofectamine as normal.

After incubating for 24 hours, cells were washed twice in PBS, trypsinised and re-suspended in DMEM N-12 medium. These were then spun down (1000 rpm, 5 minutes), washed in cold PBS, re-spun and the re-suspended in 100μl cold Western

Lysis Buffer. These were transferred to ice for 15 minutes, passed through a small gauge syringe 10 times, spun down at 13,000 rpm and the protein concentration of the supernatant assayed as described. Protein samples were stored at –80 °C, and Western blotting performed as described below.

Proteins

Choice of peptides used to raise α-Pax3 antibody

The amino acid sequence of the Pax3 protein was derived from the cDNA sequence, and used to design immunogenic peptides to raise against the Pax3 protein. Peptide sequences and modification specifications were emailed to Genosphere Biotechnologies Ltd. who synthesised, modified and finally conjugated the peptides to Keyhole Limpet Heamocyanin. This was then injected into Rabbits over several weeks, and the serum checked for immunogenicity using an ELISA with the original peptides as primary substrate. Once good titres had been obtained the un-purified sera was shipped back from the company for analysis and purification in our lab.

Protein Quantification

Protein concentration was determined using the BCA Reagent Kit (Pierce), against a known range of BSA concentrations, according to the manufacturer's instructions. Assays were conducted in a 96 well plate and absorbance at λ562 was measured on a

plate reading spectrophotometer. A standard curve was drawn, linear regression performed and the resulting equation used to calculate the concentration of total protein of samples.

Western Blotting

Western blotting was used to confirm the specificity of the α-Pax3 antibody, expression of *Pax3*, *Msx2* and *Pax7* in cell culture and embryonic tissue. The following general protocol was used in all cases; the specific antibody concentrations used were determined empirically for each serum.

SDS-PAGE

10% Tris-Glycine polyacrylamide Novex pre-cast gels (Invitrogen) were used to separate proteins in one dimension. 10μg protein was loaded on each gel after being reduced by boiling in the following mixture:

Protein Loading Mixture	n μl protein sample (10μg) 1 μl β-Mercaptoethanol 5 μl SDS 4X Sample Loading Buffer (n + 6) – 20 μl Western Lysis Buffer

Samples were boiled for at least 10 minutes at 100 °C and then loaded into a lane filled with 1X SDS Running Buffer. The gels were set up in the Xcell SureLock Mini-Cell (Invitrogen) and run for 1 hour and 40 minutes at 150V. Magic Mark (Invitrogen) was used as a ladder to enable sizing of bands.

Protein Transfer

Immediately after electrophoresis proteins were transferred onto nitrocellulose membrane. The gel was removed from the SDS-PAGE apparatus, rinsed in ddH_2O and Transfer Buffer before being placed in a sandwich between two sheets of Whatmann paper and two thick nylon sponges on the outer surface. Next to the gel inside the sandwich a piece of nitrocellulose membrane (Biorad) was placed on the side which would face the positive electrode in the transfer tank. This was then placed into a transfer tank and covered in Transfer Buffer. Transfer was conducted at 4 ^{o}C at 50mA for 16 hours. The transfer apparatus was then dismantled and the nitrocellulose stained with Amido Black to demonstrate transfer and examine equal loading of protein samples. Excess Amido Black was then washed off in ddH_2O and an image of the membrane recorded. Membranes were chopped into separate pieces at this stage if necessary.

Immunodetection

The following protocol was used during immunodetection.

1) Block membrane in Blocking Buffer for 1 hour
2) Add primary antibody at appropriate concentration, diluted in Blocking Buffer
3) Incubate with shaking at 4 ^{o}C for 16 hours
4) Wash three times in PBS-T
5) Add secondary antibody at appropriate concentration, diluted in Blocking Buffer
6) Incubate with shaking at RT for 2 hours
7) Wash three times in PBS-T

8) Detect using the ECL+ detection system (Amersham) according to manufacturer's instructions and exposing to X-Ray film

The solutions used were as follows:

Western Lysis Buffer	150mM NaCl 25mM Tris-HCl (ph 7.5) 1% Triton X-100 0.1% SDS + Complete Protease inhibitor tablets (Roche)
4X Sample Loading Buffer	0.5M Tris-HCl (pH 6.8) 10% SDS (w/v) 10% Glycerol 0.1% Bromophenol Blue
5X SDS Running Buffer	0.125M Tris-Base (pH 8.3) 0.96M glycine 0.5% SDS
Western Transfer Buffer (make fre	100mM glycine 120mM Tris-Base 200ml methanol
Amido Black	0.1% Amido Black 25% isopropanol 10% acetic acid
PBS-T	1X PBS 0.1% Tween-20
Blocking Buffer	5% powdered milk solution in PBS-T

Immunohistochemistry

Mouse embryos were obtained and dissected at specific ages as described. Embryos were then fixed in 10% paraformaldehyde for 16 hours at 4 ^{o}C and placed in 70% ethanol before being embedded in paraffin. Waxed embryos were then sectioned at 10μm thickness and placed on glass slides.

The following protocol was used for immunohistochemistry.

1) Dewax sections in xylene (twice for10 – 20 minutes)
2) Rehydrate sections in series of descending ethanols (100% - 50%)
3) Wash with PBS (3 times for 5 minutes)
4) Block endogenous peroxidases with a solution of 3% H_2O_2 and 10% methanol in PBS for 15 minutes in the dark
5) Wash with PBS-TX (3 times for 5 minutes)
6) Wash with (3 times for 5 minutes)
7) Wash in 10mM Sodium Citrate Buffer for 15 minutes
8) Boil slides in microwave for a total of 20' (5'-20') as follows:
9) 5 minutes at full power
10) top up with dH20
11) repeat up to 3 more times
12) Rest slides for 20 minutes to cool down
13) Incubate with Blocking Solution for 2 hours at RT
14) Wash with PBS-TX for 5 minutes
15) Incubate with primary antibody diluted in Blocking Solution for 16 hours at 4 ^{o}C
16) Wash with PBS-TX 5 times for 5 minutes
17) Incubate with biotinilated secondary antibody (1:200) Blocking Solution for 1 hour at RT
18) Wash with PBS-TX 5 times for 5 minutes
19) Incubate with the Streptavidine-HRP complex (1:400, ABC Kit) Blocking Solution for 1 hour at RT
20) Wash with PBS-TX twice for 5 minutes
21) Wash with PBS 3 times for 10 minutes
22) Develop with a solution of 0.03% DAB and 0.003% H_2O_2 in PBS
23) Wash slides 3-5 times in PBS
24) Counter stain with Crystal Violet if necessary
25) Dehydrate sections in a series of ascending ethanols and xylene
26) Mount the tissue with DPX

Sections were examined under an inverted light phase contrast microscope and images taken using a digital camera.

The solutions used were as follows:

PBS-TX	0.2% solution of Triton X-100 in PBS
Sodium Citrate Buffer (pH 6.0)	100mM sodium citrate
Blocking Solution	0.2% gelatine 10% goat serum in PBS-TX

Antibody Purification

After the immunogenicity of the α-Pax3 serum was confirmed, column purification was performed using Protein-G sepharose (Amersham). The sepharose was degassed under vacuum for 30 minutes at RT before being packed onto a 1cm diameter glass EconoColumn (Biorad). Flow rate was adjusted to 1ml per minute, and the column washed with 10 bed volumes of ice cold TBS. All purification was conducted in the cold room unless otherwise stated.

The volume of serum purified was calculated as follows:

Binding capacity of column (5ml) = 100mg IgG

Assume 90% binding efficiency = 90mg, and that rabbit IgG concentration is 5mg per ml, therefore 90/5 = 18ml serum applied to column.

Any debris from the serum was spun out at 15,000g for 5 minutes at 4 ^{o}C, and then applied to the column at a flow rate of 1 ml per minute. The serum was passed through the column twice. The column was then washed with 180ml ice cold TBS until no protein could be detected from the eluate using the BCA Kit (Pierce).

100μl Neutralisation Buffer was added to 20 x 1.5ml Eppendorfs as all the TBS was allowed to drain from the column. The column was transferred to RT and 15ml RT

pH 2.7 Elution Buffer was applied. 10 x 1ml fractions were collected. 15 ml of RT pH 1.9 Elution Buffer was the applied and 1ml fractions were collected. Samples were mixed immediately to ensure neutralization and placed on ice. The BCA Kit (Pierce) was then used to quantify the protein concentration and the λ562 was measured. λ562 vs. fraction number was then plotted and two peaks were identified and separated into two fractions for later testing with Western blot and immunohistochemistry. For long term storage, the fractions had BSA added to 5%, aliquoted and stored at –80 °C.

TBS	50mM Tris-HCl (pH 7.4) 150mM NaCl
Neutralization Buffer	1M Tris-HCl (pH 8.0) 1.5M NaCl 1mM EDTA
Elution Buffer pH 2.7	50mM glycine (pH 2.7)
Elution Buffer pH 1.9	50mM glycine (pH 1.9)

Chromatin Immunoprecipitation (ChIP)

Chapter 6 is dedicated to ChIP experiments, and so a detailed description of the rationale behind this method is not given here.

PCR primers were designed to amplify a region of either the promoter or downstream *cis*-regulatory elements of both the *Pax7* and *Wnt1* gene loci. PCRs were optimised for use on genomic DNA. The position of these primers and the reasoning behind their design is included in Chapter 6. ChIP primer sequences are recorded in Appendix 2.

Mouse embryos were obtained as described and sacrificed at E10.5. Embryos were dissected out and the telencephalon removed. These regions were deemed as being likely to contain tissues where the hypothesised interactions suggested from Chapters 3 and 4 (i.e. neural tube and somite / mesenchyme) might be found.

An *in vivo* ChIP methodology was designed specifically for use in this thesis as an amalgamation of *in vitro* methods used by other groups, and published on the internet. Several approaches were tested, and the following is a description of the method which proved successful. One of the major considerations in using an embryological source is the rapid and uniform fixation of the source material. Over exposure to formaldehyde would result in excessive crosslinking making subsequent enrichment steps impossible. To enable embryonic tissues to be manipulated in a manner closer to that of the tissue culture cells usually used in this type of analysis, a gentle disassociation protocol was utilised after dissection to generate a suspension of single cells. This also enabled cell counting and a uniform quantity of starting material to be used in each repeat experiment.

Dissected embryos were then immediately disassociated using the Papain Dissociation System (Worthington Biochemical Corporation) to obtain a suspension of cells in PBS. Cells were counted and equal numbers of cells used in every ChIP experiment (1×10^7). Cell suspensions were then fixed by adding formaldehyde to 1%, and incubating with gentle agitation at 37 ^{o}C for 10 minutes. The fixing process was then quenched by the addition of glycine to 125mM. The cells were then pelleted, washed in PBS, and then re-suspended in 200µl Lysis Buffer and incubated on ice for 10 minutes.

Sonication conditions were previously optimised on disassociated mouse embryos to generate fragments of 500bp to 1kb, see Figure 6.3B. This should be optimised for every individual sonciator and probe before attempting these experiments since large variation between individual equipment and probes is generally observed.

Suspensions were then sonicated to generate fragments of an appropriate length. Samples were then centrifuged at 13,000 rpm for 5 minutes at 4 °C to remove debris. Supernatants were then transferred to new tubes. 300µl fresh Lysis Buffer and 50µl protein G sepharose (Amersham) with Salmon sperm DNA (2.5 µg/µl) was added to pre-clear the lysates. The samples were then gently rotated at 4 °C for 2 hours. The beads were spun down, 6,000 rpm for 1 minute, and the supernatants transferred to fresh tubes. 20 µg of purified α-Pax3 antibody was then added and the samples rotated at 4 °C for 16 hours.

50µl Protein G Sepharose was then added to each sample, and rotated for a further 4 hours at 4 °C. Immunoprecipitated complexes were then spun down at 6,000 rpm for 1 minute and the supernatant discarded. Complexes were then washed in 500 µl of the following, spinning down to recover the beads each time (all steps performed at 4 °C):

1) Lysis Buffer, 10 minutes
2) Lysis Buffer, 5 minutes
3) Low Salt Buffer, 5 minutes (low stringency)
4) High Salt Buffer, 5 minutes (high stringency)
5) LiCl Buffer, 5 minutes (removal of non-specific chromatin – agarose interactions)
6) TE Buffer (pH 8.1), 30 minutes
7) TE Buffer (pH 8.1), 5 minutes

Finally the complexes were re-suspended in fresh Elution Buffer , and vortexed at RT for 15 minutes. The sepharose was then spun out and the supernatant transferred to a fresh tube. Formaldehyde cross linking was then reversed by adding 5µl 8M NaCl, 1µl RNaseH (Qiagen), 5µl Protinase K (Promega) and incubating at 65 °C for 16 hours.

DNA was then purified using phenol chloroform and precipitated using ammonium acetate as described. The seeDNA nucleic acid reagent (Amersham) was added during precipitation to visualise the pellet. Pellets were re-suspended in 50µl ddH_2O and 5µl ran out on an agarose gel against serial dilutions of 'input' sonicated chromatin (the source of positive control, see Chapter 6) to ensure that similar quantities of template DNA were added to each PCR reaction. 5µl of ChIP and input chromatin were then used in each PCR reaction. PCR conditions were as shown in Chapter 6 and PCR products visualised on a 2% agarose gel.

The solutions used were as follows:

Lysis Buffer	150 mM NaCl 25 mM Tris-HCl ph 7.5 1% Triton X-100 0.1% SDS 0.5 % Deoxycholate
Low Salt Buffer	0.1% SDS, 1% Triton X-100 1mM EDTA 20mM Tris-HCl, pH 8.0 150mM NaCl
High Salt Buffer	50 mM Tris-HCl, pH 8.0 500 mM NaCl 0.1 % SDS 1% Triton X-100 1 mM EDTA

LiCl Buffer	50 mM Tris, pH 8.0 1 mM EDTA 250 mM LiCl 1% NP-40 0.5% Deoxiholate
TE Buffer	10 mM Tris-HCl, pH 8.0 1 mM EDTA
Elution Buffer	1% SDS 0.1M $NaHCO_3$

Every solution had protease inhibitors added fresh before use in each experiment, and were kept at 4 °C. Complete Protease Inhibitor Cocktail tablets (Roche) were used.

Bioinformatics

DNA sequences were obtained, where available, from www.ensembl.org and annotated manually. Global alignments were performed using PipMaker (Schwartz, 2000), Jemboss, and ClustalW software, all available from www.hgmp.ac.uk. Transcription factor binding sites were predicted using the MatInspector program, available from Genomatix; data outputs were then dumped into Excel and analysed manually with this software. Cloning and DNA analysis was performed using the MacVector 7.2 software from Accelrys.

Chapter Three: *Wnt1* regulation

Introduction

In this chapter, the interaction between *Pax3* and the regulatory elements of the *Wnt1* gene are investigated. As described in Chapter 1, *Wnt1* provides an attractive potential target for regulation by *Pax3* due to both its expression pattern, timing and its apparent position as genetically downstream of the *Pax3* signal (see (Conway et al., 2000; Deardorff, 2001; Meulemans and Bronner-Fraser, 2004; Monsoro-Burq, 2004) for representative evidence). This chapter will show that, whilst *Pax3* cannot be demonstrated to have any significant regulatory effect on the 3' distal enhancer region, (Echelard et al., 1994), the identification of a putative *Pax3* consensus site 5' proximal to the transcriptional start site of the *Wnt1* gene enables a regulatory interaction between this region and the *Pax3* transcription factor to be established *in vitro*. Hypothesis One will be addressed first.

Hypothesis One

Pax3 *regulates* Wnt1 *directly, most probably through the 3' distal enhancer region,* in vivo *during the development of the neural crest.*

Wnt1 *expression is decreased in* Sp^{2H} *homozygotes*

Before establishing *Wnt1* as a direct target of regulation by *Pax3*, it was important to unequivocally demonstrate the misregulation of this gene *in vivo*. Whilst other groups have shown *Pax3* to be unperturbed in *Wnt1* mutants (Ikeya et al., 1997) and later studies have shown evidence from *in situ* hybridisations which suggest *Wnt1* is significantly downregulated in the Sp^{2H} homozygous mutant (Conway et al., 2000), no quantitative proof of this misregulation in the *Splotch* mouse has been reported. Demonstrating a change in *Wnt1* expression on a *Pax3* null background was perceived as an essential step before an investigation into the potential regulatory relationship could be taken further.

To achieve this, Quantified Reverse Transcriptase PCR (QRTPCR) was performed on RNA extracted from wild type and mutant sibling pair embryos at E9.5 as described (see Chapter 2 for a detailed description of the QRTPCRT technique). Primers pairs used were GAPLITEF/R and W1LITEF/R, (all primers are listed in Appendix Two). The assay was performed on four pairs of embryos, genotyped by PCR (primers P3GENOF/R), which were then homogenised and RNA extracted using a RNeasy Midi kit (Qiagen). RNA was then quantified using a UV spectrophotometer, and a fixed quantity added to a reverse transcriptase reaction. QRTPCR, using the SYBR Green dye (Qiagen) and a Opticon Monitor system (MJ Research), was then performed using the 55^35 program as described. Expression levels for mutant embryos were then reported as a % of wild type. A wild type standard curve was used to interpolate and the results averaged across the four sib-pairs. Blank and no RT

controls were negative, and blank fluorescence automatically subtracted from the data set by the Opticon software. These data can be seen in Figure 3.1.

This figure clearly shows a significant reduction of *Wnt1* expression of around 40% ($p = 0.003$). In contrast no detectable difference in GAPDH expression was observed in the same embryo pairs. This figure is in keeping with previously published estimates of 50% (Conway et al., 2000) and was interpreted as meaning that the levels of *Wnt1* expression in the Sp^{2H} mutant are significantly reduced in comparison to the wild type. This result does not indicate why this difference is observed. *Wnt1* may be entirely independent of *Pax3* regulation, but expressed within a cell population that is reduced in Sp^{2H} homozygous mutants. To establish a regulatory role for *Pax3*, a more detailed analysis of the regulatory elements known to control *Wnt1* expression was performed.

Pax3 *does not interact with the* Wnt1 *3' enhancer*

The expression of *Wnt1* has been faithfully recaptured by the expression of a LacZ reporter cassette driven by a 5.5kb enhancer fragment 3' distal to the transcriptional start site (Echelard et al., 1994). This region has been investigated in detail, and a number of potential transcription factor binding sites have been mapped to this region (Iler et al., 1995; Rowitch et al., 1998). To enhance this investigation a bioinformatic analysis of this 5.5kb sequence was performed using MatInspector software (MatInspector). This searches genomic sequence for significant matches to known transcription factor binding sites based on known targets and sequence affinities. Whilst over 600 sites were predicted, with a core similarity of 75% or over, only three

Figure 3.1 :
QRTPCR of *Wnt1* and *GAPDH* transcript levels in *Pax3 -/-* embryos. Levels expressed as % of wild type expression. *GAPDH* 94.01% of wild type (no difference), *Wnt1* 59.4% of wild type expression (40.6% reduction). n = 4 wild type / homozygous mutant sibling pairs. Error bars are SEM. p = 0.003 (two sample t test)

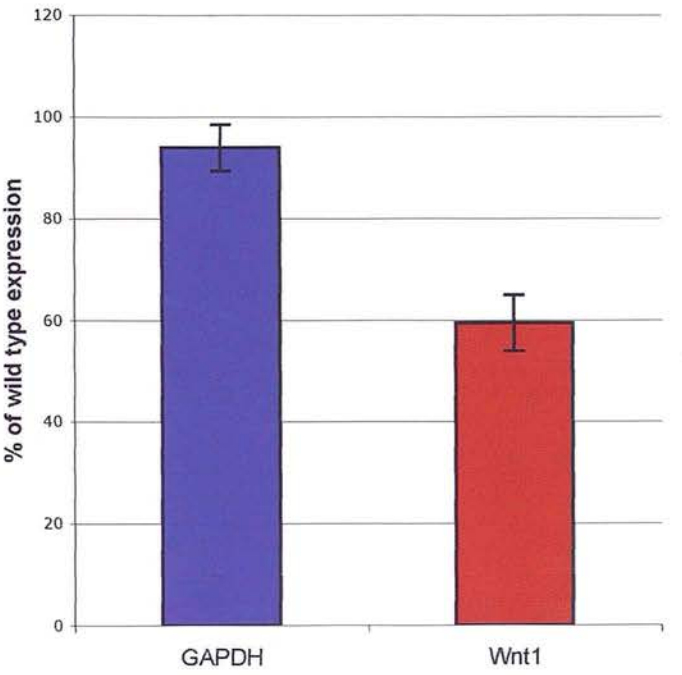

potential *Pax* binding sites were identified. These were all predicted as *Pax5* binding sites. Since *Pax3* and *Pax5* are not from the same Pax gene subfamily, and *Pax5* is thought to be primarily involved in B-lymphocyte development (Urbanek, 1994), these seemed unlikely to be potential *Pax3* binding sites.

A lack of predicted binding sites does not preclude a regulatory interaction between this fragment and the *Pax3* protein via a novel site. To investigate this possibility the 5.5kb enhancer fragment spanning this region was cloned from the pWEXP3 plasmid (A. McMahon, kind gift) as BglII fragment into the pGL3promoter Luciferase reporter construct (Promega) BamHI site and clones screened to ensure genomic orientation relative to the Luciferase ORF. The pGL3promoter construct carries a Firefly Luciferase reporter gene under the control of a weak SV40 promoter, and is designed to enable the dissection of enhancer elements. This construct was then co-transfected into NIH-3T3 cells (*Pax3* and *Wnt1* negative by RTPCR, data not shown) with a *Pax3* expression construct, pCMV-*Pax3*. The expression construct was generated by cloning full length *Pax3* cDNA from wild type E10.5 RNA by RTPCR using the primers 3/5 P3IRES to amplify full length *Pax3* cDNA. This was then TOPO cloned into pCR-II-TOPO-Blunt and sequenced using the *Pax3* sequencing primers shown in Appendix Two. Full length *Pax3* with no mutations was then sub-cloned into pCMV-Script (Stratagene) as a SacII – BamHI fragment. This generated a plasmid with the full length *Pax3* cDNA under the control of the CMV promoter. These constructs are shown in Figure 3.2A.

pCMV-Pax3 was then co-transfected into NIH-3T3 cells with pW1ELuc, and the fold induction over pGL3promoter baseline calculated for 6 triplicate runs, see Figure

Figure 3.2:
A) Illustrating *Wnt1* enhancer Luciferase reporter construct and pCMV-Pax3 expression construct, B = BglII - BamHI cloning sites.
B) Luciferase data illustrating normalised luminescence for pW1ELuc with and without *Pax3* expression (100ng pCMV-Pax3 or 100ng empty vector). Data is expressed as fold induction over pGL3promoter (pW1ELuc without *Wnt1* enhancer fragment). n = 6, error bars are SEM, induction is non-significant (p = 0.24, two sample t test)

A

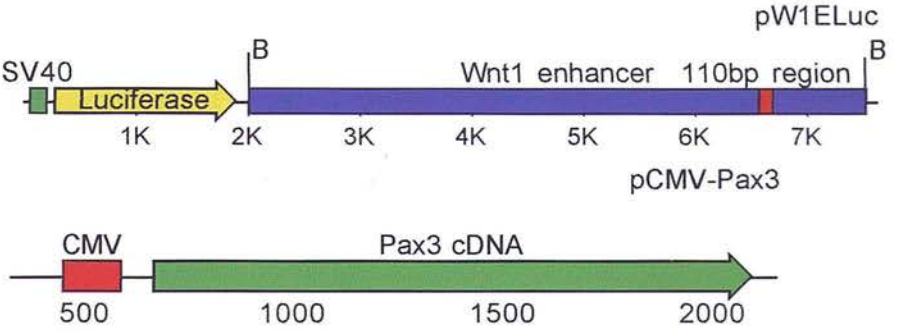

B

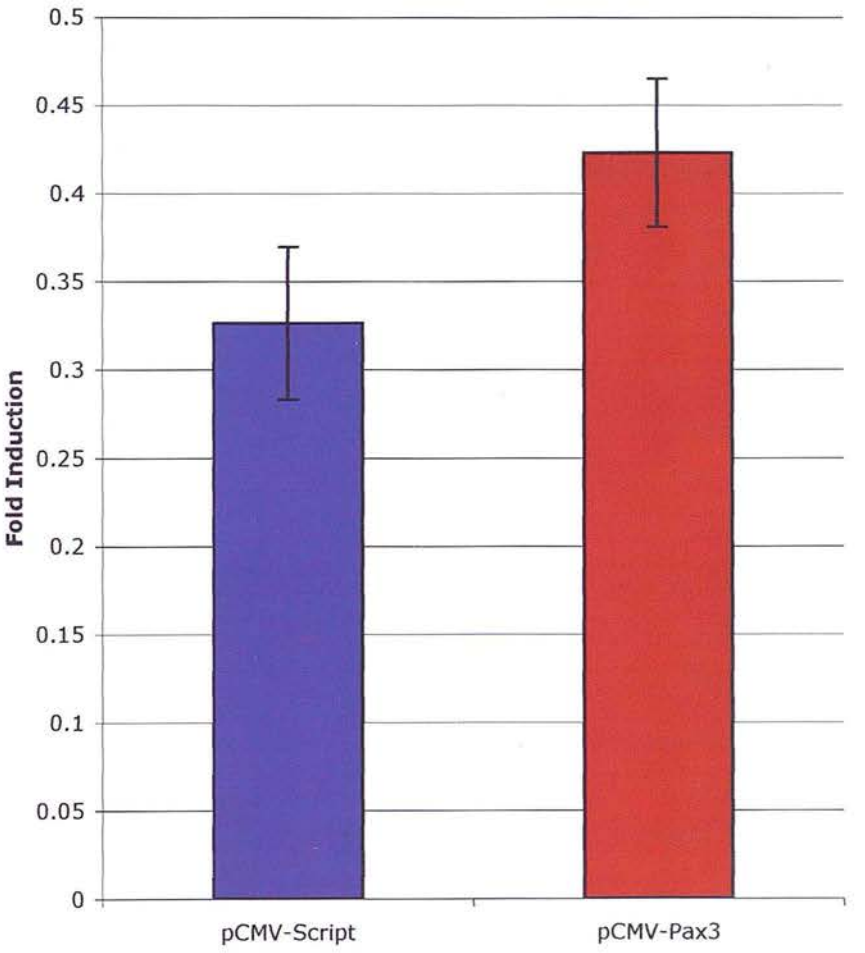

3.2B. A detailed description of the Luciferase protocol and the data treatment used in this thesis can be found in Appendix 4 and is not given here. Whilst a very slight induction was observed with the addition of pCMV-*Pax3* versus empty vector, pCMV-Script, this was not significant. The reverse enhancer orientation was also examined in this assay, but again no change in Luciferase activity could be detected on co-transfection with pCMV-*Pax3* (data not shown).

To ensure the pCMV-*Pax3* expression vector was producing full length *Pax3* protein in these cells, Western blots on protein extracts from samples transfected with pCMV-*Pax3* and those transfected with pCMV-Script were performed. The primary antibody was derived as described in Chapter 5. Un-purified serum was used in these experiments since non-specific bands enable an easy control of loading equivalence between lanes. A representative blot can be seen in Figure 3.3. This clearly shows the expression of full length *Pax3* protein in these samples (red arrow). It was concluded that the lack of Luciferase induction in these samples could not be attributed to a problem with *Pax3* expression from the pCMV-*Pax3* construct.

In this *in vitro* assay, *Pax3* could not be shown to interact with the 3' distal enhancer element of *Wnt1*.

The Wnt1 *5' promoter is* Pax3 *responsive*

Since the 3' distal enhancer of *Wnt1* did not show any reaction to *Pax3* co-expression, the 5' promoter region of the locus was then examined. The examination of this region, in spite of the control of *Wnt1* expression being generally attributed to the

Figure 3.3 :
Western blot confirming expression of Pax3 in Luciferase assay system (NB. samples taken from actual luciferase experiment and unpurified α-Pax3) Pax3 ~53KDa
+ = transfected lane, - = un-transfected lane.

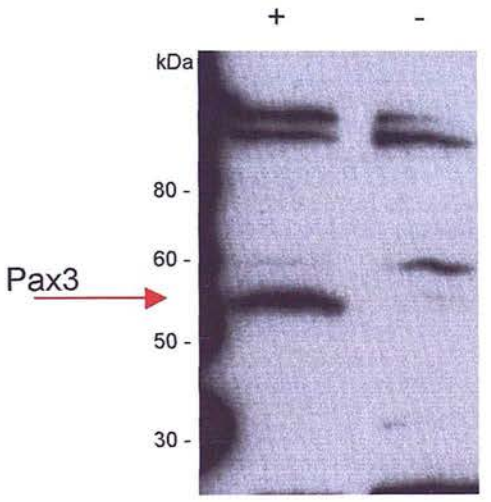

enhancer element investigated above, was seen as important for several reasons. Firstly, (Serbedzija and McMahon, 1997) reported that the expression of a *Wnt1*-LacZ transgene was altered on a *Pax3* null background. This transgenic was constructed using the WZT9B construct, and contains both the 5.5kb 3' enhancer region and a portion of the *Wnt1* genomic 5' proximal promoter (Echelard et al., 1994). Further, studies in *Xenopus* (Gao et al., 1994) have implicated this region as important in inducing reporter gene expression concomitant with neural cell specification. Also, the differentiation of P19 embryonal carcinoma cells along a neuroectodermal lineage using retinoic acid treatment has been illustrated to induce both *Pax3* (Pruitt, 1992) and the expression of *Wnt1* via an element in the 5' promoter region (St-Arnaud and Moir, 1993). Finally, the *Wnt1* promoter is essential in *Six3* mediated repression of *Wnt1* expression in the developing telencephalon (Lagutin et al., 2003), establishing a regulatory precedent for this region in anterior neural tissues.

The *Wnt1* 5' proximal promoter was then subjected to bioinformatic binding site analysis (MatInspector). This identified 178 potential transcription factor binding sites in the proximal 1.5kb upstream of the *Wnt1* gene. Several *Pax* gene consensus sites were found, including *Pax1*, *Pax4* and *Pax9*. Most importantly, one *Pax3* consensus was discovered in extreme proximity to the *Wnt1* transcriptional start site (46bp upstream). This is shown in Figure 3.4A. ClustalW local alignments were then performed on this region between human and mouse genomes, and illustrated a high degree of conservation (Figure 3.4B) suggesting functional significance. Finally, analysis of the human, mouse, *Fugu* and *Xenopus Wnt1* promoters (from (ensembl)) revealed putative *Pax3* binding sites in similar positions in all 4 species (Figure 3.4C). This site is also found

Figure 3.4 :
A) Identification of Pax3 binding consensus in the *Wnt1* 5' promoter.
B) Local alignment of human and mouse promoters showing high overall level of conservation. Red bar highlights *Pax3* consensus site.
C) Alignments showing conservation of consensus in *Xenopus*, *Fugu*, mouse and human *Wnt1* promoter regions

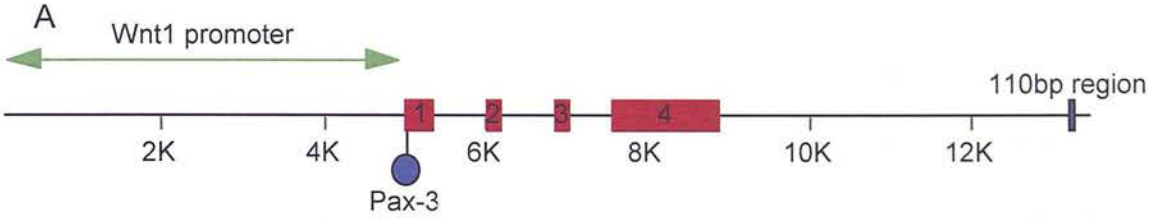

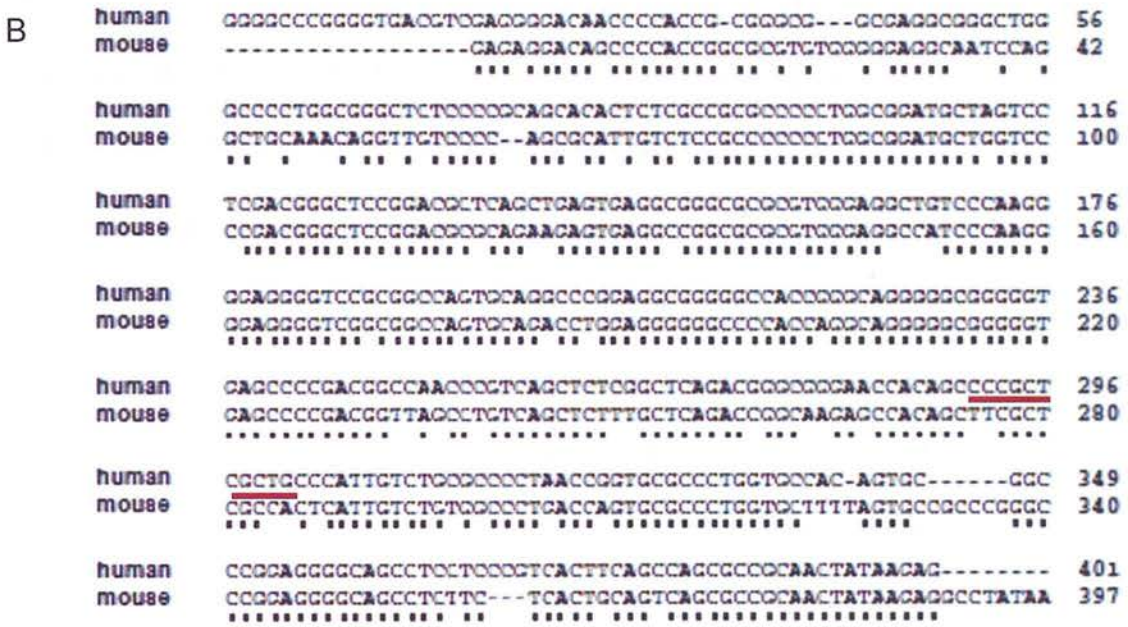

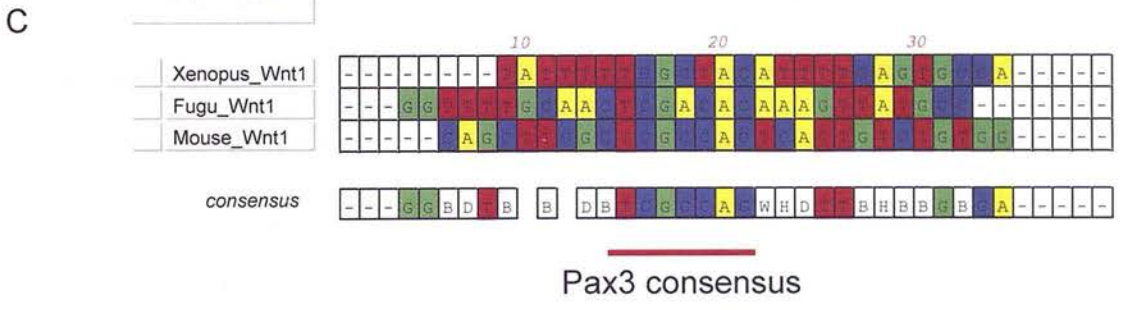

on the murine *Wnt1* promoter fragments used in the constructs examined in (Serbedzija and McMahon, 1997) and (St-Arnaud and Moir, 1993).

To investigate the possible functional significance of this conserved element, Luciferase constructs were made to test this in *Pax3* co-transfection assays. The *Wnt1* proximal promoter was obtained from pMT86 (R. Nusse, kind gift) as a 4.9kb BamHI / NcoI fragment and cloned into the BglII / NcoI sites of the pGL3basic (Promega) Luciferase reporter vector. The NcoI site in the *Wnt1* sequence contains the ATG start codon of the *Wnt1* gene. Cloning into the NcoI site of pGL3basic (also the ATG of the Luciferase ORF) positions the *Wnt1* promoter in an identical position to the Luciferase ORF as it is to the translational start of *Wnt1 in vivo*. pGL3basic contains a Firefly Luciferase ORF in a promoterless construct to enable the investigation of putative promoter elements. This construct was named pW1PLuc and is illustrated in Figure 3.5A. This was co-transfected into NIH-3T3 cells with either the pCMV-*Pax3* expression construct or empty vector. Four triplicate runs were completed for these assays, and the normalised luminescence baselined to pGL3basic background to generate fold induction. A clear induction of Luciferase activity concomitant with *Pax3* expression can be seen in Figure 3.5A.

To compare this induction with the results obtained with the pW1ELuc construct, the data was rebased to uninduced samples (i.e. co-transfections with empty vector) and illustrated in Figure 3.5B. It was concluded from this analysis that *Pax3* is able to cause induction of a reporter gene via the proximal promoter of *Wnt1*, and not via the distal enhancer element, *in vitro*.

Figure 3.5:
A) Induction of luciferase activity from pW1PLuc on co-transfection with pCMV-Pax3. Data is normalised luminescence expressed as fold induction over pG3basic (pW1PLuc without the 5.2kb Wnt1 promoter fragment). n = 4, error bars are SEM.

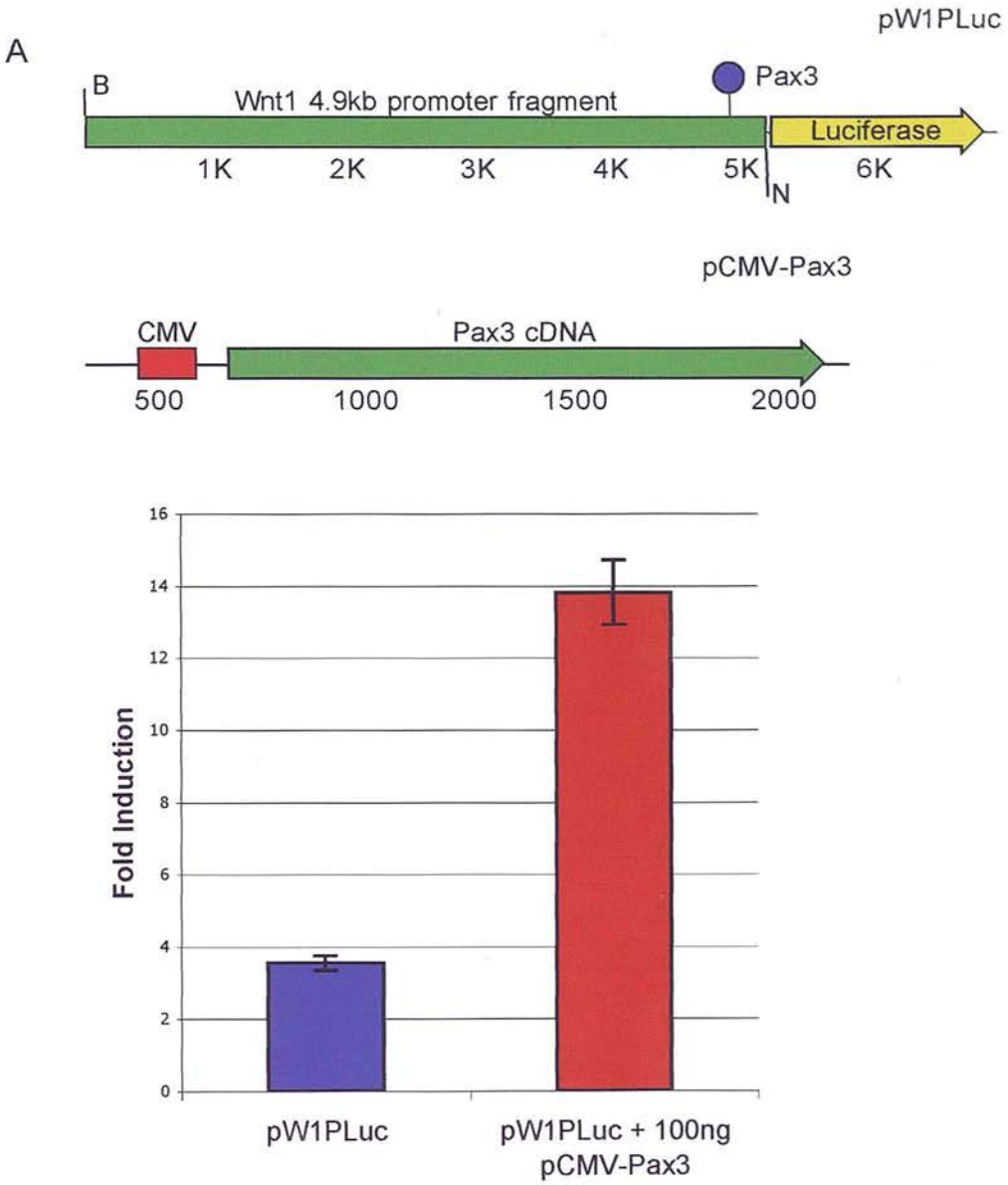

Figure 3.5:
B) Comparison of Pax3 induction of pW1PLuc and pW1ELuc. Data is normalised luminescence, fold induction over baseline (respective luciferase vectors without *Wnt1* regulatory sequence), indexed to un-induced to allow direct comparison. n = 4 and 6, respectively, error bars = SEM.

B

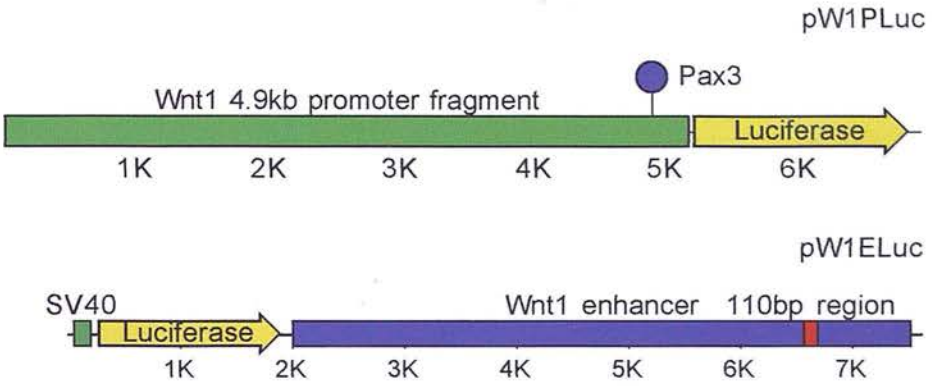

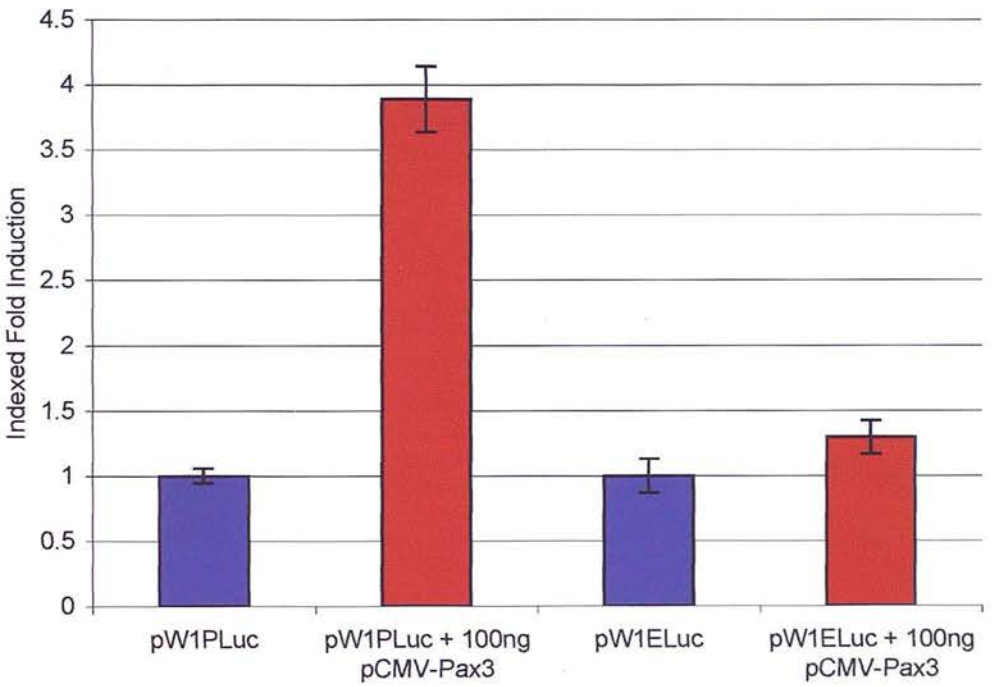

To further investigate the relationship between the *Wnt1* promoter and the *Pax3* protein a series of deletion constructs were made using restriction sites native to the element. pW1PLuc was digested with Asp718 to remove 3.7kb of sequence distal to the Luciferase ATG. The backbone was then re-ligated to generate pW1P(1.2)Luc. Similarly, twin ApaI sites were used to remove the proximal 3.1kb of the *Wnt1* promoter to generate pW1P(-1.8)Luc. In this latter construct the *Pax3* consensus site is also removed. These constructs are illustrated in Figure 3.6A. Each of these constructs were then co-transfected into NIH-3T3 cells with either pCMV-*Pax3* or empty vector, as previously described, to assay any transcriptional response to the *Pax3* protein. These results can be seen in Figure 3.6B. Clearly, whilst both pW1PLuc and pW1P(1.2)Luc retain their response to *Pax3* expression, the pW1P(-1.8)Luc construct does not. Since this latter plasmid has lost the *Pax3* consensus site identified in Figure 3.4, this data further argues for a functional role for this site in binding *Pax3*, at least *in vitro*. Finally, the pW1PLuc and pW1P(1.2)Luc were exhaustively tested in pCMV-*Pax3* co-transfection assays using a range of expression vector quantities (this was also shown to generate a proportional range of *Pax3* expression levels within the cells transfected, see Figure 4.15A). This was to ensure both specificity of *Pax3* response by illustrating a concentration dependence and to test the result reported by (Chalepakis et al., 1994) which demonstrates a biphasic transcriptional response of increasing *Pax3* concentrations when binding to reporter gene constructs carrying the NCAM promoter. This can be seen in Figure 3.6C. Whilst these data clearly demonstrate a concentration specific response to *Pax3* gene expression over the concentration range examined, no biphasic response (i.e. loss of transcriptional inductive ability at higher *Pax3* concentrations) was observed. Whilst it remains possible that in these experiments insufficient *Pax3* was co-expressed to

Figure 3.6

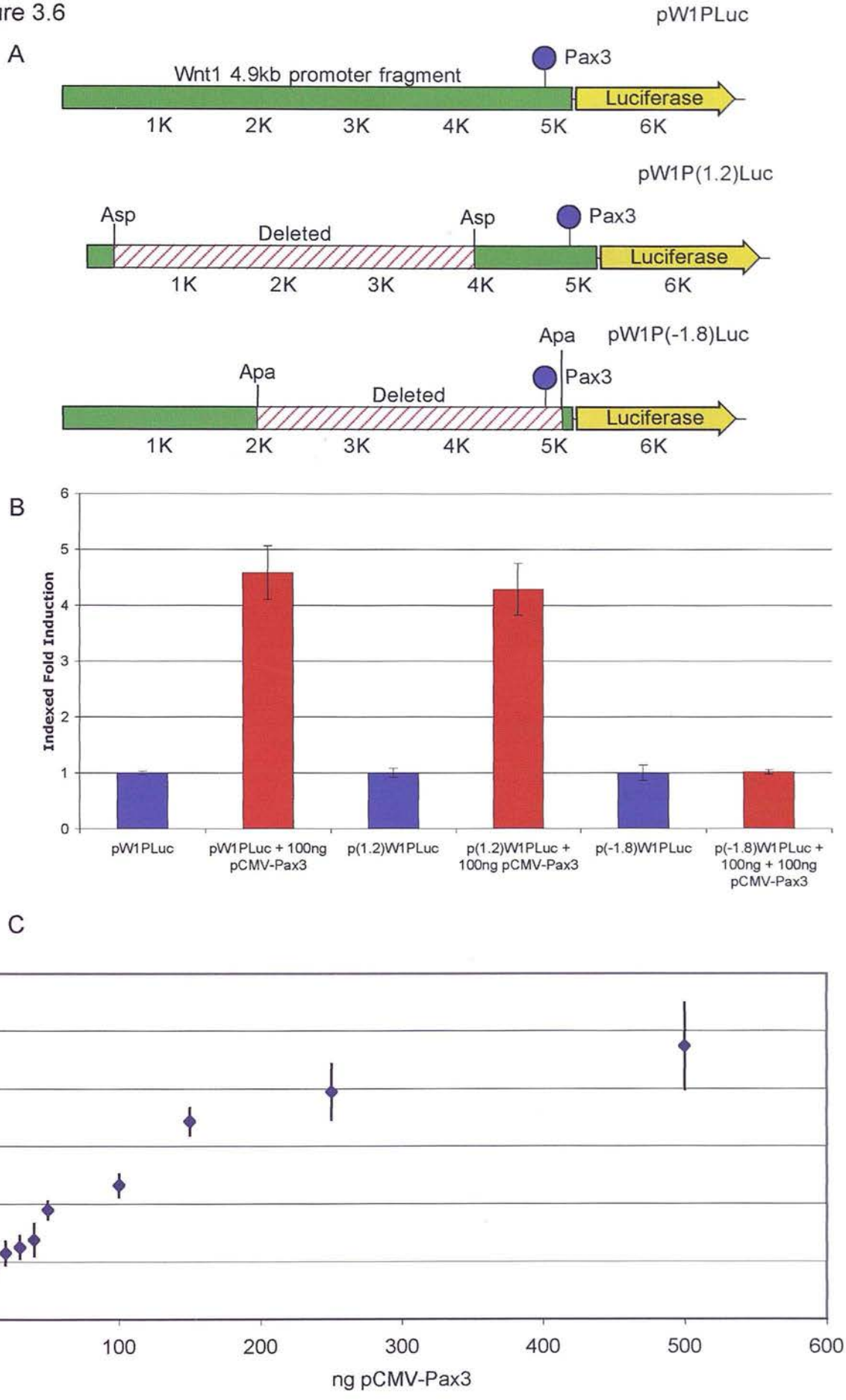
pW1PLuc
A
Wnt1 4.9kb promoter fragment
Pax3
Luciferase
1K
2K
3K
4K
5K
6K
pW1P(1.2)Luc
Asp
Deleted
Asp
Pax3
Luciferase
pW1P(-1.8)Luc
Apa
Apa
Deleted
Pax3
Luciferase
B
Indexed Fold Induction
pW1PLuc
pW1PLuc + 100ng pCMV-Pax3
p(1.2)W1PLuc
p(1.2)W1PLuc + 100ng pCMV-Pax3
p(-1.8)W1PLuc
p(-1.8)W1PLuc + 100ng + 100ng pCMV-Pax3
C
Indexed Fold Induction
ng pCMV-Pax3

Figure 3.6:
A) Schematic of pW1PLuc and deletion constructs pW1P(1.2)Luc and pW1P(-1.8)Luc, Asp = Asp718, Apa = ApaI sites
B) Luciferase data comparing the induction of the *Wnt1* promoter deletion constructs with 100ng pCMV-Pax3 vs. empty vector. Data is normalised luminescence expressed as fold induction over baseline (pG3basic) and indexed (empty vector = 1) to enable comparison between constructs. n > 3 for each data point.
C) Variation in Luciferase induction from pW1PLuc and pW1P(1.2)Luc over a range of Pax3 concentrations (expressed as ng pCMV-Pax3 plasmid used in each transfection). Data is normalised luminescence expressed as fold induction over baseline (pGL3basic) and indexed to enable comparison bewteen experiments n = 5 - 11 (depending on data point), error bars represent SEM.

generate this biphasic response, the apparent plateau of transcriptional induction from 250ng of pCMV-*Pax3* per well would suggest this is not the case. Perhaps the mode of *Pax3* transcriptional induction on the *Wnt1* and NCAM promoters differs, explaining this discrepancy.

The data presented above strongly argue that *Pax3* can bind to and transactivate the *Wnt1* promoter *in vitro*, and that this interaction occurs via the *Pax3* consensus site identified. To show that the *Pax3* consensus site is necessary and sufficient for this observed *Pax3* induction, site directed mutagenesis was performed to ablate the core binding residues, and replace them with a low affinity sequence. Primers were designed to mutate the TCGC core *Pax3* binding consensus (as defined by MatInspector and (Chalepakis and Gruss, 1995; Phelan and Loeken, 1998; Underhill, 1997), etc) to the sequence ATAA. The actual primers held a mutation in an additional base 5' to the TCGC sequence, altering the native sequence CTCGC to GATAA. The reason for this additional change is that the mouse promoter sequence contains a tandem repeat of the core consensus; TCGCTCGC. It was feared that the preceding TCGC might be able to substitute for the mutated core consensus, so the final base of this was also mutated. An alignment of these sequences can be seen in Figure 3.7A. Site directed mutagenesis was performed on pW1P(1.2)Luc using a QuikChange Site Directed Mutagenesis kit (Stratagene), and the primers W1_sub_FWD and W1_sub_REV (see Appendix 2). Clones were screened by sequencing (from the GL3 primer within the Luciferase ORF (Promega)) and aligned to the wild type sequence to confirm the specificity of the mutagenesis. The resulting plasmid was named pW1PΔLuc.

Figure 3.7 :
A) Sequence alignment of wild type and mutated Pax3 core consensus sequence
on the plasmids pW1P(1.2)Luc and pW1P<delta>, respectively
B) Luciferase data contrasting luciferase induction on co-transfection with pCMV-Pax3 between pW1P(1.2)Luc and pW1P<delta>. Mutant Wnt1 promoter shows a compete loss of Pax3 induction; co-transfection experiments with wild type promoter were conducted in tandem to ensure any loss of luciferase induction in the mutant could not be attributed to other factors. n = 3, error bars are SEM.

A

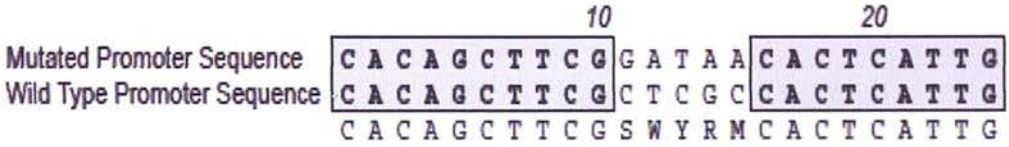

B

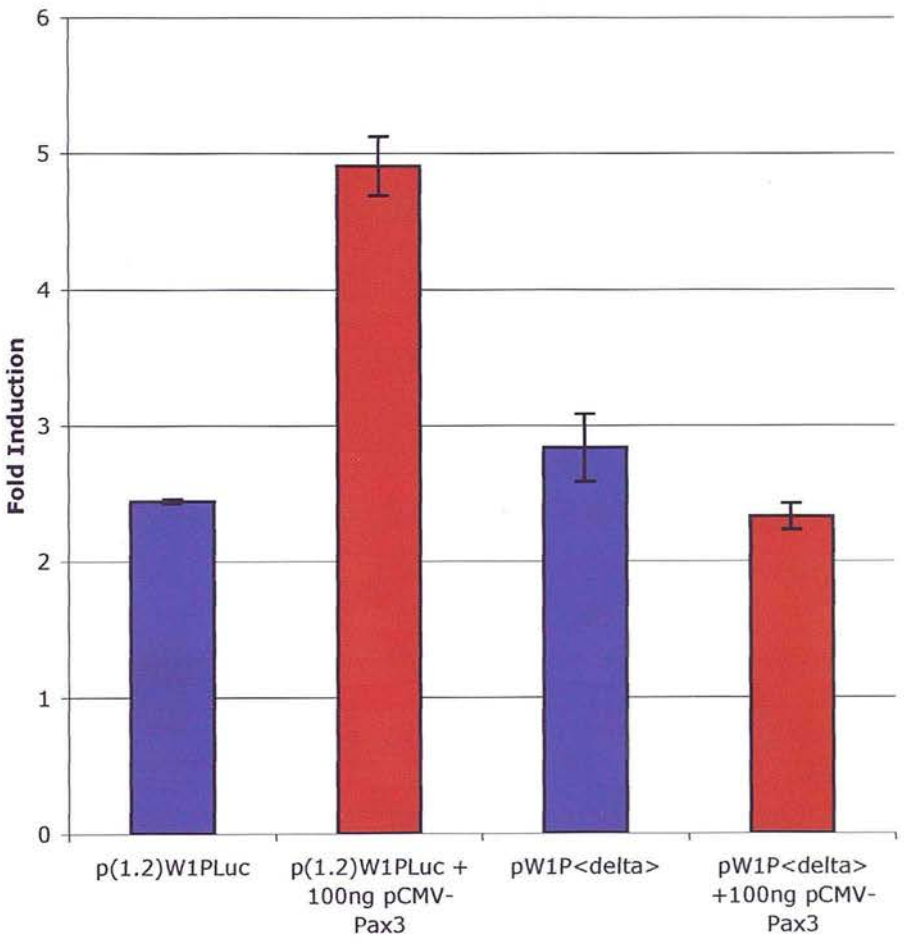

Co-transfection experiments, using pCMV-*Pax3* at levels previously shown to elicit a strong induction of Luciferase activity from the un-mutated plasmid (100ng) were then performed using pW1PΔLuc as the reporter construct. A total loss of *Pax3* induction was observed on co-transfection with the pCMV-*Pax3* plasmid. To ensure this loss of induction was due to the consensus site mutation and not a general failure of the Luciferase assay system, experiments using the un-mutated pW1PLuc reporter construct were run in tandem. No loss of *Pax3* induction was observed. These data can be seen in Figure 3.7B.

It was concluded from these experiments that the transcriptional induction driven from the *Wnt1* promoter by *Pax3* was due to the interaction of the protein with this consensus binding site.

Electrophoretic mobility shift analysis (EMSA) was not performed on this sequence. This was because the mutation incorporated into the pW1PΔLuc plasmid was based on one made by (Kwang et al., 2002). In this study, the core consensus site for *Pax3* binding to the *Msx2* promoter, TCAC (TCGC here) was mutated to GATA (GATAA here). This mutation was used to show the specificity of *Pax3* binding in a series of EMSA experiments where this mutation causes a complete loss of *Pax3* binding. Given the similarities of the core consensus sites in question, and the nature of an EMSA experiment (i.e. purified protein binding to radiolabelled oligonucleotide), an EMSA performed using the *Wnt1* promoter *Pax3* consensus described above would be an almost exact copy of the experiment reported by this group. It was decided that an EMSA could not generate a sufficiently informative result in this context and was therefore omitted.

Discussion (Hypothesis One)

The above studies address several of the issues raised by Hypothesis One. *Pax3* does appear to be able to up-regulate the expression of a reporter gene, at least *in vitro*, using the *Wnt1* regulatory elements and via a defined consensus site. This interaction does not occur via the 3' distal enhancer element but by the 5' proximal promoter, as shown here. These experiments do not confirm the occupation or biological relevance of this site *in vivo*. The experimental data reported in Chapters 5 and 6 will complete the investigation of this hypothesis by addressing this final issue.

Regulation of Wnt1 *by* Msx2

To investigate the potential role for *Wnt1* in the regulation of the cardiac neural crest, as implicated by both the Sp^{2H} mutant phenotype (Conway et al., 2000) and *Dvl2* and *Pitx2* knockout phenotypes (Hamblet, 2002) and (Kioussi, 2002), the possibility of a further regulatory interaction between *Msx2* and *Wnt1* was examined, given the data presented in (Kwang et al., 2002).

Hypothesis Two

Wnt1 transcription is directly downregulated by Msx2, most probably by the distal 3' enhancer element, in vivo *with implications for the normal development of the cardiac neural crest.*

To investigate this possibility *in vitro*, a series of luciferase co-transfection experiments were conducted in a manner analogous to that described above. Firstly, an *Msx2* expression vector was required. A search of the HGMP clone database was conducted and a potential full length *Msx2* cDNA was identified. This was ordered and sequenced to confirm this was indeed a full length and mutation free *Msx2*. The vector within which the cDNA was supplied was a CMV expression vector (pCMV-Sport6 (Invitrogen)) analogous to the one used to generate the pCMV-*Pax3* construct. Sequencing also confirmed that the *Msx2* cDNA was in the correct orientation and position to enable its expression to be driven by the CMV promoter on transfection into a mammalian cell line. This construct is illustrated in Figure 3.8.

NIH-3T3 cells were transfected with pCMV-*Msx2*, and a Western blot using an anti-Msx1/2 monoclonal obtained from the Developmental Studies Hybridoma Bank (DSHB) was then conducted on the protein extracts to confirm expression. This can be seen in Figure 3.8; the predicted molecular weight of *Msx2* is ~28kDa (ensembl). This confirms the expression of *Msx2* in cells transfected with the pCMV-*Msx2* plasmid.

The MatInspector analyses of putative transcription factor binding sites in the *Wnt1* promoter and enhancer elements were then re-examined to identify any *Msx2* consensus in these regions. This analysis revealed no *Msx2* sites in the *Wnt1* promoter

Figure 3.8 :
Schematic of pCMV-Msx2 and Western blot confirming expression in transfected NIH-3T3 cells using anti-Msx1/2 from DSHB resource.

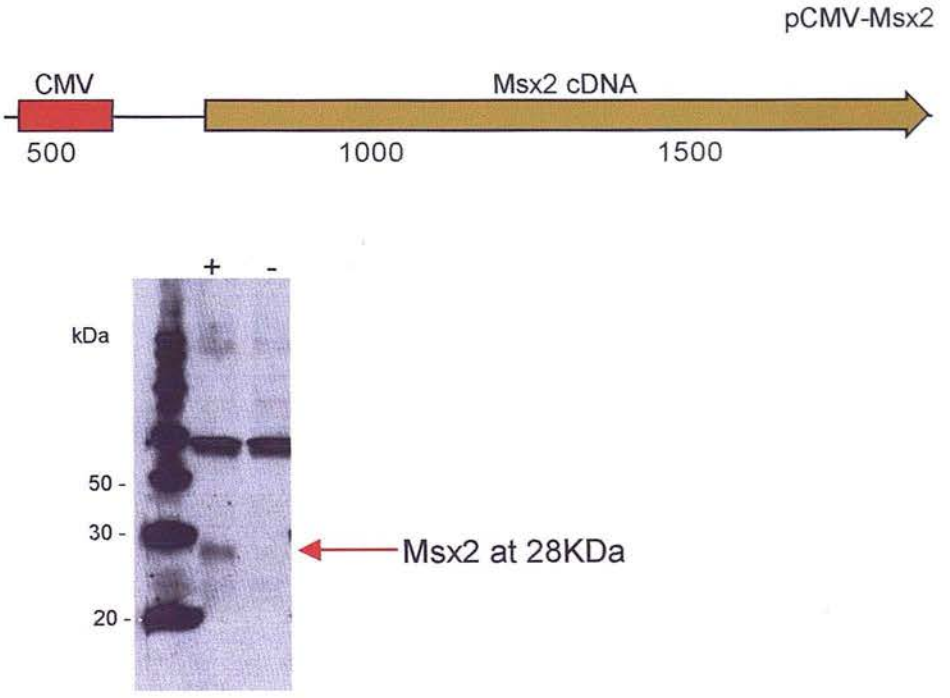

region, but an *Msx2* consensus site in the distal 3' enhancer. Furthermore, this site was found to lie within the conserved 110bp element shown by (Rowitch et al., 1998) to control *Wnt1* expression in the early neural plate and developing brain. This site is illustrated in Figure 3.9B.

To investigate this further, co-transfections of the pCMV-*Msx2* vector and the pW1PLuc and pW1P(1.2)Luc reporter plasmids were performed. No consistent response to *Msx2* co-expression could be observed over a range of pCMV-*Msx2* concentrations with either plasmid, see Figure 3.9A. The pCMV-*Msx2* construct was then tested with the pW1ELuc plasmid, see Figure 3.9B. This experiment illustrated a potentially interesting and highly significant repression of around 50% at 250ng pCMV-*Msx2*, n = 3.

To analyse this interaction further, a series of deletion constructs were made of the *Wnt1* enhancer. In these constructs the 5.5kb *Wnt1* enhancer fragments present in pW1ELuc was restricted further by BamHI and SpeI digests to extract internal fragments. The backbone was then re-ligated to generate the serial deletion plasmids pW1E(bam)Luc and pW1E(spe)Luc. These are illustrated in Figure 3.10A. Neither of these constructs carry a deletion for the *Msx2* consensus site predicted by MatInspector analysis. Deleting a small region containing this site in the plasmid by restriction digest proved impossible. Two MbiI sites were observed flanking a small region containing the *Msx2* consensus and the highly conserved 110bp element within the larger enhancer region. Since the presence of other MbiI sites elsewhere within the backbone prevented a conventional deletion, the inverse experiment was performed. In this case, the 816bp MbiI fragment was then extracted from a digest of

Figure 3.9

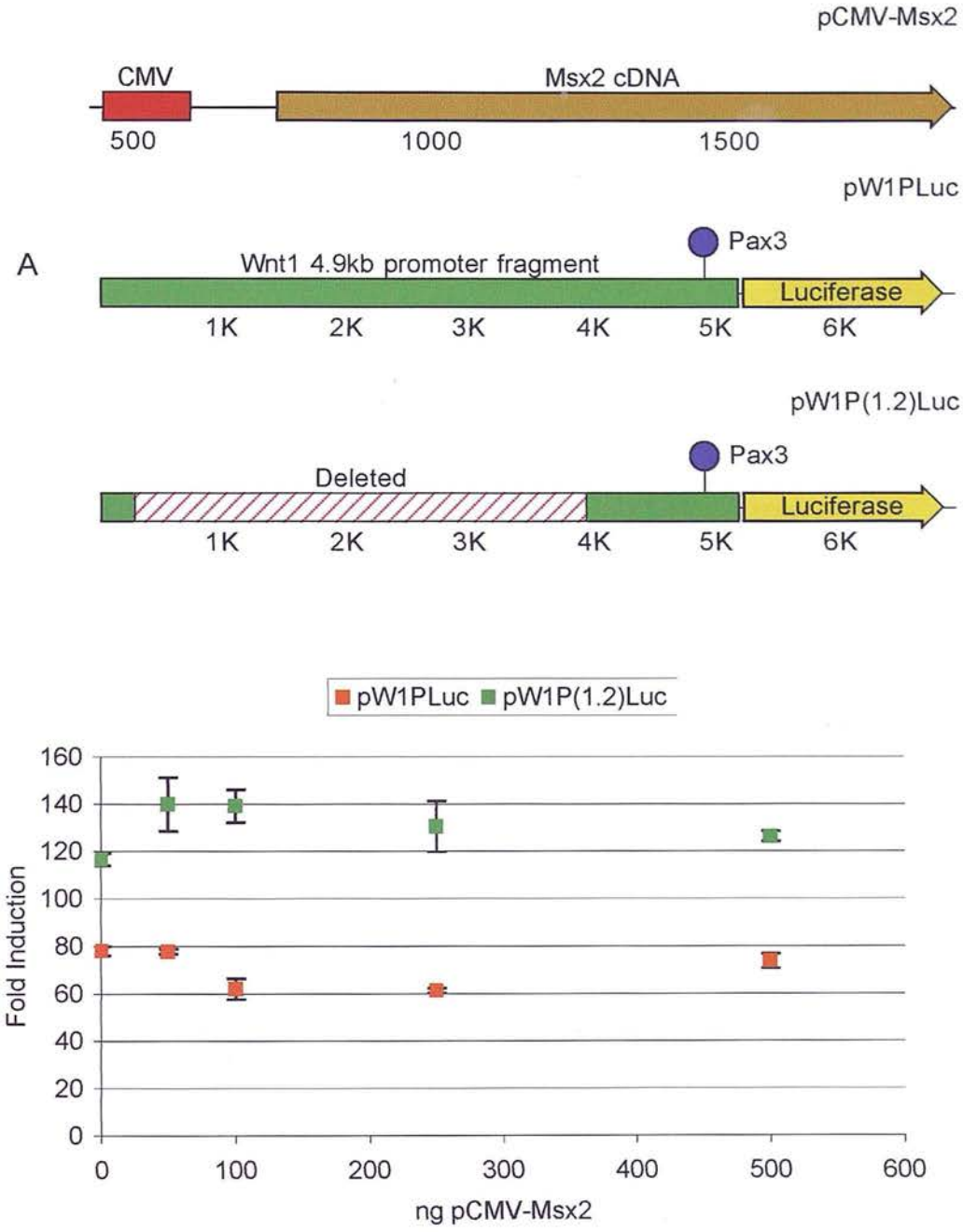
pCMV-Msx2
CMV
Msx2 cDNA
500
1000
1500
pW1PLuc
A
Wnt1 4.9kb promoter fragment
Pax3
Luciferase
1K
2K
3K
4K
5K
6K
pW1P(1.2)Luc
Deleted
Pax3
Luciferase
1K
2K
3K
4K
5K
6K
pW1PLuc
pW1P(1.2)Luc
Fold Induction
160
140
120
100
80
60
40
20
0
0
100
200
300
400
500
600
ng pCMV-Msx2

Figure 3.9:
A) *Wnt1* promoter constructs used to test the response of the Wnt1 promoter to co-expression with Msx2 (from pCMV-Msx2). Luciferase response to co-expression with Msx2. Data expressed as fold induction over baseline (pGL3basic). n = 3, error bars represent SEM
B) *Wnt1* enhancer construct used to test the response of the Wnt1 enhancer to co-expression with Msx2. Luciferase response expressed as fold induction over baseline (pGL3promoter). n = 3, error bars represent SEM.

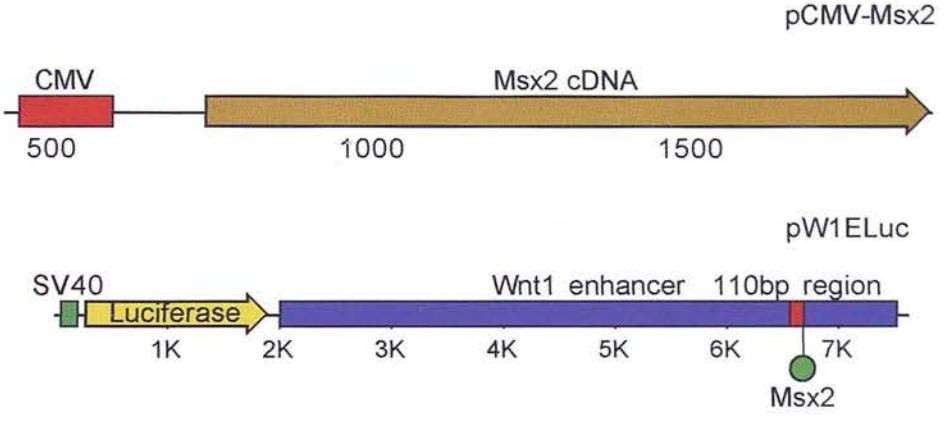

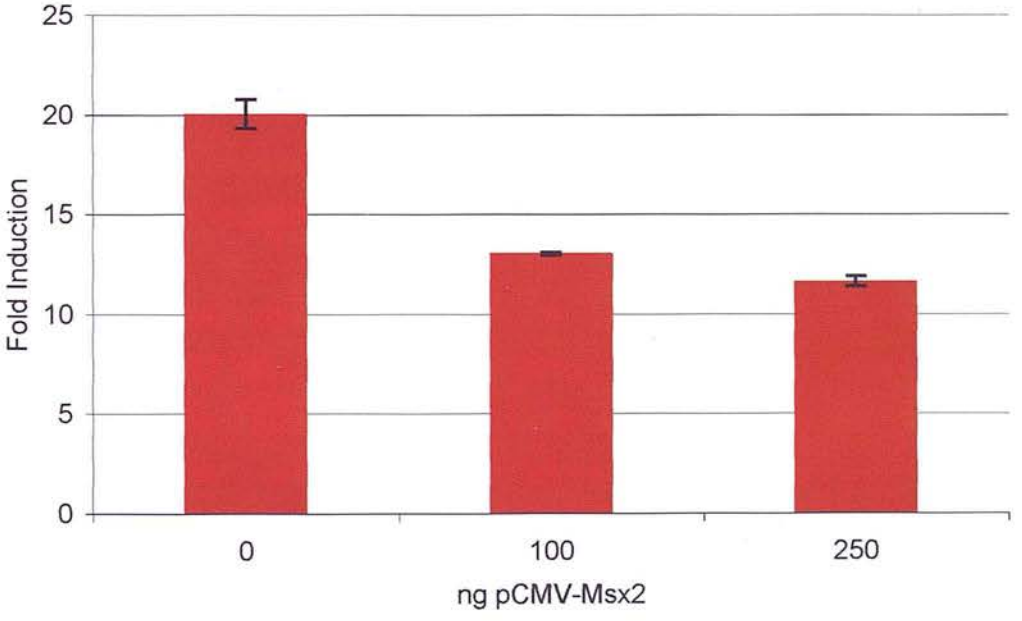

the pW1ELuc plasmid and then shuttled into an empty pGL3Promoter vector restricted with SmaI. This not only extracts the *Msx2* containing fragment from the *Wnt1* enhancer, but also places it within a different context within the Luciferase reporter vector. Since this region has been shown to behave as a canonical enhancer element by other groups (Echelard et al., 1994; Rowitch et al., 1998) and is therefore thought to be position and orientation independent, this was hoped to have no adverse effect on the ability of this element to respond to *Msx2*. This construct is also illustrated in Figure 3.10A

Co-transfection with pCMV-*Msx2* expression plasmid revealed that neither the pW1E(bam)Luc nor the pW1E(spe)Luc reporter plasmids demonstrated any significant loss of *Msx2* inhibition. Both of these plasmids retain the *Msx2* consensus site. When *Msx2* was co-expressed with the pW1E(mbi)Luc plasmid with the *Msx2* containing fragment shuttled into a new vector, an almost identical level of repression was observed. These data can be seen in Figure 3.10B and 3.10C. (N.B. Previous controls (see the Luciferase Assay subsection in Chapter 2) were performed to ensure that the SV40 weak promoter carried on the pGL3promoter vector did not respond to *Msx2* co-expression).

From the above it was concluded that the *Wnt1* enhancer, and not the *Wnt1* promoter, was able to respond to *Msx2* to repress transcription of a reporter gene. Furthermore, this repressive response could be mapped to an 816bp region containing an *Msx2* consensus binding site within an area of the *Wnt1* enhancer demonstrated by previous studies to be both highly evolutionarily conserved and of great regulatory

Figure 3.10

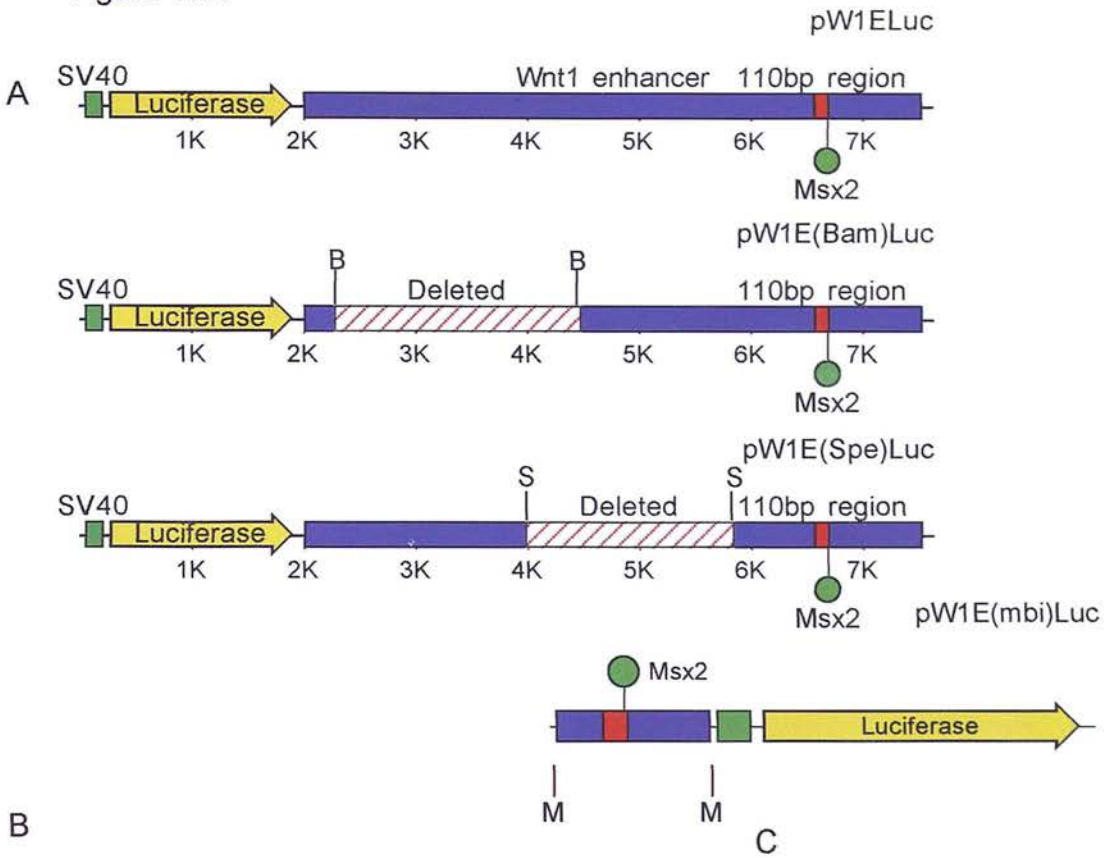
A
pW1ELuc
SV40
Luciferase
Wnt1 enhancer
110bp region
1K
2K
3K
4K
5K
6K
7K
Msx2
pW1E(Bam)Luc
B
B
Deleted
pW1E(Spe)Luc
S
S
pW1E(mbi)Luc
M
M

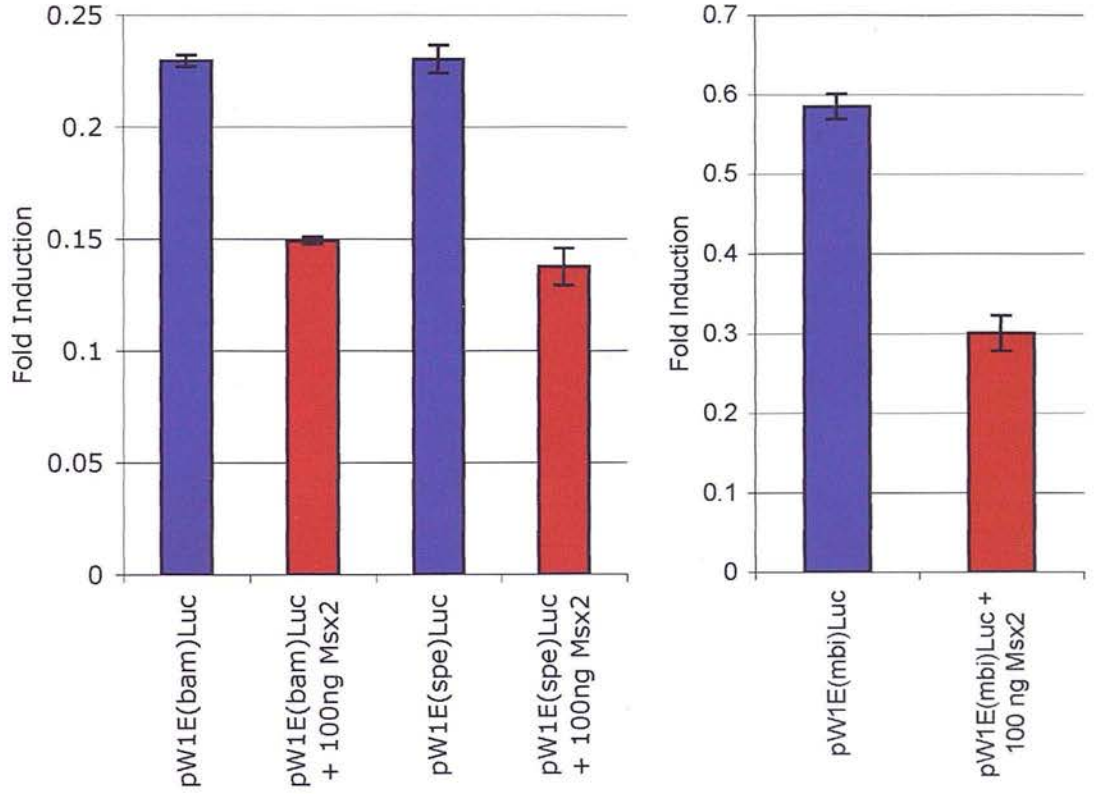
B
Fold Induction
0.25
0.2
0.15
0.1
0.05
0
pW1E(bam)Luc
pW1E(bam)Luc + 100ng Msx2
pW1E(spe)Luc
pW1E(spe)Luc + 100ng Msx2

C
Fold Induction
0.7
0.6
0.5
0.4
0.3
0.2
0.1
0
pW1E(mbi)Luc
pW1E(mbi)Luc + 100 ng Msx2

Figure 3.10:
A) Schematic of *Wnt1* enhancer deletion constructs used to dissect the response of the *Wnt1* enhancer to co-expression with Msx2. B = BamHI, S = SpeI, M = MbiI sites used in cloning
B) Luciferase response of deletion constructs to co-expression with 100ng pCMV-Msx2.Data expressed as fold induction over baseline (pGL3promoter), n = 3,error bars represent SEM
C) Luciferase response of pW1E(Mbi)Luc construct to co expression with 100ng pCMV-Msx2.Data expressed as fold induction over baseline (pGL3promoter), n = 3,error bars represent SEM

significance. Unfortunately, attempts to mutate this site with site directed mutagenesis were not be performed due to time constraints within this project.

Pax3 *and* Msx2*: a regulatory relationship at the* Wnt1 *locus?*

Any possible role of *Wnt1* regulation in the development of the cardiac neural crest is likely to be extremely complex. The above study, however, has demonstrated that, *in vitro*, there is the possibility that *Pax3* may act to induce the expression of *Wnt1* via its promoter and that *Msx2* may conversely inhibit *Wnt1* expression via its 3' enhancer. The basis for much of this hypothesis in terms of the cardiac neural crest is derived from a study by (Kwang et al., 2002) where they demonstrate that *Msx2* is a downstream target for negative regulation by *Pax3*, and its expression domain is expanded in the Sp^{2H} mutant background (See Chapter 1 for a full discussion of these findings). It would be interesting to examine the possibility that the inhibition of *Wnt1* expression by *Msx2* can further be overridden by the induction of *Pax3* binding to the *Wnt1* promoter. This would give *Pax3* two mechanisms through which to ensure the correct level of *Wnt1* expression in the wild type; both inhibition of *Msx2* expression, as established by (Kwang et al., 2002), and also through the alleviating the repression of *Wnt1* by *Msx2* via an interaction on the regulatory elements of this gene.

To begin to examine this possibility *in vitro*, a construct was made carrying both the *Pax3* responsive *Wnt1* promoter and the *Msx2* responsive *Wnt1* enhancer. This construct was named pW1EPLuc and was made by shuttling the *Wnt1* promoter fragment from pW1P(1.2)Luc as an Asp718 – NcoI fragment into the same sites on the pW1E(bam)Luc reporter construct. This construct is illustrated in Figure 3.11A.

Figure 3.11:
A) Schematic of construct pW1EPLuc, A = Asp718 N = NcoI sites used in cloning
B) Luciferase response of pW1EPLuc on co-transcfection with 250ng pCMV-Script (blue), 250ng pCMV-Msx2 (orange) and 250ng of both pCMV-Msx2 and pCMV-Pax3. n = 9, 3 and 3, repectively. * p = 0.0072, ** = 0.0001 (two sample t test)

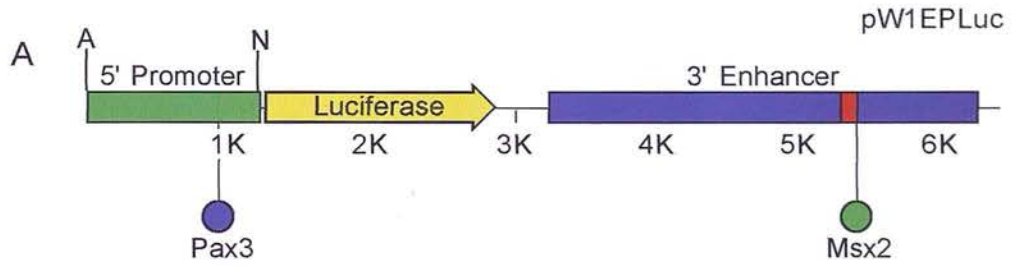

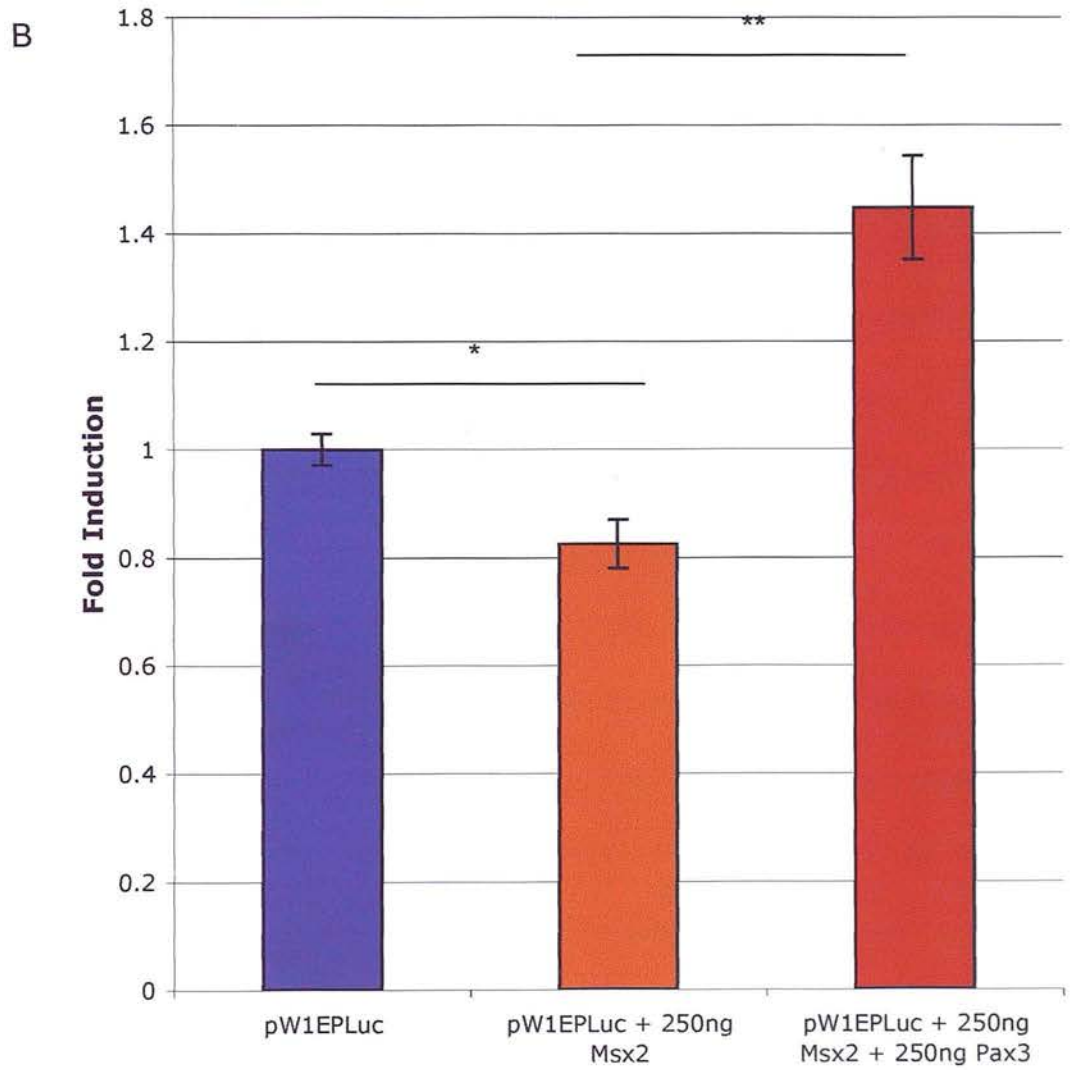

pW1EPLuc was co-transfected with pCMV-*Msx2* to show that *Msx2* was still able to significantly inhibit the transcription of the Luciferase reporter in this context. Next pCMV-*Pax3* was also co-transfected with pCMV-Msx2 and it was demonstrated that the induction by *Pax3* via the *Wnt1* promoter was clearly able to override any inhibitory effect mediated by *Msx2* in this experimental system, see Figure 3.11B.

This enables the very tentative conclusion that *Pax3* may be able to alleviate any repression of *Wnt1* expression generated by *Msx2*. Obviously, there are numerous substantial flaws with this final piece of analysis, and these results should be interpreted with great caution. Firstly, the relative levels of expression of *Msx2* and *Pax3* from their respective expression constructs could not be meaningfully assessed; even Western blotting could not control for differing affinities of the two antibodies. It is impossible in this system to control for the levels of protein produced. An alleviation of repression by *Pax3* could simply be a reflection of the pCMV-*Pax3* plasmid producing significantly more protein than pCMV-*Msx2*. Secondly, the observable level of repression from *Msx2* co-expression with the pW1EPLuc reporter is inherently much lower than with the pW1ELuc family of reporters. This is because the endogenous activity of the *Wnt1* promoter in the NIH-3T3 line is very low compared to that driven from the SV40 weak promoter found on all pGL3promoter derived vectors used to generate the pW1ELuc vectors (no cell line naturally expressing *Wnt1* has been reported). Any reduction of expression in this context is necessarily going to be difficult to observe. Finally, this experiment contains four variables (two regulatory elements and two transcription factors) and is therefore almost impossible to meaningfully control. This data should be treated with extreme

caution and is presented here merely as a final observation of a potential relationship, rather than as proof of any interaction.

Discussion (Hypothesis Two)

The above studies address the issues raised by hypothesis two in a number of ways. It was demonstrated that *Msx2* can repress reporter gene expression *in vitro* and that this occurs via the 3' enhancer element as predicted. The responsive region was mapped to an 816bp MbiI fragment containing an *Msx2* consensus, but mutagenesis of this fragment was not conducted. It is concluded that this repression is likely to be mediated by this binding site, in light of the other evidence presented. Finally, evidence is provided that the inductive ability of *Pax3* mediated by the *Wnt1* promoter may be able to override the inhibitory effects of *Msx2* on the *Wnt1* enhancer, although this is a tentative conclusion. None of the above experiments demonstrate occupancy of these sites *in vivo*. This aspect of hypothesis one and hypothesis two is addressed in Chapter 6.

Chapter Four: *Pax7* regulation

Introduction

In this chapter regulatory elements for the *Pax7* gene are described, and potential direct regulatory interaction between these and the *Pax3* protein tested and mapped *in vitro*. *Pax7* represents an interesting potential target of *Pax3* regulation not only due to its developmentally dynamic expression pattern (Jostes et al., 1990) or role in the development of regenerating muscle from an adult stem cell population (Seale et al., 2000), but also due to the existing controversy over the relationship between these two genes in the mouse (Borycki et al., 1999; Relaix et al., 2004). A range of both wet and dry approaches were used to characterise the mouse *Pax7* genomic locus, identify a number of interesting features and map a candidate region for both a 5' proximal promoter and a regulatory feature within intron 1. These were then verified experimentally in a *Pax7* expressing cell line (C2C12) and a *Pax3* response determined.

Pax7 *regulatory regions: Bioinformatics*

Since no information on the mouse *Pax7* genomic locus had been reported, and no regulatory regions had been experimentally verified, a bioinformatic analysis of the *Pax7* gene was performed. Using the mouse genome sequence database 100kb on either side of the predicted mouse *Pax7* gene was downloaded and used in subsequent

analyses (ensembl). Firstly, the exons and introns were mapped using the published mouse cDNA sequence (Ziman et al., 2001). The mouse *Pax7* locus is shown in Figure 4.1A, and shows a similar genomic organisation to that reported for human *PAX7* (Vorobyov et al., 1997).

In the search for gene regulatory elements, the obvious starting point is the 5' end of the gene which is likely to contain a minimal promoter driving transcription. To this end, ~10kb around exon 1 (N.B. since the 5'UTR for the mouse *Pax7* gene had not been determined experimentally, 'exon 1' refers to the coding sequence from the ATG start site through to the first intron boundary) was subjected to a NIX analysis (HGMP). This uses a range of sequence analysis software to identify putative features of genomic sequence, taking into account species of origin and size of fragment. This analysis identified a CpG island, a putative promoter region and a potential RNA polymerase II start site, all 5' proximal to exon 1 (within 1kb upstream). These are illustrated in Figure 4.1B.

To take this analysis a step further, the mouse *Pax7* locus was then analysed in tandem with the human *Pax7* genomic region. Comparative sequence analysis can be used to identify likely regions of regulatory significance in non-coding DNA on the basis of sequence conservation. The assumption is that sequence changes in important genomic elements (i.e. coding or regulatory sequences) will be strongly selected against in evolution. Similarly, sequences encoding no genetic information can be mutated without any adverse effect on the fitness of the organism and are therefore not selected against. If a region of non-coding DNA is conserved at the sequence level between two species which shared a common ancestor millions of years ago, this

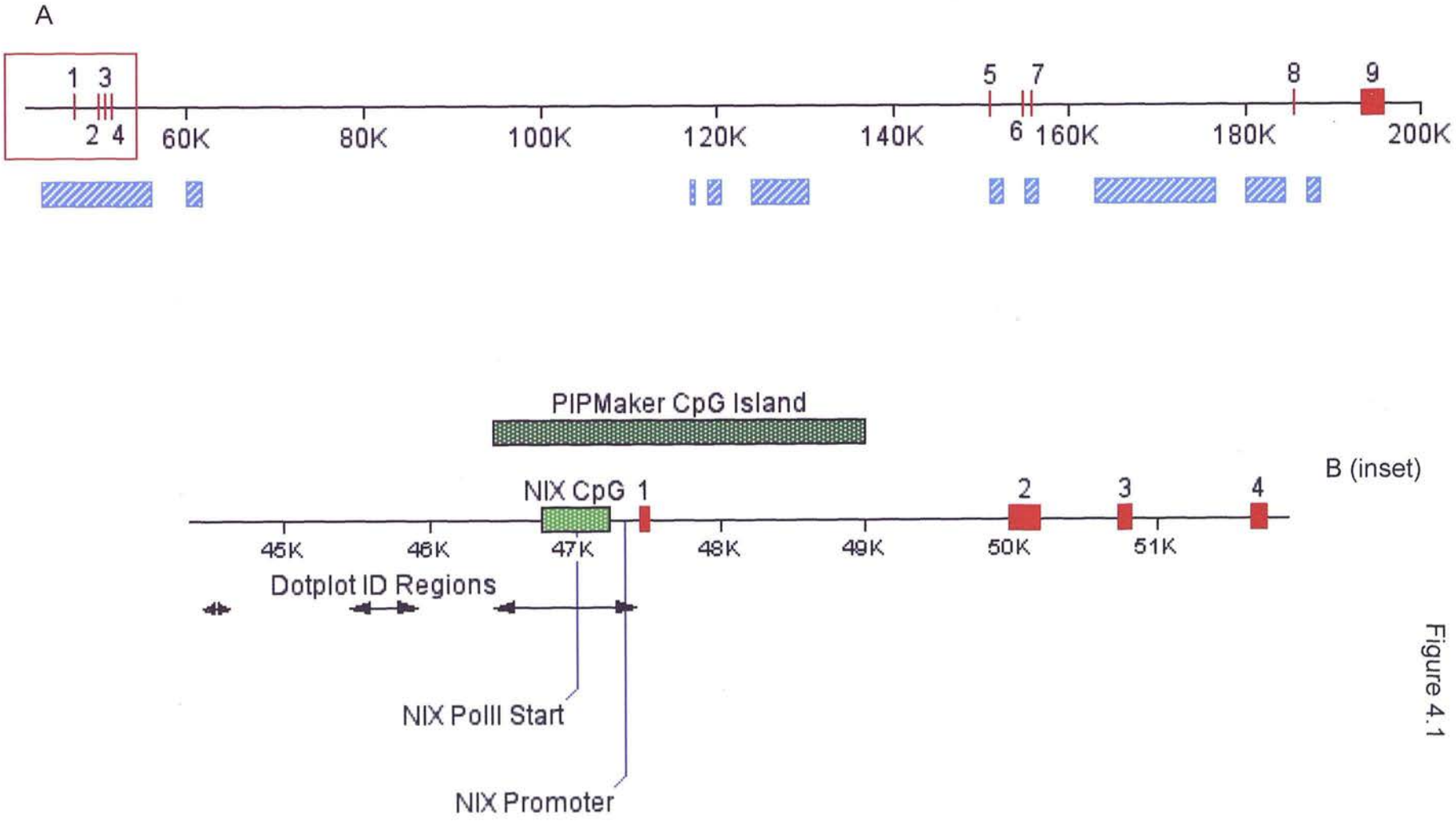
A
1 3
2 4
5 7
8 9
6
60K
80K
100K
120K
140K
160K
180K
200K
PIPMaker CpG Island
B (inset)
NIX CpG 1
2 3 4
45K
46K
47K
48K
49K
50K
51K
Dotplot ID Regions
NIX PolII Start
NIX Promoter

Figure 4.1

C

Figure 4.1

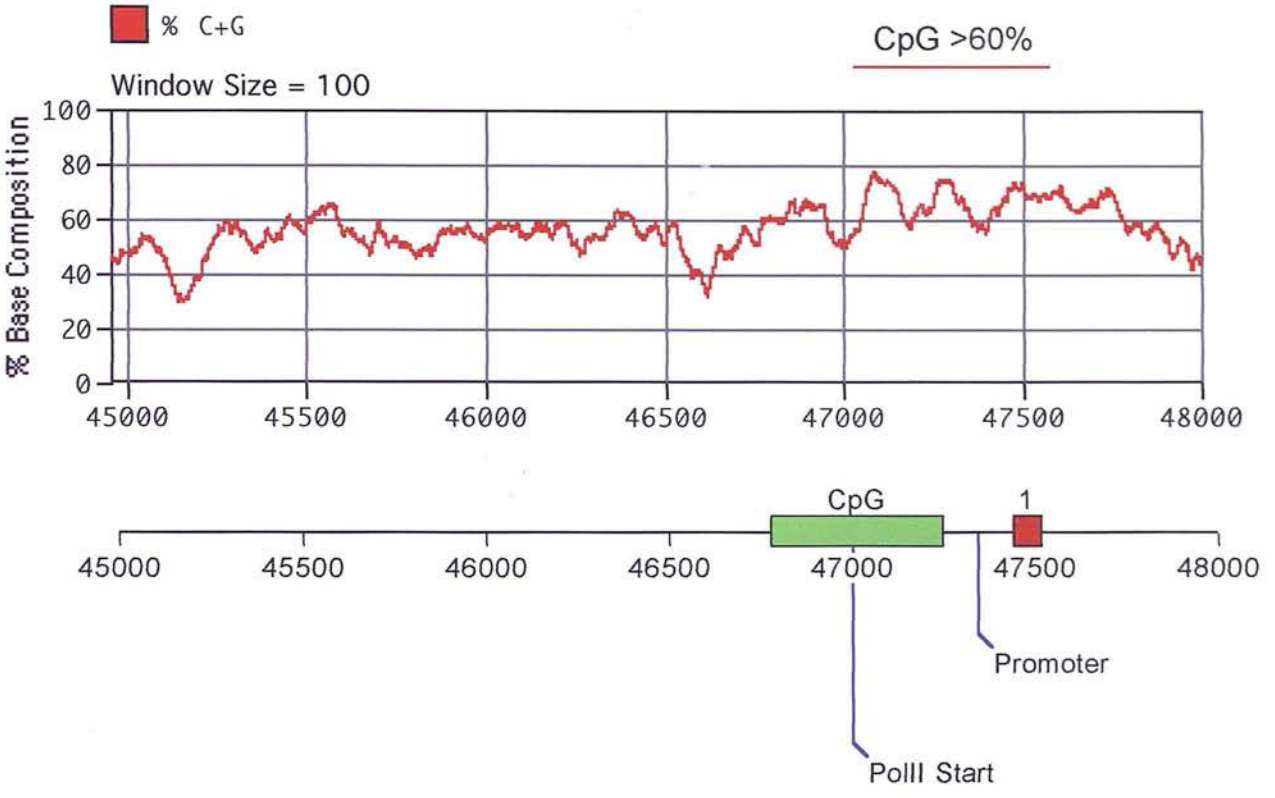
% C+G
CpG >60%
Window Size = 100
% Base Composition
100
80
60
40
20
0
45000
45500
46000
46500
47000
47500
48000
CpG
1
Promoter
PolII Start

D

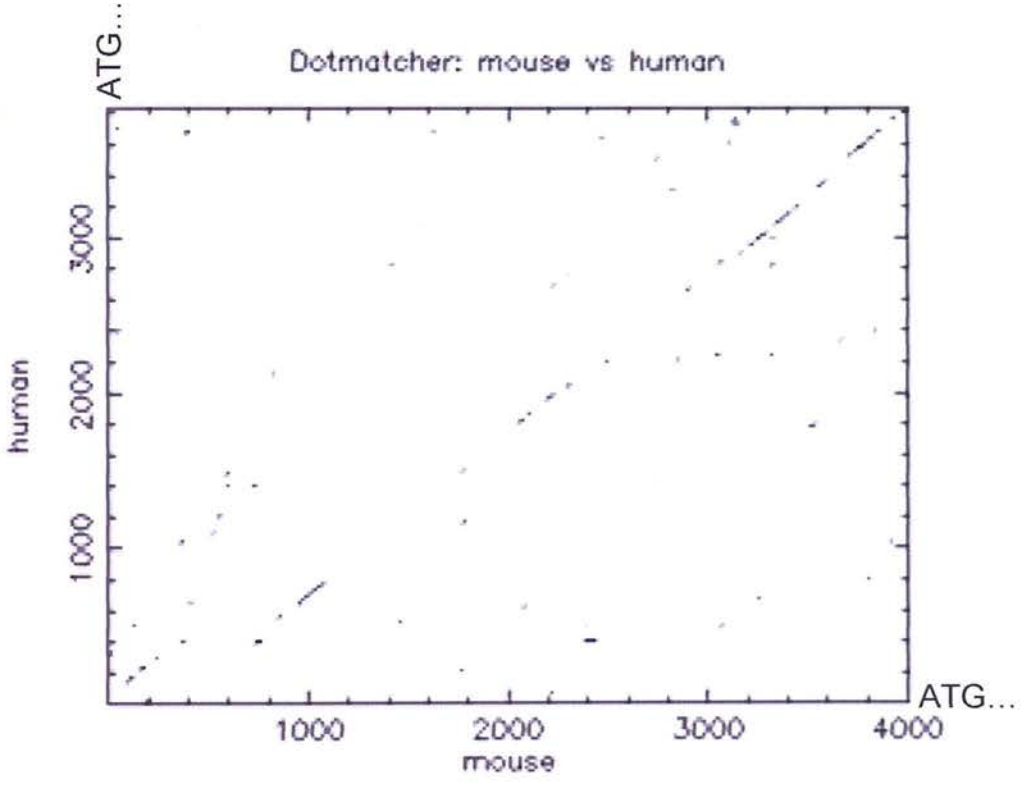
Dotmatcher: mouse vs human
ATG...
human
1000
2000
3000
ATG...
1000
2000
3000
4000
mouse

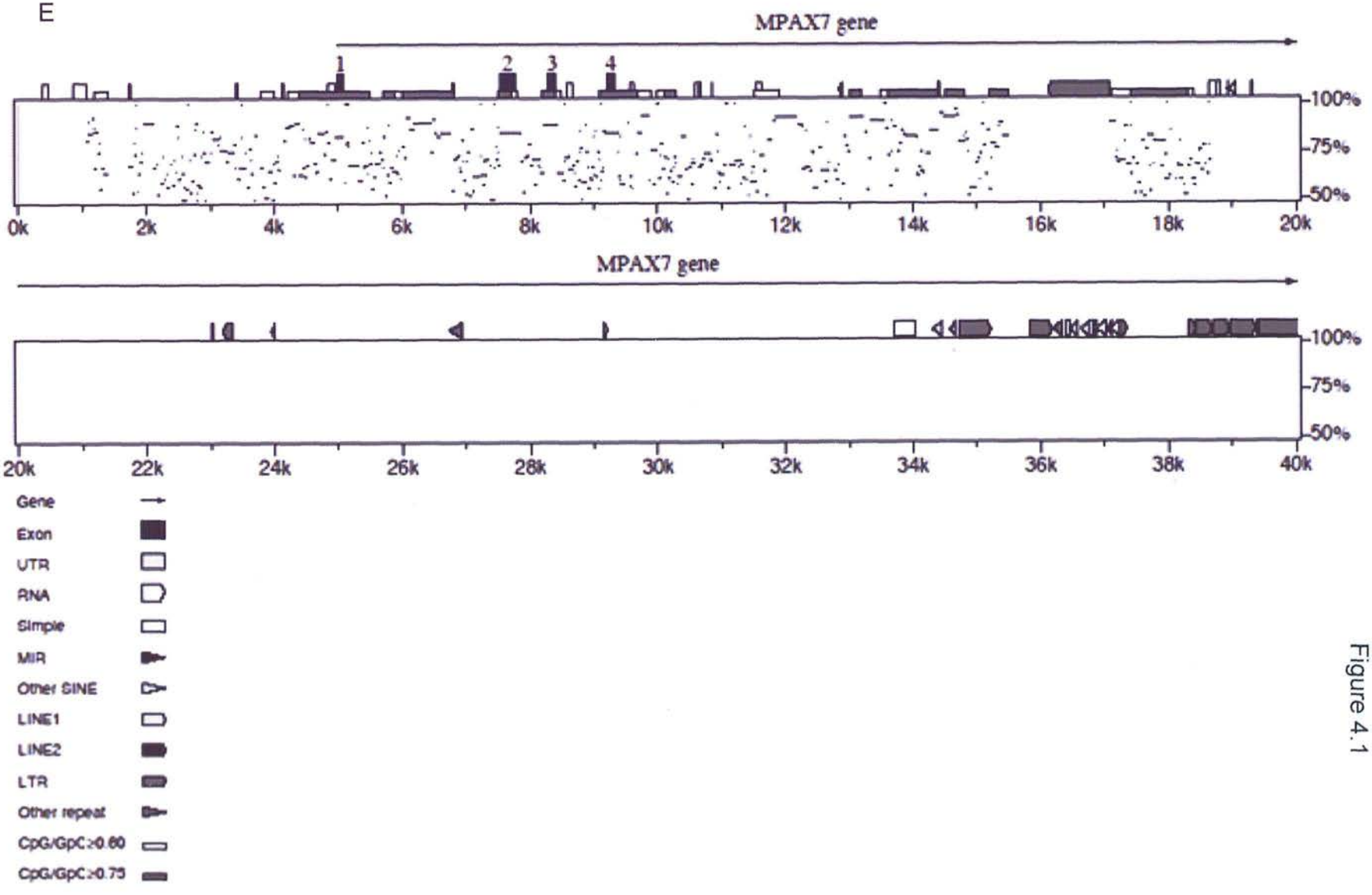
E
MPAX7 gene
1
2
3
4
100%
75%
50%
0k
2k
4k
6k
8k
10k
12k
14k
16k
18k
20k
MPAX7 gene
100%
75%
50%
20k
22k
24k
26k
28k
30k
32k
34k
36k
38k
40k
Gene
Exon
UTR
RNA
Simple
MIR
Other SINE
LINE1
LINE2
LTR
Other repeat
CpG/GpC>0.60
CpG/GpC>0.75

Figure 4.1

Figure 4.1:
N.B. Exon 1 in all figures starts at ATG of coding sequence.
A) Annotated *Pax7* locus, spanning 200kb. Red boxes are exons predicted from cDNA sequences, shaded blue boxes represent areas of significant PIPMaker identified homology of >60% between human and mouse genomic sequences (see Figure 4.1E, and appendix 3 for a complete output).
B) Inset of 5' end of *Pax7* locus shown in A. Shows relative positions of exons 1 - 4, CpG islands predicted by NIX and PIPMaker analyses, RNA PolII and promoter sites identified by NIX, and regions of homology identified by Jemboss Dotmatcher software (see Figure 4.1D)
C) %C+G plot for 3kb around *Pax7* exon 1 (upper) and corresponding genomic locus (lower) showing NIX identified features. %C+G calculated as moving average from window of 100 bp. Note increase in CG content proximal to the 5' end of exon 1 (red line).
D) Dotmatcher dotplot of human (y axis) vs mouse genomic (x axis) *Pax7* locus upstream of ATG. Sequences of high position and sequence identity represented by a diagonal line of dots between the two axis. Results summarised graphically in Figure 4.1B. (Window size = 10, Threshold = 23, Blossum matrix)
E) PIPMaker output for the first 40kb of the *Pax7* locus. Showing CpG islands, repetitive sequences, exons and percentage identity to human sequence (dots in vertical dimension running beneath genomic locus in horizontal plane represent % identity at that point)

homology can be interpreted as a potentially important site of regulation (see (Cooper and Sidow, 2003; Wasserman and Sandelin, 2004) for review).

Firstly a simple alignment program, representing regions of homology between two sequences as a dot plot was performed. Regions of significant homology are summarised in Figure 4.1B and the Dotmatcher output (HGMP) shown in Figure 4.1D for the 5kb immediately upstream of exon 1. The presence of a CpG island in this region also potentially infers a regulatory significance (Cross and Bird, 1995). The MacVector program was then used to independently analyse the CG content regions upstream of exon 1, and also identified a CpG island in the upstream 1kb (Figure 4.1C). Finally, the PIPMaker suite was used to compare the entire genomic *Pax7* locus between human and mouse (Schwartz, 2000). The sample output can be seen in Figure 4.1E, and complete output in Appendix 3. This program found clear regions of homology in the sequences upstream of exon 1, and also identified a CpG island across the 2.5kb surrounding exon 1 (Figure 4.1B). The PIPMaker output can be seen in summary in Figure 4.1A as blue boxes demarcating regions of high human – mouse homology (>60%) next to the corresponding genomic region. Since a number of different bioinformatics programs had identified significant homologies between human and mouse sequences, and several other features of potential regulatory importance, it was concluded that the 1-1.5kb upstream of exon 1 provided an attractive candidate location for a *Pax7* promoter.

Pax7 *regulatory regions: 5'UTR mapping*

Bioinformatics can only identify regions of potential regulatory interest. To clone and test the *Pax7* promoter, it was necessary to first characterise the 5' untranslated region (5'UTR) of the *Pax7* transcript. This is because the regions of homology identified upstream of the coding exon 1 may represent novel upstream non-coding exons, rather than a promoter element, therefore positioning the transcriptional start site for the gene elsewhere. A schematic of the *Pax7* transcript, with a hypothetical 1kb 5'UTR drawn for illustrative purposes, can be seen in figure 4.2A. Several groups have studied the *Pax7* 5'UTR in humans, using two different techniques, and these results are summarised in figure 4.2B. In all cases, the 5'UTR reported represented an extension of the first coding exon, and not a novel upstream non-coding exon.

To investigate the 5'UTR of the mouse *Pax7* gene a number of different approaches were employed. Firstly, primer extension (PEXT) was used to size the 5'UTR of the mouse *Pax7* transcript. A schematic of this protocol can be seen in Figure 4.3A. Briefly, an antisense primer (kinase labelled at the 5' end with ^{32}P) anneals to the *Pax7* mRNA coding sequence, and the reverse transcriptase (RT) enzyme is then used to extend a cDNA from this point to the end of the 5' end of the 5'UTR. This is a quick method of approximately sizing the 5'UTR of *Pax7* from a number of different sources. These results are shown in Figure 4.3B. Several gels are shown illustrating results from using different *Pax7* mRNA sources and extending with different primers. Two 5'UTR sizes were repeatably (7 PEXT experiments, 4 different RNA sources / preparations) obtained from this method, corresponding to a 5'UTR of 300 – 500bp and another of around 100bp (after correction for the positioning of the antisense primers within the coding region of *Pax7*). These are referred to as High M_r and Low M_r, respectively. The Low M_r band indicates a 5'UTR corresponding to one

Figure 4.2:
N.B. *Pax7* 5'UTR shown is for illustrative purposes only
A) Mouse *Pax7* transcript illustrating positions of all 9 exons, 5'UTR, start (ATG) and stop (TGA) codons and 5'Cap (5' terminal 7-methylguanine) at the very distal end of the mRNA
B) Table of published data to date highlighting source material, technique used and 5'UTR length obtained

A

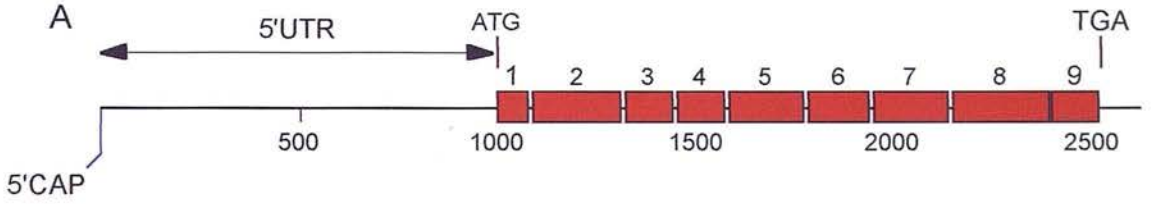

B

Reference	Source RNA	Experimental Method	5'UTR size
Schafer, B. et al 1994	Human A673 cells	5' RACE	103 bp
Vorobyov, E. et al 1997	Human ARMS tumor	5'RACE	599 bp
Murmann, O. et al 2000	Human A673 cells	5'RACE Primer Extension	95bp to 60bp 70bp
Syagailo, Y. et al 2002	Human skeletal muscle	5'RACE Primer Extension	655bp 640bp and 664 bp

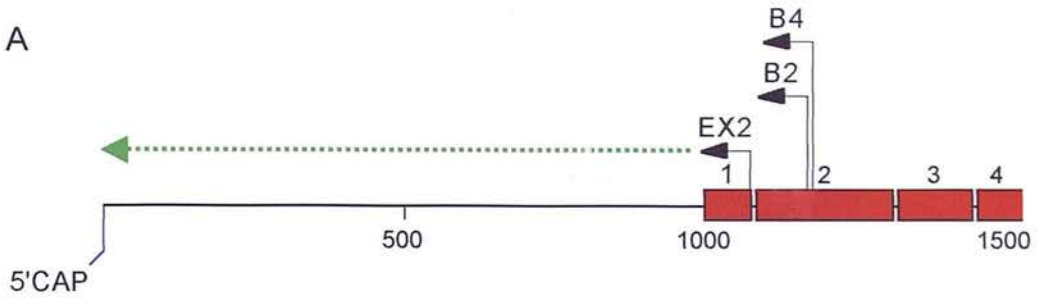

Figure 4.3:
N.B. *Pax7* 5'UTR shown is for illustrative purposes only
A)illustration of 5' end of *Pax7* mRNA, showing positions of primers EX2, B2 and B4 used in primer extension experiments shown in 4.3B and others. Primers are complementary to coding sequence and anneal 78bp (EX2), 171bp (B2) and 183bp (B4) downstream of the ATG at their 5' ends. Primers are radiolabelled at the 5' end, annealed to *Pax7* mRNA and RT activity used to extend along the 5'UTR to the 5'CAP. ssDNA products are then ran out on acrylamide and sized according to kinase labeled ladder. Size of fragment - distance from 5' end of primer to ATG = size of 5'UTR
B) Representative images of primer extension gels, showing banding pattern obtained (pBR322(MspI) ladder used in every case)
Bi and Bii:
Primer EX2 used. Lane 1 = C2C12 total RNA, 2 = C2C12 mRNA, 3 = C2C12 total RNA, 4 = E11.5 total RNA, 5 = E11.5 total RNA from a Pax3 -/- embryo. Illustrating PEXT products at 350 - 600 bp (high Mr) and 160 - 180 (low Mr)
Biii)
All lanes are E11.5 mRNA, Primers EX2, B2 and B4 used as marked. Illustrating PEXT products for EX2 at high and low M_r as for Bi and ii (red lines), and corresponding bands for primers B2 and B4 (blue lines), taking into account differing positions of primer annealing sequences within the *Pax7* transcript (green arrow designates a non-specific band caused by gel drying)

Bi Bii Figure 4.3

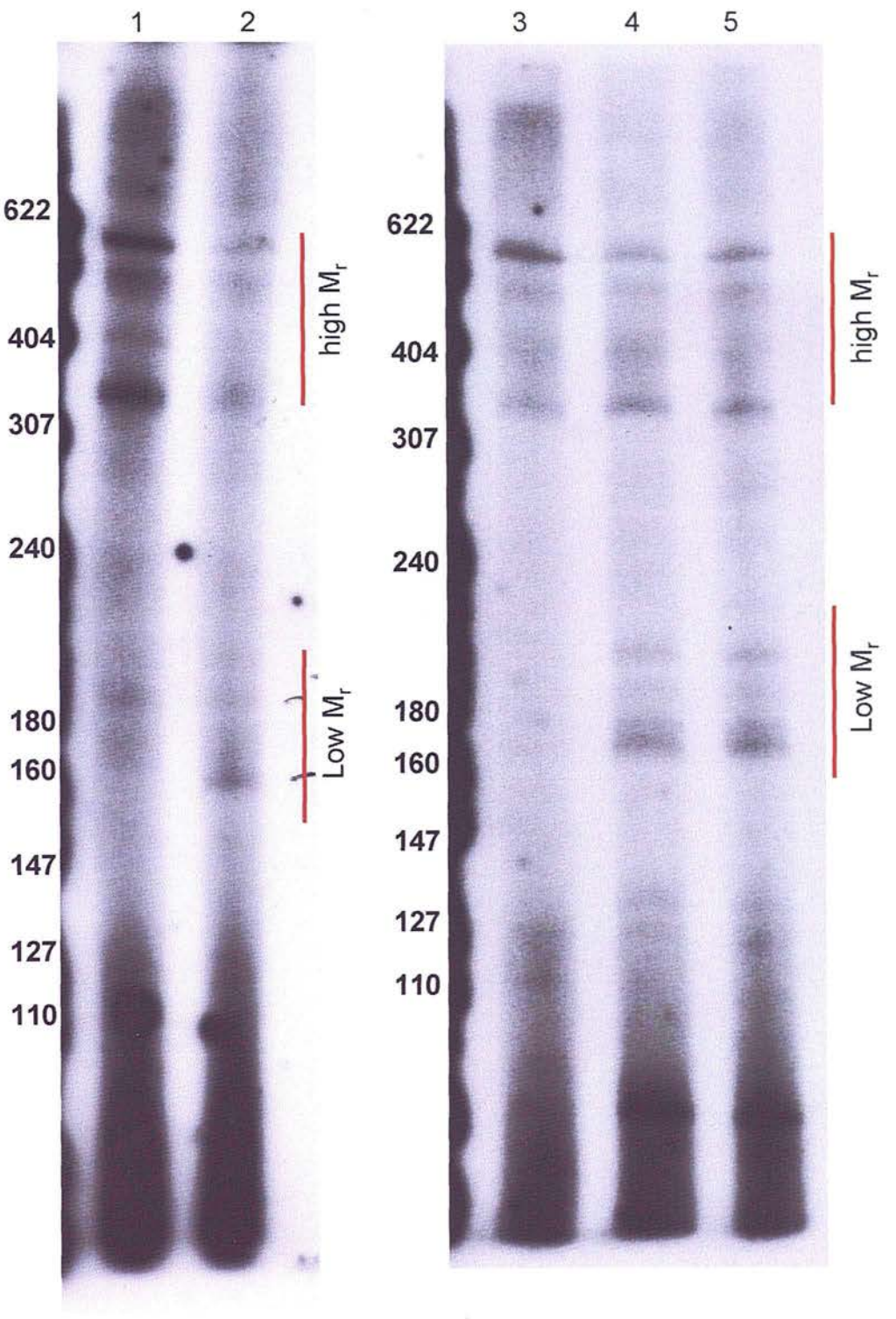

Figure 4.3

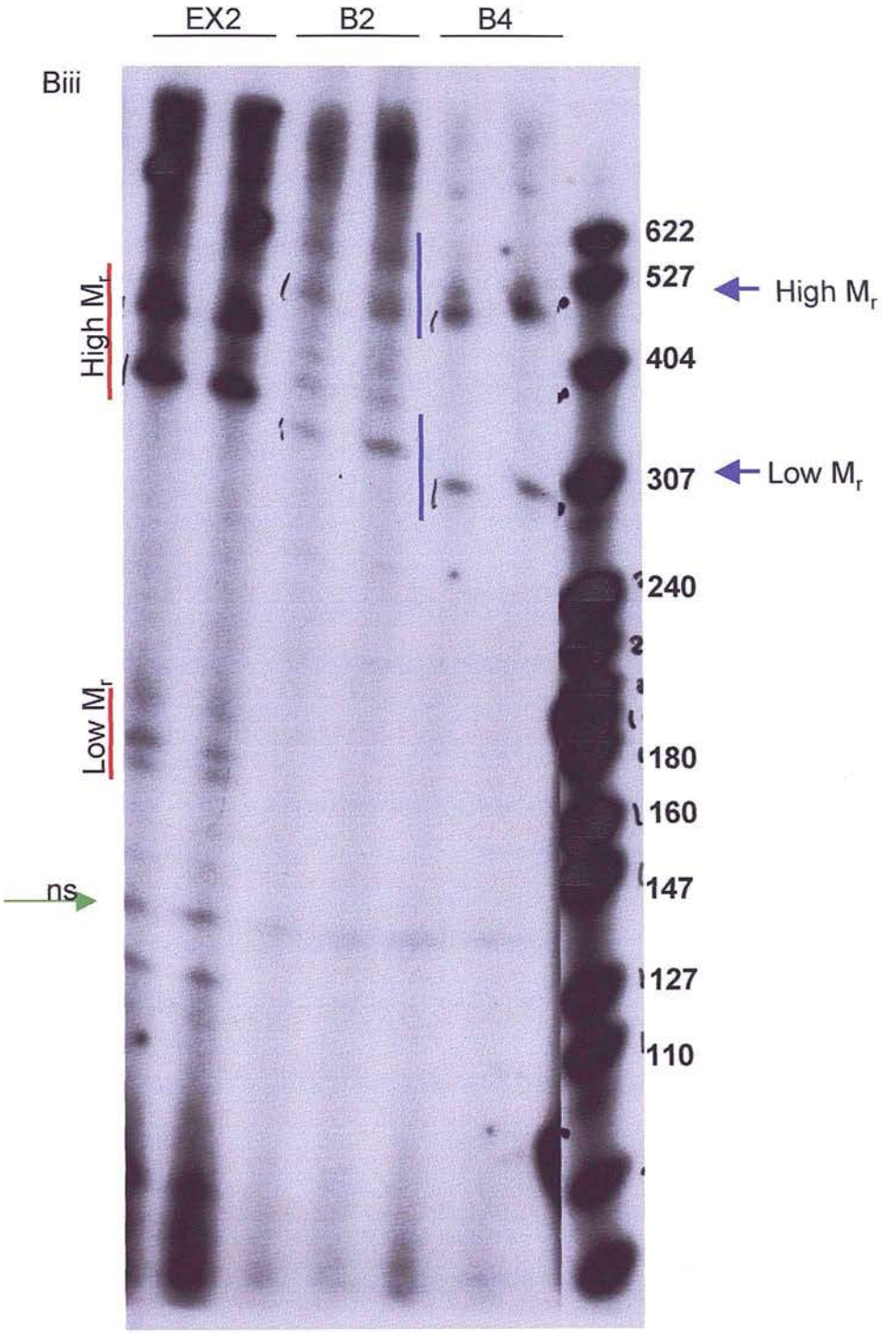
EX2
B2
B4
Biii
High M_r
Low M_r
ns
622
527
404
307
240
180
160
147
127
110
High M_r
Low M_r

previously published for human *Pax7*, see Figure 4.2B, but the High M_r bands are novel.

Since the 5'UTR sizes obtained in the PEXT experiments represented fragment sizes which would be easily amplifiable by PCR, a 5'RACE (Rapid Amplification of cDNA Ends) methodology was then used to try and clone and sequence these fragments from wild type embryo RNA. Two different kits were used, see Chapter Two, to minimise experimental artefacts due to specific methodologies. Nested PCR was used from the *Pax7* coding region, see Figure 4.4A, and the product TOPO-cloned for sequencing. Over 40 clones were sequenced and 18 of these were found to be carrying an insert. The results can be seen in the alignment in Figure 4.4B. A range of 5'UTR sequences were cloned, ranging from 93bp (which would correspond to the Low M_r bands observed in the PEXT experiments) to 11bp. All of these sequences align exactly to the genomic sequence upstream of the *Pax7* coding region.

Interestingly, no clone which would correspond to the High M_r bands observed in the PEXT gels could be identified by 5'RACE. Bands of ~500bp were sometimes seen when running out amplification products, but these proved to be unclonable in spite of several attempts.

Finally, in an attempt to characterise the High M_r bands from the PEXT experiments and confirm the results from the 5'RACE, a Ribonuclease Protection Assay (RPA) was performed. A riboprobe was made by amplifying 770bp of the *Pax7* upstream sequence by PCR, see Figure 4.5A, using primers P7RT1L/R. This was then sub-cloned into pBSII(KS) as a 686bp Asp718 – FspI fragment to generate pP7RiboProbe,

Figure 4.4:
N.B. *Pax7* 5'UTR shown is for illustrative purposes only
A) Schematic of 5'RACE reaction: nested PCR using two gene specific primers annealing at the 5' end of the *Pax7* transcript were used to amplify the *Pax7* 5'UTR with primers annealed to the distal end after an appropriate RT step
B) Alignment of the 5'RACE products obtained. Reference line (bottom) represents mouse genomic sequence from ensembl and positions ATG of coding sequence. Sequences color coded to enable visualization of alignment.

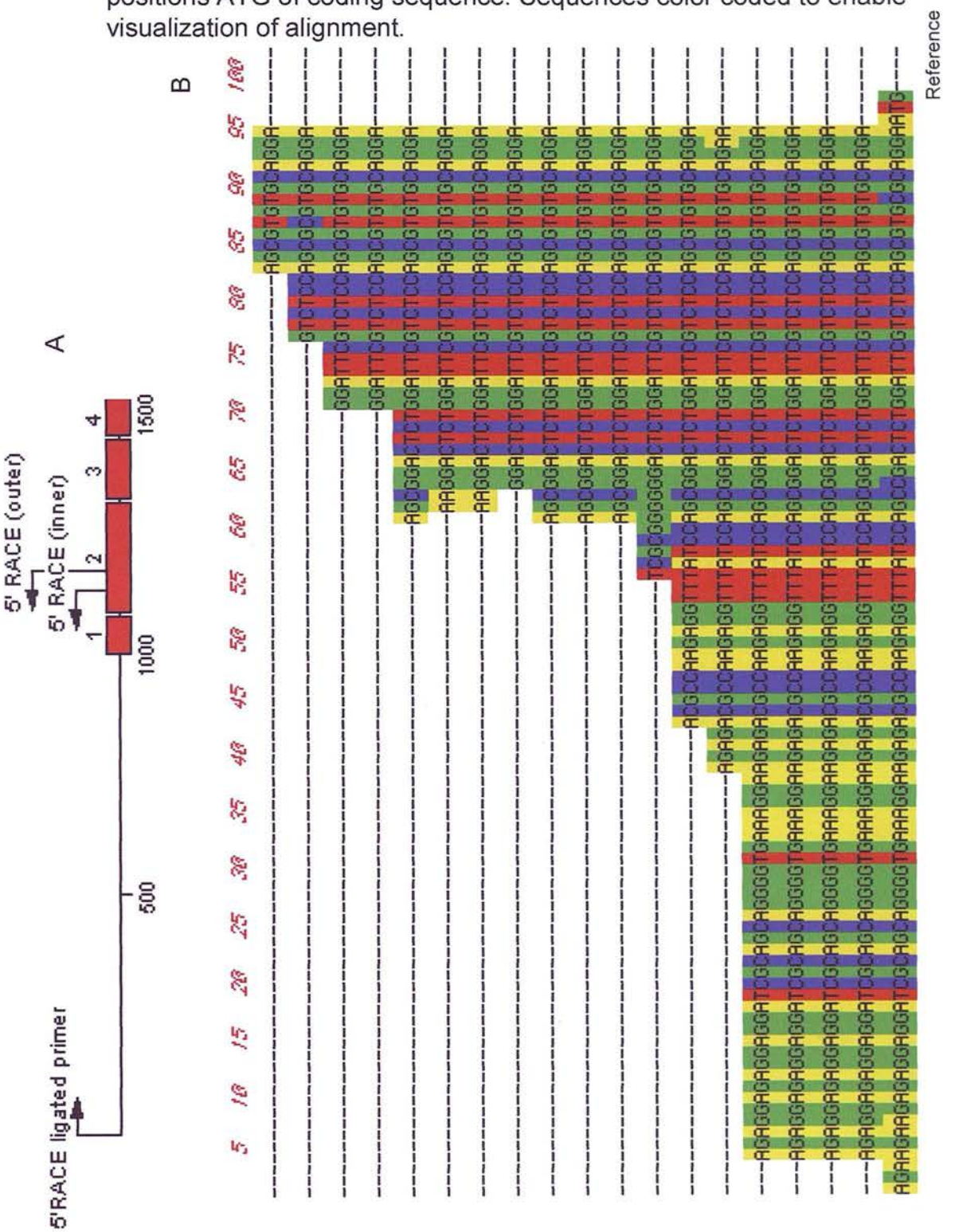

and confirmed by sequencing. Figure 4.5A illustrates the position of this riboprobe and the predicted sizes of protected fragments which would be obtained from the High M_r , Low M_r , and 5'RACE 5'UTR's (assuming the High M_r bands are not obtained from novel exons upstream of this probe binding site). The RPA gel is shown in Figure 4.5B for a C2C12 total RNA sample and an E11.5 total RNA sample. Protected fragments present in both RPA's are at 74, 105 and 135bp, in agreement with the PEXT and 5'RACE data. No larger protected fragment which would correspond to the High M_r bands observed in the PEXT gels could be detected.

To summarise the above data, a plot of 5'UTR length and frequency of observation has been drawn in Figure 4.6. This shows that all 3 methods employed agree on a 5'UTR length of around 100bp. Both 5'RACE and RPA experiments indicate this 5'UTR represents an upstream extension of the coding region and not a novel 5' exon for *Pax7*. This is in agreement with some data published for the human *Pax7* locus (Murmann et al., 2000; Schafer et al., 1994). This UTR also contains a stop TGA codon on the + strand 40bp upstream of the *Pax7* ATG. The existence of several shorter 5'UTR's determined by 5'RACE, and several repeatable larger PEXT fragments is puzzling, however. It is worthy to note that this region of genomic DNA is extremely CG and repeat rich. These sequences are reportedly often difficult for RT enzymes and polymerases to metabolise properly *in vitro*, and may explain the foreshortened 5'RACE products observed. The reliance of this method on PCR and cloning, which may preferentially select for shorter products, could explain why these fragments are observed in RACE clones but not by either PEXT or RPA. The repeated observation of a larger set of PEXT products is more difficult to explain. Whist several groups have reported longer 5'UTR's for the human *Pax7* gene

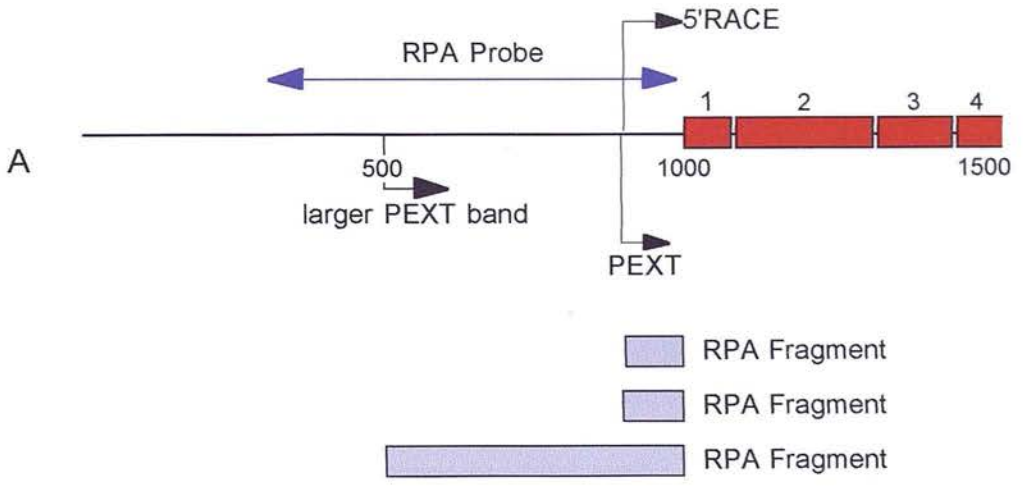

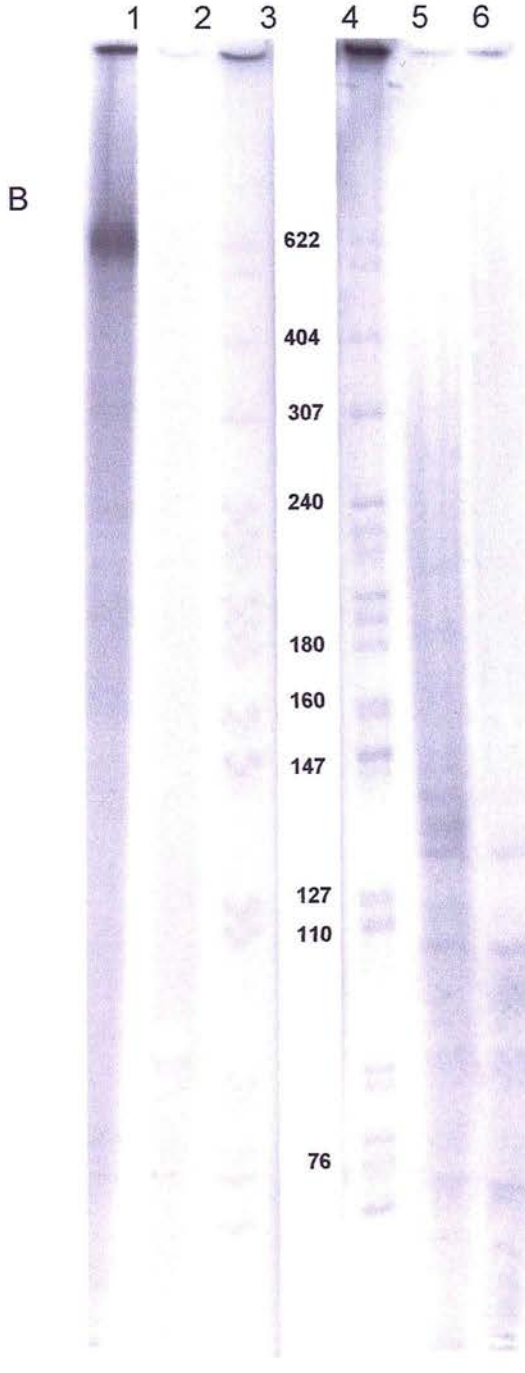

Figure 4.5

Lanes:
1 = Positive control, undigested probe
2 = Negative control, (NIH-3T3 RNA)
3 = pBR322(MspI) ladder
4 = pBR322(MspI) ladder
5 = RPA, C2C12 RNA
6 = RPA E11.5 embryo RNA

Figure 4.5:
N.B. *Pax7* 5'UTR shown is for illustrative purposes only
A) Illustration of *Pax7* mRNA, showing 5'UTR's predicted so far by 5'RACE and primer extension (PEXT). The riboprobe cloned and used in the RPA shown in B is positioned in blue (685bp). The predicted fragments are shown below (to scale). A 5'UTR in agreement with RACE and the smaller primer extension products would generate protected fragments of around 100bp. 5'UTR's of the size predicted by the larger primer extension product would generate protected fragments of around 350 - 500 bp (only 500bp fragment shown here for simplicity) from the same riboprobe. Populations of transcripts containing both should generate fragments of both sizes.
B) RPA gel, visualized on a phosphorimager. Band and ladder sizes as marked, lane key as shown. Note no evidence of any bands corresponding to the larger primer extension products shown in Figure 4.3

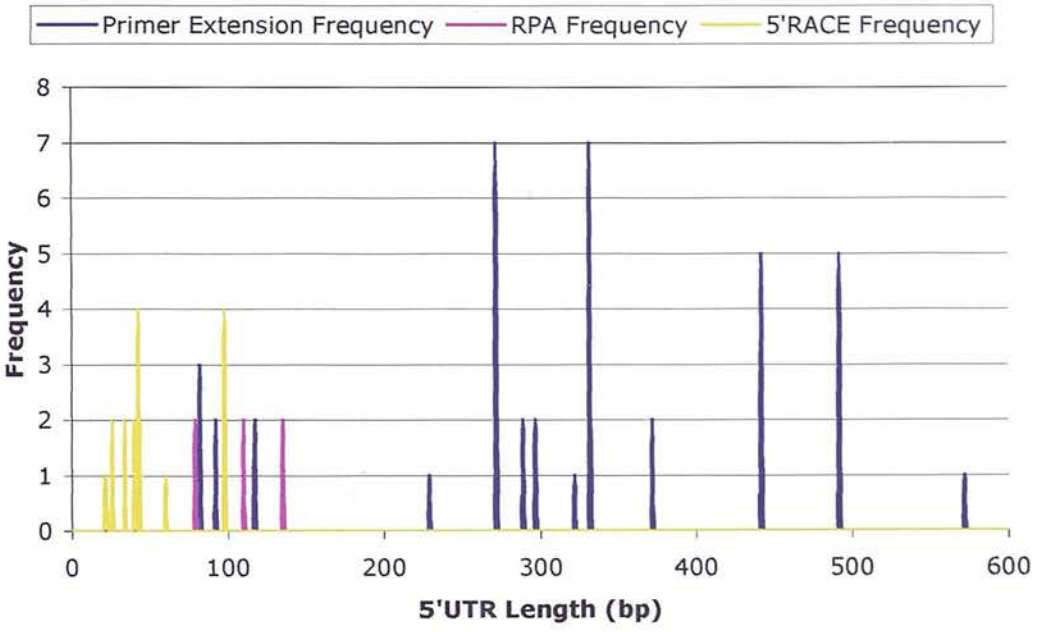

Figure 4.6:
Summary graph of all experiments performed to determine the length of the mouse *Pax7* 5'UTR. The graph is a plot of length of 5'UTR (x axis) against frequency of experimental observation (y axis). Primer extension is represented by the blue trace (n = 40), RPA is pink (n = 6) and 5'RACE is yellow (n = 18). All methods cluster a predicted 5'UTR at around 100 bp (in the region reported by Schafer et al 1994 and Lang et al 2003) but primer extension repeatedly determines a longer extension products from ~300 to 500 bp (in the region reported by Vorobyov et al 1997, Murmann et al 2000 and Syagailo et al 2002) which has not been detected by either 5'RACE or RPA

(Syagailo et al., 2002; Vorobyov et al., 1997), these are all at least 150bp bigger than the bands observed in these PEXT experiments, and since these were also 5' extensions of the *Pax7* coding sequence and not novel upstream exons, these should also have been detected by RPA. It is possible that these PEXT bands represent 5'UTR's of genes other than *Pax7*. Since three different primers all show extension products in this region, the most likely candidate for this would be *Pax3*, given the level of homology of between *Pax3* and *Pax7*. C2C12 cells do not express *Pax3* (data not shown and (Borycki et al., 1999)) and give PEXT products of this size. It would therefore seem unlikely that this PEXT product represents an accidental extension of the *Pax3* 5'UTR. Furthermore, all primers were subjected to BLAST analysis to ensure specificity during the design process. The data presented here does not adequately explain this observation, and further investigation is needed. Given the convergence of all three methodologies on a transcriptional start site of around 100bp upstream of the *Pax3* coding sequence, it was decided for the purposes of this thesis to take this as the major transcriptional start site for mouse *Pax7*.

Pax7 *5' Promoter: Cloning*

Since the 5' extent of the *Pax7* transcript was taken to include around 100bp of sequence upstream of the coding region, it was reasoned that the genomic sequence upstream of this, containing a CpG island and a high level of homology to the equivalent region in the human genome, might contain a minimal promoter for the mouse *Pax7* gene. In the human, a similar homologous region has been shown to confer *Pax7* promoter activity in cell culture (Murmann et al., 2000; Syagailo et al., 2002).

To investigate this experimentally, this region of the *Pax7* locus was cloned. Initially, a mouse genomic PAC library was screened using a 520bp probe (made by amplifying human genomic DNA (primers P7HYB1L/R) and TOPO-cloning into pCR-II-TOPO-TA to generate pP7HYB). The predicted hybridisation region is illustrated in Figure 4.7. Several positive clones were identified and these were then confirmed by Southern blot. Figure 4.8A and B illustrate the position of the probe used (a 770bp PCR product amplified from mouse genomic DNA using primers P7RT1L/R) and fragment sizes predicted from the mouse genomic sequence. PAC clones were digested using the restriction enzymes indicated and Southern blotting performed, see Figure 4.8C. Clone I4 gave positive signals of the correct size in each case and was used to clone the *Pax7* promoter region.

Since this region proved resistant to cloning via conventional methods, TEPCR was used to TOPO clone a 3.5kb fragment into pCR-XL-TOPO using primers PAX7PROML/R to generate p3.5TOPO. The insert was then sequenced completely, and a 3kb (BamHI – FspI) putative promoter fragment was then shuttled into pGL3basic, (via an intermediate construct, see appendix one), generating p3.0Luc, see Figure 4.9A and B. To test the proximal 1kb region of human – mouse homology initially identified by bioinformatics, two deletion constructs were made using tandem Asp718 or BglII sites to delete the distal and proximal regions of this putative promoter region, respectively (Figure 4.9B). These were named p1.5Luc (distal deletion) and p-1.8Luc (proximal deletion).

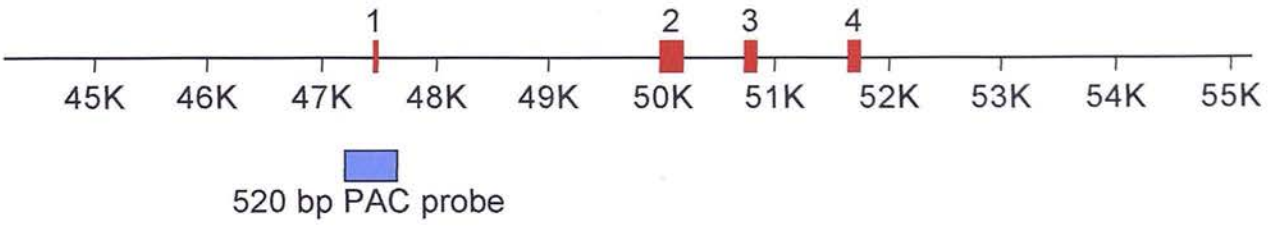

Figure 4.7:
Pax7 genomic locus showing predicted hybridization of 520bp fragment (cloned into pP7HYB, human sequence) used to probe a mouse genomic PAC library

Figure 4.8:
A) Illustration of *Pax7* locus and predicted restriction sites used in Southern blotting to verify validity of PAC clones
B) Table of enzymes and predicted restriction fragments
C) Representative Southern blots of PAC clone I4 showing predicted fragments

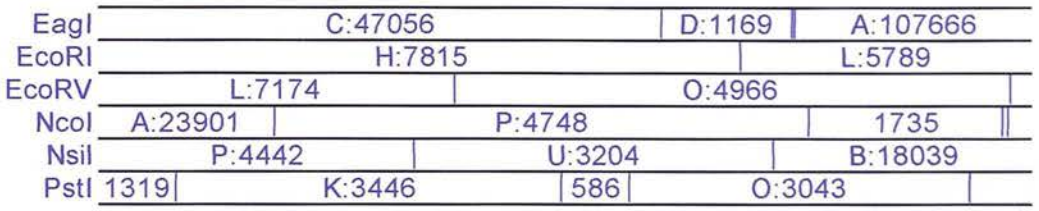

A

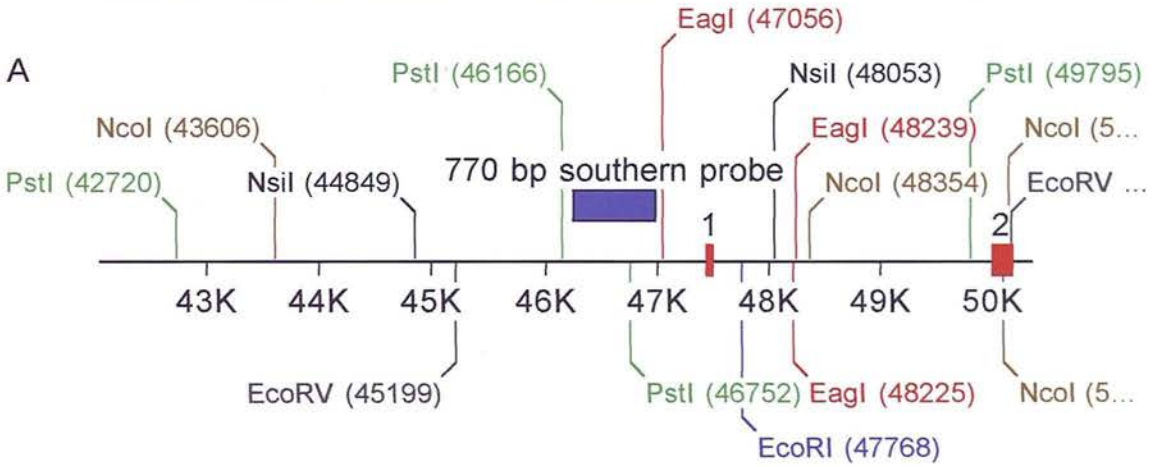

B

Enzyme	Predicted kb Fragment Size(s)	Hybridization Observed?
AvaII	0.338 and 0.797	✓
EcoRI	7.815	✓
EcoRV	4.966	✓
PstI	0.586 and 3.043	✓
EagI	47.056	✓
NcoI	4.748	✓
NsiI	3.204	✓

Figure 4.8

C

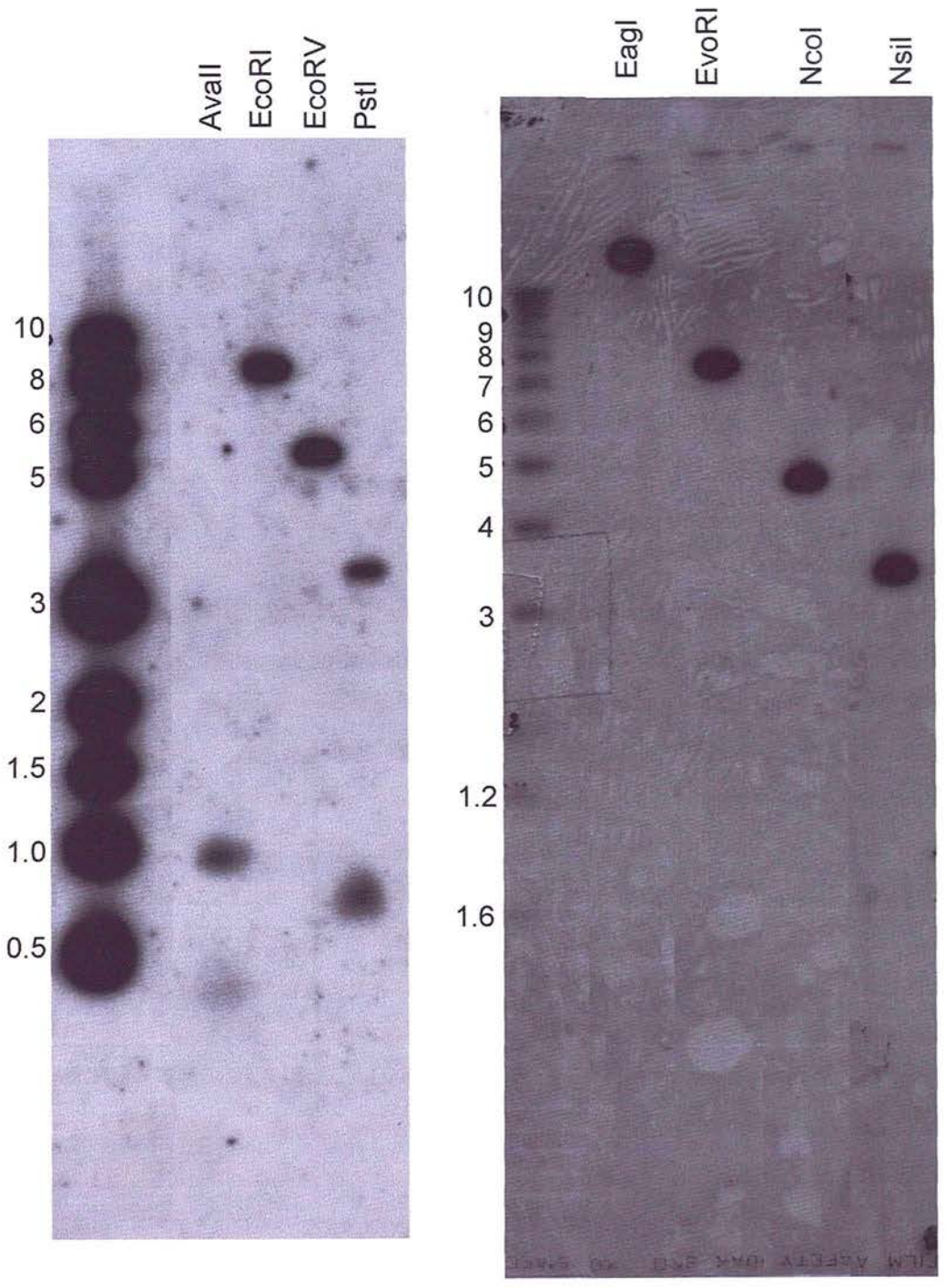
AvaII
EcoRI
EcoRV
PstI
10
8
6
5
3
2
1.5
1.0
0.5
EagI
EvoRI
NcoI
NsiI
10
9
8
7
6
5
4
3
1.2
1.6

To test the ability of these regions of proximal genomic sequence to drive Luciferase reporter gene expression, these plasmids were transfected into the C2C12 mouse myoblast cell line which is *Pax7* positive. Figure 4.9C illustrates these results. A detailed description of the Luciferase protocol and the data treatment used in this thesis can be found in Appendix 4 and is not dealt with here. In the C2C12 cell line, the constructs p3.0Luc and p1.5Luc were clearly able to drive reporter gene expression over baseline (pGL3basic, or empty vector). In the construct p-1.8Luc, where the sequence proximal to the transcriptional start site has been deleted, no induction could be observed. This enabled the proximal 1.5kb of mouse genomic sequence to be established as a *Pax7* minimal promoter in the C2C12 cell line.

During the bioinformatic analysis of this region of the mouse genome, a potential regulatory element within the first intron of the *Pax7* gene was also identified. This region was highlighted by the PIPMaker program as having >91% homology between human and mouse sequences. Given that the coding sequences for *Pax7* generally only demonstrate 75 – 80% identity, this represented a potentially interesting feature. This is illustrated in Figure 4.10A. To investigate experimentally, the region was cloned using TEPCR from the I4 PAC clone, with primers P7INT1REGF/B (containing BamHI sites) and directly into the BamHI site (3' to the Luciferase ORF) of both pGL3promoter and p1.5Luc. Both orientations of the element were cloned and screened with restriction digests, before sequencing to confirm insertion. These constructs are represented in Figure 4.10B, and were named pI1RLuc and p1.5I1RLuc.

Figure 4.9

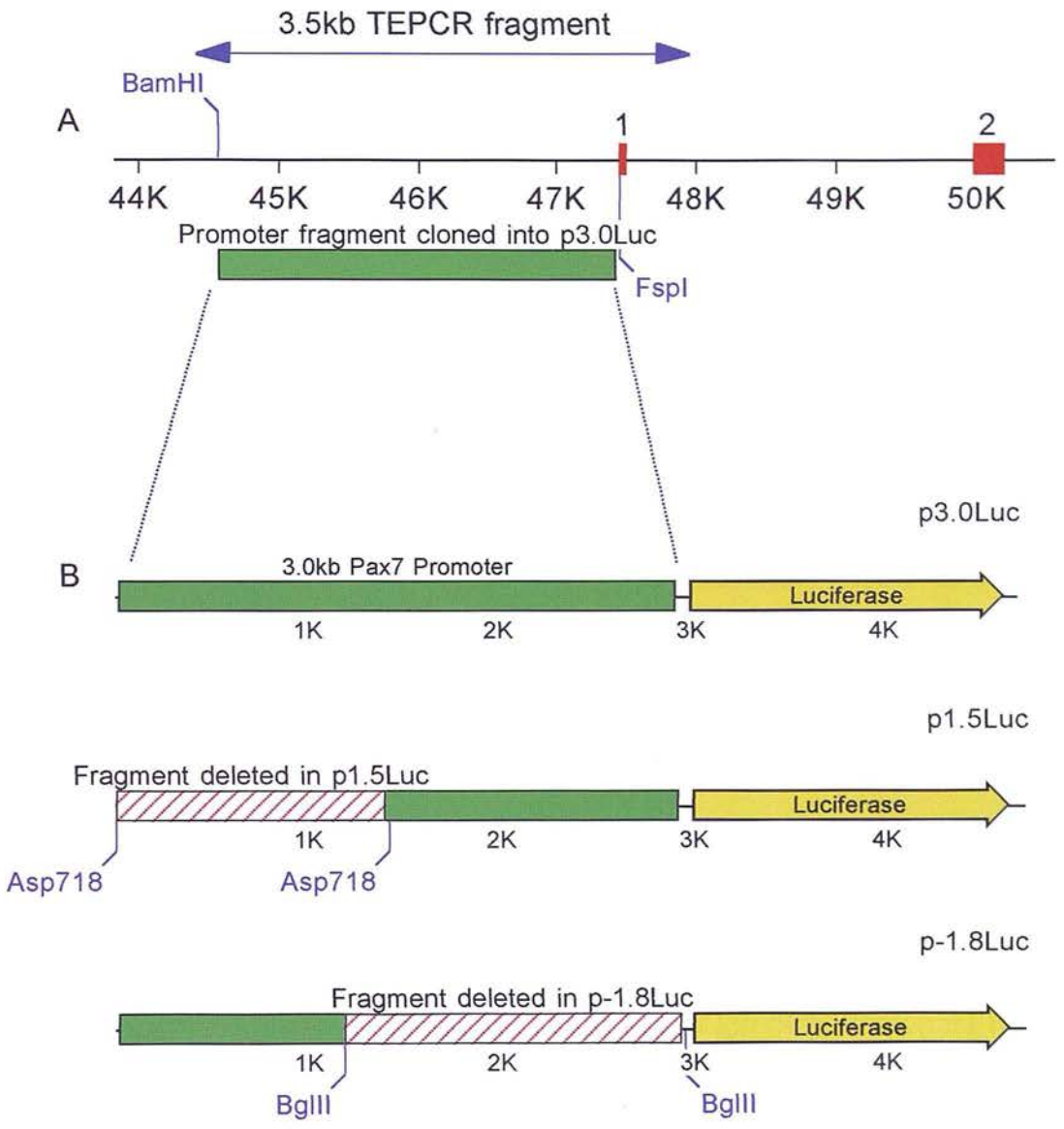
3.5kb TEPCR fragment
BamHI
A
1
2
44K
45K
46K
47K
48K
49K
50K
Promoter fragment cloned into p3.0Luc
FspI
p3.0Luc
B
3.0kb Pax7 Promoter
Luciferase
1K
2K
3K
4K
p1.5Luc
Fragment deleted in p1.5Luc
Luciferase
1K
2K
3K
4K
Asp718
Asp718
p-1.8Luc
Fragment deleted in p-1.8Luc
Luciferase
1K
2K
3K
4K
BglII
BglII

C

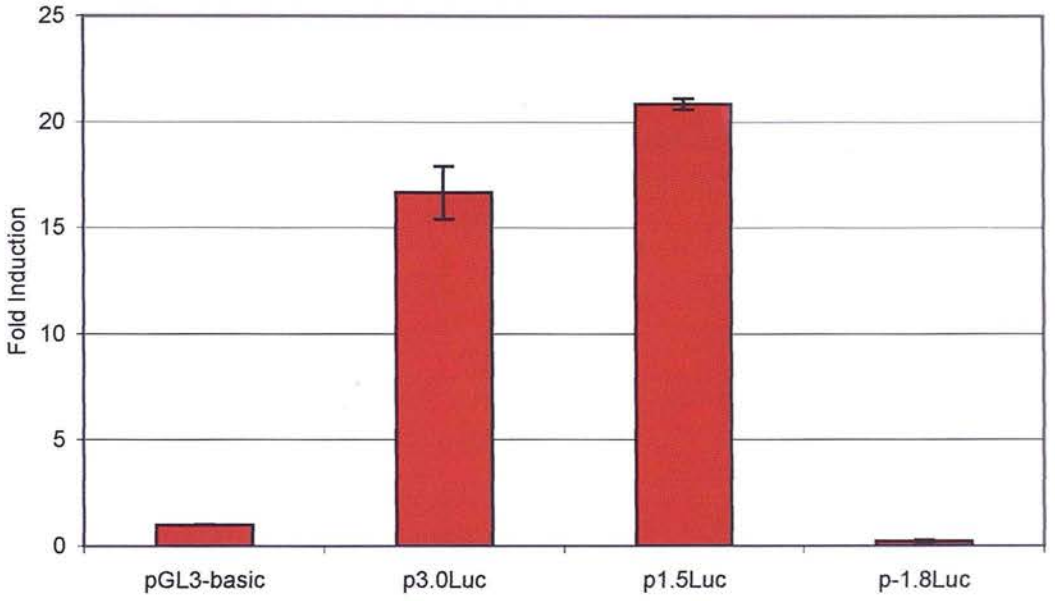

Figure 4.9:
A) Genomic locus of Pax7 showing region cloned by TEPCR into p3.5TOPO, and the BamHI and FspI sites then used to clone a 3kb fragment into pGL3basic via shuttling through pIntermediate1 (pBSII backbone)
B) p3.0Luc, p1.5Luc and p-1.8Luc constructs showing regions deleted and restriction sites used.
C) Luciferase data of Pax7 promoter luciferase plasmids on transfection into the Pax7 expressing C2C12 cell line. Data is normalised luminescence expressed as fold induction over baseline (pGL3basic). n = 3, error bars are SEM

Figure 4.10

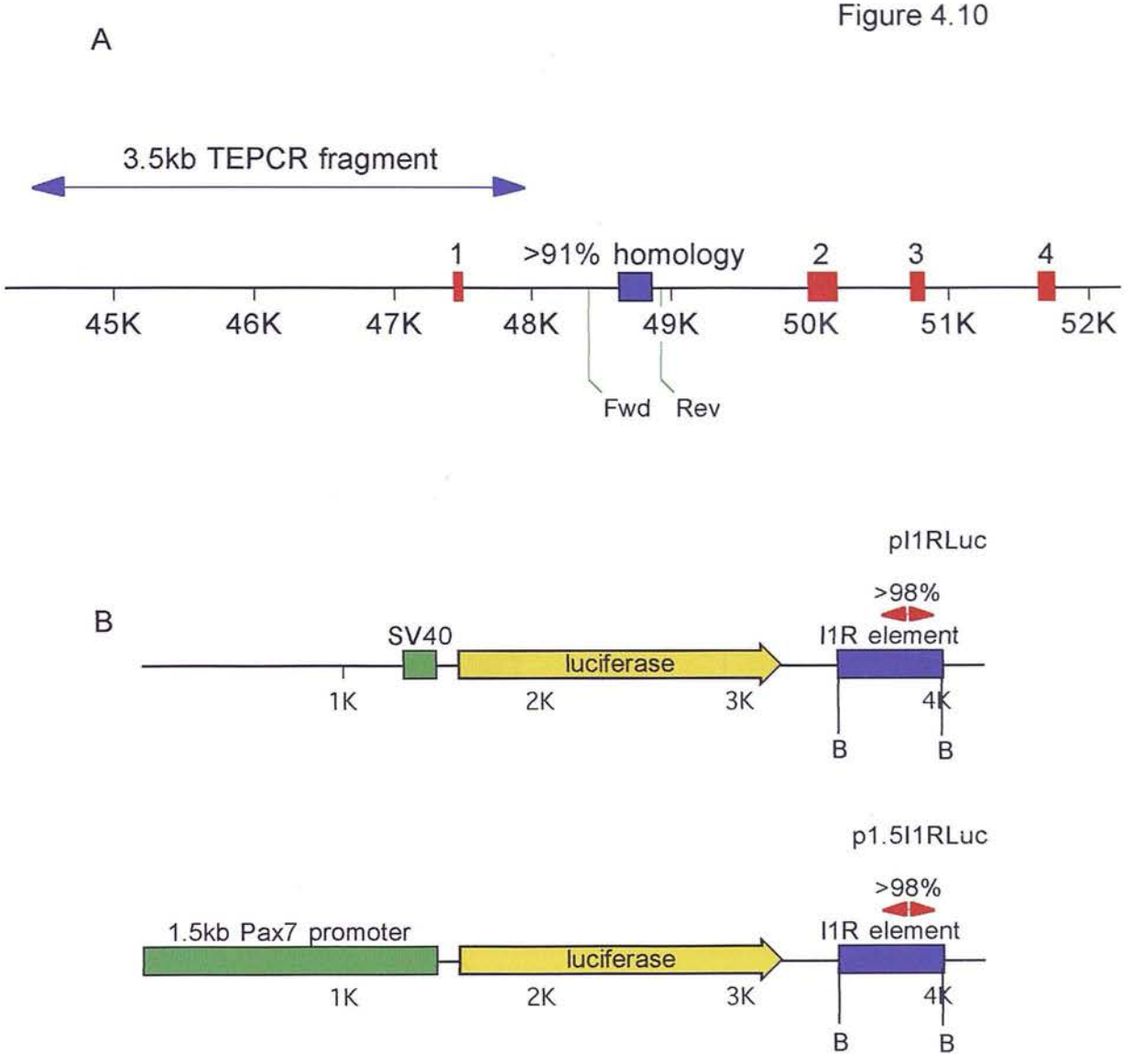
A
3.5kb TEPCR fragment
1
>91% homology
2
3
4
45K
46K
47K
48K
49K
50K
51K
52K
Fwd
Rev
pI1RLuc
B
SV40
luciferase
I1R element
>98%
1K
2K
3K
4K
B
B
p1.5I1RLuc
1.5kb Pax7 promoter
luciferase
I1R element
>98%
1K
2K
3K
4K
B
B

Figure 4.10

C

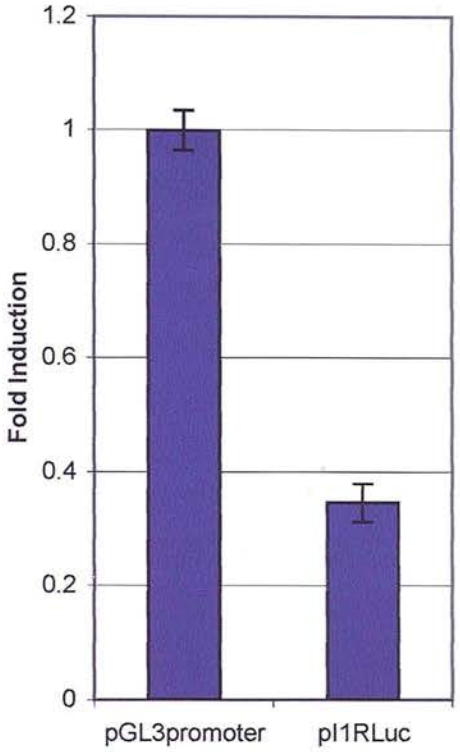
1.2
1
0.8
0.6
0.4
0.2
0
Fold Induction
pGL3promoter
pI1RLuc

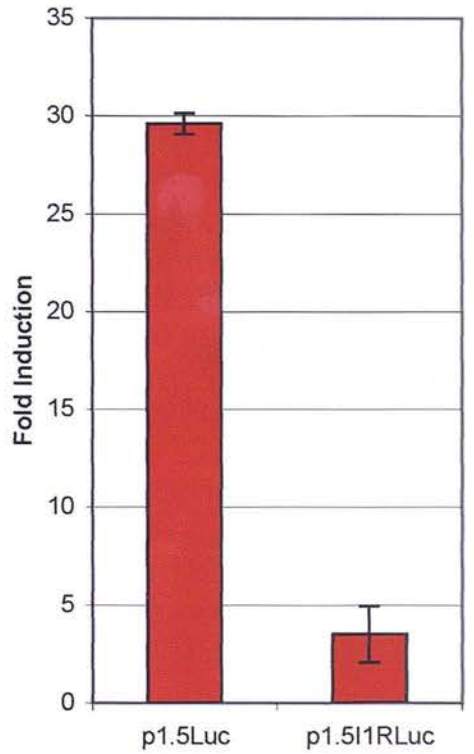
35
30
25
20
15
10
5
0
Fold Induction
p1.5Luc
p1.5I1RLuc

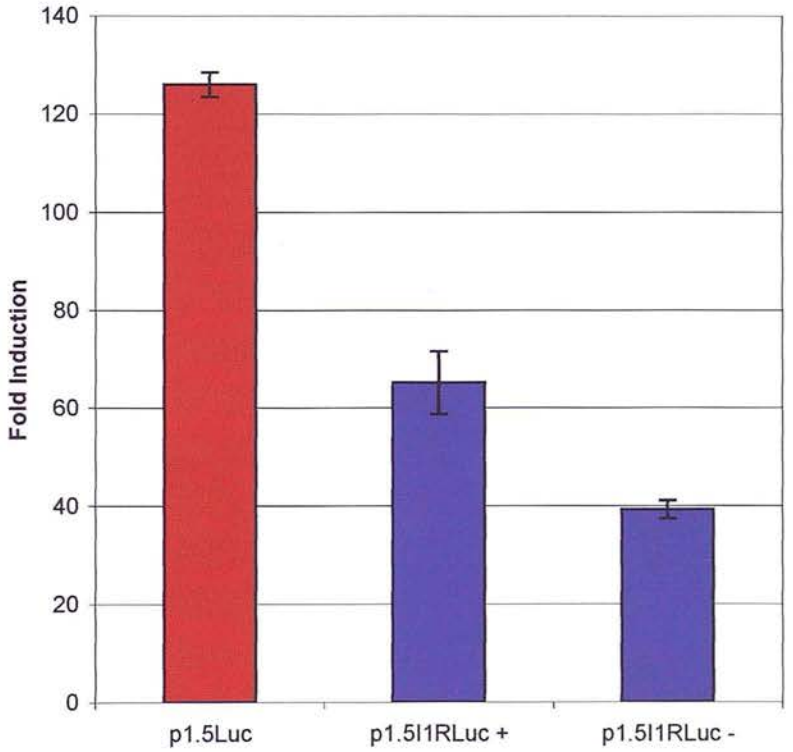
140
120
100
80
60
40
20
0
Fold Induction
p1.5Luc
p1.5I1RLuc +
p1.5I1RLuc -

Figure 4.10:
A) Schematic of *Pax7* genomic locus showing region of very high sequence conservation between human and mouse genomes (>91%). Since this homology is greater than that demonstrated for the exon sequences, primers were designed to amplify and clone this sequence into Luciferase reporter vectors (shown). B = BamHI sites engineered into PCR product and used for cloning into pGL3Promoter and p1.5I1RLuc
B) pI1RLuc and p1.5I1RLuc reporter vectors used to test the effects of the highly conserved sequence found within intron one. The I1R fragment was cloned behind the Luciferase ORF in plasmids containing the SV40 weak and *Pax7* endogenous promoters, respectively.
C) Luciferase data showing the silencing effects of the I1R element on reporter gene activity driven by both the SV40 and *Pax7* endogenous promoters (top panels). The silencing effect is also orientation independent (bottom panel). Data is normalised luminescence, expressed as fold induction over empty vector (pGL3promoter and pGL3basic). n = 3, error bars are SEM.

To test the effects of this element on transcription, these plasmids were transfected into the C2C12 cell line as before, and levels of reporter gene expression examined with and without the I1R insert. These data are shown in Figure 4.10C. The I1R element demonstrated a robust silencing activity which was both promoter and orientation independent. This silencing activity was also observed in NIH-3T3 cells (data not shown). It was therefore hypothesised that this element may also function to regulate *Pax7* expression *in vivo* through the binding of inhibitory elements.

Regulation of Pax7 *by* Pax3

The identification of some potential regulatory regions within the *Pax7* locus now enables the final hypothesis described in Chapter One to be investigated.

Hypothesis Three

Pax7 is directly downregulated by Pax3, in vitro *and* in vivo*, via defined regulatory elements and with implications for the development of both neural and mesodermal tissues.*

To test this hypothesis, the regulatory regions identified above were initially subjected to a bioinformatic analysis to identify potential transcription factor binding sites using the MatInspector program (MatInspector). Both the minimal promoter and I1R element were analysed in this way. One *Pax3* binding consensus was identified in the proximal promoter region. Local alignment using the ClustalW program illustrated

that this region of the *Pax7* promoter is highly conserved between human and mouse, and this consensus is present in both species, see Figure 4.11A. Figure 4.11B positions this site in both p3.0Luc and p1.5Luc.

To test the *Pax3* responsiveness of this site *in vitro*, these constructs were co-transfected into C2C12 with and without the pCMV-*Pax3* expression construct, as described previously (see Chapter Three). These data are shown in Figure 4.11C. Despite relatively high variation in normalised luminescence, no significant change in reporter gene expression could be obtained for either construct. This indicates that *Pax3* cannot interact with this promoter consensus *in vitro*. To ensure this result was not an artefact of cell line activity, these experiments were also conducted in the NIH-3T3 cell line; and an identical result was obtained (data not shown).

Since the hypothesis under investigation predicts that *Pax3* down regulates *Pax7* activity, and a silencing element was identified at the *Pax7* locus, it was decided to investigate any potential interaction between *Pax3* and this element in spite of a failure of MacVector to identify any consensus binding sites. A similar approach was adopted and pI1RLuc (Figure 4.12A) was co-transfected with and without the pCMV-*Pax3* expression vector, and the changes in normalised luminescence recorded. Again, no change in fold induction was observed, Figure 4.12B, indicating this element does not respond to *Pax3* co-expression *in vitro*.

Finally, the p1.5I1RLuc construct was tested. This construct contains both the *Pax7* proximal promoter and the I1R element around the Luciferase ORF, Figure 4.13A. This was co-transfected into C2C12 cells with and without pCMV-*Pax3*, in a repeat

A


mouse ----------GTCATTCGGCTTAACTTCTGGCCGAGCCCGGCGGGTGGAGGCGGACT 3740
human TTCTGCCAGGCGCATCAGCCCGCACAACTTCTGGCCGAGGC-AGCCGGCAGAGGCGGACT 3559
*** * ** ********** * ** ** **********
mouse ---TGGGGTTGGAGTGTTTGTTTGTTTGAACTTCCTTGTCGCCACCTTCCACTCCTCCCG 3797
human TGGGGTTGGAGTGTTTGTTTGTTTGAACTTCCTCGTCGTCGCCACCTTCCCTCCCCCCAA 3619
******** ********** ** **
mouse CCCCCACCTCACCCC-CCCCCGCGCCCAGCTTCTGGAAGGGGCGCGTCTGCAACCGGGTG 3856
human CCTCCAACCCACCTCACCCCCCTCCCCAGCTTCTGGACGCGTT-TGACTGCAGCCAGGGG 3678
** *** * **** * ***** ********** * * * ***** ** ** *

Figure 4.11

Figure 4.11:
A) CustalW alignment of mouse and human *Pax7* promoter regions showing high level of homology and position of *Pax3* consensus sequence (highlighted). Consensus site has been gapped in mouse by alignment software but is clearly present in both species
B) Illustration of p3.0Luc and p1.5Luc showing position of *Pax3* consensus site
C) Luciferase response to co-transfection with the pCMV-Pax3 expression plasmid. No significant change in reporter gene expression observed, n = 3 error bars are SEM. Data expressed as fold induction over baseline (pGL3basic).

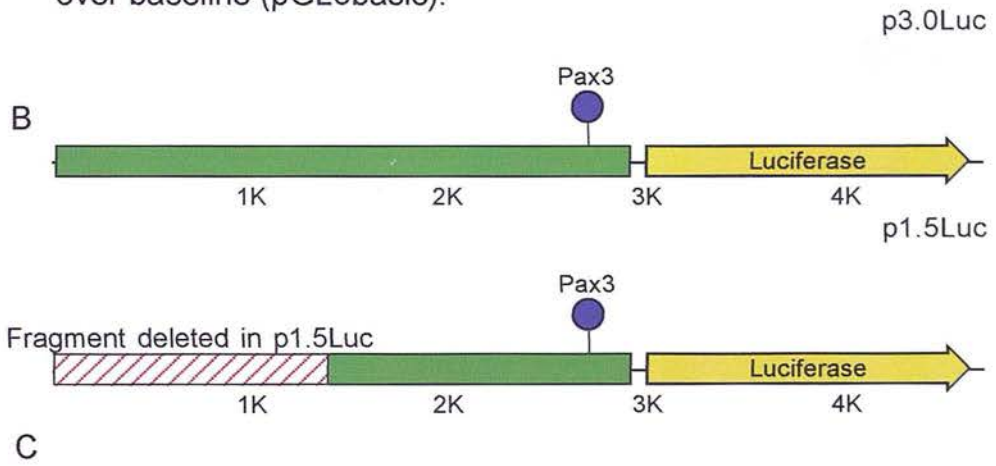

C

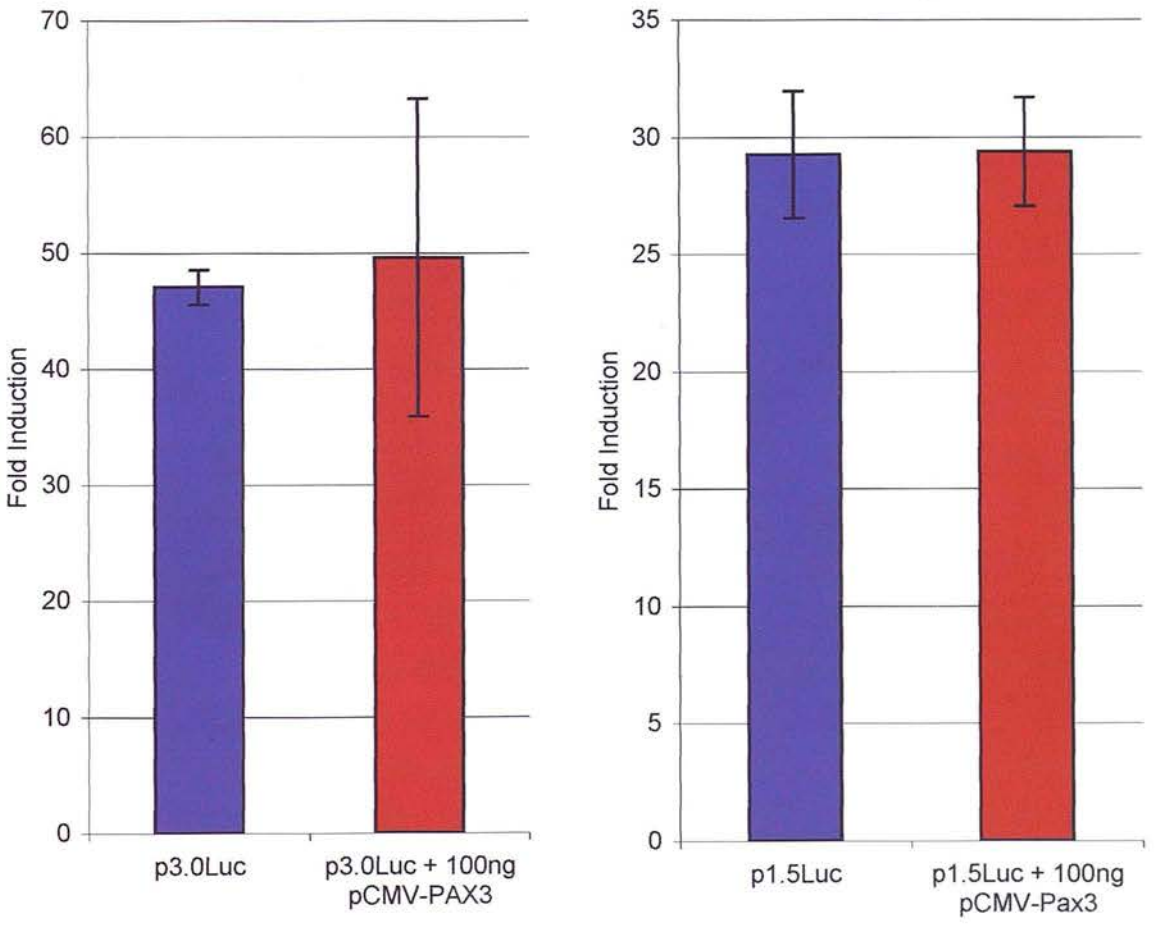

Figure 4.12:
A) Plasmid pI1RLuc
B) No change in reporter gene activity on co transfection with pCMV Pax3, n = 3 error bars are SEM.

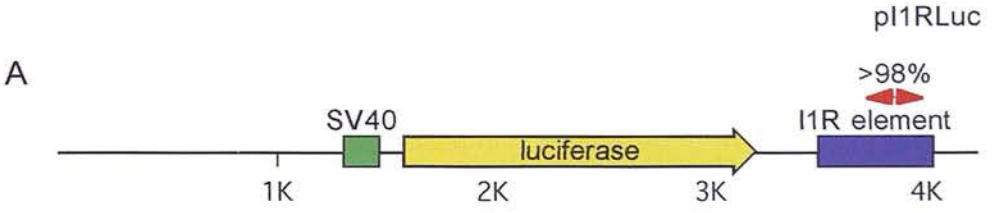

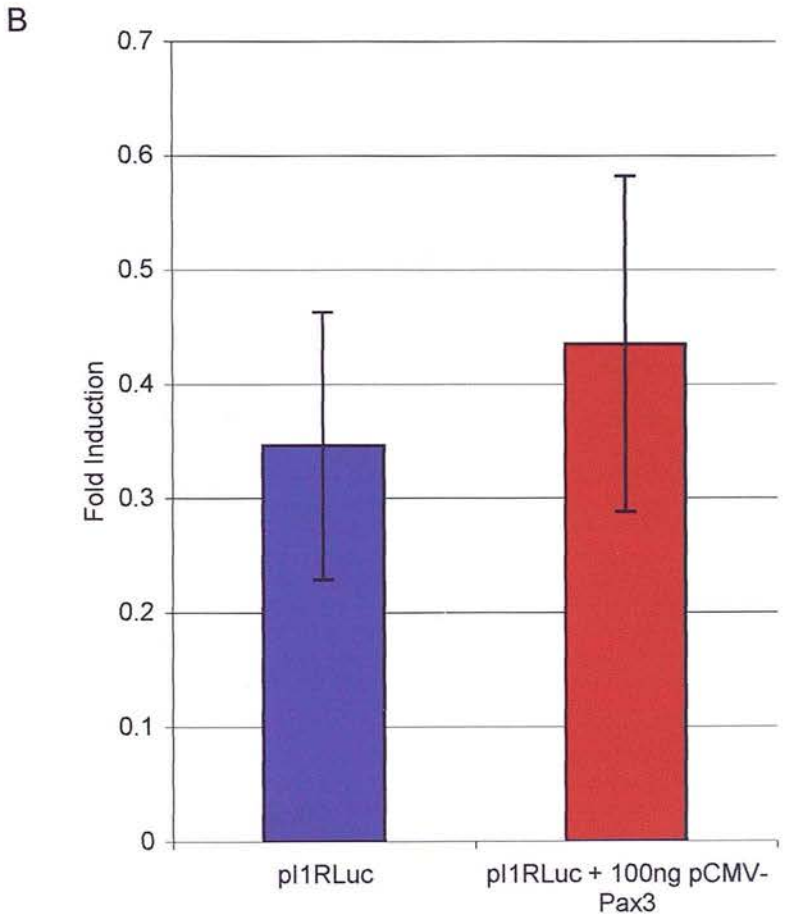

Figure 4.13

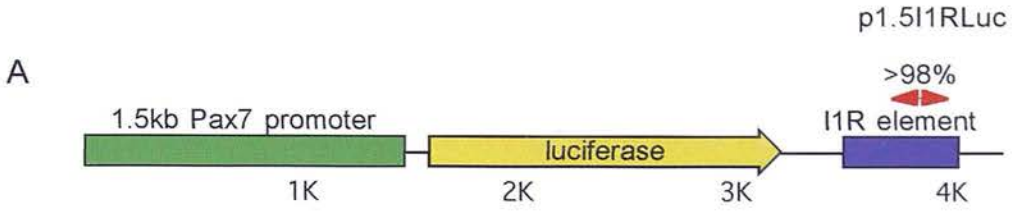
A
p1.5I1RLuc
>98%
1.5kb Pax7 promoter
luciferase
I1R element
1K
2K
3K
4K

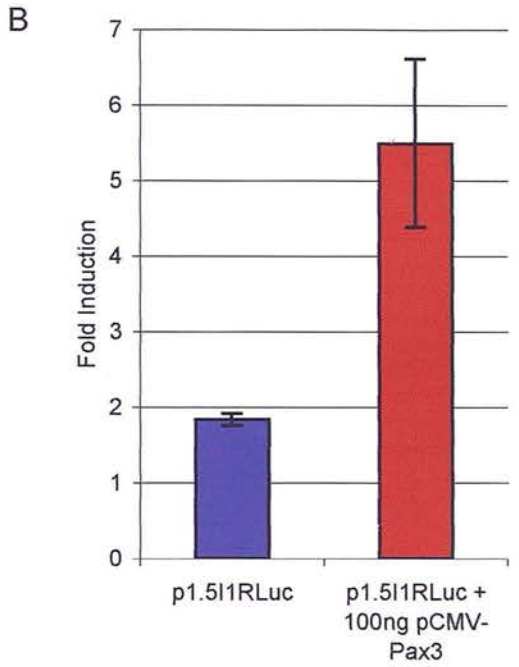
B
Fold Induction
0
1
2
3
4
5
6
7
p1.5I1RLuc
p1.5I1RLuc + 100ng pCMV-Pax3

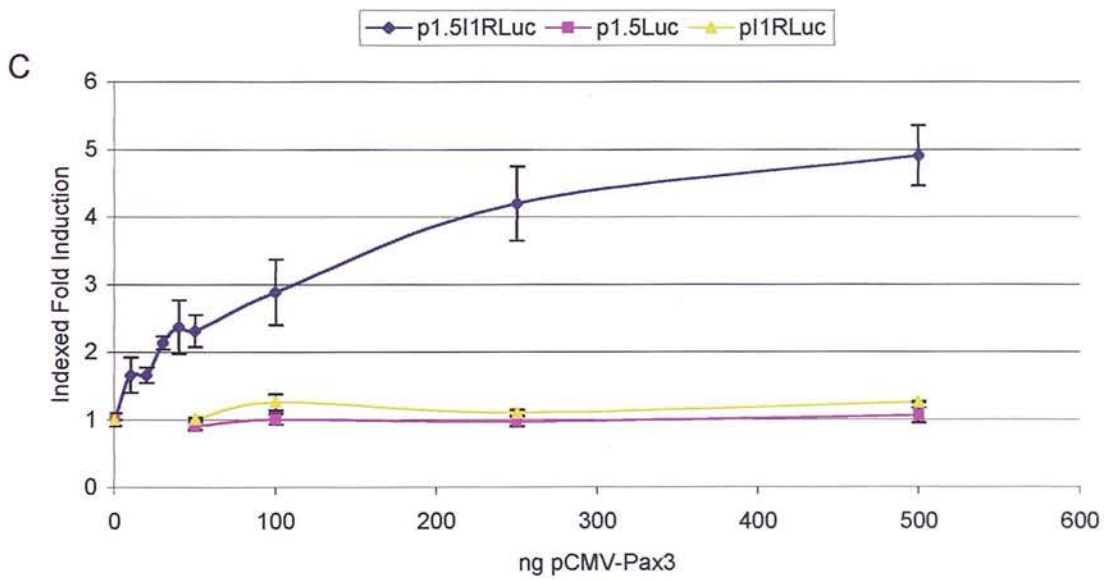
C
p1.5I1RLuc
p1.5Luc
pI1RLuc
Indexed Fold Induction
0
1
2
3
4
5
6
0
100
200
300
400
500
600
ng pCMV-Pax3

Figure 4.13:
A) Plasmid p1.5I1RLuc
B) Pax3 response to co-transfection of p1.5I1RLuc with 100ng pCMV-Pax3. A clear induction in Luciferase activity is observed, n = 3 error bars are SEM.
C) To test the observations in Figures 3.11, 3.12 and B, a range of ng quantities of pCMV-Pax3 were co-transfected with each of p1.5Luc, pI1RLuc and p1.5I1RLuc. An induction of reporter gene activity is observed only on co-transfection of the pCMV-Pax3 expression construct with p1.5I1RLuc (containing both the *Pax7* promoter *and Pax7* intron 1 silencer element). Blue trace is p1.5I1RLuc, pink is p1.5Luc, yellow is pI1RLuc. Data is expressed as normalised luminescence fold induction over baseline and indexed to 0ng pCMV-Pax3 to enable direct comparison between data sets. n = 3 - 5 (dependant on data point) error bars are SEM.

of the above, and this time a clear response to *Pax3* co-expression was obtained, Figure 4.13B. To test this response further, and to ensure a concentration dependent response to *Pax3*, a range of quantities of pCMV-*Pax3* were co-transfected for each of the plasmids p1.5Luc, pI1RLuc, and p1.5I1RLuc. Only the latter construct responded to pCMV-*Pax3* co-transfection over the range investigated, see Figure 4.13C.

Interestingly, this result implies that *Pax3* can interact with the *Pax7* regulatory elements defined here, at least *in vitro*, but that this interaction would appear to 'de-repress' the silencing effect of the I1R element, rather than being a simple activating or inhibitory relationship.

Since the reporter gene assays described above do not indicate whether *Pax3* is interacting with the promoter or silencer element, it remained possible that the *Pax3* consensus identified by the MatInspector analysis mediates this response. To investigate this possibility, the core consensus *Pax3* binding site within the *Pax7* promoter was mutated using site directed mutagenesis. The p1.5I1RLuc plasmid was used with the QuikChange Site Directed Mutagenesis kit (Stratagene) and primers P7_sub_FWD/REV. Clones were screened by direct sequencing to confirm substitution of the core consensus TCGC to ATAA, Figure 4.14A. Reporter gene co-transfections were repeated using this mutated construct (pP7P<delta>) and the original p1.5I1RLuc plasmid. No change to the *Pax3* response was observed, see Figure 4.14B, indicating that *Pax3* does not bind to this consensus sequence to mediate its effect in this system.

Figure 4.14:
A) Site directed mutagenesis of the *Pax3* consensus site in the *Pax7* promoter sequence alignment
B) Luciferase response of p1.5I1RLuc and pP7P<delta> illustrating no change in Pax3 response on co-transfection with 250ng pCMV-Pax3. Data is fold induction over baseline (pGL3basic), n = 4, error bars are SEM

A

B

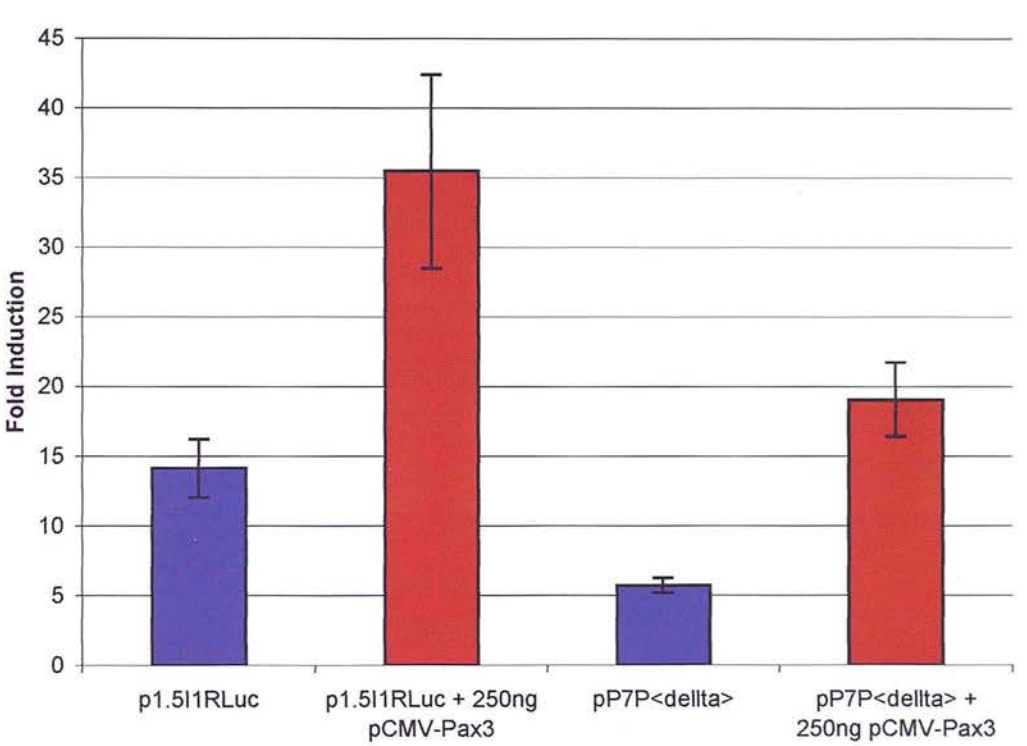

Finally, since this 'de-repression' of *Pax7* regulatory elements by *Pax3* was not predicted in the literature, and is in fact in direct contradiction to data presented by (Borycki et al., 1999) for the expression of *Pax3* in the C2C12 cell line, Western blotting analysis of *Pax3* and *Pax7* was performed to see if the implied changes in *Pax7* regulation could be observed at the protein level in C2C12 cells. The *Pax3* anti-serum (rabbit) described in Chapter 5 and the DSHB α-*Pax7* (mouse) were used for all pCMV-*Pax3* quantities used in the above reporter gene assays. A β-actin antibody (goat) was also used to control for loading differences on the *Pax7* blot, after stripping. This result can be seen in Figure 4.15A.

These data show that, as more pCMV-*Pax3* is transfected into the C2C12 cells, more *Pax3* protein is made. They also indicate that the level of *Pax7* protein expressed by these cells is initially undetectable in this assay, but is induced by increasing quantities of *Pax3*. The β-actin control indicates that this change is not an artefact of loading. To contrast this result, a northern blot published by (Borycki et al., 1999) is included in Figure 4.15B, clearly showing a loss of *Pax7* activity in C2C12 cells stabling expressing *Pax3*.

Discussion (Hypothesis Three)

The aims of this chapter were to first try and establish experimentally some regions of the mouse *Pax7* genomic locus that might control expression of this gene *in vivo* and then to use these elements to test the third hypothesis outlined in Chapter One. Since no regulatory elements had been defined for the mouse *Pax7* gene at the start of this

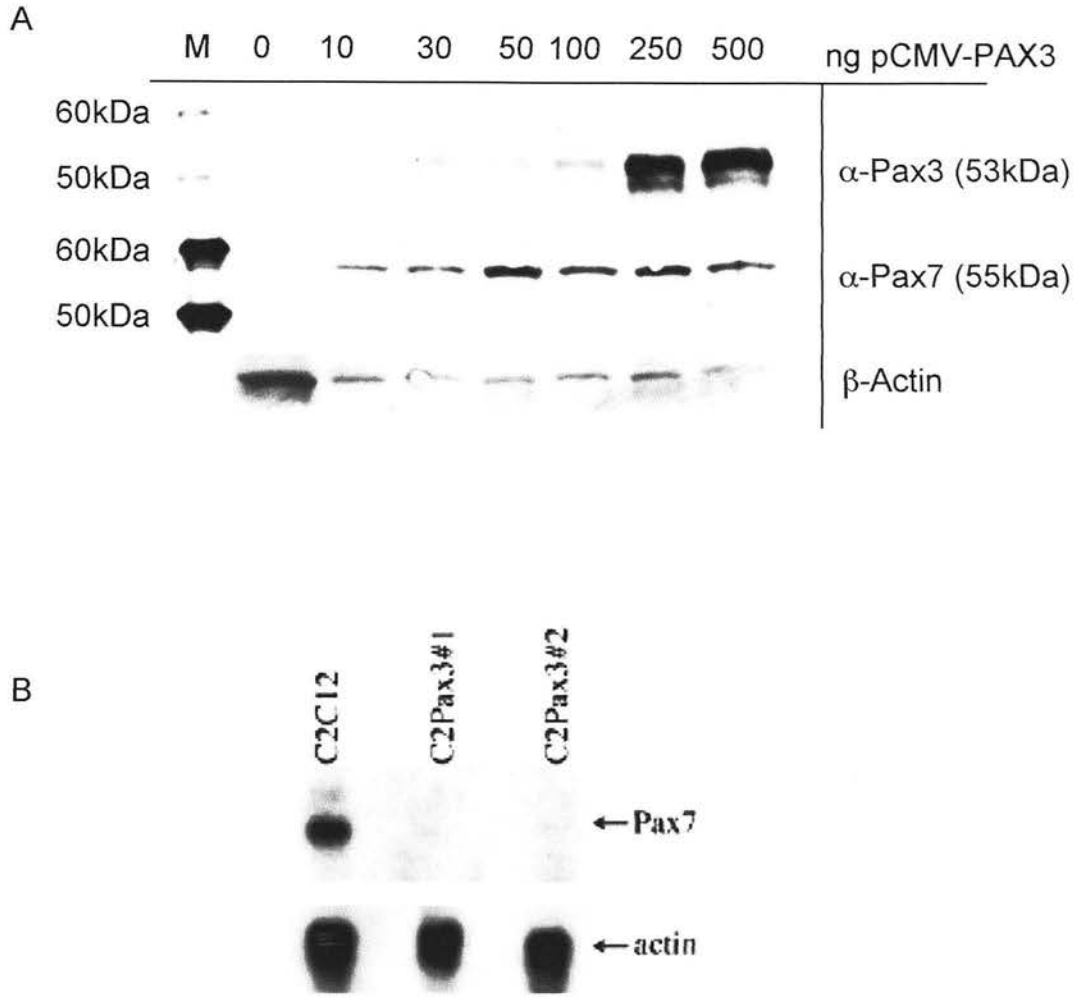

Figure 4.15:
A) Western blotting for Pax3, Pax7 and β-Actin from C2C12 cells transfected with 0 - 500ng pCMV-Pax3, showing increase in *Pax3* protein and *Pax7* protein (β-Actin shown as lane loading control)
B) Contrasting evidence from Borycki, A. et al 1999, of a Northern blot illustrating *Pax7* RNA levels from two C2C12 cell lines stably transfected with a Pax3 expression construct

project, the minimal promoter was perceived as good starting point. To this end a comprehensive bioinformatic analysis was performed over the entire *Pax7* region, and highly conserved CpG island was identified in the 1 – 2kb upstream of the *Pax7* coding exon. To ensure this region could act as a minimal promoter, the 5'UTR of the *Pax7* gene was also characterised in the mouse to see if upstream, non-coding exons could be detected. Since the coding sequence of the *Pax7* gene covers around 200kb of genomic DNA the potential existence of upstream exons, which would position any minimal promoter away from the area identified by bioinformatics, had to be considered. The results from PEXT, 5'RACE and RPA indicated a definite transcriptional start site around 100bp upstream of the start of the *Pax7* coding sequence. This is in agreement with some reports published concerning the human *Pax7* gene (Murmann et al., 2000; Schafer et al., 1994). PEXT repeatably demonstrated a second population of 5'UTR's of between 300 – 500bp. This product was not detected in 5'RACE or RPA experiments. It was concluded that, given the range of sources of RNA used in the PEXT experiments, this seemed unlikely to be an artefact of PEXT methodology. Previous reports have indicated *Pax7* may have a longer (600 – 650bp) 5'UTR, which would be closer to the size reported here (Syagailo et al., 2002; Vorobyov et al., 1997). None of these researchers report a novel non-coding exon, however. Since the start of this project, one paper analysing the *Pax7* promoter in the mouse has been published (Lang et al., 2003). This group conclude that the *Pax7* 5'UTR is 73bp, and encodes no novel exons. Whilst this is in agreement with my data, the evidence presented by this group does not rule out the possibility of larger 5'UTR's. Given the heterogeneity of actual start sites reported for this gene, and the extremely high CG content of the proximal sequence, it possible a discrete single start site for *Pax7* does not exist. In other systems, such conditions

have been attributed as causative factors for a 'stuttery' transcriptional start sites, (Ayoubi and Van den Ven, 1996), where transcription starts at numerous places within a defined region. This may explain the differences observed between both the data obtained from different techniques here, and that reported in the literature. Importantly, no novel upstream exons have been reported for *Pax7*, allowing a putative promoter region to be positioned here.

This region was cloned and used in reporter gene assays in *Pax7* positive cell lines, and promoter activity mapped to the proximal 1.5kb. Initial bioinformatic analyses also indicated a highly conserved element within intron one. This was cloned and found to act as a canonical silencer element *in vitro*. This element was also identified by (Lang et al., 2003) and shown in transgenic assays to act as a Pons-specific enhancer, in contrast to the role indicated here.

To address hypothesis three, the minimal promoter was assayed for an *in vitro* response to *Pax3* in co-transfection assays, since a *Pax3* consensus had been identified in this region. This did not demonstrate a response, nor did the I1R silencer. When both elements were carried on the same reporter vector, a *Pax3* dependant 'de-repression' of reporter gene activity was observed. Mutagenesis indicated this activity was not mediated by the *Pax3* binding consensus identified in the promoter.

Finally, the effect of *Pax3* expression on endogenous C2C12 *Pax7* expression was conducted by Western blotting. Interestingly, a clear induction of *Pax7* was observed with increasing quantities of *Pax3*. This was in contrast to previously published reports

It was concluded from the above that *Pax3* is able to effect the transcription of *Pax7* *in vitro*, but that this regulation may be from either the proximal promoter or the I1R element identified above. Therefore hypothesis three can be partially confirmed; *Pax3* does seem to have an effect on the regulatory elements defined here *in vitro*, but the mechanism and *in vivo* significance of that effect is unclear. Chapter Six will attempt to investigate which of these elements, if any, are occupied by the *Pax3* protein *in vivo*, and attempt to establish a role for *Pax3* in the regulation of *Pax7* in an embryonic context.

Chapter Five: Generation of a novel α-Pax3 antibody

Introduction

Chromatin Immunoprecipitation (ChIP) requires relatively large (μg) quantities of specific antibody, to reduce background and increase the sensitivity and specificity of detection. At the start of this project, only one anti-Pax3 antibody had been described (Stark, 1997). This was a rabbit polyclonal derived by another group, and therefore not reliably available in large quantities. The decision was made to raise and design a new anti-Pax3 antibody, using specific peptide sequences, to enable multiple ChIP experiments to be performed and optimised. This chapter describes the methods used to design and raise a rabbit polyclonal antibody to specific peptide sequences within the *Pax3* protein. The anti-sera obtained were characterised using both Western blotting and immunohistochemistry to confirm detection of the Pax3 epitope at the correct molecular weight and expression pattern. One of the sera was then selected and purified to obtain mono-specificity on Western blot and clean expression patterns with immunohistochemistry.

Peptide Design and Antibody Production

The Pax3 sequence and predicted structure were considered in the design of the peptides used to generate anti-Pax3 sera. From X-ray analyses of both Paired domains (Xu, 1995) and structural dissections of Pax3 (Chalepakis et al., 1994) it has been

shown that the N-terminal regions contain the DNA binding domains, whilst the C-terminus of the protein is involved in recruiting transcriptional complexes. The C-terminus of the Pax3 protein sequence was examined to identify possible immunogenic peptide sequences. It was reasoned that the N-terminal DNA binding domains may contain less structural epitopes accessible to an antibody when bound to DNA due to conformational restrictions and the possible presence of associated co-factors or the RNA polymerase machinery. The C-terminal portion of the related Pax6 protein has been hypothesised to be less structurally ordered on contact with DNA than the paired domain (Xu, 1999). Structural disorder has been cited as a possible factor increasing the immunogencity of an epitope experimentally due to its increased availability for antibody binding. Furthermore, since ChIP depends upon transcription factor – DNA contact peptides in the N-terminal portion of the protein would be undesirable since they may disrupt protein – DNA interactions.

Figure 5.1 shows the full peptide sequence of Pax3, and highlights the peptide sequences initially considered for immunisation. Peptides A and B were chosen. Peptide A represents the natural C-terminus of Pax3, contains ~60% polar residues (green) one charged residue (lysine at position 12 - red) and the negatively charged carboxyl group at position 16. Peptide A was chemically modified to include an cysteine residue at the very N-terminus; this was to enable chemical linkage to the carrier protein (Keyhole Limpet Haemocyanin) via the sulphydryl group. Peptide B is a shorter peptide, has an overall negative charge, and is also composed of ~60% polar residues. This peptide was chemically modified to amidate the C-terminus; since this sequence is internal in the protein this would better represent the chemical environment of the N-terminal region of this sequence. Analysis of the C-terminus of

Figure 5.1:
A) Scale drawing of the Pax3 polypeptide. Major features illustrated; yellow boxes show the position of peptide sequences A, B, and C.
B) Peptide sequences (green = polar, red = charged side chains).
C) Antigenicity and flexibility plots for the C-terminus of Pax3; Peptide A and B sequences highlighted in red.

A

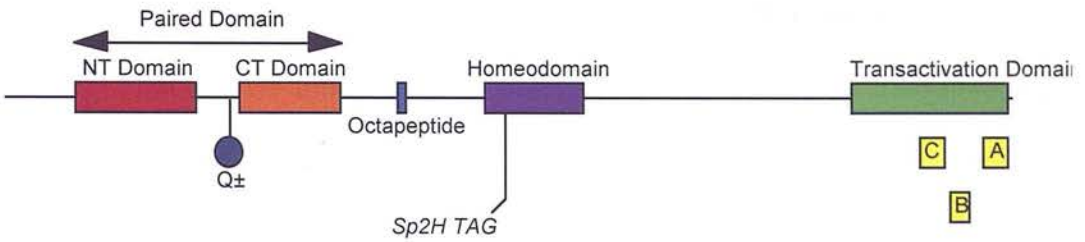

B

Peptide A :TGYQYGQYGQSKPWTF
Peptide B :CPPTYSTAGYSMD
Peptide C : EHMKNVDSLPTSQPYC

C

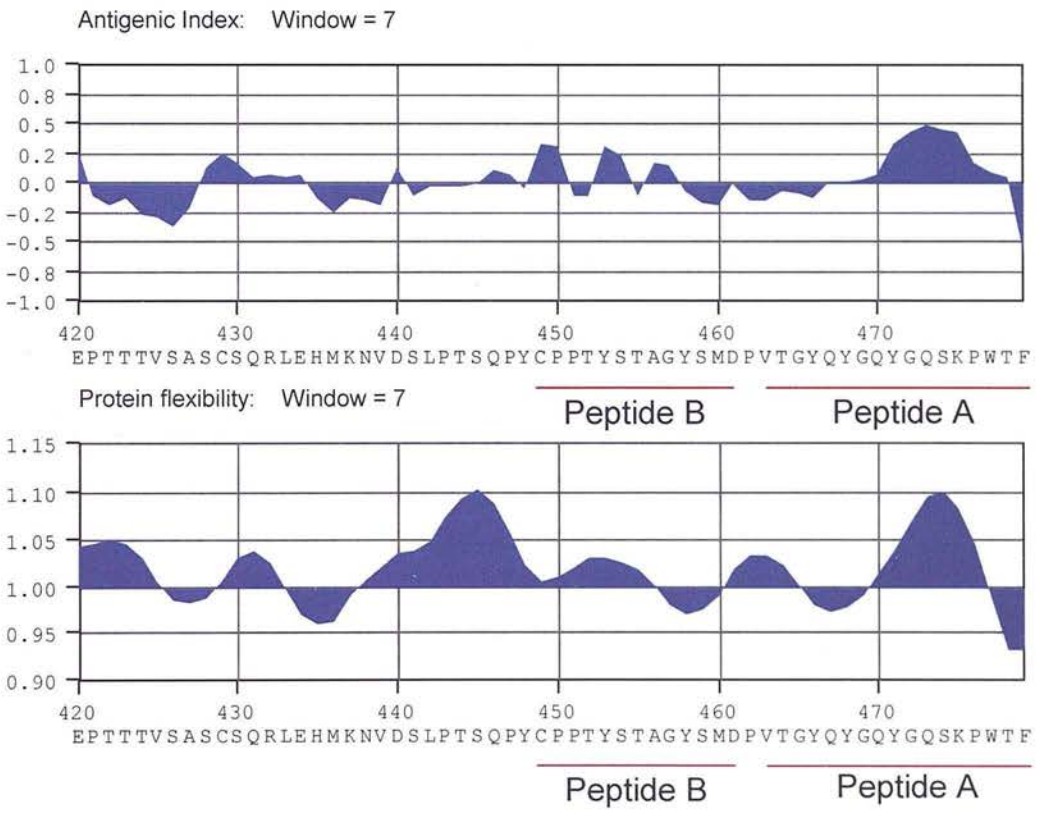

the protein using MacVector antigenicity index and flexibility plot prediction software further illustrated that these peptide sequences represented regions of the protein which had both high flexibility and antigenicity (Figure 5.1C). Peptide C was initially identified as potentially antigenic sequence, but was ultimately not used as this epitope was considered too far into the protein, risking the epitope being occluded by tertiary structure in the intact protein. Also bioinformatic analysis suggested a low antigenicity index (Figure 5.1C). Anti-sera were raised in rabbits as described in Chapter 2; two rabbits were immunised for each peptide, generating four batches of anti-sera.

Verification of α-Pax3 immunogenicity

To evaluate the sera obtained from immunisation with peptides A and B, Western blotting was performed on NIH-3T3 cells transiently transfected with pCMV-*Pax3* plasmid, as described in Chapter Two. The pCMV-*Pax3* plasmid contains a full length *Pax3* cDNA driven by a strong (CMV) promoter, and was used in these experiments as a source of *in vitro* expressed *Pax3* protein. NIH-3T3 were previously shown not to express Pax3, as detectable by RTPCR (data not shown). Mock transfected NIH-3T3 cells (transfected with the pCMV-Script plasmid) were therefore used as a source of negative control protein. All four sera were tested by comparing pre-immune with post immune sera (to ensure any bands observed were the result of immunisation against the Pax3 peptides), on protein extracts from transfected and mock-transfected NIH-3T3 cultures. Serum generated from peptide A (rabbit 1) gave the best potential-band at this stage and was therefore used in all later experiments.

Peptide A (rabbit 2) and one of the rabbits immunised with peptide B did also generate Pax3 bands, but these were weaker and therefore not used (data not shown).

Figure 5.2A shows the initial Western blot for the peptide A serum, comparing pre and post-immune sera on protein samples containing Pax3 and matched negative controls. The Pax3 band, at 53 kDa is highlighted in the post-immune western. Western blotting conditions were further optimised, Figure 5.2B, to reduce background. The antibody was then used to detect Pax3 protein from NIH-3T3 (± pCMV-Pax3), C2C12 (±pCMV-Pax3) and E11.5 wild type and Sp^{2H} homozygous mutant (Pax3 null) mice (Figure 5.2C). As Figure 5.1A illustrates, the Sp^{2H} mutations would truncate any protein product from the *splotch* allele before the peptide sequences used to raise the anti-sera. Therefore no *Pax3* protein should be detectable by Western blot in extracts from Sp^{2H} homozygous mutant embryos.

To further confirm the specificity of the serum to Pax3, immunohistochemistry was then attempted using the un-purified serum. Unfortunately the background levels on all sections examined was too high to enable specific expression patterns to be reliably determined (data not shown). This is perhaps unsurprising given the number of non-specific bands observed on Western blots using this serum.

Antibody Purification

ChIP requires a source of anti-serum as specific as possible. To prepare the anti-Pax3 serum for ChIP, and to enable its use in immunohistochemistry, a protein-G column purification, followed by a two step acid elution, protocol was used. After washing,

Figure 5.2:
A) Western blot using serum from rabbits immunised with peptide A. Comparison of pre-immune serum with post-immune serum on NIH-3T3 transfected with pCMV-Pax3 expression plasmid or empty vector (±). Pax3 pro-band highlighted.
B) Western blot optimised using serum from rabbits immunised with peptide A. Pax3 clearly visible at ~53kDa, and specific to cell transfected with pCMV-Pax3.
C) Western blot showing presence of Pax3 in wild-type E11.5 embryos (lane 1), cells transfected with pCMV-Pax3 (lanes 3 and 5). Homozygous *Splotch* embryo protein was loaded in lane 2. Lanes 4 and 6 represent protein extracts from cells lines transfected with empty vector.

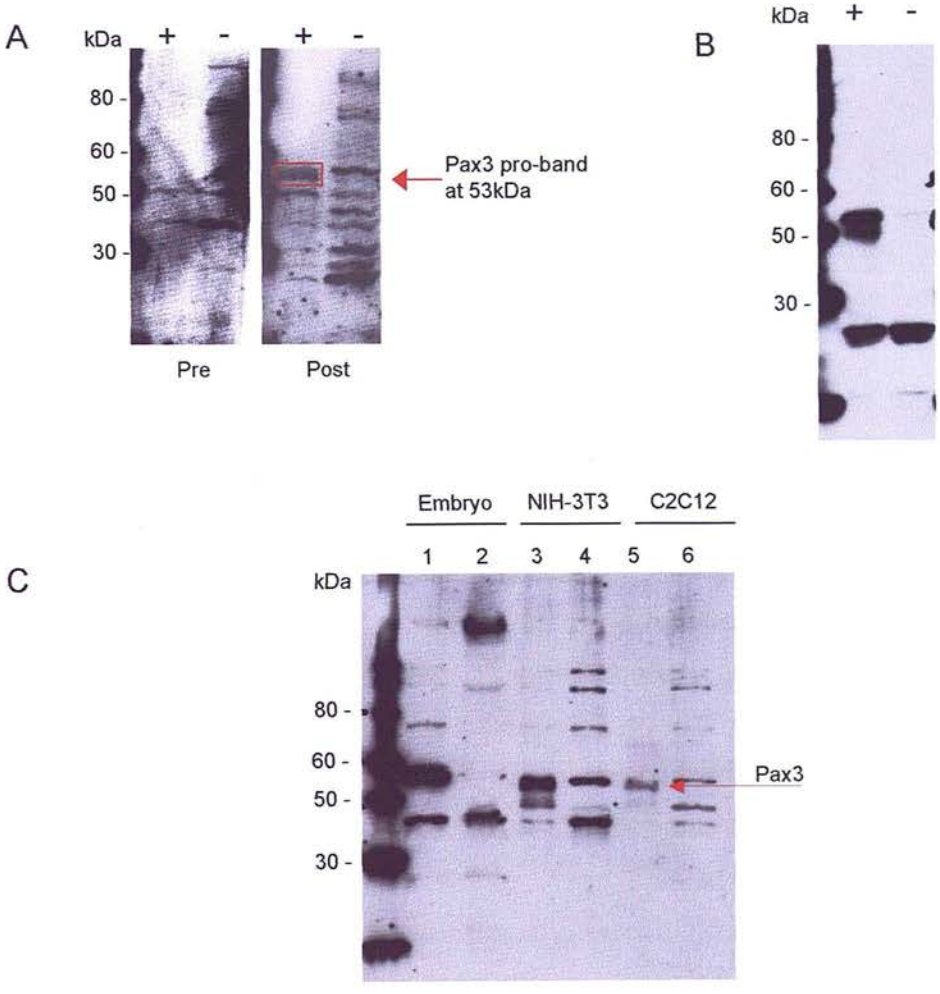

elute was collected in 1 minute intervals (1ml) and the protein concentration determined by Bradford assay. A plot of protein concentration (expressed as OD at λ562) vs. elution volume can be seen in Figure 5.3.

A clear elution peak can clearly be seen between elution volumes pH2.7(5) and pH2.7(9). These volumes were combined and referred to as α-Pax3(HT) (High Titre). The slow tail-off in protein concentration between volumes pH2.7(10) and pH2.7(14) was interpreted as a potential second peak, poorly resolved due to the relative crudity of the protein concentration assay. These elutes were also combined and referred to as α-Pax3(LT) (Low Titre). The mean (OD = 0.15 n = 6, SD = 0.004) blank (background) OD λ562 is shown on the plot for reference. No protein over background could be detected in any of the samples eluted with the pH1.9 buffer. These were discarded.

α-Pax3(HT) and α-Pax3(LT) were therefore tested using the Western blot parameters outlined above (Figure 5.4A). This clearly shows that, whilst both fractions contain an anti-Pax3 immunogenicity, the α-Pax3(HT) still retains many of the non-specific bands previously described for the unpurified serum. This is possibly due to the use of a protein-G column, which binds IgG heavy chain irrespective of immunospecificity, rather than a peptide A specific column. The α-Pax3(LT), however, gave an extremely clear signal at the appropriate M_r for Pax3. During the process of deriving and purifying this antibody, a monoclonal anti-Pax3 resource became available from the DSHB (Developmental Studies Hybridoma Bank, Iowa). To compare specificities, Western blots were performed comparing the two antibodies (DSHB and α-Pax3(LT)) under identical conditions (Figure 5.4B). The DSHB antibody gave a

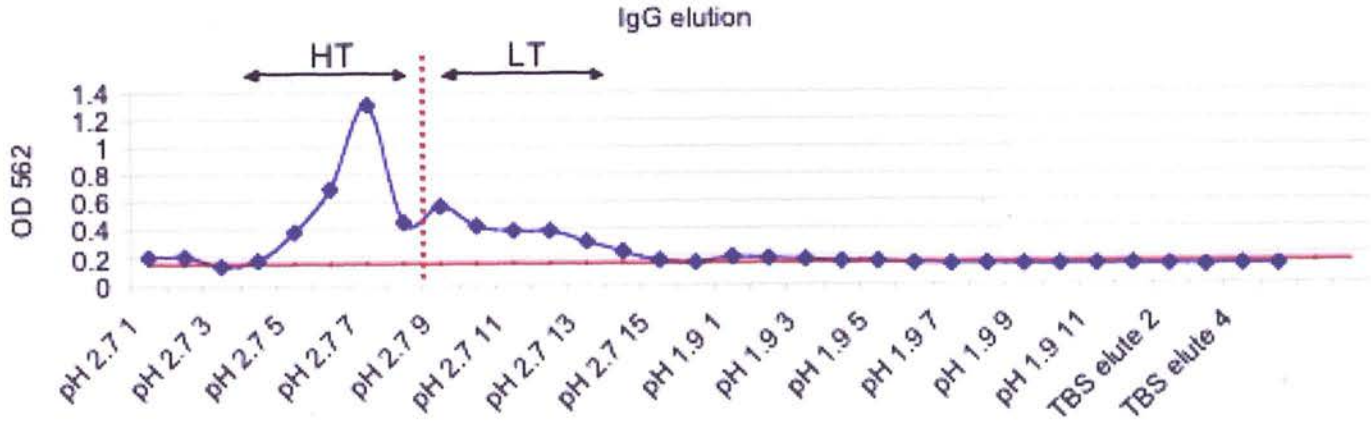

Figure 5.3: IgG acid elution curve to generate monospecific anti-Pax3 antisera. Time (volume) of sample eluted from column is plotted against OD562 (protein concentration). HT = samples collated to generate α-Pax3(HT), LT = samples collated to generate α-Pax3(LT). Solid red line represents background protein concentration in eluate.

Figure 5.4:
A) Western blot on NIH-3T3 cells transfected with either pCMV-Pax3 (+) or empty vector (-). Comparing the LT and HT α-Pax3 fractions collected
B) Western blot on NIH-3T3 cells transfected with either pCMV-Pax3 (+) or empty vector (-). Comparing α-Pax3(LT) with the monoclonal antibody from the DSHB

A

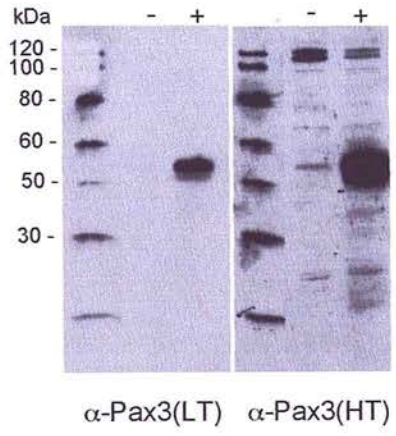

B

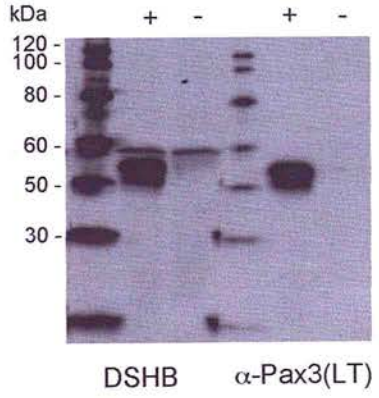

non-specific band of about 60kDa which was absent from the α-Pax3(LT) westerns. This correspond with Western blots obtained using a sample of the source polyclonal used to derive this monoclonal (A kind gift from M. Goulding, data not shown) when verifying the production of Pax3 from transfected NIH-3T3 cells. Since ChIP requires as mono-specific an antibody as possible, and the fact that the DSHB antibody was produced from the C-terminal 183 residues, rather than a specific peptide sequence (Venters et al., 2004), the α-Pax3(LT) was chosen for the ChIP experiments. α-Pax3(LT) is henceforth referred to as α-Pax3.

α-Pax3 Immunohistochemistry

Given the specificity of the α-Pax3 polyclonal on Western blot, immunohistochemistry on wax embedded, transverse sectioned, wild-type E12.5 mouse embryos was performed. Figure 5.5A illustrates a transverse section showing clear specific staining in dorsal neural tube (NT), dorsal root ganglion (DRG) and facial mesenchyme. Figure 5.5B is a high-power image of the same section, showing nuclear staining in both NT and DRG cells, as expected for a transcription factor, and 5.5C a high power image from another section, illustrating Pax3 positive cells delaminating from the dorsal edge of the NT, possibly neural crest. Also illustrated are comparative sections from published work (Dottori et al., 2001) and (Terzic and Saraga-Babic, 1999). Since the purpose of this exercise was to confirm the Pax3 specificity of the α-Pax3 polyclonal produced, further expression analysis was not performed. The lack of a comprehensive publication detailing Pax3 protein expression

Figure 5.5:
A) Transverse section through E12.5 WT embryo. Pax3 expression in dorsal neural tube (NT), facial mesenchyme (FM) and dorsal root ganglia (DRG).
B) High power image of inset highlighted in A. Note Pax3 expression in migrating neural crest cells (NC).
C) Comparison of similar published images illustrating Pax3 expression. Human 9 week fetus Pax3 immuno (Terzic et al 1999), Mouse E12.5 transverse section Pax3 immuno (Pax3 = red and yellow signal) (Dottori et al 2001), another high power transverse section showing nuclear Pax3 staining.

A

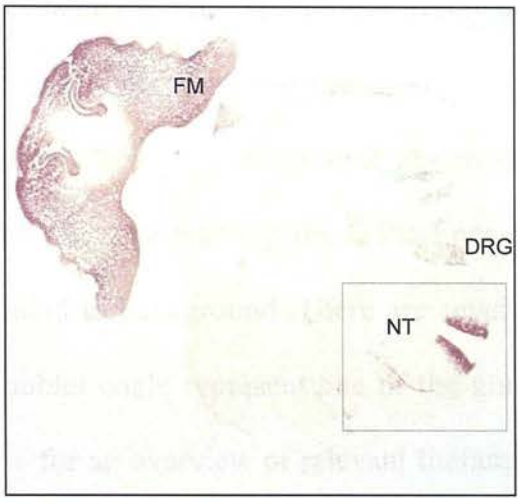

B

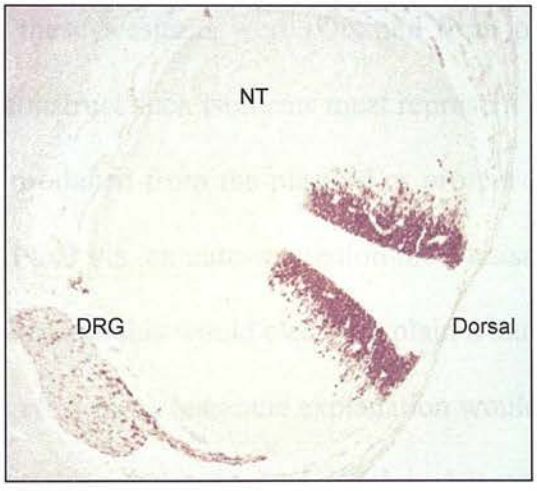

C

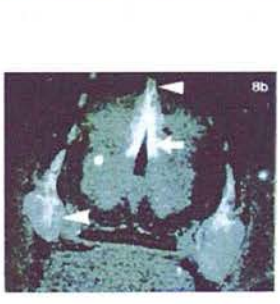

Terzic et a 1999

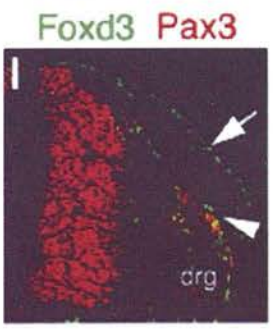

Dottori et al 2001

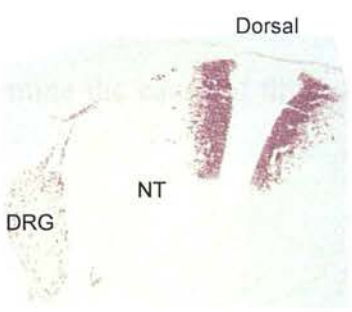

across a developmental series would make this anti-serum a potentially attractive tool for future investigators, however.

Discussion

The α-Pax3 polyclonal described here was then aliquoted and stored appropriately for ChIP, described in Chapter 6. All experiments described in this thesis using an α-Pax3 antibody were performed using the above polyclonal. One interesting aspect of all Western blots shown here, whichever antibody was used, was the presence of a doublet (see Figure 5.4B). This was specific to Pax3 positive lanes only, and therefore could not be attributed to background. There are several possible explanations for this. Firstly, the doublet could represent one of the glutamine or exon isoforms of Pax3 (see Chapter 1 for an overview of relevant literature). Since many of the Pax3 bands detected on these westerns were obtained from protein driven from a Pax3 cDNA expression construct such isoforms must represent either novel splicing events within the mRNA produced from the plasmid or protein produced from the cells on genomic copies of Pax3 via an auto-regulation mechanism. Pax3 may have different phosphorylation states and this would clearly explain a band migrating a different rate on an SDS-PAGE gel. A more mundane explanation would be that the doublet simply represents a common degradation product which is detected in transfected cells due to the high quantities of Pax3 produced in these transfections. Further investigation is required to differentiate between these possibilities and determine the cause of this doublet.

Chapter Six: *in vivo* Chromatin immunoprecipitation

Introduction

In this chapter the occupancy of the transcription factor binding sites previously investigated on the *cis*-regulatory target sequences identified will be tested *in vivo*. This will bring together the *in vitro* studies that have attempted to establish a possible role for the regulation of *Wnt1* and *Pax7* by *Pax3*. To this end the anti-*Pax3* antibody, designed and purified as described in Chapter 5, and the anti-Msx1/2 antibody obtained from the DSHB were used to develop specific Chromatin Immunoprecipitation (ChIP) assays on mouse embryonic tissue. This technique allows the localisation of transcription factor binding sites to specific regions of genomic DNA. The data described below confirms the *in vitro* observations for the *Pax3* regulation of *Wnt1* via the 5' proximal promoter region, raises some interesting possibilities for the interaction of *Msx2* with these regulatory elements, and resolves the uncertainty over the location of *Pax3* interaction within the *Pax7* genomic locus.

ChIP: an overview

The ChIP technique isolates and enriches DNA sequences which are involved in protein-DNA interactions. The technique was originally designed for use with chromatin remodelling proteins (such as DNA methyltransferases and histone deacetylases) but has since been adapted for a number of other assays to assess any

kind of protein-DNA interaction (Ren, 2000b). An increasingly widely used application of this technology is the characterisation of transcription factors binding to target sequences within the genome. Generally this technique has been used to examine these interactions in cell culture, due to the relative ease of obtaining large amounts of source material, but the demand for *in vivo* ChIP to examine the validity of findings (such as those outlined in Chapters 3 and 4) in the tissues and organisms of interest is growing.

A schematic of the ChIP process is shown in Figure 6.1. In the first stage, the transcription factor under investigation is assumed to bind to and activate / repress transcription of its target gene by binding to appropriate sequences within the genome (stage I - II). At this point the embryo or tissue is dissected and disassociated into single cells as rapidly as possible, and the cell suspensions treated with formaldehyde. The formaldehyde acts as a chemical cross linking agent between proteins (generally between the ε-amino group of lysine residues and adjacent amide bonds) and between proteins and DNA (between lysine residues and the NH_2 exocyclic moiety of adenine, guanine or cytosine (Siomin, 1973) –interestingly this requires the DNA to be at least partially denatured, or for the protein to be making close contact with the bases through the major or minor grooves of the DNA molecule. Both of these are thought to occur during the interaction of a transcription factor with its target sequence), see stage III. The transcription factor is then effectively 'trapped' on its target genomic sequence. The cells are then placed in detergent-based lysis buffer and subjected to sonication to disrupt the cell and nuclear membranes and to break the chromatin into fragments of a desired size, stage IV. The tissue sample has now been broken into a pool of chromatin fragments with transcription factors, histones, and other DNA

Figure 6.1

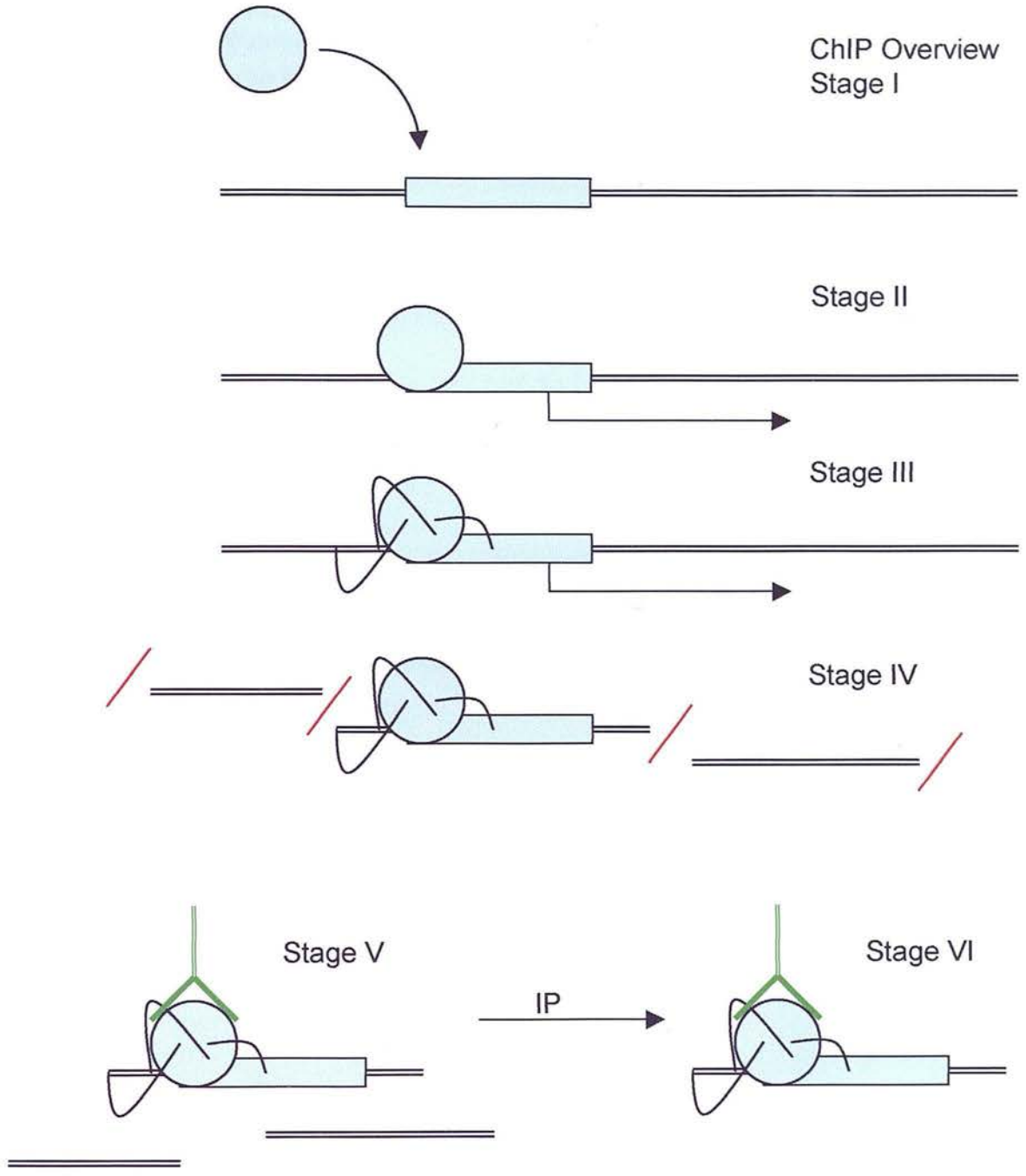
ChIP Overview
Stage I
Stage II
Stage III
Stage IV
Stage V
IP
Stage VI
Stage VII
PCR or cloning
and sequencing =
verification of target
site occupancy

Figure 6.1:
Schematic of *in vivo* ChIP protocol.
Stage I: Transcription factor (circle) of interest is binds target element (box) on genomic DNA (line) in appropriate tissue / developmental stage
Stage II: Transcription factor drives / alters expression of target gene
Stage III: Cells / tissue extracted and treated with weak formaldehyde treatment to crosslink proteins and DNA *in situ* (curved lines)
Stage IV: Crosslinking quenched, and cells lysed. Crosslinked protein - DNA complexes sonicated to break up genomic DNA into smaller fragments
Stage V: Antibody specific to transcripiton factor of interest the added to pool of sonicated protein-DNA complexes
Stage VI: Immunoprecititation performed to isolate Antibody - transcription factor - DNA complexes
Stage VII: Protein - DNA complexes uncrosslinked, proteins and antibodies degraded with proteases, and DNA isolated by phenol - choloroform. Primers specific to the regulatory regions being tested for transcription factor occupancy then used to screen pool of DNA fragments and amplify sequences if present.

associated proteins bound co-valently. To enrich specifically for those complexes containing the transcription factor under investigation, an immunoprecipitation is performed using an antibody raised against the protein of interest (stage VI). Once all unwanted species have been washed away, the antibody – transcription factor – DNA complexes (stage VI) are then eluted from the IP and the formaldehyde cross links reversed using heat and halide (typically Cl^-). The proteins (antibody and transcription factor) and any co-purifying RNA are then enzymatically digested. This should leave a population of DNA fragments, of broadly uniform size due to the sonication process employed, which were bound to the transcription factor under investigation. These are then phenol chloroform purified and re-suspended in clean ddH_2O.

At this stage the occupancy of a specific site can be tested by designing flanking PCR primers and testing the pool of precipitated fragments for the presence of this site (stage VII). Enrichment can be meaningfully assessed by also attempting to amplify a genomic sequence to which the factor is known / thought not to bind to. It is important to ensure that the second sequence is not too close to the putative binding sequence so as not to co-purify on the same fragment. This makes the sonication step essential; care must be taken to ensure all chromatin is fragmented to a size sufficiently small that these two amplicons cannot occupy the same fragment, but large enough to ensure that both test primers can anneal to the same target fragment and enable PCR amplification to occur. A positive control PCR of 'input' chromatin (i.e. sonicated chromatin from the source sample which is phenol chloroform purified without any intermediate immunoprecipitation) and a negative control 'no antibody' PCR (i.e. a sonicated chromatin sample where water instead of antibody was added at the IP stage).

Alternatively the populations of enriched fragments can be cloned and sequenced, or applied to genome coverage microarrays. Both of these endpoints are generally used to identify novel target sequences and, whilst not being experimentally utilised in this study, will be discussed in more detail later.

Thesis findings: an overview

Figure 6.2 presents a diagrammatic review of the findings so far described in this thesis and the interactions that the following ChIP experiments were designed to investigate. Figure 6.2A summarises the *in vitro* interactions suggested between *Pax3* and the *Wnt1* regulatory elements in an *in vivo* context. Illustrated is the mouse genomic *Wnt1* region, highlighting the four exons, the distal 110bp enhancer (blue box) and the *Pax3* consensus site contained within the 1.2kb proximal promoter region (green arrow). Deletion and site directed mutagenesis studies have strongly suggested that this *Pax3* consensus may mediate an active binding site for the *Pax3* protein *in vivo*. ChIP was performed on these regions using the purified anti-*Pax3* polyclonal antibody described in Chapter 5 to confirm *in vivo* occupation of this site, and not the *Wnt1* distal enhancer.

Figure 6.2B summarises the putative relationship of the *Msx2* protein with the *Msx2* consensus binding site in the *Wnt1* distal enhancer, in the context of the mouse genomic *Wnt1* locus. This interaction was supported by deletion and transposition studies using luciferase reporter vectors *in vitro*. No mutagenesis experiments were conducted on this site during this investigation. ChIP using the anti-Msx1/2 antibody

Figure 6.2

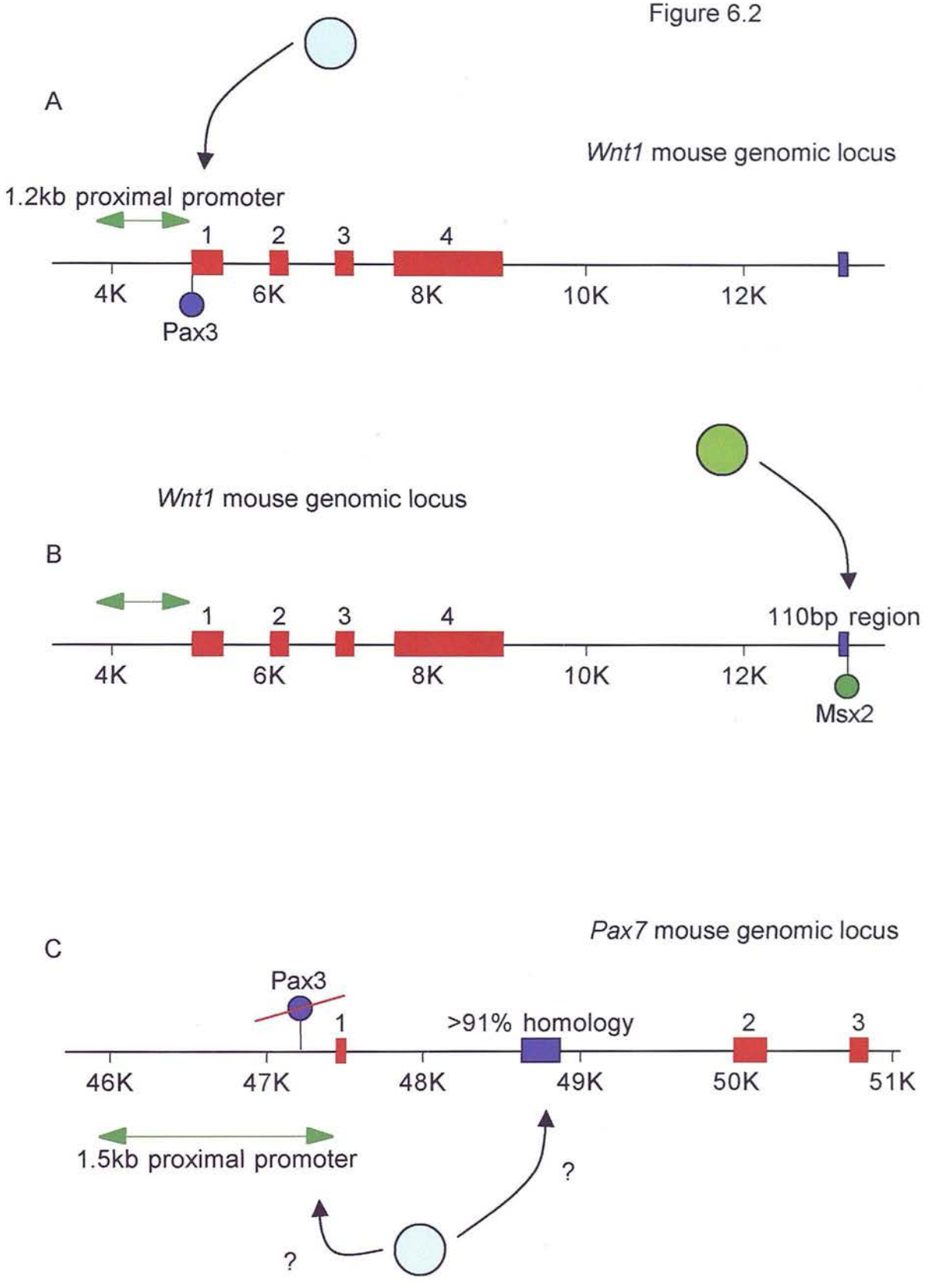
A
Wnt1 mouse genomic locus
1.2kb proximal promoter
1
2
3
4
4K
6K
8K
10K
12K
Pax3
Wnt1 mouse genomic locus
B
1
2
3
4
110bp region
4K
6K
8K
10K
12K
Msx2
C
Pax7 mouse genomic locus
Pax3
1
>91% homology
2
3
46K
47K
48K
49K
50K
51K
1.5kb proximal promoter
?
?

Figure 6.2:
A) Summary of model proposed from *in vitro* data described in Chapter 3 and in investigation of hypothesis one. Pax3 binds to and transactivates the Wnt1 proximal promoter via a defined Pax3 consensus site, confirmed by mutagenesis and deletion studies
B) Model proposed from *in vitro* data and investigation of hypothesis two described in Chapter 3. Msx2 binds to the Wnt1 distal enhancer (within the conserved 110bp element, see Echelard et al 1994) to repress transcription, confirmed by deletion and translocation studies
C) Model proposed by *in vitro* data described in Chapter 4 and in investigation of hypothesis three. Pax3 binds to either the 1.5kb proximal promoter or the highly conserved I1R element within intron one of the Pax7 locus, but not via the Pax3 consensus site present in the promoter region. Confirmed by mutagenesis and deletion studies

was used to try and show the *in vivo* occupation of *Msx2* at this site, and not the *Wnt1* proximal promoter, and is discussed below.

Figure 6.2C summarises the *in vitro* data obtained during an investigation into the relationship between *Pax3* and the *Pax7* regulatory elements *in vitro*. The *Pax7* genomic locus is shown, illustrating the first three coding exons, the 1.5kb proximal promoter and the I1R silencer within intron 1. Luciferase experiments demonstrated that both the proximal promoter and the I1R element were necessary to observe a *Pax3* driven transcriptional effect, although this was a de-repression (contrary to the relationship previously described by one group), and was not mediated by the *Pax3* consensus in the 5' proximal promoter (as determined by site directed mutagenesis). To try and see if either of these sites were occupied by *Pax3 in vivo*, and support the findings of Chapter 4 as potentially biologically significant (rather than an artefact of the Luciferase assay system), ChIP using the *Pax3* antibody and primers specific to these regions was also performed.

ChIP: technical considerations

To examine the role of *Pax3* or *Msx2* in the transcriptional contexts described above and in previous chapters, it was necessary to utilise the correct embryonic tissues. The role of *Pax3* in regulating *Wnt1* transcription has been hypothesised to occur during the development of the murine neural tube, when both *Pax3* and *Wnt1* are being expressed, see Chapter 1. Similarly, any interaction between *Msx2* and the *Wnt1* locus is hypothesised to occur in the developing cardiac neural crest, also found within and around the dorsal neural tube. Finally the interaction between *Pax3* and the *Pax7*

locus has been hypothesised to be in both the somitic mesoderm, limb bud and neural tube. Embryos were collected at E10.5, and the neural tube, forelimb bud and mesoderm dissected as shown in figure 6.3A. Care was taken to remove telencephalon and any tissues caudal to the forelimb bud. E10.5 is a little late to isolate tissues containing migrating neural crest cells. However, one of the major technical difficulties in performing *in vivo* ChIP is obtaining enough starting material to generate an amplifiable pool of DNA fragments at the end of the procedure. Trials with embryos from ages ranging from E8.5 to E12.5 were initially performed. The most reliable ChIP fractions (generating consistently strong positive control PCR products for all amplicons described below) were generated by embryos at E10.5. Since it was felt that a compromise had to be made experimentally between embryo age and reproducibility of data, E10.5 embryos, dissected as shown, were used in the following ChIP assays.

The sonication of genomic DNA to the correct size is an essential stage in the design and implementation of ChIP experiments. Figure 6.3B shows the optimisation of sonication conditions. The left panel represents DNA extracted from E10.5 dissected, disassociated and fixed embryos which were then sonicated under a range of conditions. Conditions which favoured the generation of fragment sizes between 500bp and 1kb were used in all following experiments and example sonications can be seen from four embryo preparations in the right panel. This average size of DNA fragment length is large enough to enable all of the ChIP PCR reactions to amplify (product range between 282 and 595bp) but small enough to ensure that the two amplicons cannot fall entirely on the same fragment (minimum distance between

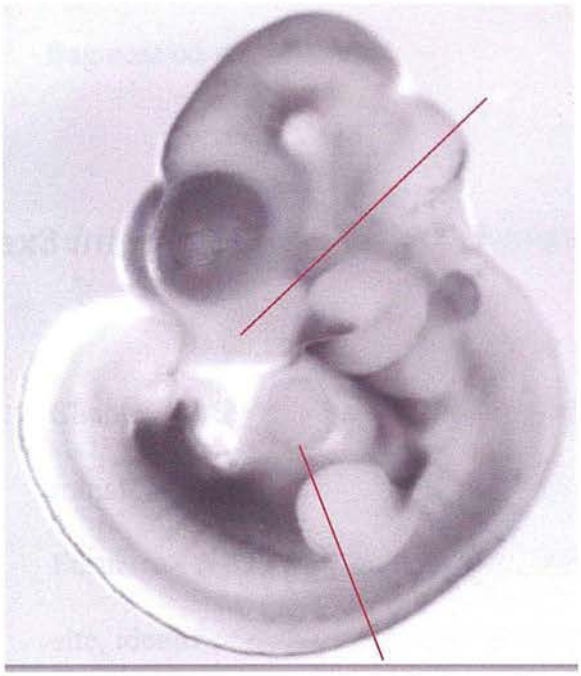

Figure 6.3:
A) Image of an E10.5 embryo showing locations of dissection when preparing sample for ChIP analysis (red lines). Mid / Forebrain and regions below the forelimb bud were discarded.
B)Agarose gels to illustrate the optimisation of sonication conditions to generate genomic DNA fragments of 0.5 - 1kb. Left panel shows initial optimisation of conditions for fixed, embryonic chromatin. Bar indicates increasing sonication power, U denotes un-sonicated chromatin. Right panel illustrates sample sonicated chromatin showing required fragmentation in four samples. Red line denotes 1kb level.

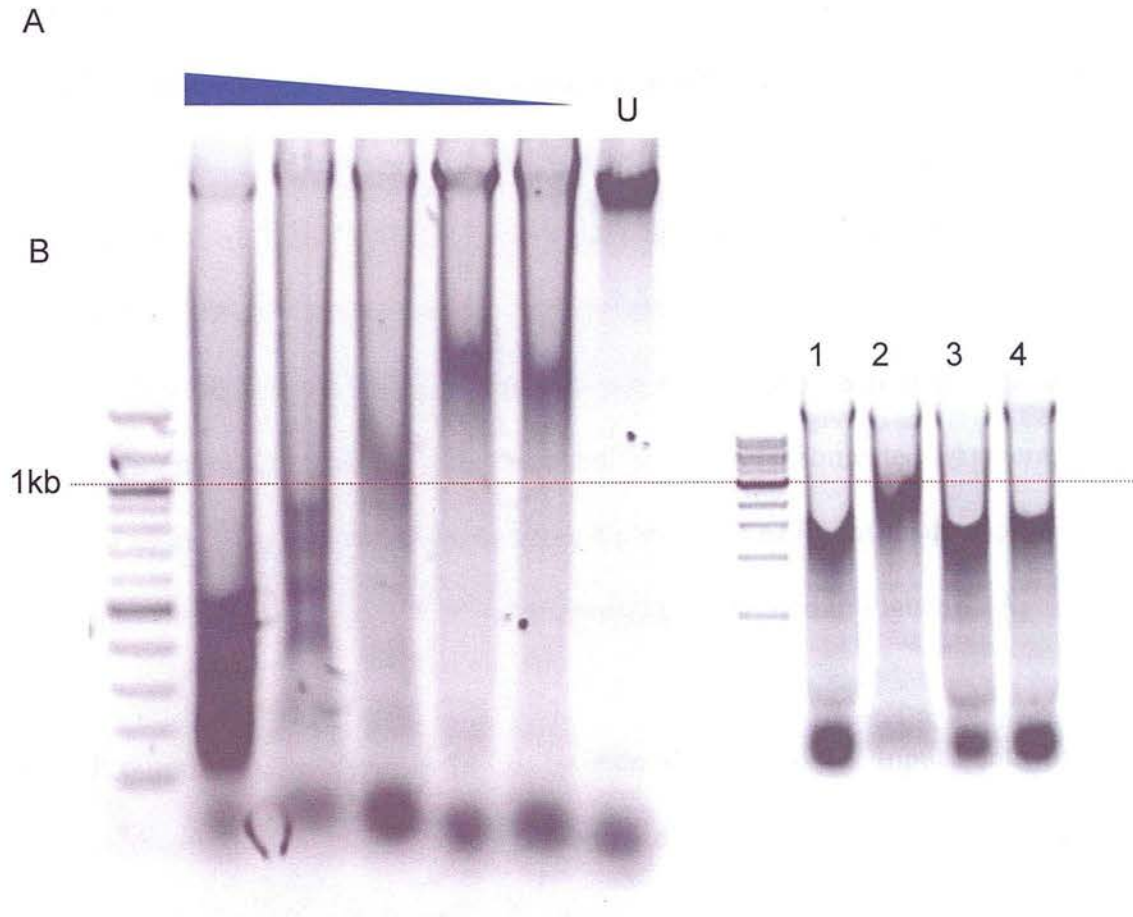

amplicons is 2.127kb on the *Pax7* locus) thus preventing a false positive signal due to fragment co-purification.

Pax3 *interacts with the Wnt1 proximal promoter* in vivo

Chapter 3 provides strong evidence from both QRTPCR *in vivo* and Luciferase co-transfection assays *in vitro* that *Wnt1* represents a direct target of *Pax3* regulation. Furthermore this interaction appears to be mediated via a *Pax3* consensus binding site, identified by bioinformatic analysis and confirmed with mutagenesis, in the *Wnt1* proximal promoter region. To test occupancy of this site *in vivo* ChIP assays were performed as described. Primers were designed to amplify the *Wnt1* genomic locus at either the 5' proximal promoter region (a 541bp product flanking the *Pax3* consensus, primers W1_PROM_CHIP_FWD/REV) or the 3' distal enhancer (a 282bp product containing the 110bp conserved element and the *Msx2* consensus binding site, primers W1_ENHAN_CHIP_FWD/REV). These sites are separated by 8.789kb of genomic DNA and therefore are unlikely to be contained on the same sonicated fragment. An illustration of the *Wnt1* genomic locus, showing exons, *Pax3* consensus and primer binding sites (labelled W1P and W1E respectively) is illustrated in Figure 6.4A.

The ChIP output for this experiment can be seen in Figure 6.4B. Input control was positive, indicating both fragments are present and competent to be amplified from the pre-IP pool of DNA and no antibody control negative, indicating that any bands observed are due to specific antibody binding during the IP. A clear positive signal is observed for three different wild type E10.5 dissected embryos, showing *Pax3* is

A

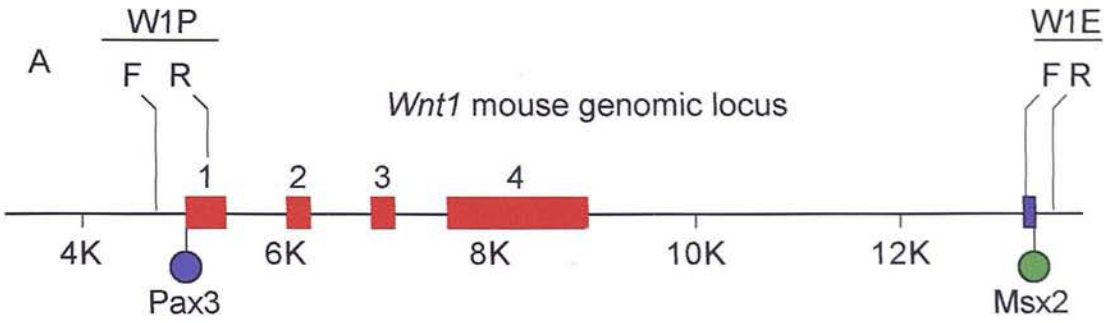

Fragment	PCR	Size
Wnt1 Promoter (W1P)	55^30	541 bp
Wnt1 Enhancer (W1E)	56^30	282 bp

B

Input
(positive control)

Embryo 1

Embryo 2

Embryo 3

No Antibody
(negative control)

Figure 6.4:
A Genomic Wnt1 locus showing ChIP primer binding sites, and table of predicted mplicon sizes
B) PCR products of anti-Pax3 ChIP using primers specific to the Wnt1 locus. Wnt1 promoter positive in all three experiments, confirming occupancy of this site *in vivo* by Pax3

bound to the *Wnt1* promoter region and not the distal enhancer at this stage in development an in these tissues.

This enables the conclusion that *Pax3* mediates the transcriptional upregulation of *Wnt1 in vivo* via the 5' proximal promoter and the *Pax3* consensus site described and in agreement with hypothesis one.

Msx2 *may associate with the Wnt1 locus* in vivo

Chapter 3 also provides evidence that the *Msx2* transcription factor may mediate the repression of *Wnt1* transcription through the binding of a consensus site in the 3' distal enhancer. These experiments were conducted in response to a study performed by (Kwang et al., 2002) where the misregulation of *Msx2* in the *Pax3* homozygous mutant was shown to be responsible for the cardiac phenotype observed in these animals. Given the importance of the *Wnt – Dvl2* pathway in the development of the cardiac outflow tract in a second series of studies (Hamblet, 2002), it was postulated here that the Wnt signal involved could be *Wnt1*, and that the expansion of *Msx2* expression in the *Splotch* mutant was able to repress *Wnt1* expression in these migratory cardiac neural crest. To test this hypothesis, the *cis*-regulatory elements of *Wnt1* were tested in co-transfection assays with an *Msx2* expression construct. A repressive activity of *Msx2* was observed in association with the *Wnt1* 3' distal enhancer. This was mapped with deletion and transposition constructs to a region of the enhancer containing a highly conserved 110bp element and an *Msx2* consensus site.

To test occupancy of this site *in vivo*, ChIP assays were performed on three wild type E10.5 embryos, dissected as described. Identical conditions and PCR primers to those used to test the occupancy of *Pax3* in the *Wnt1* promoter were employed here. These, and the position of the *Msx2* consensus site, are illustrated in Figure 6.5A. The Msx1/2 antibody obtained from the DSHB was used in the IP stage of these assays.

Figure 6.5B illustrates the ChIP output for these experiments. Unfortunately, whilst the positive and negative controls were correct, the ChIP assays themselves did not give a consistent or easily interpretable result. Two of the embryos assayed gave positive signals for both the promoter and the enhancer, whereas the third gave no signal at all. There are several ways in which to interpret this data. Firstly it is possible that the experiment simply did not work properly and has simply given random signals. More repeats are necessary to determine if this is the case. Given that the *Pax3* ChIP worked consistently under identical conditions for this locus other possible causative factors are considered. Assuming that the third embryo examined simply did not work the presence of bands in both the promoter and enhancer lanes may suggest a number of other outcomes. It is possible that *Msx2* is binding to one or other region of the *Wnt1* locus, but the sonication did not separate the two fragments efficiently or these regions were in close physical proximity and were bound together during the formaldehyde treatment. Since this was not the case for the *Pax3* ChIP illustrated in Figure 6.4 using identical source tissues and cross linking conditions, this would seem improbable. It is possible that *Msx2* was bound to both the promoter and enhancer regions in these tissues, although the lack of *in vitro* response from the *Wnt1* promoter fragments to the *Msx2* protein would argue against this. One major fault with this experiment was the use of a bi-specific anti Msx1/2 antibody. Clearly

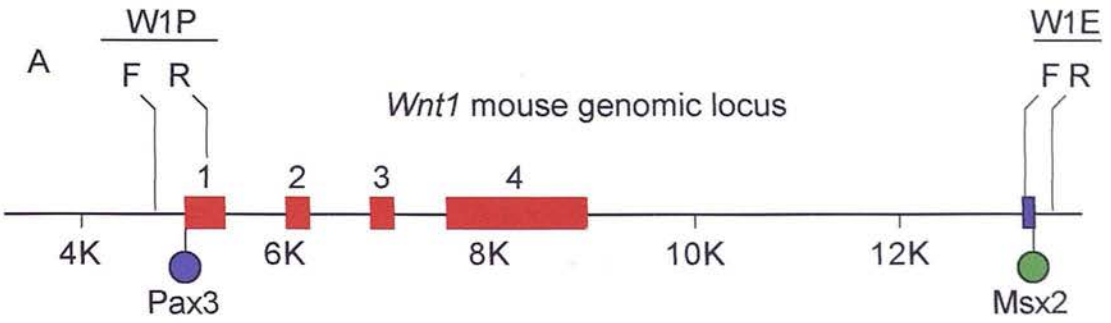

Fragment	PCR	Size
Wnt1 Promoter (W1P)	55^30	541 bp
Wnt1 Enhancer (W1E)	56^30	282 bp

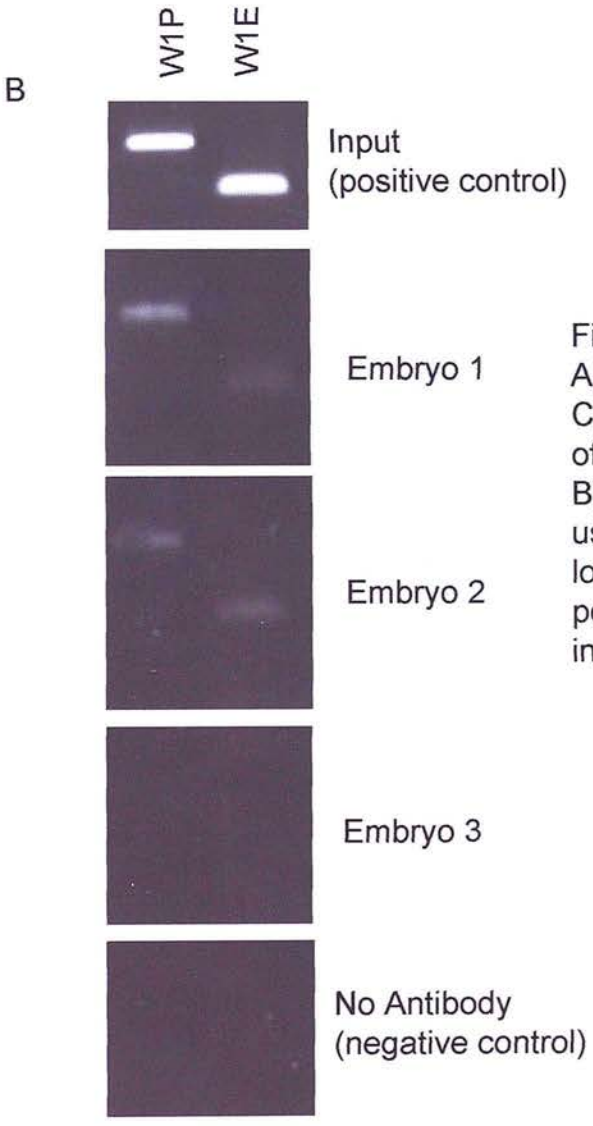

Figure 6.5:
A) Genomic Wnt1 locus showing ChIP primer binding sites, and table of predicted amplicon sizes
B) PCR products of anti-Msx1/2 ChIP using primers specific to the Wnt1 locus. Wnt1 promoter and enhancer positive in two experiments, negative in one.

this cannot differentiate between the binding of either protein to the *Wnt1* regulatory elements, and may account for the observed result. Further investigation is obviously required, perhaps using a mono-specific antibody or site directed mutagenesis of the *Msx2* site within the *Wnt1* enhancer. It is tentatively concluded that *Msx2* is found in association with the *Wnt1* locus *in vivo,* although the precise position of this interaction is unclear. This is therefore in partial agreement with second hypothesis presented in this thesis, although much further work is required.

Pax3 *binds to the* Pax7 *I1R element* in vivo

Chapter 4 presents data which both establishes two regulatory elements potentially controlling *Pax7* expression in the mouse genome, and presents data that *Pax3* may interact with one or both of these elements to regulate the transcription of *Pax7 in vivo*. Luciferase assay experiments investigating the interaction of *Pax3* with either the *Pax7* proximal promoter (as established by activity in the C2C12 cell line and by (Lang et al., 2003)) or the I1R silencer revealed that both elements were required to generate a response *in vitro*. The mutagenesis of a *Pax3* binding site consensus in the *Pax7* proximal promoter region did not abrogate this effect (in contrast to the *Pax3* binding site in the *Wnt1* promoter) indicating that the interaction was not mediated through that site.

To examine if *Pax3* does indeed interact with the *Pax7* locus *in vivo*, and whether the interaction is through the promoter or I1R silencer element, ChIP was performed on the *Pax7* locus on dissected E10.5 mouse embryos. Primers were designed to amplify a 595bp region of the *Pax7* promoter (primers P7_PROM_CHIP_FWD/REV) or a

546bp region of the *Pax7* intron 1 silencer (P7_INTRON_CHIP_FWD/REV). The *Pax7* genomic locus with these primers positioned and showing the first three exons, *Pax3* consensus binding site and I1R element can be seen in Figure 6.6A.

ChIP assays were then performed using the *Pax3* antibody described in Chapter 5 on three wild type embryos; the positive and negative controls were correct in each case. Figure 6.6B illustrates that the ChIP assay repeatably enriched for fragments carrying the I1R element and not the *Pax7* proximal promoter or *Pax3* consensus site. This confirms the mutagenesis result, and suggests that *Pax3* is interacting with the *Pax7* locus via the I1R silencer element *in vivo*.

Whilst this result enables hypothesis three to be partially accepted this, and the work described in this thesis, does not fully resolve whether *Pax3* is acting to repress as suggested by (Borycki et al., 1999), de-repress as suggested by Chapter 4's Luciferase data, or do nothing at all as suggested by (Relaix et al., 2004) the *Pax7* gene. The occupancy of a site within a highly conserved element of apparent regulatory function would argue against *Pax3* paying no role whatsoever in the transcription of *Pax3*. It is possible that the de-repression observed in Chapter 4 reflects an artefact of the Luciferase assay whereby the absence of *Pax3* co-factors, usually present *in vivo*, enables the *Pax3* transcription factor to mediate an unusual effect. Since *Pax3* carries domains for both transcriptional activation and repression of target genes (Chalepakis and Gruss, 1995; Lang, 2005)) an observation of this nature *in vitro* would not be entirely unsurprising. This would not be in keeping with the clear up-regulation of *Pax7* protein observed from C2C12 cells transfected with increasing quantities of *Pax3*, shown in Figure 4.15. Clearly further work, to resolve this issue *in vivo* and to

A

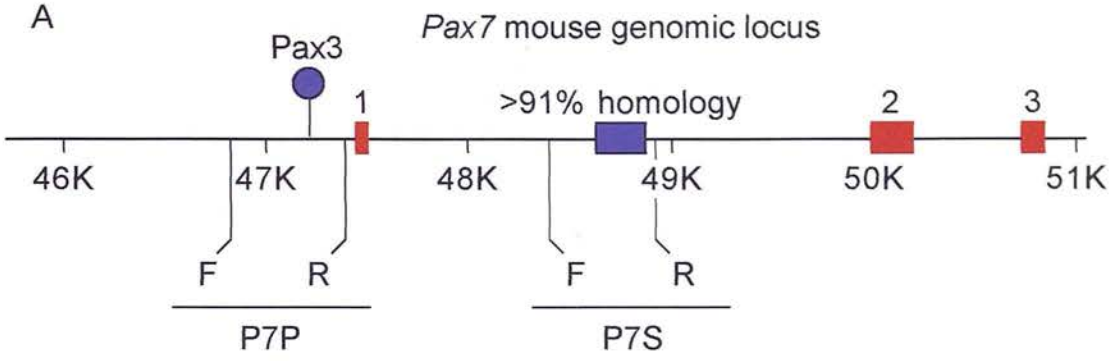

Fragment	PCR	Size
Pax7 Promoter (P7P)	57^30	595 bp
Pax7 Silencer (P7S)	55^30	546 bp

B

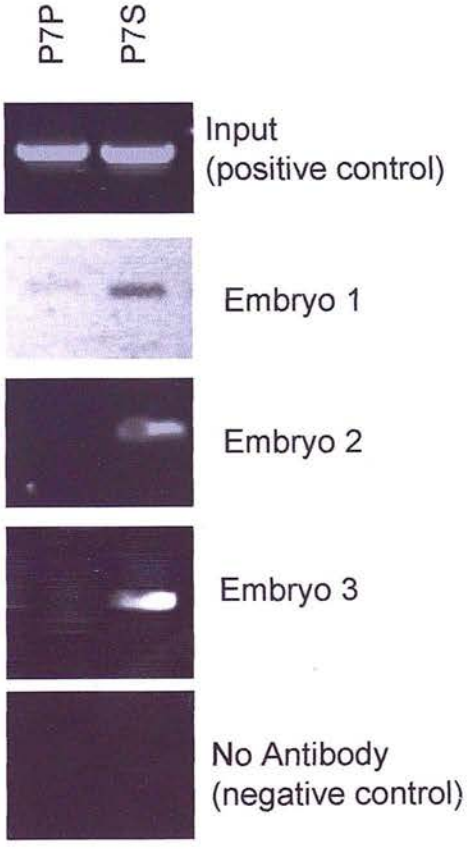

Figure 6.6:
A) Genomic Pax7 locus showing ChIP primer binding sites, and table of predicted amplicon sizes
B) PCR products of anti-Pax3 ChIP using primers specific to the Pax7 locus. The Pax7 silencer within intron is specifically amplified in each experiment, confirming Pax3 binding to this region *in vivo*

map the binding of *Pax3* to the I1R element precisely, is needed. Given the role *Pax7* plays in both embryonic development and adult stem cell derived muscle regeneration in the adult, a greater understanding of *Pax7* regulation may also be of therapeutic value.

Conclusions

In the above chapter a series of ChIP experiments, bringing together and testing the observations made in the Chapters 3 and 4 with the antibody designed and described in Chapter 5, are described. *Pax3* has been shown to associate with the *Wnt1* promoter and the *Pax7* I1R silencer *in vivo*, via a defined and as yet undefined binding site, respectively. *Msx2* may have some association with the *Wnt1* locus *in vivo*, although the data presented here is inconclusive and much work remains to be done to complete this analysis. Importantly, the above data validates the use of the *Pax3* antibody with *in vivo* ChIP and paves the way for the use of these tools for a high level analysis of *Pax3* function in development.

Chapter Seven: Discussion

In this thesis a series of direct transcriptional interactions were postulated from published studies on *Pax3*. Methodologies to test these interactions were developed for *in vitro* and *in vivo* analyses. In the post-genomic era it is increasingly important to dissect precisely the genetic interactions involved in biological processes. Transcription is one of the first lines of regulation between the information encoded within the genome and the translation of that information into biochemically active material. It is essential that this process is studied in detail and that gene regulatory networks and relationships are reliably established.

The process of transcription transfers coding sequences in DNA to an RNA format that is then translated into protein by the cellular ribosomal machinery. The RNA polymerases and factors constituting the general transcriptional holoenzyme are the same irrespective of gene, cell type, tissue, or even organism (Ayoubi and Van den Ven, 1996). The proteins that recruit the polymerases to the correct position on the genome are myriad and form one of the major regulatory points in this process. These transcription factors bind to specific sequences in the *cis*-regulatory regions of genes and mediate their upregulation (i.e. recruitment of the polymerase machinery and/or chromatin remodelling factors) or inhibition depending on their precise biological context. One of the problems faced in experimental biology is that the techniques used to examine such protein – DNA interactions precisely *in vitro* are often difficult to confirm in an *in vivo* context. A relationship observed with *in vitro* techniques will

not necessarily be borne out in an *in vivo* setting, nor is an *in vivo* approach always practical when examining relationships of this kind experimentally.

In this thesis, the developing mouse embryo was used as a model system to examine transcriptional interactions between *Pax3* and its targets. An *in vitro* approach was used in the first instance to map these interactions precisely. This was then followed by ChIP to confirm these interactions *in vivo*. It is hoped that this technique could then be applied to other *Pax3* – target interactions, or even be scaled up to scan the mouse genome for equivalent sites demonstrating *Pax3* binding *in vivo* to enable a fuller understanding of this important gene's function in development.

Pax3 and Wnt1

Chapter 1 outlines some of the developmental roles *Pax3* is known to have in the developing mouse embryo. One of the earliest post-gastrulation events is the induction of cells fated to become the nervous system from the ectoderm, known as neurulation (see (Copp, 2003) for review). *Pax3* is intimately associated with this process, and the expression of this gene in the developing neuroectoderm is one of the earliest observable markers of the future spinal cord (Bang, 1997; Goulding et al., 1991). The roles of *Pax3* in the development of these tissues are varied, and much work has been done to characterise the effects of both *Pax3* overexpression (Tremblay et al., 1996) and mutation (see (Epstein et al., 1991; Epstein, 1996) and references within Chapter 1 for overview). Assaying the direct targets of *Pax3* is important when considering the role of this factor in development. This will also

enable the separation of direct and indirect effects of *Pax3* when manipulating this factor in these systems.

Wnt signalling is also fundamental to the patterning of the developing embryo, and several Wnt genes are expressed in the developing nervous system (Miller, 2001; Parr, 1993). Whilst *Wnt8* has been shown to be one of the inductive factors establishing *Pax3* expression in the developing neural folds (Bang et al., 1999) the expression of *Wnt1* in the neural tube has been shown to be follow *Pax3* temporally (Deardorff, 2001) and the expression of neural crest cell marker genes, such as *slug*, has been shown to depend upon a *Pax3* mediated Wnt signal (Monsoro-Burq, 2004; Sato, 2005). The observation that *Wnt1* expression levels are reduced on a *Pax3* null background (Conway et al., 2000) but that *Pax3* expression levels remain unchanged on a *Wnt1* mutant background (Ikeya et al., 1997) suggest that *Pax3* is genetically upstream of *Wnt1* and led to the investigation of the following hypothesis:

Hypothesis One

Pax3 up regulates Wnt1 transcription directly, probably through the 3' distal enhancer region, in vivo *during the development of the neural crest.*

This hypothesis was tested in Chapters 3 and 6. In Chapter 3 this problem was initially addressed by sub-cloning the 5.5kb 3' distal *Wnt1* enhancer, first defined as necessary and sufficient to recreate the *Wnt1* expression pattern in the developing mouse CNS by (Echelard et al., 1994) into a series of Luciferase reporter constructs. An interaction between the 3' distal *Wnt1* enhancer and *Pax3* could not be detected.

Bioinformatic analysis had identified a *Pax3* consensus within the *Wnt1* 5' proximal promoter region. Despite the inability of the *Wnt1* proximal promoter to drive reporter gene expression in a faithful reproduction of the *Wnt1* expression pattern in the mouse, this region of DNA has been shown to be important in a regulatory context (Lagutin et al., 2003). The 5' proximal promoter was then also cloned into a Luciferase reporter construct and shown to be *Pax3* responsive. Deletion studies confirmed that this interaction was mediated by a region of the *Wnt1* promoter carrying the *Pax3* consensus site. The specifity of this interaction was finally confirmed by site directed mutagenesis.

These experiments illustrated that *Pax3* was competent to up-regulate the transcription of a reporter gene under the control of the *Wnt1* 5' proximal promoter. To confirm this interaction *in vivo*, ChIP was conducted using an antibody designed specifically for this purpose. This experiment confirmed the occupancy of *Pax3* specifically on this region of mouse genomic DNA, and not on the distal 3' enhancer.

This enables hypothesis one to be concluded, with the modification that *Pax3* is binding to the proximal promoter and not the distal enhancer element of this gene. This result sits well with previous studies examining the roles of these genes in the development of the neural tube and induction of neural crest. A model of the proposed interactions can be seen in Figure 7.1 (Brault et al., 2001; Dickinson et al., 1994; Ikeya et al., 1997; Monsoro-Burq, 2004; Sato, 2005; Serbedzija and McMahon, 1997). Whilst other factors must clearly regulate the expression of *Wnt1* in addition to *Pax3* (i.e. Msx1 (Lallemand, 2003; Monsoro-Burq, 2004), or WiF (St-Arnaud and Moir, 1993)), the above data in conjunction with the observed reduction of *Wnt1*

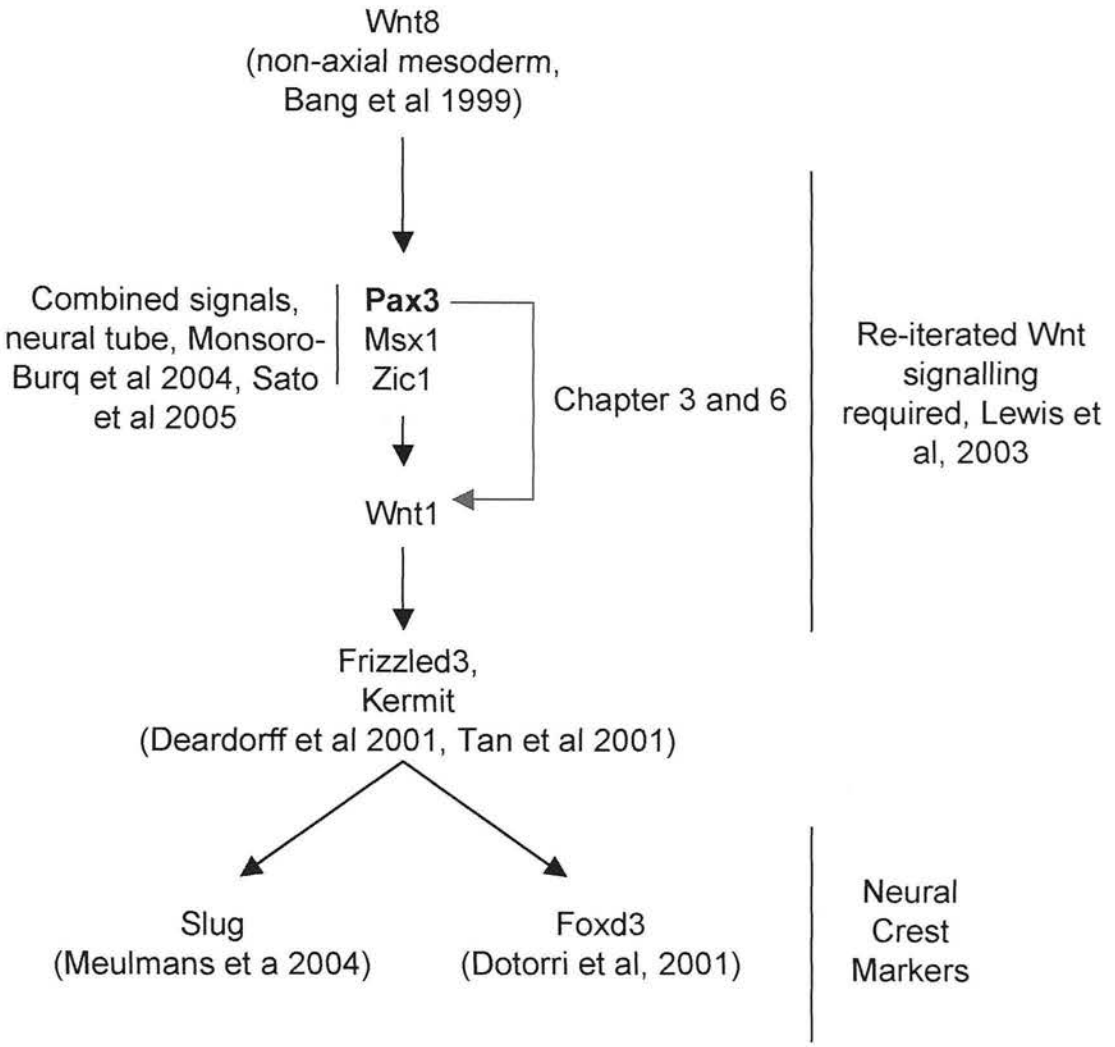

Figure 7.1:
A summary of the genetic network involved in neural crest induction, some of the factors involved, and the proposed position of the Pax3 - Wnt1 relationship determined by this thesis

expression by around 40 (Chapter 3) – 50% (Conway et al., 2000) on a *Pax3* null background clearly implicates *Pax3* as an important regulator of *Wnt1* expression *in vivo*.

Only one study to date, (Burstyn-Cohen, 2004), has cited evidence that *Wnt1* may lie upstream of *Pax3* in the chick. The data presented by this group does not differentiate between specific Wnt signals, however, and has only demonstrated that *Pax3* is downstream of a canonical Wnt signal. Since *Pax3* has been shown to be induced in the neural plate by Wnt8 in previous work in *Xenopus* (Bang et al., 1999), and given that the rostrocaudal wave of *Pax3* expression is widely held to precede that of *Wnt1* (see (Deardorff, 2001) for a time course analysis of dorsal neural tube markers in *Xenopus*), the role of *Wnt1* as an inducer of *Pax3* expression in the neural tube seems unlikely.

When a *Wnt1*-LacZ transgene was crossed onto a *Pax3* null background a clear loss of migrating LacZ positive neural crest cells was observed (Serbedzija and McMahon, 1997). The possibility that a *Pax3* – *Wnt1* interaction may play a role in events after the induction of the neural crest population was also considered. Mice carrying a mutation in the *Dvl2* gene (*Dvl2* is a downstream component of both canonical and PCP Wnt signalling pathways) share an identical cardiac neural crest phenotype to *Pax3* mutant mice (Briata, 2003; Clevers, 2002; Hamblet, 2002; Kioussi, 2002). This places *Wnt1* in an attractive position to act as the Wnt signal in this process. This would also link the *Pax3* and *Dvl2* cardiac outflow tract phenotypes with a common mechanism. A mutation in *Pax3* would reduce the expression of *Wnt1* in cardiac neural crest, thus inhibiting signalling through the *Wnt/Dvl2/Pitx2* pathway and

generating a cardiac outflow tract phenotype. Another interesting feature of this pathway is the partially non-cell autonomous nature of the Sp^{2H} cardiac phenotype (Chan et al., 2004; Conway et al., 1997a; Mansouri et al., 2001), again implicating a secreted signal such as *Wnt1* in the development of these tissues. Finally, one group has noted in cardiac neural crest ablation experiments that defects in the developing chick heart actually begin to manifest whilst the migrating cells would still be populating the pharyngeal arches (i.e. before reaching the heart) (Waldo, 1999). One of these defects was in Ca^{2+} transients, a measure of excitation – contraction coupling, and is a phenotype also observed in *Pax3* mutant embryos (Creazzo, 1998). *Wnt1*, signalling via β-catenin, has also been shown to regulate the expression of the *connexin43* gene (critical in the formation of gap junctions in the heart which mediate the electronic coupling in cardiac tissues) (Zhaowei, 2000). *Wnt1*-cre targeted inactivation of β-catenin also generates defects in neural crest derived structures and cell survival (Brault et al., 2001). It is tempting to speculate that *Wnt1*, as a target of *Pax3* and signalling via β-catenin, mediates these effects *in vivo*.

Msx2 and Wnt1

To establish a role for *Wnt1* as a possible effector of *Pax3* function during cardiac development the findings of (Kwang et al., 2002) needed to be addressed. In this study *Pax3* was shown to negatively regulate the *Msx2* gene in the neural crest. In the Sp^{2H} -/- mouse, the *Pax3* null phenotype generates an expanded expression domain of *Msx2* at the level of the post-otic neural tube (the area from which the cardiac neural crest originate (Chan et al., 2004)). This upregulation of *Msx2* on a *Pax3* null

background was shown to be causative in the development of the *Splotch* cardiac phenotype, since a double *Msx2/Pax3* homozygous mutant genotype rescues this defect specifically. It was reasoned that if *Wnt1* is also an effector of *Pax3* signalling in the development of the cardiac neural crest, *Msx2* should act to downregulate *Wnt1* expression.

Therefore hypothesis two was also investigated:

Hypothesis Two

Wnt1 transcription is directly downregulated by Msx2, most probably by the distal 3' enhancer element, in vivo *with implications for the normal development of the cardiac neural crest.*

To investigate this hypothesis the *Msx2* protein was co-expressed in a series of Luciferase transfection experiments, and a responsive element mapped to a region of the *Wnt1* enhancer containing a highly conserved 110bp sequence (first defined as necessary and sufficient for LacZ transgene expression in the *Wnt1* domain of the mouse midbrain (Rowitch et al., 1998)) and an *Msx2* binding site (Chapter 3). Unfortunately, mutational analysis of this site was not performed and the information obtained from a series of ChIP experiments using the DSHB Msx1/2 antibody was inconclusive (Chapter 6). It was tentatively concluded that *Msx2* might associate with the *Wnt1* locus *in vivo*, but more experiments are required to confirm this association. Also, ChIP experiments using both a specific *Msx2* antibody and possibly using isolated neural crest cells would help to clarify this result.

The hypotheses outlined above were designed to identify and test possible direct interactions between *Pax3* and target gene *cis*-regulatory sequences both *in vitro* and *in vivo*. The developmental systems outlined above and in Chapter 1 are presented as a relevant context for these interactions. To understand what the relationship between *Pax3*, *Wnt1* and *Msx2* may be functionally during development, the data described here can now be used to design specific transgenic experiments (for example the mutation of the *Pax3* binding site in the *Wnt1* promoter in a transgenic line, or assaying for a rescue phenotype if the *Pax3* gene is expressed under the control of the *Wnt1* regulatory elements on a Sp^{2H} -/- background) to test these relationships further.

Pax3 and Pax7

Another developmental system was chosen for the second candidate target of *Pax3* regulation. The controversy over the role which *Pax3* may play in the regulation of *Pax7* is described in Chapter 1 (see (Borycki et al., 1999; Relaix et al., 2004)). To test any possible direct regulatory interaction between *Pax3* and its sister *Pax* family member a similar approach to that outlined for *Wnt1* was adopted, see Chapter 4. Beceause regulatory regions for the *Pax7* gene had not been described for the mouse the identification of these regions formed the initial part of the investigation into this candidate target.

Three techniques were used to try and position putative *Pax7* promoter regions on the basis of the size and sequence of the *Pax7* 5'UTR. All techniques converged on a

5'UTR of around 100bp of upstream genomic sequence, which was consistent with a paper published subsequently on the mouse *Pax7* promoter. This study evidenced a 5'UTR of 73bp although the PEXT gel presented by this group does indicate faint bands at higher and lower molecular weights (Lang et al., 2003). One interesting exception in my data was the presence of consistently larger PEXT products, indicating a second transcriptional start site at a different location for the mouse *Pax7* gene. Studies in human (Syagailo et al., 2002) have also reported a larger 5'UTR (~650bp), and the methods presented in (Lang et al., 2003) may have missed a larger PEXT product for technical reasons (running the PEXT products on a sequencing gel may mean larger (>500bp) fragments do no resolve). 5'RACE may not have amplified these larger fragments due to technical issues with the PCR and cloning basis of this protocol and the CG and repeat rich nature of the genomic sequence in question. The lack of confirmation of these larger fragments by RPA is puzzling; this may indicate the presence of an upstream exon in the mouse *Pax7* gene outside of the region covered by the RPA probe. It is interesting to note that, of the six studies to date characterising the mouse and human *Pax7* 5'UTR's, no definitive consensus on the transcriptional start has been reached. It is possible that a defined start site may not exist for this gene. The existence of promoters with multiple transcriptional start sites has long been accepted and may even be of regulatory importance (see (Ayoubi and Van den Ven, 1996) for review). Of the LacZ reporter transgenics reported in (Lang et al., 2003), even those containing 10kb of genomic sequence upstream of the *Pax7* transcriptional start did not fully recreate the *Pax7* binding pattern. This implies that additional regulatory elements to those reported here and in (Lang et al., 2003) must be involved in the regulation of this gene. It is possible the larger PEXT product observed here can be explained in this manner. Perhaps the PIPMaker alignment

output, shown in Appendix 3, could be used as a starting point to identify regions of putative regulatory importance.

The I1R silencer within intron 1 was also reported by (Lang et al., 2003) although this element was not isolated and tested. Interestingly, they report that, in transgenic mice carrying both the I1R element and 4kb of proximal *Pax7* genomic sequence, the I1R silencer seems to act as a pons-specific enhancer with respect to LacZ staining.

Once candidate regulatory regions for the *Pax7* gene had been described the following hypothesis was investigated:

Hypothesis Three

Pax7 is directly downregulated by Pax3, in vitro *and* in vivo*, via defined regulatory elements and with implications for the development of both neural and mesodermal tissues.*

In this study we cloned a minimal *Pax7* promoter, restricted to 1.5kb by activity in C2C12 cells, and the I1R element both individually and together in a series of Luciferase reporter constructs. These were co-transfected with *Pax3* to test the above hypothesis. It was discovered that both elements were required on a reporter construct to elicit a response to *Pax3*. This response was a de-repression of the I1R silencing activity of the *Pax7* promoter observed for these constructs *in vitro*. This relationship was unexpected since, if any regulatory interaction existed between *Pax3* and *Pax7* at all, it had been proposed to be negative (Borycki et al., 1999). Mutagenesis confirmed

that the *Pax3* response was not via a *Pax3* consensus in the *Pax7* promoter region, and ChIP indicated that *Pax3* bound the I1R element *in vivo*. These data confirm that *Pax7* is a direct target of *Pax3*, but imply a positive relationship which is at odds with one published account of *Pax7* expression on a *Pax3* null genotype (Borycki et al., 1999). Future work should map this *Pax7* binding site on the I1R element precisely through mutagenesis, and then a transgenic approach should be adopted to interpret the developmental significance of this. QRTPCR was attempted for *Pax7* between wild type and Sp^{2H} -/- embryos, but a consistent result could not be obtained despite several attempts (data not shown). Recent work identifying a *Pax3* and *Pax7* dependant population of skeletal muscle progenitor cells highlights the importance these genes have in adult muscle regeneration (Relaix, 2005). Establishing a regulatory interaction between these factors may therefore be significant in this context.

Pax3 *ChIP: future directions*

The establishment of direct vs. indirect targets for the action of *Pax3* and other developmentally important transcription factors is essential in the interpretation and investigation of the function of these genes *in vivo*. Previous attempts have been made using a microarray approach (Mayanil et al., 2001) to screen for candidate targets of *Pax3*. The inability of these techniques to differentiate between primary and secondary effects of *Pax3* function make the meaningful interpretation of these data difficult.

It is intended that the ChIP technique designed in this thesis may be used as a way of rapidly testing direct functional relationships between *Pax3* and potential target genes *in vivo*. In addition to testing specific DNA - protein interactions, ChIP can be used in combination with genome wide arrays or CpG island arrays to screen for sites of direct transcription factor occupation (Buck, 2004; Hanlon, 2004; Weinmann, 2002). This approach, whilst relatively new in mammals due to limitations in the microarrays and bioinformatics available, has been used with great success in yeast (Lee, 2002; Lieb, 2001; Ren, 2000a). It is hoped that the validation of ChIP in mouse embryonic tissues described here will be used in future to screen for direct transcriptional targets of *Pax3* during development.

Appendix 1: Constructs and cloning strategies

Plasmid Name	Cloning Strategy Outline
pP3IRESEGFP / pP3IRES	RTPCR from E10 RNA using Primers 3/5 P3IRES, topo cloned and then shuttled using the SacII-BamHI sites form the primers into pIRES-2-EGFP (Clontech)
pW1ELuc	Wnt-1 enhancer plasmid (McM -pWEXP3) BglII fragment of 5.4kb using a BglII / SalI double digest and then cloned into pGL3Promoter (Promega) BamHI site.
pW1PLuc	pMT86 (JOM) digested with BamHI/NcoI to generate 4.89kb promoter fragment. This cloned into pGL3Basic BglII/NcoI sites.
pP7HYB	PAC Library Pax-7 promoter screen. Human DNA amplified using P7HYB1L / 2R primers, 520bp product topoisomerased into vector.
pP7Probe	PCR topo clone using P7RT1I/R primers to generate 770bp product (across the CpG island of Pax-7 5' proximal region)
pCMV-Pax-3	pP3IRES (SacII - BamHI) into pCMV-Script (stratagene) (SacII - BamHI).
p3.5TOPO	Pax-7 promoter fragment TEPCR cloned from I4 PAC and crystal violet extracted before topoisomerasing into pCR-XL-TOPO (invitrogen). HindIII screened to check orientation.
pP7P-EGFP	See Step 1, above.
pP7RiboProbe	Take pP7Probe and clone a 686bp Pax-7 promoter fragment using Asp718 - FspI and insert into pBSII(KS) with Asp718 - EcoRV. BamHI or HindIII can be used to linearise at either end (or double to confirm fragment) to synth. riboprobe from with T3 or T7, depending on sense or antisense being required.
p3.0Luc	p3.5TOPO (BamHI - FspI) -take 2.8kb frag into pBSII(KS) (BamHI-EcoRV) to create pIntermediate1 (below) and then digest pIntermediate1 with SacI - XhoI - FspI triple, extract the 2.9kb frag and insert into pGL3basic (promega) via SacI - XhoI. NB. p3.0Luc called p3.5Luc in earlier notes, re-named to be more accurate.
pIntermediate1	See above

p1.5Luc	Take p3.0Luc, digest with Asp718, excise 1.404kb frag of upstream promoter, re-ligate backbone to generate p1.5Luc with proximal 1.5kb of Pax-7 promoter.
p-1.8Luc	Take p3.0Luc, digest with BglII, excise 1.755kb of Pax-7 promoter proximal to ATG of Luciferase. Re-ligate backbone to generate Luciferase construct with distal 1.8kb of Pax-7 promoter (deleted in p1.5Luc) controlling Luciferase.
pI1RLuc	TEPCR PAC DNA using P7INT1REGF/B, generate 546bp, digest frag with BamHI (sites in primers), clone into BamHI site of pGL3Promoter (both orientations, orientation screen performed by SacI / ApaI / XbaI triple digest)
p1.5I1RLuc	TEPCR PAC DNA using P7INT1REGF/B, generate 546bp, digest frag with BamHI (sites in primers), clone into BamHI site of p1.5Luc (both orientations, orientation screen performed by SacI / ApaI / XbaI triple digest).
pW1P(1.2)Luc	pW1PLuc, Asp718 digest to delete the distal 3.5kb of Wnt-1 promoter
pW1P(-1.8)Luc	pW1PLuc, ApaI digest to delete the proximal 3.0kb of Wnt-1 promoter (mis-named) KEEPS 250bp upstream of ATG so a better plasmid than p(-1.8)Luc which only keeps 50bp
pP7SP6RiboProbe	pP7RiboProbe, BamHI - HindIII extraction of 686bp frag and then cloning into pGEM-3ZF using BamHI - HindIII. Linearise with BamHI later for SP6 transcription of riboprobe for RPA
pCMV-MSx2	Ordered from HGMP, seq to ensure full length cDNA and correct orientation wrt CMV prom (originally pCMV-Sport (Invitrogen?)
pW1E(Bam)Luc	pW1ELucBF (BamHI) -fragment excised and vector re-ligated to make enhancer deletion construct
pW1E(Spe)Luc	pw1ELucBF (SpeI) -fragment excised and vector re-ligated to make enhancer deletion construct

pW1E(Mbi)Luc	pw1ELucBF (MbiI), 816bp fragment carrying putative Msx2 response element excised and re-ligated into pGL3Promoter (Promega) SmaI site and then screened for orientation using
pW1EPLuc	pW1P(1.2)Luc (Asp718 - NcoI), take 1.236kb fragment, ligate into pW1E(Bam)Luc (Asp718 - NcoI) 7.937 backbone fragment (loose 277bp containing the SV40 minimal promoter used in pGL3Promoter based vectors).
pW1PΔLuc	Site directed mutagenesis of Pax-3 core consensus in the Wnt-1 promoter sequence on this plasmid. CTCGC - GATAA.
pP7PΔLuc	Site directed mutagenesis of Pax-3 core consensus in the Pax-7 promoter sequence on this plasmid. TCGC - ATAA.

Appendix 2: Primer List

Primer Name	Sequence (5' - 3')
P3GENOF	AAGCAGCGCAGGAGCAGAACC
P3GENOR	CCTCGGTAAGCTTCGCCCTCT
W1LITEF	CGCTCTCTTCCAGTTCTCAGACAC
W1LITER	CAGGATGGCAAAAGGGTTCG
GAPLITEF	GGGTGTGAACCACGAGAAAT
GAPLITER	CCTTCCACAATGCCAAAGTT
3P3IRES	GATACAGGATCCTAGAACGTCCAACAAGGCTTACTTTG
5P3IRES	TGTATCGCAGGAAGAGCCCGCGAACGTCCAAGGCTTACTTTG
NT - reverse	TGTCACCTTGGGTTTGCTG
E1L	GCTGTGCCCAGGATGATG
E4L	GAGTTCTATCAGCCGCATCC
E4R	CCATCGATGCTGTGTTTAGC
E6L	GCAAGATGGAGGAAACAA
E6R	GGTAAGAGTGCTCCGACAGC
E7L	CCGTGTCAGATCCCAGTAGC
E7R	GATGGAGGCACAAAGCTGTC
E8R	GCCCATACTGGTAGCCTGTG
CT - forward	CTTTCAACCATCTCATTCCG
W1_sub_FWD	CGGCAAGAGCCACAGCTTCGGATAACACTCATTGTCTGTGGCCCTG
W1_sub_REV	CAGGGCCACAGACAATGAGTGTTATCCGAAGCTGTGGCTCTTGCCG
EX2	AACTACCCGCGCACCGGCTTCCCCC
B2	CCGAACCACATCCGTCACAA
B4	CACATCCGTCACAAGATAGTGGAA
5'RACE (outer)	CTGCCGAACCACATCCGTCACAAG
5' RACE (inner)	TCAATCAGCTTGGTGGGGTCTTCA
P7RT1L	CCAAGAGGTTTATCCAGCCGA
P7RT1R	TTGATGAAGACCCCACCAAGC
P7HYB1L	GTAGAGTAAGAACCGGACACCG
P7HYB2R	CAACTGAATGATCAGGAGTCAGG
P7PROML	CCCTGCTGGATGTGAAATCG
P7PROMR	CGGTCTGGTGGAGTGGAAATAG
P7INT1REGF	GTAGATGGATCCTTAGCCGCCCCTCTTGTCATTG
P7INT1REGB	AGTTTAGGATCCCTACCGCCCCCTCTTTACTTTC
P7_sub_FWD	AGTGTTTGTTTGTTTGAACTTCCTTGGATATACCTTCCACTCCTCCCGCCCC
P7_sub_REV	GGGGCGGGAGGAGTGGAAGGTATATCCAAGGAAGTTCAAACAAACAAACACT

P7_PROM_CHIP_FWD	CCCTCGCTTTTCCTCTTGTGTTC
P7_PROM_CHIP_REV	GCCAAGAGGTTTATCCAGCCGA
P7_INTRON_CHIP_FWD	TTAGCCGCCCCTCTTGTCATTG
P7_INTRON_CHIP_REV	GAAAGTAAAGAGGGGGCGGTAG
W1_PROM_CHIP_FWD	GGGACAGAGGAGACGGACTTC
W1_PROM_CHIP_REV	CATCACTGCCCTCACCGCT
W1_ENHAN_CHIP_FWD	CGTCAGCCTGGATTAATCTTCG
W1_ENHAN_CHIP_REV	CGTTCACGTAGTGTCTCCCAA

Appendix 3: PIPMaker Output

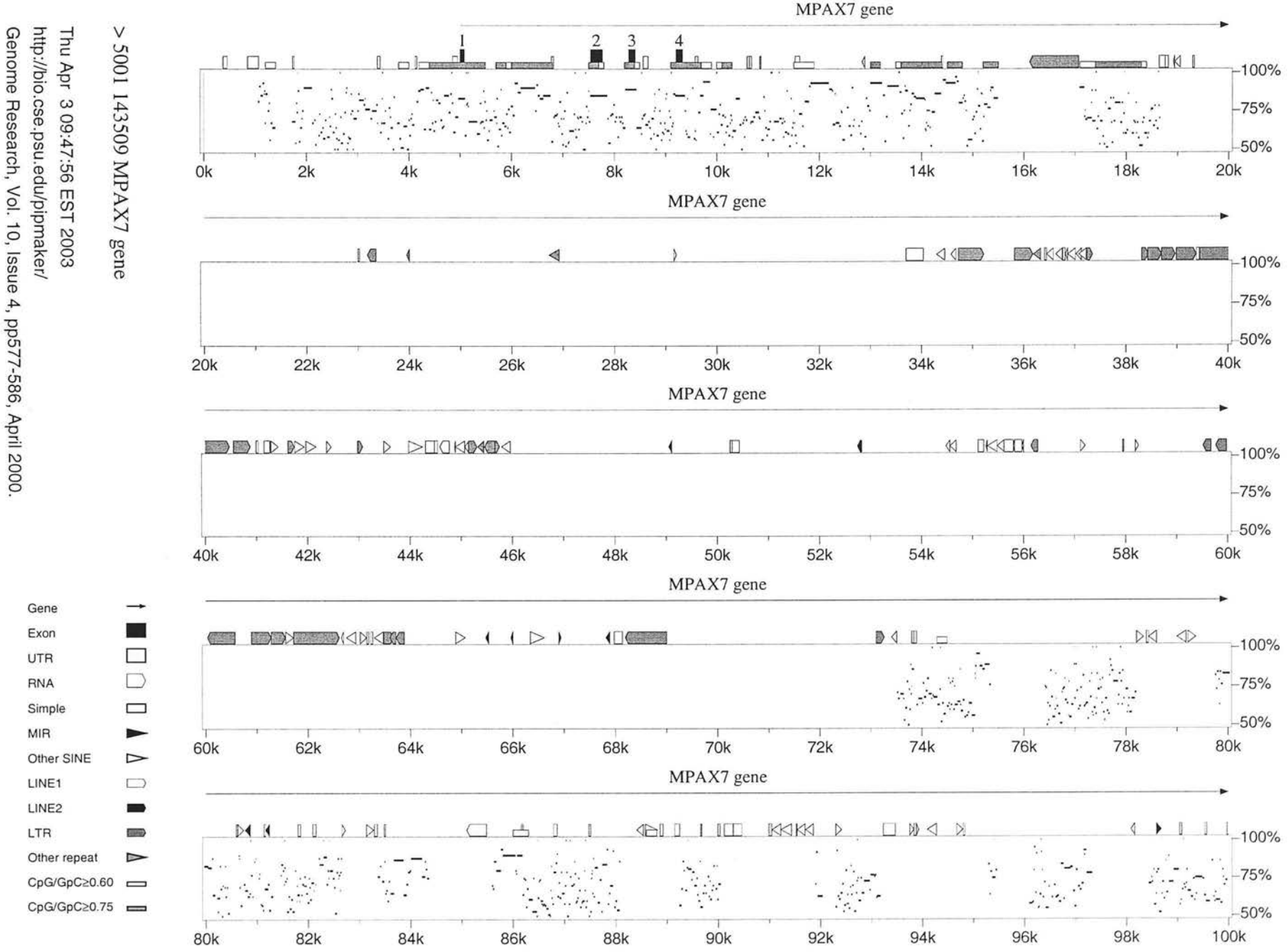
> 5001 143509 MPAX7 gene
Thu Apr 3 09:47:56 EST 2003
http://bio.cse.psu.edu/pipmaker/
Genome Research, Vol. 10, Issue 4, pp577-586, April 2000.
MPAX7 gene
1
2
3
4
100%
75%
50%
0k
2k
4k
6k
8k
10k
12k
14k
16k
18k
20k
20k
22k
24k
26k
28k
30k
32k
34k
36k
38k
40k
40k
42k
44k
46k
48k
50k
52k
54k
56k
58k
60k
60k
62k
64k
66k
68k
70k
72k
74k
76k
78k
80k
80k
82k
84k
86k
88k
90k
92k
94k
96k
98k
100k
Gene
Exon
UTR
RNA
Simple
MIR
Other SINE
LINE1
LINE2
LTR
Other repeat
CpG/GpC≥0.60
CpG/GpC≥0.75

> 5001 143509 MPAX7 gene

Thu Apr 3 09:47:56 EST 2003
http://bio.cse.psu.edu/pipmaker/
Genome Research, Vol. 10, Issue 4, pp577-586, April 2000.

Appendix 4: Luciferase Assay Data Treatment

Luciferase transfections were performed as above using the Promega DLR Assay system and a TD-20/20 Luminometer (Turner Biosystems). There were two distinct types of Luciferase assay performed in this thesis. The nature and purpose of these, and the way in which the data has been processed in each case, are described here.

Luciferase assays are transient transfection experiments where the expression of the Luciferase reporter gene can be used to infer the properties of various *cis*-regulatory elements *in vitro*. Whilst these methods generally involve plasmid DNA in secondary cell lines and are therefore not subject to all of the levels of gene regulation thought to occur in an *in vivo* context (i.e. chromatin remodelling, post-transcriptional modification, etc), the benefit of these methods is their rapid reproducibility and the chance to carefully dissect functional elements of non-coding DNA in much greater detail than would otherwise be practical.

In this thesis all Luciferase assays were conducted as transfections in 24 well plates, using a final total of 1.5μg DNA in each well. This was to ensure no variability in transfection efficiency arose from different quantities of DNA in each experiment. Between two and four plasmids were simultaneously transfected into cells in any one transfection. In all cases a reporter vector, carrying the Firefly Luciferase ORF under the control of various pieces of DNA, was transfected simultaneously with an identical quantity of a second plasmid carrying a *Renilla* Luciferase ORF whose transcription is controlled by a known element (either the SV40 or Thymidine Kinase promoters). Both gene products are enzymes capable of metabolising specific

substrates with the concomitant production of light. In these assays the metabolite specific for the Firefly luciferase gene is added first, and the quantity of light produced over a fixed period of time (10 seconds) is measured by the Luminometer. The quantity of light produced is directly proportional to the quantity of enzyme produced, as predicted by Michaelis-Menten kinetics where rate, v, is related to concentration of enzyme by the relationship:

$$v = V_{max}.[S] / K_m+[S]$$

where $V_{max} = k_2.[E_{total}]$, [S] = concentration of enzyme substrate, and k_2 and K_m represent kinetic constants. Where substrate is constant and in great excess (i.e. so $\Delta[S] \rightarrow 0$ over the time course observed), increasing the concentration of enzyme ($[E_{total}]$) will increase the rate of reaction and therefore the quantity of light produced over a fixed period. A detailed derivation of this relationship can be found in (Price, 2001).

After the first measurement of light produced by the Firefly Luciferase has been made, the reaction in the sample is quenched chemically and a second substrate is added which is specific to the *Renilla* Luciferase enzyme. This activity is then measured in the same way. Since the first reaction is quenched before the second reading, two independent and specific Luciferase activity readings can be taken from the one sample. This is important since the second measurement of the *Renilla* Luciferase activity is made to control for the differences in transfection efficiency, cell lysis, etc which may vary. If the first reading increases by 50% between a treated and untreated sample, for example, and the second reading remains constant it is

assumed that the treatment has increased the transcription of the Firefly Luciferase gene by 50% through interacting with whichever DNA sequences are controlling its transcription. If both readings increase by 50%, it is assumed that this change is due to differences in experimental conditions.

The first Luciferase reading is therefore divided by the second reading to correct for this type of experimental variation and the resulting ratio, called *normalised luminescence* throughout, is taken as the real measure of variation between samples.

Data is expressed as the mean value of several transfections. Each experimental run was performed in triplicate, to ensure each transfection was repeatable within a run, and then experimental runs repeated at least three times to generate data. Each reading on the Luminometer was also taken twice to ensure no variability in luminescence could be observed within the same sample over the time period assayed (i.e. that $\Delta[S] \rightarrow 0$ is true).

In the first type of assay, the measurement of the basal activity of a putative promoter element is examined. In these assays normalised luminescence is measured for transfections where the Firefly Luciferase gene is placed under the control of a specific piece of DNA (such as the *Wnt1* promoter). Two plasmids are co-transfected in each case (a test firefly Luciferase plasmid and a control *Renilla* Luciferase plasmid). Data is gathered for these transfections and expressed as fold induction. This is the number of times greater (or smaller) the normalised luminescence for these samples is over a baseline. In this case the baseline is defined as the normalised luminescence obtained for sample transfected with the Firefly Luciferase gene under

the control of the empty vector sequences (specifically the pGL3basic or pGL3promoter plasmids).

In the second type of experiment the effect of co-transfecting an expression plasmid containing the ORF of a transcription factor of interest with plasmids containing the Firefly Luciferase gene under the control of specific regulatory element is performed. The normalised luminescence of samples transfected with differing ratios of expression construct to empty expression construct are compared. Three or four plasmids are transfected in each case; Firefly reporter, *Renilla* control, expression construct and/or empty expression construct to ensure the total quantity of DNA added remains constant (this is also to ensure a consistent amount of CMV promoter, driving expression of the transcription factor of interest, is added to prevent 'squelching' or an expression data artefact due to competition of strong promoters for RNA polymerase machinery in the cell). In these experiments fold induction of normalised luminescence over baseline is generally reported.

Occasionally, it was necessary to represent data as 'indexed fold induction'. This was used to compare between samples where a direct comparison of fold induction was not possible. This was always for one of two reasons. Firstly, when considering the interaction of a transcription factor with either a promoter element or an enhancer element a meaningful comparison is impossible. This is because the two vectors used as baseline (pGL3basic or pGL3promoter, respectively) have very different inherent Luciferase activities. As a result, the actual numbers generated for fold induction are different. Secondly, when comparing effects of co-expression across a large data set or between different reporter plasmids of different sizes, the differences in absolute

value of fold induction was observed to vary, although the relative changes were similar. For example, one data set might generate a change in fold induction of 0.1 to 10 whilst another might generate 10 to 1000. Clearly, the relative effect of treatment is identical, but an efficient comparison of the absolute values is impossible. Since all these experiments are concerned with the changes induced by co-expression of a particular cDNA, not the relationship to background observed in each separate experimental run, these data were indexed by setting the fold induction observed for the untreated sample (i.e., 0ng pCMV-Pax3) at 1. In these cases, relative or indexed fold induction is reported (essentially the % change induced by a specific quantity of expression plasmid) to enable direct comparison.

Finally, control experiments where pGL3basic and pGL3promoter empty reporter constructs were co-transfected with a range of quantities of pCMV-script, pCMV-Pax3 and pCMV-Msx2 expression constructs, using both pRL-TK and pRLSV40 *Renilla* transfection control plasmids were performed. No change in baseline Luminescence was ever observed for any of these controls (i.e. < 3-5%, data not shown).

Bibliography

Ai, Z., Fischer, A., Spray, D. C., Brown, A. M. and Fishman, G. I. (2000). Wnt-1 regulation of connexin43 in cardiac myocytes. *J Clin Invest* **105**, 161-71.

Amthor H, C. B., Patel K. (1999). A molecular mechanism enabling continuous embruonic muscle growth -a balance between proliferation and differentiation. *Development* **126**, 1041 - 1053.

Amthor H, C. B., Weil M, Patel K. (1998). The importance of timing differentiation during limb muscle development. *Current Biology* **8**, 642 - 652.

Antoine Bach, Y. L., Marie-Anne Nicola, Casto Ramos, Luc Mathis, Mathilde Maufras, and Benoît Robert. (2003). Msx1 is required for dorsal diencephalon patterning. *Development* **130**, 4025 - 4036.

Apuzzo S, A. A., Fortin AS, Gros P. (2004). Cross-talk between the Paired Domain and the Homeodomain of Pax3. *Journal of Biological Chemistry* **279**, 33601-33612.

Apuzzo, S. and Gros, P. (2002). Site-specific modification of single cysteine Pax3 mutants reveals reciprocal regulation of DNA binding activity of the paired and homeo domain. *Biochemistry* **41**, 12076-85.

Aruga J, T. T., Homma S, Mikoshiba K. (2002). Zic1 promotes the expansion of dorsal neural tube progenitors in spina cord by inhibiting neuronal differentiation. *Dev Biol* **244**.

Auerbach, R. (1954). Analysis of the development effects of a lethal mutation in the house mouse. *J. Exp. Zool.* **127**, 305 -329.

Augustine, K., Liu, E. T. and Sadler, T. W. (1993). Antisense attenuation of Wnt-1 and Wnt-3a expression in whole embryo culture reveals roles for these genes in craniofacial, spinal cord, and cardiac morphogenesis. *Dev Genet* **14**, 500-20.

Ayoubi, T. and Van den Ven, W. (1996). Regulation of gene expression by alternative promoters. *FASEB J* **10**, 453 - 460.

Bach, A. e. a. (2003). Msx1 is required for dorsal diencephalon patterning. *Development* **130**, 4025 - 4036.

Bachrach, E., Li, S., Perez, A. L., Schienda, J., Liadaki, K., Volinski, J., Flint, A., Chamberlain, J. and Kunkel, L. M. (2004). Systemic delivery of human microdystrophin to regenerating mouse dystrophic muscle by muscle progenitor cells. *Proc Natl Acad Sci U S A* **101**, 3581-6.

Bajanca, F. and Thorsteinsdottir, S. (2002). Integrin expression patterns during early limb muscle development in the mouse. *Mech Dev* **119 Suppl 1**, S131-4.

Bang, A. G., Papalopulu, N., Goulding, M. D. and Kintner, C. (1999). Expression of Pax-3 in the lateral neural plate is dependent on a Wnt-mediated signal from posterior nonaxial mesoderm. *Dev Biol* **212**, 366-80.

Bang AG, P. N., Kintner C, Goulding MD. (1997). Expression of Pax3 is initiated in the early neural plate by posteriorizing signals produced by the organiser and by posterior non-axial mesoderm. *Developmental* **124**, 2075 - 2085.

Barber, T. D., Barber, M. C., Cloutier, T. E. and Friedman, T. B. (1999). PAX3 gene structure, alternative splicing and evolution. *Gene* **237**, 311-9.

Barber, T. D., Barber, M. C., Tomescu, O., Barr, F. G., Ruben, S. and Friedman, T. B. (2002). Identification of target genes regulated by PAX3 and PAX3-FKHR in embryogenesis and alveolar rhabdomyosarcoma. *Genomics* **79**, 278-84.

Barr, F. G. (2001). Gene fusions involving PAX and FOX family members in alveolar rhabdomyosarcoma. *Oncogene* **20**, 5736-46.

Barr, F. G., Fitzgerald, J. C., Ginsberg, J. P., Vanella, M. L., Davis, R. J. and Bennicelli, J. L. (1999). Predominant expression of alternative PAX3 and PAX7 forms in myogenic and neural tumor cell lines. *Cancer Res* **59**, 5443-8.

Begum S, E. N., Cheung A, Wilkins O, Der S, Hamel PA. (2005). Cell-type specific regulation of distinct sets of gene targets by Pax3 and Pax3/FKHR. *Oncogene* **24**, 1860-1872.

Bendall, A. J., Ding, J., Hu, G., Shen, M. M. and Abate-Shen, C. (1999). Msx1 antagonizes the myogenic activity of Pax3 in migrating limb muscle precursors. *Development* **126**, 4965-76.

Bladt F, R. D., Isenmann S, Aguzzi A, Birchmeier C. (1995). Essential role for the c-met receptor in the migration of myogenic precursor cells into the limb bud. *Nature* **376**, 768 - 771.

Bober, E., Franz, T., Arnold, H. H., Gruss, P. and Tremblay, P. (1994). Pax-3 is required for the development of limb muscles: a possible role for the migration of dermomyotomal muscle progenitor cells. *Development* **120**, 603-12.

Borycki, A. G., Li, J., Jin, F., Emerson, C. P. and Epstein, J. A. (1999). Pax3 functions in cell survival and in pax7 regulation. *Development* **126**, 1665-74.

Brault, V., Moore, R., Kutsch, S., Ishibashi, M., Rowitch, D. H., McMahon, A. P., Sommer, L., Boussadia, O. and Kemler, R. (2001). Inactivation of the beta-catenin gene by Wnt1-Cre-mediated deletion results in dramatic brain malformation and failure of craniofacial development. *Development* **128**, 1253-64.

Briata P, I. C., Corte G, Moroni C, Rosenfeld MG, Chen CY, Gherzi R. (2003). The Wnt/B-Catenin/Pitx2 pathway controls the turnover of Pitc2 and other unstable mRNAs. *Molecular Cell* **12**, 1201 - 1211.

Brohmann H, J. K., Birchmeier C. (2000). The role of Lbx1 in the migration of muscle precursor cells. *Development* **127**, 437 - 445.

Buck MJ, L. J. (2004). ChIP-chip: considerations for the design, analysis and application of genome wide ChIP experiments. *Genomics* **83**, 349 - 360.

Buckingham, M. (2001). Skeletal muscle formation in vertebrates. *Curr Opin Genet Dev* **11**, 440-8.

Buckingham, M., Bajard, L., Chang, T., Daubas, P., Hadchouel, J., Meilhac, S., Montarras, D., Rocancourt, D. and Relaix, F. (2003). The formation of skeletal muscle: from somite to limb. *J Anat* **202**, 59-68.

Burstyn-Cohen T, S. J., Sela-Donenfeld D, Kalcheim C. (2004). Canonical Wnt activity regulates trunk neural crest delamination linking BMP/noggin signalling with G1/S transition. *Development* **131**, 5327 - 5339.

Bustin, S. A. (2000). Absolute quantification of mRNA using real-time reverse transcription polymerase chain reaction assays. *Journal of Molecular Endocrinology* **25**, 169 - 193.

Cao, Y. and Wang, C. (2000). The COOH-terminal transactivation domain plays a key role in regulating the in vitro and in vivo function of Pax3 homeodomain. *J Biol Chem* **275**, 9854-62.

Capdevila J, T. C., Johnson RL. (1998). Control of dorsoventral somite patterning by Wnt1 and B-catenin. *Dev Biol* **193**, 182 - 914.

Carmona R, G.-I. M., Macias D, Perez-Pomares JM, Garcia-Garrido L, Munoz-Chapuli R. (2000). Immunolocalisation of the transcription factor Sug in the developing avian heart. *Anat Embryol* **201**, 103 - 109.

Chalepakis, G. and Gruss, P. (1995). Identification of DNA recognition sequences for the Pax3 paired domain. *Gene* **162**, 267-70.

Chalepakis, G., Jones, F. S., Edelman, G. M. and Gruss, P. (1994). Pax-3 contains domains for transcription activation and transcription inhibition. *Proc Natl Acad Sci USA* **91**, 12745-9.

Chan, W. Y., Cheung, C. S., Yung, K. M. and Copp, A. J. (2004). Cardiac neural crest of the mouse embryo: axial level of origin, migratory pathway and cell autonomy of the splotch (Sp2H) mutant effect. *Development* **131**, 3367-79.

Chen AE, G. D., Fan CM. (2004). Protein Kinase A signalling via CREB controls myogenesis induced by Wnt proteins. *Nature* **433**, 317-22.

Chi, N. C. and Epstein, J. A. (2002). Getting your Pax straight: Pax proteins in development and disease. *Trends in Genetics* **18**, 41 - 47.

Christ, B. and Brand-Saberi, B. (2002). Limb muscle development. *Int J Dev Biol* **46**, 905 - 914.

Clevers, H. (2002). Inflating cell numbers by Wnt. *Molecular Cell*, 1260 - 1261.

Conway, S. J., Bundy, J., Chen, J., Dickman, E., Rogers, R. and Will, B. M. (2000). Decreased neural crest stem cell expansion is responsible for the conotruncal heart defects within the splotch (Sp(2H))/Pax3 mouse mutant. *Cardiovasc Res* **47**, 314-28.

Conway, S. J., Henderson, D. J. and Copp, A. J. (1997a). Pax3 is required for cardiac neural crest migration in the mouse: evidence from the splotch (Sp2H) mutant. *Development* **124**, 505-14.

Conway, S. J., Henderson, D. J., Kirby, M. L., Anderson, R. H. and Copp, A. J. (1997b). Development of a lethal congenital heart defect in the splotch (Pax3) mutant mouse. *Cardiovasc Res* **36**, 163-73.

Cooper, G. M. and Sidow, A. (2003). Genomic regulatory regions: insights from comparative sequence analysis. *Curr Opin Genet Dev* **13**, 604 - 610.

Copp AJ, G. N., Murdoch JN. (2003). The genetic basis of mammalian neuralation. *Nature Reviews Genetics* **4**, 784 - 793.

Creazzo TL, G. R., Leatherbury L, Conway SJ, Kirby ML. (1998). Role of cardiac neural crest cells in cardiovascular development. *Annual Rev. Physiol.* **60**, 267 - 286.

Cross, S. H. and Bird, A. P. (1995). CpG Islands and genes. *Curr Opin Genet Dev* **5**, 309 - 314.

Czerny, T. (1993). DNA sequence recognition by Pax proteins: bipartite structure of the paired domain and its binding site. *Genes Dev* **7**, 2048 - 2061.

Daston G, L. E., Olivier M, Goulding M. (1996). Pax3 is necessary for migration but not differentiation of limb muscle precursors in the mouse. *Development* **122**, 1017 - 1027.

Deardorff MA, T. C., Saint-Jeannet JP, Klein PS. (2001). A role for frizzled 3 in neural crest development. *Development* **128**, 3655 - 3663.

Denetclaw WF Jr, C. B., Ordahl CP. (1997). Location and growth of epaxial myotome precursor cells. *Development* **124**, 1601 - 1610.

Dickinson, M. E., Krumlauf, R. and McMahon, A. P. (1994). Evidence for a mitogenic effect of Wnt-1 in the developing mammalian central nervous system. *Development* **120**, 1453-71.

Dietrich S, S. F., Lumsden A. (1997). Control of dorsoventral pattern in the chick paraxial mesoderm. *Development* **124**, 3895 - 3908.

Dottori, M., Gross, M. K., Labosky, P. and Goulding, M. (2001). The winged-helix transcription factor Foxd3 suppresses interneuron differentiation and promotes neural crest cell fate. *Development* **128**, 4127-38.

Dreyfus, P. A., Chretien, F., Chazaud, B., Kirova, Y., Caramelle, P., Garcia, L., Butler-Browne, G. and Gherardi, R. K. (2004). Adult bone marrow-derived stem cells in muscle connective tissue and satellite cell niches. *Am J Pathol* **164**, 773-9.

Du S, L. E., Strzelecki D, Rajput P, Xia SJ, Gottesman DM, Barr FG. (2005). Co-expression of aternatively spliced forms of PAX3, PAX7, PAX3-FKHR and PAX7-FKHR with distinct DNA binding and transactivation properties in rhabdomyosarcoma. *Int J Cancer* **Epub -ahead of print**.

Eccles MR, H. S., Legge M, Kumar R, Fox J, Zhou C, French M, Tsai RW. (2002). PAX genes in development and disease: the role of PAX2 in urogenital tract development. *Int J Dev Biol* **46**, 535-544.

Echelard, Y., Vassileva, G. and McMahon, A. P. (1994). Cis-acting regulatory sequences governing Wnt-1 expression in the developing mouse CNS. *Development* **120**, 2213-24.

ensembl. *http://www.ensembl.org*.

Epstein, D. J., Vekemans, M. and Gros, P. (1991). Splotch (Sp2H), a mutation affecting development of the mouse neural tube, shows a deletion within the paired homeodomain of Pax-3. *Cell* **67**, 767-74.

Epstein, J. A. (1996). Pax3, neural crest and cardiovascular development. *TCM* **6**, 255 - 261.

Epstein, J. A., Li, J., Lang, D., Chen, F., Brown, C. B., Jin, F., Lu, M. M., Thomas, M., Liu, E., Wessels, A. et al. (2000). Migration of cardiac neural crest cells in Splotch embryos. *Development* **127**, 1869-78.

Epstein, J. A., Shapiro, D. N., Cheng, J., Lam, P. Y. and Maas, R. L. (1996). Pax3 modulates expression of the c-Met receptor during limb muscle development. *Proc Natl Acad Sci U S A* **93**, 4213-8.

Fan CM, L. C., Tessier-Lavigne M. (1997). A role for Wnt proteins in induction of dermomyotome. *Dev Biol* **191**, 160 - 165.

Farrell M, W. K., Li YX, Kirby ML. (1999). A novel role for cardiac neural crest in heart development. *J Clin Invest* **103**, 1499 - 1507.

Fedtsova, N., Perris, R. and Turner, E. E. (2003). Sonic hedgehog regulates the position of the trigeminal ganglia. *Dev Biol* **261**, 456-69.

Fortin, A. S., Underhill, D. A. and Gros, P. (1998). Helix 2 of the paired domain plays a key role in the regulation of DNA-binding by the Pax-3 homeodomain. *Nucleic Acids Res* **26**, 4574-81.

Franz T, K. R., Surani MA, Halata Z, Grim M. (1993). The Splotch mutation interferes with muscle development in the limbs. *Anat Embryol* **187**, 153 - 160.

Galibert, M. D., Yavuzer, U., Dexter, T. J. and Goding, C. R. (1999). Pax3 and regulation of the melanocyte-specific tyrosinase-related protein-1 promoter. *J Biol Chem* **274**, 26894-900.

Gao, X., Kuiken, G. A., Baarends, W. M., Koster, J. G. and Destree, O. H. (1994). Characterization of a functional promoter for the Xenopus wnt-1 gene on vivo. *Oncogene* **9**, 573-81.

Garcia-Castro MI, M. C., Bronner-Fraser M. (2002). Ectodermal Wnt function as a neural crest inducer. *Science* **297**, 848 - 851.

Glogarova, K. and Buckiova, D. (2004). Changes in sialylation in homozygous Sp2H mouse mutant embryos. *Birth Defects Res A Clin Mol Teratol* **70**, 142 - 152.

Goulding, M., Lumsden, A. and Paquette, A. J. (1994). Regulation of Pax-3 expression in the dermomyotome and its role in muscle development. *Development* **120**, 957-71.

Goulding, M. D., Chalepakis, G., Deutsch, U., Erselius, J. R. and Gruss, P. (1991). Pax-3, a novel murine DNA binding protein expressed during early neurogenesis. *Embo J* **10**, 1135-47.

Goulding MD, L. A., Gruss P. (1993). Signals from the notocord and floor plate regulate the region specific expression of two Pax genes in the developing spinal cord. *Development* **117**, 1001 - 1016.

Grifone R, D. J., Houbron C, Souil E, Niro C, Seller MJ, Hamard G, Maire P. (2005). Six1 and Six4 homeoproteins are required for Pax3 and Mrf expression during myogenesis in the mouse. *Development* **132**, ePub ahead of print.

Gros J, M. M., Thome V, Marcelle C. (2005). A common somitic origin for embryonic musce progenitors and satellite cells. *Nature* **434**, epub ahead of print.

Gross MK, M.-R. L., Velasquez T, Nakatsu MN, Jagla K, Goulding M. (2000). Lbx1 is required for muscle precursor migration along a lateral pathway into the limb. *Development* **127**, 413 - 424.

Habener, J. and Stoffers, D. (1998). A newly discovered role of transcription factors involved in pancreas development and the pathogenesis of diabetes mellitus. *Proc Assoc Am Physicians* **110**, 12-21.

Hamblet NS, L. N., Ruiz-Lozano P, Wang J, Yang Y, Luo Z, Mei L, Chien KR, Sussman DJ, Wynshaw-Boris A. (2002). Dishevelled 2 is essential for cardaic

outflow tract development, somite segmentation and neural tube closure. *Development* **129**, 5827 - 5838.

Hanlon SE, L. J. (2004). Progress and challenges in profiling the dynamics of chromatin and transcription factor binding with DNA microarrays. *Curr Opin Genet Dev* **14**, 697 - 705.

Heiko Peters, A. N., Klaus Kratochwil, and Rudi Balling. (1998). Pax9 deficient mice lack pharyngeal pouch derivatives and teeth and exhibit craniofacial and limb abnormalities. *Genes Dev* **12**, 2735-2747.

Henderson, D. J., Conway, S. J. and Copp, A. J. (1999). Rib truncations and fusions in the Sp2H mouse reveal a role for Pax3 in specification of the ventro-lateral and posterior parts of the somite. *Dev Biol* **209**, 143-58.

Henderson, D. J., Ybot-Gonzalez, P. and Copp, A. J. (1997). Over-expression of the chondroitin sulphate proteoglycan versican is associated with defective neural crest migration in the Pax3 mutant mouse (splotch). *Mech Dev* **69**, 39-51.

HGMP. http://www.hgmp.mrc.ac.uk, (ed.

Hill RE, F. J., Hogan BL, Ton CC, Saunders GF, Hanson IM, Prosser J, Jordan T, Hastie ND, van Heyningen V. (1991). Mouse *small eye* results from mutations in a paired-like homeobox containing gene. *Nature* **354**, 522 - 525.

Holland, L. Z., Schubert, M., Kozmik, Z. and Holland, N. D. (1999). AmphiPax3/7, an amphioxus paired box gene: insights into chordate myogenesis, neurogenesis, and the possible evolutionary precursor of definitive vertebrate neural crest. *Evol Dev* **1**, 153-65.

Hollenbach, A. D., McPherson, C. J., Lagutina, I. and Grosveld, G. (2002). The EF-hand calcium-binding protein calmyrin inhibits the transcriptional and DNA-binding activity of Pax3. *Biochim Biophys Acta* **1574**, 321-8.

Hollenbach, A. D., Sublett, J. E., McPherson, C. J. and Grosveld, G. (1999). The Pax3-FKHR oncoprotein is unresponsive to the Pax3-associated repressor hDaxx. *Embo J* **18**, 3702-11.

Ikeya, M., Lee, S. M., Johnson, J. E., McMahon, A. P. and Takada, S. (1997). Wnt signalling required for expansion of neural crest and CNS progenitors. *Nature* **389**, 966-70.

Iler, N., Rowitch, D. H., Echelard, Y., McMahon, A. P. and Abate-Shen, C. (1995). A single homeodomain binding site restricts spatial expression of Wnt-1 in the developing brain. *Mech Dev* **53**, 87-96.

JacksonLabs. In *http://www.jax.org*, (ed.

Jiang X, R. D., Soriano P, McMahon AP, Sucov HM. (2000). Fate of the mammalian cardiac neural crest. *Development* **127**, 1607 - 1616.

Jostes, B., Walther, C. and Gruss, P. (1990). The murine paired box gene, Pax7, is expressed specifically during the development of the nervous and muscular system. *Mech Dev* **33**, 27-37.

Kassar-Duchossoy L, G.-M. B., Gomes D, Rocancourt D, Buckingham M, Shinin V, Tajbakhsh S. (2004). Mrf4 determines skeletal muscle identity in Myf5:MyoD double mutant mice. *Nature* **431**, 466 - 471.

Kay, P. H., Mitchell, C. A., Akkari, A. and Papadimitriou, J. M. (1995). Association of an unusual form of a Pax7-like gene with increased efficiency of skeletal muscle regeneration. *Gene* **163**, 171-7.

Kay, P. H. and Ziman, M. R. (1999). Alternate Pax7 paired box transcripts which include a trinucleotide or a hexanucleotide are generated by use of alternate 3' intronic splice sites which are not utilized in the ancestral homologue. *Gene* **230**, 55-60.

Kioussi C, B. P., Baek SH, Rose DW, Hamblet NS, Herman T, Ohgi KA, Lin C, Gleiberman A, Wang J, Brault V, Ruiz-Lozano P, Nguyen HD, Kemler R, Glass CK, Wynshaw-Boris A, Rosenfeld MG. (2002). Identificaiton of a Wnt/Dvl/B-Catenin - Pitx2 pathway mediating cell-type-specific proliferation during development. *Cell* **111**, 673 - 685.

Kioussi, C., Gross, M. K. and Gruss, P. (1995). Pax3: a paired domain gene as a regulator in PNS myelination. *Neuron* **15**, 553-62.

Kos R, R. M., Johnson RL, Erickson CA. (2001). The winged - helix transcription factor Foxd3 is important for establishing the neural crest lineage and repressing melanogenesis in avian embryos. *Development* **128**, 1467 - 1479.

Kozmik Z, C. T., Busslinger M. (1997). Alternatively spliced insertions in the paired domain restrict the DNA sequence specificity of Pax6 and Pax8. *Embo J* **16**, 6793 - 6803.

Kuhlbrodt, K., Herbarth, B., Sock, E., Hermans-Borgmeyer, I. and Wegner, M. (1998). Sox10, a novel transcriptional modulator in glial cells. *J Neurosci* **18**, 237-50.

Kwang, S. J., Brugger, S. M., Lazik, A., Merrill, A. E., Wu, L. Y., Liu, Y. H., Ishii, M., Sangiorgi, F. O., Rauchman, M., Sucov, H. M. et al. (2002). Msx2 is an immediate downstream effector of Pax3 in the development of the murine cardiac neural crest. *Development* **129**, 527-38.

LaBonne, C. and Bronner-Fraser, M. (1998). Neural crest induction in Xenopus: evidence for a two signal model. *Development* **125**, 2403 - 2414.

LaBonne, C. and Bronner-Fraser, M. (1999). Moecular Mechanisms of Neural Crest Formation. *Annual Rev. Cell Dev. Biol.* **15**, 81 - 112.

Laclef, C., Hamard, G., Demignon, J., Souil, E., Houbron, C. and Maire, P. (2003). Altered myogenesis in Six1-deficient mice. *Development* **130**, 2239-52.

Lagutin, O. V., Zhu, C. C., Kobayashi, D., Topczewski, J., Shimamura, K., Puelles, L., Russell, H. R., McKinnon, P. J., Solnica-Krezel, L. and Oliver, G. (2003). Six3 repression of Wnt signaling in the anterior neuroectoderm is essential for vertebrate forebrain development. *Genes Dev* **17**, 368-79.

Lam, P. Y., Sublett, J. E., Hollenbach, A. D. and Roussel, M. F. (1999). The oncogenic potential of the Pax3-FKHR fusion protein requires the Pax3 homeodomain recognition helix but not the Pax3 paired-box DNA binding domain. *Mol Cell Biol* **19**, 594-601.

Lang, D., Brown, C. B., Milewski, R., Jiang, Y. Q., Lu, M. M. and Epstein, J. A. (2003). Distinct enhancers regulate neural expression of Pax7. *Genomics* **82**, 553-60.

Lang, D. and Epstein, J. A. (2003). Sox10 and Pax3 physically interact to mediate activation of a conserved c-RET enhancer. *Hum Mol Genet* **12**, 937-45.

Lang D, L. M., Huang L, Engleka KA, Zhang M, Chu EY, Lipner S, Skoultchi A, Millar SE, Epstein JA. (2005). Pax3 functions at a nodal point in melanocyte stem cell differentiation. *Nature* **433**, 884-887.

Lee TI, R. N., Robert F, Odom DT, Bar-Joseph Z, Gerber GK, Hannett NM, Harbison CT, Thompson CM, Simon I, Zeitlinger J, Jennings EG, Murray HL, Gordon DB, Ren B, Wyrick JJ, Tagne JB, Volkert TL, Fraenkel E, Gifford DK, Young RA. (2002). Transcriptional regulatory networks in Saccharomyces cerevisiae. *Science* **298**, 799 - 805.

Lewis JL, B. J., Modrell M, Ragland JW, Moon RT, Dorsky RI, Raible DW. (2003). Reiterated Wnt signalling during zebrafish neural crest development. *Development* **131**, 1299 - 1308.

Li, J., Liu, K. C., Jin, F., Lu, M. M. and Epstein, J. A. (1999). Transgenic rescue of congenital heart disease and spina bifida in Splotch mice. *Development* **126**, 2495-503.

Lieb, J. D., Xiaole L., Botstein D., P. Brown. (2001). Promoter spceific binding of Rap1 revealed by genome wide maps of protein DNA association. *Nature Genetics* **28**, 327 - 334.

Liem KF Jr, T. G., Jessell TM. (1997). A role for the roof plate and its resident TGF-B related proteins in neuronal patterning in the dorsal spinal cord. *Cell* **91**, 127 - 138.

Livak, K. J. and Schmittgen, T. D. (2001). Analysis of relative gene expression data using real time quantitative PCR and the 2.exp(-delta,deltaCt) method. *Methods* **25**, 402 - 408.

Logan CY, N. R. (2004). The Wnt signalling pathway in development and disease. *Annual Rev. Cell Dev. Biol.* **20**, 781 - 810.

Mansouri, A. (1998). Follicular cells of the thyroid gland require Pax8 gene function. *Nature Genetics* **19**, 87-90.

Mansouri A, H. M., Gruss P. (1996). Pax genes and their roles in cell differentiation and development. *Curr Opin Cell Biol* **8**, 851-857.

Mansouri, A., Pla, P., Larue, L. and Gruss, P. (2001). Pax3 acts cell autonomously in the neural tube and somites by controlling cell surface properties. *Development* **128**, 1995-2005.

Mansouri, A., Stoykova, A., Torres, M. and Gruss, P. (1996). Dysgenesis of cephalic neural crest derivatives in Pax7-/- mutant mice. *Development* **122**, 831-8.

Maroto, M., Reshef, R., Munsterberg, A. E., Koester, S., Goulding, M. and Lassar, A. B. (1997). Ectopic Pax-3 activates MyoD and Myf-5 expression in embryonic mesoderm and neural tissue. *Cell* **89**, 139-48.

MatInspector, G.-. Transcription factor binding site prediction software. *http://www.genomatix.org*.

Matsunaga, E., Araki, I. and Nakamura, H. (2001). Role of Pax3/7 in the tectum regionalization. *Development* **128**, 4069-77.

Mayanil, C. S., George, D., Freilich, L., Miljan, E. J., Mania-Farnell, B., McLone, D. G. and Bremer, E. G. (2001). Microarray analysis detects novel Pax3 downstream target genes. *J Biol Chem* **276**, 49299-309.

McMahon, A. P. and Bradley, A. (1990). The Wnt-1 (int-1) proto-oncogene is required for development of a large region of the mouse brain. *Cell* **62**, 1073-85.

McMahon JA, T. S., Zimmerman LB, Fan CM, Harland RM, McMahon AP. (1998). Noggin mediated antagonism of BMP signalling is required for growth and patterning of the neural tube and somite. *Genes Dev* **12**, 1438 - 1452.

Mennerich, D. and Braun, T. (2001). Activation of myogenesis by the homeobox gene Lbx1 requires cell proliferation. *Embo J* **20**, 7174-83.

Mennerich D, S. K., Braun T. (1998). Pax3 is necessary but not sufficient for Lbx1 expression in myogenic precursor cells of the limb. *Mech Dev* **73**, 147 - 158.

Meulemans, D. and Bronner-Fraser, M. (2004). Gene regulatory interactions in Neural Crest evolution and development. *Developmental Cell* **7**, 291 - 299.

Milewski, R. C., Chi, N. C., Li, J., Brown, C., Lu, M. M. and Epstein, J. A. (2004). Identification of minimal enhancer elements sufficient for Pax3 expression in neural crest and implication of Tead2 as a regulator of Pax3. *Development* **131**, 829-37.

Miller, J. R. (2001). The Wnts. *Genome Biology* **3**, 3001.1 - 3001.15.

Monsoro-Burq, A. H., Duprez, D., Watanabe, Y., Bontoux, M., Vincent, C., Brickell, P. and Le Douarin, N. (1996). The role of bone morphogenetic proteins in vertebral development. *Development* **122**, 3607-16.

Monsoro-Burq AH, F. R., Harland RM. (2003). Neural crest induction by paraxial mesoderm in Xenopus embryos requires FGF signals. *Development* **130**, 3111 - 3124.

Monsoro-Burq AH, W. E., Harland R. (2004). Msx1 and Pax3 cooperate to mediate FGF8 and WNT signals during Xenopus neural crest induction. *Developmental Cell* **8**, 167 - 178.

Murmann, O. V., Niggli, F. and Schafer, B. W. (2000). Cloning and characterization of the human PAX7 promoter. *Biol Chem* **381**, 331-5.

Natoli, T. A., Ellsworth, M. K., Wu, C., Gross, K. W. and Pruitt, S. C. (1997). Positive and negative DNA sequence elements are required to establish the pattern of Pax3 expression. *Development* **124**, 617-26.

Nusse, R., Theunissen, H., Wagenaar, E., Rijsewijk, F., Gennissen, A., Otte, A., Schuuring, E. and van Ooyen, A. (1990). The Wnt-1 (int-1) oncogene promoter and its mechanism of activation by insertion of proviral DNA of the mouse mammary tumor virus. *Mol Cell Biol* **10**, 4170-9.

Odelberg SJ, K. A., Keating MT. (2000). Dedifferentiation of mammaian myotubes induced by Msx1. *Cell* **103**, 1099 - 1109.

Pani, L., Horal, M. and Loeken, M. R. (2002). Rescue of neural tube defects in Pax-3-deficient embryos by p53 loss of function: implications for Pax-3- dependent development and tumorigenesis. *Genes Dev* **16**, 676-80.

Parr BA, S. M., Vassileva G, McMahon AP. (1993). Mouse Wnt genes exhibit discrete domains of expression in early embryonic CNS and limb buds. *Development* **119**, 247 - 261.

Pearce D, M. W., Miner JN, Yamamoto KR. (1998). Glucocorticoid receptor transcriptional activity determined by spacing of receptor and nonreceptor DNA sites. *Journal of Biological Chemistry* **273**, 30081-30085.

Phelan, S. A. and Loeken, M. R. (1998). Identification of a new binding motif for the paired domain of Pax-3 and unusual characteristics of spacing of bipartite recognition elements on binding and transcription activation. *J Biol Chem* **273**, 19153-9.

Pourquie O, C. M., Breant C, Le Douarin NM. (1995). Control of somite patterning by signals from the lateral plate. *Proc Natl Acad Sci U S A* **92**, 3219 - 3223.

Price, N. C., et al. (2001). Principles and problems in physical chemistry for biochemists: Oxford University Press.

Pritchard C, G. G., Hollenbach AD. (2003). Alternative splicing of Pax3 produces a transcriptionally inactive protein. *Gene* **305**, 61-69.

Pruitt, S. C. (1992). Expression of Pax3 and neuroectoderm-inducing activities during differentiation of P19 embryonal carcinoma cells. *Development* **116**, 573 - 583.

Puppo, F., Griseri, P., Fanelli, M., Schena, F., Romeo, G., Pelicci, P., Ceccherini, I., Ravazzolo, R. and Patrone, G. (2002). Cell-line specific chromatin acetylation at the Sox10-Pax3 enhancer site modulates the RET proto-oncogene expression. *FEBS Lett* **523**, 123-7.

Relaix, F., Polimeni, M., Rocancourt, D., Ponzetto, C., Schafer, B. W. and Buckingham, M. (2003). The transcriptional activator PAX3-FKHR rescues the

defects of Pax3 mutant mice but induces a myogenic gain-of-function phenotype with ligand-independent activation of Met signaling in vivo. *Genes Dev* **17**, 2950-65.

Relaix F, R. D., Mansouri A, Buckingham M. (2005). A Pax3/Pax7 dependant population of skeletal muscle progenitor cells. *Nature* **434**, epub ahead of print.

Relaix, F., Rocancourt, D., Mansouri, A. and Buckingham, M. (2004). Divergent functions of murine Pax3 and Pax7 in limb muscle development. *Genes Dev* **18**, 1088-105.

Ren B, R. F., Wyrick JJ, Aparicio O, Jennings EG, Simon I, Zeitlinger J, Schreiber J, Hannett N, Kanin E, Volkert TL, Wilson CJ, Bell SP, Young RA. (2000a). Genome wide locaiton and function of DNA binding proteins. *Science* **290**, 2306 - 2310.

Ren B, R. F., Wyrick JJ, Aparicio O, Jennings EG, Simon I, Zeitlinger J, Schreiber J, Hannett N, Kanin E, Volkert TL, Wilson CJ, Bell SP, Young RA. (2000b). Genome-wide location and function of DNA binding proteins. *Science* **290**, 2306 - 2309.

Ridgeway, A. G. and Skerjanc, I. S. (2001). Pax3 is essential for skeletal myogenesis and the expression of Six1 and Eya2. *J Biol Chem* **276**, 19033-9.

Roth, J. F., Shikama, N., Henzen, C., Desbaillets, I., Lutz, W., Marino, S., Wittwer, J., Schorle, H., Gassmann, M. and Eckner, R. (2003). Differential role of p300 and CBP acetyltransferase during myogenesis: p300 acts upstream of MyoD and Myf5. *Embo J* **22**, 5186-96.

Rowitch, D. H., Echelard, Y., Danielian, P. S., Gellner, K., Brenner, S. and McMahon, A. P. (1998). Identification of an evolutionarily conserved 110 base-pair cis-acting regulatory sequence that governs Wnt-1 expression in the murine neural plate. *Development* **125**, 2735-46.

Saint-Jeannet, J. P., He, X., Varmus, H. E. and Dawid, I. B. (1997). Regulation of dorsal fate in the neuraxis by Wnt-1 and Wnt-3a. *Proc Natl Acad Sci U S A* **94**, 13713-8.

Sambrook, J. and Russell, D. (2005). Molecular Cloning: A Laboratory Manual.

Sato T, S. N., Sasai Y. (2005). Neural crest induction by co-activation of Pax3 and Zic1 genes in Xenopus ectoderm. *Development*, 2355 - 2363.

Satokata I, M. L., Ohshima H, Bei M, Woo I, Nishizawa K, Maeda T, Takano Y, Uchiyama M, Heaney S, Peters H, Tang Z, Maxson R, Maas R. (2000). Msx2 deficiency in mice causes pleitropic defects in bone growth and ectodermal organ formation. *Nature Genetics* **24**, 391 - 395.

Scaal M, B. A., Dathe V, Sachs M, Cann G, Christ B, Brand-Saberi B. (1999). SF/HGF is a mediator between limb patterning and muscle development. *Development* **126**, 4885 - 4893.

Schafer, B. W., Czerny, T., Bernasconi, M., Genini, M. and Busslinger, M. (1994). Molecular cloning and characterization of a human PAX-7 cDNA expressed in normal and neoplastic myocytes. *Nucleic Acids Res* **22**, 4574-82.

Schmidt M, T. M., Munsterberg A. (2000). Expression of B-catenin in the developing chick myotome is regulated by myogenic signals. *Development* **127**, 4105 - 4113.

Schwartz S, Z. Z., Frazer KA, Smit A, Riemer C, Bouck J, Gibbs R, Hardison R, Miller W. (2000). PIPMaker - A web server for aligning two genomic DNA sequences. *Genome Res* **10**, 577 - 586.

Seale, P., Ishibashi, J., Scime, A. and Rudnicki, M. A. (2004). Pax7 Is Necessary and Sufficient for the Myogenic Specification of CD45(+):Sca1(+) Stem Cells from Injured Muscle. *PLoS Biol* **2**, E130.

Seale, P., Sabourin, L. A., Girgis-Gabardo, A., Mansouri, A., Gruss, P. and Rudnicki, M. A. (2000). Pax7 is required for the specification of myogenic satellite cells. *Cell* **102**, 777-86.

Selleck, M. and Bronner-Fraser, M. (1995). Origins of the avian neural crest: the role of neural plate - epidermal interactions. *Development* **121**, 525 - 538.

Serbedzija, G. N. and McMahon, A. P. (1997). Analysis of neural crest cell migration in Splotch mice using a neural crest-specific LacZ reporter. *Dev Biol* **185**, 139-47.

Siomin YA, S. V., Poverenny AM. (1973). The reaction of formaldehyde with deoxynucleotides and DNA in the prescence of amino acids and lysine rich histone. *Biochim Biophys Acta* **331**, 27 - 32.

St-Arnaud, R. and Moir, J. M. (1993). Wnt-1-inducing factor-1: a novel G/C box-binding transcription factor regulating the expression of Wnt-1 during neuroectodermal differentiation. *Mol Cell Biol* **13**, 1590-8.

Stamataki, D., Kastrinaki, M., Mankoo, B. S., Pachnis, V. and Karagogeos, D. (2001). Homeodomain proteins Mox1 and Mox2 associate with Pax1 and Pax3 transcription factors. *FEBS Lett* **499**, 274-8.

Stark MR, S. J., Bronner-Fraser M, Marcelle C. (1997). Neural tube - ectoderm interactions are required for trigeminal placode formation. *Development* **124**, 4287 - 4295.

Sung Hee Baek, C. K., Paola Briata, Degeng Wang, H. D. Nguyen, Kenneth A. Ohgi, Christopher K. Glass, Anthony Wynshaw-Boris, David W. Rose, and Michael G. Rosenfeld. (2003). Regulated subset of G1 growth-control genes in response to derepression by the Wnt pathway. *Proc Natl Acad Sci U S A* **100**, 3245 - 3250.

Syagailo, Y. V., Okladnova, O., Reimer, E., Grassle, M., Mossner, R., Gattenlohner, S., Marx, A., Meyer, J. and Lesch, K. P. (2002). Structural and functional characterization of the human PAX7 5'-flanking regulatory region. *Gene* **294**, 259-68.

Tajbakhsh, S., Rocancourt, D., Cossu, G. and Buckingham, M. (1997). Redefining the genetic hierarchies controlling skeletal myogenesis: Pax-3 and Myf-5 act upstream of MyoD. *Cell* **89**, 127-38.

Takada S, S. K., Shea MJ, Vassileva G, McMahon JA, McMahon AP. (1994). Wnt3a regulates somite and tailbud formation in the mouse embryo. *Genes Dev* **8**, 174 - 189.

Tan C, D. M., Saint-Jeannet JP, Yang J, Arzoumanian A, Klein PS. (2001). Kermit, a frizzled interacting protein regulates frizzed 3 signalling in neural crest development. *Development* **128**, 3665 - 3674.

Terzic, J. and Saraga-Babic, M. (1999). Expression pattern of PAX3 and PAX6 genes during human embryogenesis. *Int J Dev Biol* **43**, 501-8.

Thomas KR, C. M. (1990). Targeted disruption of the murine int-1 proto-oncogene resulting in severe abnormalities in midbrain and cerebellar development. *Nature* **346**, 847 - 850.

Thomas, K. R., Musci, T. S., Neumann, P. E. and Capecchi, M. R. (1991). Swaying is a mutant allele of the proto-oncogene Wnt-1. *Cell* **67**, 969-76.

Thomas, M., Lazic, S., Beazley, L. and Ziman, M. (2004). Expression profiles suggest a role for Pax7 in the establishment of tectal polarity and map refinement. *Exp Brain Res* **156**, 263-73.

Tomescu, O., Xia, S. J., Strezlecki, D., Bennicelli, J. L., Ginsberg, J., Pawel, B. and Barr, F. G. (2004). Inducible short-term and stable long-term cell culture

systems reveal that the PAX3-FKHR fusion oncoprotein regulates CXCR4, PAX3, and PAX7 expression. *Lab Invest* **84**, 1060-70.

Torres M, G.-P. E., Dressler GR, Gruss P. (1995). Pax2 controls multiple steps of urogenital development. *Development* **121**, 4057-4065.

Tremblay P, D. S., Mericskay M, Schubert FR, Li Z, Paulin D. (1998). A crucial role for Pax3 in the development of the hypaxial musculature and the long range migration of muscle precursors. *Dev Biol* **203**, 49 -61.

Tremblay, P., Pituello, F. and Gruss, P. (1996). Inhibition of floor plate differentiation by Pax3: evidence from ectopic expression in transgenic mice. *Development* **122**, 2555-67.

Trinklein, N. D. e. a. (2003). Identification and functional analysis of human transcriptional promoters. *Genome Res* **13**, 308 - 312.

Tsukamoto, K., Nakamura, Y. and Niikawa, N. (1994). Isolation of two isoforms of the PAX3 gene transcripts and their tissue-specific alternative expression in human adult tissues. *Hum Genet* **93**, 270-4.

Tzahor, E. and Lassar, A. B. (2001). Wnt signals from the neural tube block ectopic cardiogenesis. *Genes Dev* **15**, 255-60.

Underhill DA and Gros P. (1997). The paired domain regulates DNA binding by the homeodomain within the intact Pax3 protein. *Journal of Biological Chemistry* **272**, 14175-14182.

Urbanek P, W. Z., Fetka I, Wagner EF, Busslinger M. (1994). Complete block of early B cell differentiation and altered patterning of the posterior midbrain in mice lacking Pax5/BSAP. *Cell* **79**, 901-912.

van den Hoff MJ, M. A. (2000). Cardiac Neural Crest: the holy grail of cardiac abnormalities? *Cardiovasc Res* **47**, 212 - 216.

van Ooyen A, N. R. (1984). Structure and nucleotide sequence of the putative mammary oncogene int-1; proviral insertions leave the protein coding domain intact. *Cell* **39**, 233 - 240.

van Tilborg MA, L. J., Kruiskamp M, Teuben J, Boelens R, Yamamoto KR, Kaptein R. (2000). Mutations in the glucocorticoid receptor DNA-binding domain mimic an allosteric effect of DNA. *J Mol Biol* **301**, 947-958.

Venters, S. J., Argent, R. E., Deegan, F. M., Perez-Baron, G., Wong, T. S., Tidyman, W. E., Denetclaw, W. F., Jr., Marcelle, C., Bronner-Fraser, M. and Ordahl, C. P. (2004). Precocious terminal differentiation of premigratory limb muscle precursor cells requires positive signalling. *Dev Dyn* **229**, 591-9.

Villanueva S, G. A., Ruiz P, Mayor R. (2002). Posteriorisation by FGF, Wnt, and Retenoic Acid is required for neural crest induction. *Dev Biol* **241**, 289 - 301.

Vogan, K. J. and Gros, P. (1997). The C-terminal subdomain makes an important contribution to the DNA binding activity of the Pax-3 paired domain. *J Biol Chem* **272**, 28289-95.

Vogan, K. J., Underhill, D. A. and Gros, P. (1996). An alternative splicing event in the Pax-3 paired domain identifies the linker region as a key determinant of paired domain DNA-binding activity. *Mol Cell Biol* **16**, 6677-86.

Vorobyov, E., Mertsalov, I., Dockhorn-Dworniczak, B., Dworniczak, B. and Horst, J. (1997). The genomic organization and the full coding region of the human PAX7 gene. *Genomics* **45**, 168-74.

Wallin J, W. J., Koseki H, Fritsch R, Christ B, Balling R. (1994). The role of Pax1 axial skeleton development. *Development* **120**, 1109 - 1121.

Wasserman, W. and Sandelin, A. (2004). Applied bioinformatics for the identification of regulatory elements. *Nature Reviews Genetics* **5**, 276-287.

Weinmann AS, Y. P., Oberley MJ, Huang TH, Farnham PJ. (2002). Isolating human transcrption factor targets bby coupling ChIP and CpG island microarray analysis. *Genes Dev* **16**, 235 - 244.

Wheat W, F. D., Lennox H, Krautkramer SR, Gentile LN, McIntosh LP, Hagman J. (1999). The highly conserved B-hairpin of the Paired DNA-binding domain is required for assembly of Pax-Ets Ternary complexes. *Mol Cell Biol* **19**, 2231 - 2241.

Wiggan, O. and Hamel, P. A. (2002). Pax3 regulates morphogenetic cell behavior in vitro coincident with activation of a PCP/non-canonical Wnt-signaling cascade. *J Cell Sci* **115**, 531-41.

Williams BA, O. C. (1994). Pax3 expression in segmental mesoderm marks early stages in myogenic cell specification. *Development* **120**, 785 - 796.

Xu HE, R. M., Xu W, Epstein JA, Maas RL, Pabo CO. (1999). Crystal structure of the human Pax6 paired domain - DNA complex reveals specific roles for the linker region and carboxy-terminal subdomain in DNA binding. *Genes Dev* **13**, 1263 - 1275.

Xu W, R. M., Jun S, Desplan C, Pabo CO. (1995). Crystal structure of a paired domain - DNA complex at 2.5A resolution reveals structural basis for Pax developmental mutations. *Cell* **80**, 639 - 650.

Zhao, P. and Hoffman, E. P. (2004). Embryonic myogenesis pathways in muscle regeneration. *Dev Dyn* **229**, 380-92.

Zhaowei A, F. A., Spray D, Brown A, Fishman G. (2000). Wnt1 regulation of connexin43 in cardiac myocytes. *J Clin Invest* **105**, 161 - 171.

Ziman, M. R., Fletcher, S. and Kay, P. H. (1997). Alternate Pax7 transcripts are expressed specifically in skeletal muscle, brain and other organs of adult mice. *Int J Biochem Cell Biol* **29**, 1029-36.

Ziman, M. R. and Kay, P. H. (1998a). A conserved TN8TCCT motif in the octapeptide-encoding region of Pax genes which has the potential to direct cytosine methylation. *Gene* **223**, 303-8.

Ziman, M. R. and Kay, P. H. (1998b). Differential expression of four alternate Pax7 paired box transcripts is influenced by organ- and strain-specific factors in adult mice. *Gene* **217**, 77-81.

Ziman, M. R., Thomas, M., Jacobsen, P. and Beazley, L. (2001). A key role for Pax7 transcripts in determination of muscle and nerve cells. *Exp Cell Res* **268**, 220-9.

Zlotogora J, L. I., Bar-David S, Ergaz Z, Abeliovich D. (1995). Homozygosity for Waardenburg syndrome. *Am J Hum Genetics* **56**, 1173 - 1178.